Understanding the role of scale in assessing sediment and nutrient loads from Coastal Plain watersheds delivered to the Chesapeake Bay

Mohammad Nayeb Yazdi

Dissertation submitted to the faculty of the Virginia Polytechnic Institute and State University in partial fulfillment of the requirements for the degree of

Doctor of Philosophy
In
Biological Systems Engineering

David J. Sample
Durelle. T Scott
Adil A. Godrej
Robert W. Burgholzer
Karen S. Kline

June 25, 2020
Virginia Beach, Virginia

Keywords: Watershed models, stormwater, land use, retention pond, nursery, pollutant loads, urban and agricultural runoff

Understanding the role of scale in assessing sediment and nutrient loads from Coastal Plain watersheds delivered to the Chesapeake Bay

Mohammad Nayeb Yazdi

ABSTRACT

Urban and agricultural runoff is the principal contributor to non-point source (NPS) pollution and subsequent impairments of streams, rivers, lakes, and estuaries. Urban and agricultural runoff is a major source of sediment, nitrogen (N) and phosphorus (P) loading to receiving waters. Coastal waters in the southeastern U.S. are vulnerable to human impacts due to the proximity to urban an agricultural land uses, and hydrologic connection of the Coastal Plain to receiving waters. To mitigate the impacts of urban and agricultural runoff, a variety of stormwater control measures (SCMs) are implemented. Despite the importance of the Coastal Plain on water quality and quantity, few studies are available that focus on prediction of nutrient and sediment runoff loads from Coastal Plain watersheds. The overall goals of my dissertation are to assess the effect of urban and agricultural watershed on coastal waters through monitoring and modeling, and to characterize treatment performance of SCMs. These goals are addressed in four independent studies. First, we developed the Storm Water Management Model (SWMM) and the Hydrologic Simulation Program-Fortran (HSPF) models for an urbanized watershed to compared the ability of these two models at simulating streamflow, peak flow, and baseflow. Three separate monitoring and modeling programs were conducted on: 1) six urban land uses (i.e. commercial, industrial, low density residential, high density residential, transportation, and open space); 2) container nursey; and 3) a Coastal Plain retention pond. This study provides methods for estimating watershed pollutant loads. This is a key missing link in implementing watershed improvement strategies and selecting the most appropriate urban BMPs at the local

scale. Results of these projects will help urban planners, urban decision makers and ecological experts for long-term sustainable management of urbanized and agricultural watersheds.

Understanding the role of scale in assessing sediment and nutrient loads from Coastal Plain watersheds delivered to the Chesapeake Bay

Mohammad Nayeb Yazdi

General Audience Abstract

Urban and agricultural runoff is a major source of sediment, nitrogen (N) and phosphorus (P) loading to receiving waters. When in excess, these pollutants degrade water quality and threaten aquatic ecosystems. Coastal waters in the southeastern U.S. are vulnerable to human impacts due to the proximity to urban an agricultural landuse. To mitigate the impacts of urban and agricultural runoff, a variety of stormwater control measures (SCMs) are implemented. The overall goals of my dissertation are to assess the effect of urban and agricultural watershed on coastal waters through monitoring and modeling, and to characterize treatment performance of SCMs. These goals are addressed in four independent studies. First, we developed two watershed models the Storm Water Management Model (SWMM) and the Hydrologic Simulation Program-Fortran (HSPF) to simulate streamflow, peak flow, and baseflow within an urbanized watershed. Three separate monitoring programs were conducted on: (1) urban land uses (i.e. commercial, industrial, low density residential, high density residential, transportation, and open space); (2) container nursey; and (3) a Coastal Plain retention pond. These studies provided methods for estimating watershed pollutant loads. Results of these projects will help urban planners and ecological experts for long-term sustainable management of urbanized and agricultural watersheds.

ACKNOWLEDGEMENTS

The journey of completing this degree has been a great experience for me. Foremost, I would like to thank my advisors David Sample and Scott Durelle for their continued support and guidance throughout my PhD program.

In addition, I would like to express thanks to my committee members Adil Godrej, Karen Kline, and Robert Burgholzer for providing valued input and feedback. I would like to thank specially James Owen for his advice and comments on agricultural side of my project, and thank you to the Clean WateR3 research team that funded one part of this project. I would like to thank Xixi Wang, Michael Harrison, Mehdi Ketabchy, Nasrin Alamdari, and lab members for all of their help in this project. They all are great colleagues who made this research possible. I would like to acknowledge all staff and faculty at the Hampton Roads AREC for helping me to have a great time in Virginia Beach. I also thank all my friends who made my life in the U.S. more comfortable and blessed, especially Piotr Zaczynski.

Finally, and most importantly, I am deeply thankful and blessed for my Mom, Dad, and Sisters who support me, encourage me, comfort me, and pray for me.

TABLE OF CONTENTS

LIST OF TABLES

LIST OF FIGURES

LIST OF ABBREVIATIONS

ADD	Antecedence dry day
API	Average Precipitation Intensity
BMP	Best Management Practice
CC	Climate Change
CI	Confidence Intervals
CO	Commercial
CV	Coefficient of Variation
DO	Dissolved Oxygen
DP	Dissolve Phosphorus
DW	Dynamic Wave
EC	Electrical Conductivity
EMC	Event Mean Concentrations
ET	Evapotranspiration
GA	Green-Ampt
GI	Green Infrastructure
GIS	Geographic Information System
GSA	Global Sensitivity Analysis
HDR	High Density Residential
HRT	Hydrologic Residence Time
HSPF	Hydrologic Simulation Program-Fortran
HW	Hydraulic Width
IMPLND	Impervious Land Segments
IN	Industrial
KW	Kinematic Wave
LDR	Low Density Residential
LID	Low Impact Development
MPI	Maximum Precipitation Intensity
NOAA	National Oceanic and Atmospheric Administration
NPS	Non-Point Source
NRCS	Natural Resources Conservation Service
NSE	Nash-Sutcliffe Efficiency
NSQD	National Stormwater Quality Database
ORP	Oxidation/Reduction Potential
OS	Open Space
PBIAS	Percent Bias
PCA	Principal Component Analysis
PCs	Principal Components
Pde	Precipitation Depth
Pdu	Precipitation Duration
PERLND	Pervious Land
PF	Precipitation Frequency
PP	Particulate P
PSD	Particle Size Distribution

QA/QC	Quality Assurance/Quality Control
RC	Runoff Coefficient
RCHRES	Routing Through Reaches
RE	Removal Efficiency
RR	Runoff Reduction
SA	Sensitivity Analysis
SCMS	Stormwater Control Measures
SCS	Soil Conservation Service
SSURGO	Soil Survey Geographic database
SWMM	Storm Water Management Model
TMDL	Total Maximum Daily Load
TN	Total Nitrogen
TP	Total Phosphorus
TR	Transportation
TRB	Tailwater Recover Basins
TSS	Total suspended solids
VA-DCR	Virginia Department of Conservation and Recreation

Chapter 1. Introduction

Dead zones are hypoxic (low-oxygen) areas found within coastal waters. Since the mid-1900s, the occurrence of dead zones has doubled each decade (Altieri and Gedan, 2015; Diaz and Rosenberg, 2008; Rabalais et al., 2010). Dead zones are widespread across the globe and a detrimental anthropogenic threat to marine ecosystems worldwide (Diaz and Rosenberg, 2008). The increase in the number, size, and severity of dead zones is a direct response to increasing nutrient inputs resulting in the eutrophication of estuaries and coastal waters (Altieri and Gedan, 2015). The development of eutrophication in coastal hypoxia begins with increased nutrient levels; in response, algae grow exponentially. Eventually the algae die, settling to the bottom. The degradation of this organic matter consumes available oxygen, resulting in hypoxic conditions, leading to fish kills. As nutrients and organic matter in the sediments accumulate, the timespan of hypoxic conditions increases, and the concentration of dissolved oxygen (DO) continues to fall and anoxia can become a long-term seasonal condition (Diaz and Rosenberg, 2008).

Hypoxia within the Chesapeake Bay, the largest estuary in the U.S. (USEPA, 2010a), has been observed over the last 70 years (Hagy et al., 2004), resulting in degradation to the coastal ecosystem and commercial fisheries (Kemp et al., 2005). To reduce the nutrients and sediment delivered to the Bay, the U.S. Environmental Protection Agency instituted the Chesapeake Bay Total Maximum Daily Load (TMDL) program (USEPA, 2010b). The goal of the CB TMDL is to reduce nitrogen (N), phosphorous (P) and sediment loads by treating targeted sources of these constituents, which stem from a wide variety of point and nonpoint sources (NPS) of pollution (Shenk and Linker, 2013; USEPA, 2010b). While significant investments have been made to treat or remove wastewater point source loadings from the Bay (Hendriks and Langeveld, 2017;

USEPA, 2003), urban runoff (as a NPS of pollution) is thought to be one of the largest contributors of excess N, P, and sediment, which is currently discharged untreated for the most part (Bettez and Groffman, 2012; Gold et al., 2017). The largest NSP in urban runoff is suspended solids (Muñoz and Panero, 2008; Schwartz et al., 2017). Fine particle sediments are easily suspended and conveyed to receiving waters (Liu et al., 2015).

Runoff volume, timing and magnitudes of streamflow during storm events have also increased due to urbanization and channelization, largely from the decrease in infiltration and the conversion of creeks into storm drains (Hester and Bauman, 2013; Li et al., 2013; Liu et al., 2015). Increased runoff and decreased residence time, results in more streams erosion and less time for treatment and/or natural "filtering", respectively, resulting in the conveyance of substantially increased N, P, and sediment (DeLorenzo et al., 2012; Gold et al., 2017; Rosenzweig et al., 2011; Stephansen et al., 2014). These processes thus result in increased transport of N, P, and sediment to the Bay. A variety of practices have been implemented to mitigate the impacts of urbanization on quantity and quality of stormwater. Collectively, these are known as best management practices (BMPs), or stormwater control measures (SCMs). SCMs can be small, decentralized practices that utilize infiltration and or evapotranspiration to reduce runoff volume and improve water quality through a variety of unit processes (Lucas and Sample, 2015; Palla and Gnecco, 2015). These are known as low impact development (LID) practices, or green infrastructure (GI). The central principle of LID design is to mimic or restore pre-development hydrology and water quality (Damodaram et al., 2010; Golden and Hoghooghi, 2017; Liu et al., 2014). SCMs may also include large, centralized facilities such as retention ponds or underground tanks that primarily remove pollutants through settling, but may also use biological uptake (USEPA, 2016).

Most of the southeast U.S. lies within the Coastal Plain physiographic province, an area of approximately 1.2 million km^2 (Hupp, 2000). In the U.S., there was 40% growth in the population of coastal zones between 1970 and 2010, and by 2020 is projected to increase by 8% (NOAA, 2017). In addition, coastal portions of the southeastern U.S. are expected to nearly double in urbanization over the next 50 years (Terando et al., 2014). Consequently, coastal waters in the southeastern U.S. will become particularly vulnerable to human impacts due to the proximity and hydrologic connection of the Coastal Plain to receiving waters (Beckert et al., 2011; Phillips and Slattery, 2006). Due to its proximity of the Chesapeake Bay to urban areas and hydrologic connection of the Coastal Plain to receiving waters, the Coastal Plain portion of the CB watershed could become critical in terms of its potential impact on water quality (Beckert et al., 2011; Phillips and Slattery, 2006). Further, water tables in coastal areas are high, decreasing soil infiltration in coastal area and increasing surface pollutant transport to the CB during storm events (Basha, 2011; Munõz-Carpena et al., 2018). Despite the importance of the Coastal Plain on water quality and quantity of receiving waters, few studies are available that focus on prediction of nutrient and sediment runoff loads to the CB generated from Coastal Plain watersheds.

A variety of watershed models are available to: (1) simulate hydrology and water quality in runoff, streams, and water bodies; (2) evaluate the impacts of urban development; and (3) investigate effectiveness of watershed restoration strategies (Borah et al., 2019; Niazi et al., 2017). Two commonly used watershed models include the U.S. Environmental Protection Agency's (USEPA) Storm Water Management Model (SWMM) (USEPA, 2018), and the Hydrologic Simulation Program-Fortran (HSPF) (USEPA, 2014). SWMM is a dynamic/physically-based hydrologic and hydraulic model which is used to simulate runoff

quantity and quality during discrete events and continuous periods (Huber and Dickinson, 1988; James et al., 2010; Rossman, 2010). HSPF is a comprehensive process-based watershed model that simulates watershed hydrology and water quality (Bicknell et al., 2001; Linsley et al., 1975). Both SWMM and HSPF were developed by the USEPA. SWMM has specific functionality for simulation of SCMs and LID.

Overall, urban runoff delivered from the Coastal Plain is one of the largest sources of nutrients and sediment loading delivered to the CB (Howarth et al., 2002; National Research Council, 2000; Rebich et al., 2011). Developing an effective strategy for decreasing sediment and associated nutrients in stormwater is important for the CB watershed. However, there is lack of information on: (1) sediment and nutrient export from Coastal Plain watersheds during the storm events that represent the majority of water/sediment/nutrient export; (2) sediment and nutrient export from each urban and agricultural land uses, and (3) effect of SCMs in Coastal Plain on removal stormwater sediment and nutrient. This information gap can be addressed through selective monitoring of runoff quantity and quality from dominant land uses and SCM performance in Coastal Plain area. This dissertation is organized to address the following objectives

1.1 Goals and Objectives

The goal of this research is improving the understanding of urban and agricultural watershed behavior through monitoring and modeling, and in improving treatment performance of SCMs. To advance this goal, the following objectives will be addressed:

- Assessing the performance of HSPF and SWMM for simulating streamflow regimes in an urban watershed.

- Assessing the role of land use characteristics on urban stormwater quality, and estimating watershed pollutant loads
- Evaluating water quality of storm and irrigation runoff from a container nursery and comparing these with urban land uses in Coastal Plain area.
- Investigating the effect of a Coastal Plain retention pond in potentially reducing or buffering downstream loads to the Bay.

1.2 Dissertation Organization

This dissertation is composed of six chapters. Chapter 1 explains about dead zones in the CB and the strategies for reducing runoff pollutants delivered to the CB from coastal areas. Chapters 2-5 are allocated to aforementioned objectives of this research. All these four chapters (2-5) have been published or will be submitted for publication in peer-reviewed journals. The author of this dissertation was the lead author on all four manuscripts. Chapter 6 contains the overall conclusion of this research.

1.3 References for Chapter 1:

Altieri, A.H., Gedan, K.B., 2015. Climate change and dead zones. Glob. Chang. Biol. 21, 1395–1406. doi:10.1111/gcb.12754

Basha, H.A., 2011. Infiltration models for soil profiles bounded by a water table. Water Resour. Res. 47. doi:10.1029/2011WR010872

Beckert, K.A., Fisher, T.R., O'Neil, J.M., Jesien, R. V., 2011. Characterization and Comparison of Stream Nutrients, Land Use, and Loading Patterns in Maryland Coastal Bay Watersheds. Water, Air, Soil Pollut. 221, 255–273. doi:10.1007/s11270-011-0788-7

Bettez, N.D., Groffman, P.M., 2012. Denitrification Potential in Stormwater Control Structures and Natural Riparian Zones in an Urban Landscape. Environ. Sci. Technol. 46, 10909–10917. doi:10.1021/es301409z

Bicknell, B.R., Imhoff, J.., Kittle Jr, J.., Jobes, T.., Donigian Jr, A.., Johanson, R., 2001. Hydrological simulation program–fortran: HSPF, version 12 user's manual. AQUA TERRA Consult. Mt. View, Calif.

Borah, D.K., Ahmadisharaf, E., Padmanabhan, G., Imen, S., Mohamoud, Y.M., 2019. Watershed Models for Development and Implementation of Total Maximum Daily Loads. J. Hydrol. Eng. 24, 03118001. doi:10.1061/(ASCE)HE.1943-5584.0001724

Carey, R.O., Migliaccio, K.W., Brown, M.T., 2011. Nutrient discharges to Biscayne Bay, Florida: Trends, loads, and a pollutant index. Sci. Total Environ. 409, 530–539. doi:10.1016/j.scitotenv.2010.10.029

Damodaram, C., Giacomoni, M.H., Prakash Khedun, C., Holmes, H., Ryan, A., Saour, W., Zechman, E.M., 2010. Simulation of Combined Best Management Practices and Low Impact Development for Sustainable Stormwater Management1. JAWRA J. Am. Water Resour. Assoc. 46, 907–918. doi:10.1111/j.1752-1688.2010.00462.x

DeLorenzo, M.E., Thompson, B., Cooper, E., Moore, J., Fulton, M.H., 2012. A long-term monitoring study of chlorophyll, microbial contaminants, and pesticides in a coastal residential stormwater pond and its adjacent tidal creek. Environ. Monit. Assess. 184, 343–359. doi:10.1007/s10661-011-1972-3

Diaz, R.J., Rosenberg, R., 2008. Spreading dead zones and consequences for marine ecosystems. Science 321, 926–9. doi:10.1126/science.1156401

Gold, A.C., Thompson, S.P., Piehler, M.F., 2017. Water quality before and after watershed-scale implementation of stormwater wet ponds in the coastal plain. Ecol. Eng. 105, 240–251. doi:10.1016/j.ecoleng.2017.05.003

Golden, H.E., Hoghooghi, N., 2017. Green infrastructure and its catchment-scale effects: an emerging science. Wiley Interdiscip. Rev. Water 5, e1254. doi:10.1002/wat2.1254

Hagy, J.D., Boynton, W.R., Keefe, C.W., Wood, K. V., 2004. Hypoxia in Chesapeake Bay, 1950–2001: Long-term change in relation to nutrient loading and river flow. Estuaries 27, 634–658. doi:10.1007/BF02907650

Hendriks, A.T.W.M., Langeveld, J.G., 2017. Rethinking Wastewater Treatment Plant Effluent Standards: Nutrient Reduction or Nutrient Control? Environ. Sci. Technol. 51, 4735–4737. doi:10.1021/acs.est.7b01186

Hester, E.T., Bauman, K.S., 2013. Stream and retention pond thermal response to heated summer runoff from urban impervious surfaces. J. Am. Water Resour. Assoc. 49, 328–342. doi:10.1111/jawr.12019

Howarth, R.W., Sharpley, A.N., Walker, D., 2002. Sources of nutrient pollution to coastal waters in the United States: Implications for achieving coastal water quality goals. Estuaries 25, 656–676. doi:10.1007/BF02804898

Huber, W.C., Dickinson, R.E., 1988. Storm Water Management Model , Version 4 : User's Manual 720. doi:EPA/600/3-88/001a

Hupp, C.R., 2000. Hydrology, geomorphology and vegetation of costal plain rivers in the south-eastern USA. Hydrol. Process. 14, 2991–3010. doi:10.1002/1099-1085(200011/12)14:16/17<2991::AID-HYP131>3.0.CO;2-H

James, W., Rossman, L.A., James, W.R.., 2010. User's guide to SWMM5.

Keller, T.A., Shenk, G.W., Williams, M.R., Batiuk, R.A., 2011. Development of a new indicator of pollutant loads and its application to the Chesapeake Bay watershed. River Res. Appl. 27, 202–212. doi:10.1002/rra.1351

Kemp, W.M., Boynton, W.R., Adolf, J.E., Boesch, D.F., Boicourt, W.C., Brush, G., Cornwell,

J.C., Fisher, T.R., Glibert, P.M., Hagy, J.D., Harding, L.W., Houde, E.D., Kimmel, D.G., Miller, W.D., Newell, R.I.E., Roman, M.R., Smith, E.M., Stevenson, J.C., 2005. Eutrophication of Chesapeake Bay: Historical trends and ecological interactions. Mar. Ecol. Prog. Ser. 303, 1–29. doi:10.3354/meps303001

Li, H., Harvey, J.T., Holland, T.J., Kayhanian, M., 2013. Corrigendum: The use of reflective and permeable pavements as a potential practice for heat island mitigation and stormwater management. Environ. Res. Lett. 8, 049501. doi:10.1088/1748-9326/8/4/049501

Linsley, R.K., Kohler, M.A., Paulhus, J., 1975. HYDROLOGY FOR ENGINEERS, 2nd ed. New York : McGraw-Hill.

Liu, A., Goonetilleke, A., Egodawatta, P., 2015. Role of Rainfall and Catchment Characteristicson Urban Stormwater Quality.

Liu, W., Chen, W., Peng, C., 2014. Assessing the effectiveness of green infrastructures on urban flooding reduction: A community scale study. Ecol. Modell. 291, 6–14. doi:10.1016/J.ECOLMODEL.2014.07.012

Lucas, W.C., Sample, D.J., 2015. Reducing combined sewer overflows by using outlet controls for Green Stormwater Infrastructure: Case study in Richmond, Virginia. J. Hydrol. 520, 473–488. doi:10.1016/J.JHYDROL.2014.10.029

Munõz-Carpena, R., Lauvernet, C., Carluer, N., 2018. Shallow water table effects on water, sediment, and pesticide transport in vegetative filter strips-Part 1: Nonuniform infiltration and soil water redistribution. Hydrol. Earth Syst. Sci. 22, 53–70. doi:10.5194/hess-22-53-2018

Muñoz, G., Panero, M., 2008. Sources of suspended solids to the New York/New Jersey harbor watershed.

National Research Council, 2000. Clean coastal waters : understanding and reducing the effects of nutrient pollution. National Academy Press.

Niazi, M., Nietch, C., Maghrebi, M., 2017. Stormwater management model: Performance review and gap analysis, Journal of Sustainable Water in the Built Environment. doi:10.1061/JSWBAY.0000817.

NOAA, 2017. American population lives near the coast [WWW Document]. Natl. Ocean. Atmos. Adm. URL https://oceanservice.noaa.gov/facts/population.html

Palla, A., Gnecco, I., 2015. Hydrologic modeling of Low Impact Development systems at the urban catchment scale. J. Hydrol. 528, 361–368. doi:10.1016/J.JHYDROL.2015.06.050

Phillips, J.D., Slattery, M.C., 2006. Sediment storage, sea level, and sediment delivery to the ocean by coastal plain rivers. Prog. Phys. Geogr. 30, 513–530. doi:10.1191/0309133306pp494ra

Rabalais, N.N., Díaz, R.J., Levin, L.A., Turner, R.E., Gilbert, D., Zhang, J., 2010. Dynamics and distribution of natural and human-caused hypoxia. Biogeosciences 7, 585–619. doi:10.5194/bg-7-585-2010

Rebich, R.A., Houston, N.A., Mize, S. V., Pearson, D.K., Ging, P.B., Evan Hornig, C., 2011. Sources and Delivery of Nutrients to the Northwestern Gulf of Mexico from Streams in the

South-Central United States. J. Am. Water Resour. Assoc. 47, 1061–1086. doi:10.1111/j.1752-1688.2011.00583.x

Rosenzweig, B.R., Smith, J.A., Baeck, M.L., Jaffé, P.R., 2011. Monitoring Nitrogen Loading and Retention in an Urban Stormwater Detention Pond. J. Environ. Qual. 40, 598. doi:10.2134/jeq2010.0300

Rossman, L.A., 2010. Storm water management model user's manual, version 5.0. Cincinnati: National Risk Management Research Laboratory, Office of Research and Development, US Environmental Protection Agency.

Schwartz, D., Sample, D.J., Grizzard, T.J., 2017. Evaluating the performance of a retrofitted stormwater wet pond for treatment of urban runoff. Environ. Monit. Assess. 189, 256. doi:10.1007/s10661-017-5930-6

Shenk, G.W., Linker, L.C., 2013. Development and Application of the 2010 Chesapeake Bay Watershed Total Maximum Daily Load Model. JAWRA J. Am. Water Resour. Assoc. 49, n/a-n/a. doi:10.1111/jawr.12109

Stephansen, D.A., Nielsen, A.H., Hvitved-Jacobsen, T., Arias, C.A., Brix, H., Vollertsen, J., 2014. Distribution of metals in fauna, flora and sediments of wet detention ponds and natural shallow lakes. Ecol. Eng. 66, 43–51. doi:10.1016/j.ecoleng.2013.05.007

Terando, A.J., Costanza, J., Belyea, C., Dunn, R.R., McKerrow, A., Collazo, J.A., 2014. The Southern Megalopolis: Using the Past to Predict the Future of Urban Sprawl in the Southeast U.S. PLoS One 9, e102261. doi:10.1371/journal.pone.0102261

USEPA, 2018. Storm Water Management Model (SWMM) [WWW Document]. URL https://www.epa.gov/water-research/storm-water-management-model-swmm (accessed 1.11.19).

USEPA, 2016. Operating and Maintaining Underground Storage Tank Systems: Practical Help and Checklists.

USEPA, 2014. Hydrological Simulation Program - FORTRAN (HSPF).

USEPA, 2010a. Chesapeake Bay Phase 5 Community Watershed Model [WWW Document]. U.S Environ. Prot. Agency.

USEPA, 2010b. Chesapeake Bay Total Maximum Daily Load for Nitrogen, Phosphorus and Sediment [WWW Document]. US Environ. Prot. Agency. URL https://www.epa.gov/chesapeake-bay-tmdl

USEPA, 2003. Decision on petition for rulemaking to address nutrient pollution from significant point sources in the Chesapeake Bay watershed [WWW Document]. U.S. Environ. Agency. URL https://www.epa.gov/sites/production/files/2015-12/documents/chesapeake-foundation-bay-petition.pdf

Zhang, Q., Brady, D.C., Ball, W.P., 2013. Long-term seasonal trends of nitrogen, phosphorus, and suspended sediment load from the non-tidal Susquehanna River Basin to Chesapeake Bay. Sci. Total Environ. 452–453, 208–221. doi:10.1016/j.scitotenv.2013.02.012

Chapter 2. An Evaluation of HSPF and SWMM for Simulating Streamflow Regimes in an Urban Watershed

Mohammad Nayeb Yazdi, Mehdi mina, David J. Sample, Durelle Scott, and Hehuan Liao

Submitted: January 2019

To: *Environmental Modelling & Software*

Status: Published May 2019. DOI: 10.1016/j.envsoft.2019.05.008

Abstract

Hydrologic models such as the Storm Water Management Model (SWMM) and the Hydrologic Simulation Program-Fortran (HSPF) are widely used to assess the impacts of urbanization on receiving waters. We compared the ability of these two models at simulating streamflow, peak flow, and baseflow from an urbanized watershed. The most sensitive hydrologic parameters for HSPF were related to groundwater; for SWMM, it was imperviousness. Both models simulated streamflow adequately; however, HSPF simulated baseflow better than SWMM, while, SWMM simulated peak flow better than HSPF. Global Sensitivity Analysis showed that variability of streamflow for SWMM was higher than that of HSPF, while variability of baseflow for HSPF was greater than that of SWMM. Further, analysis of extreme storm events indicated that the runoff coefficient for SWMM was slightly greater than HSPF for recurrence intervals of 1, 2, 5, and 10-yr.; the opposite was the case for higher recurrence intervals.

Keywords: HSPF, SWMM, Streamflow, Baseflow, Peak flow, Sensitivity analysis.

2.1 Introduction

Urbanization alters watershed hydrology by increasing imperviousness and channelizing or piping natural drainageways (Hester and Bauman, 2013; Li et al., 2013; Liu et al., 2015). These changes reduce infiltration, increase runoff volume, accelerate the time to runoff peak (lag time), and reduce baseflow to streams (Chen et al., 2017; Lacher et al., 2019; Locatelli et al., 2017; Rosburg et al., 2017). Increasing runoff volume results in higher streambank and channel erosion (Whitney et al., 2015; Yousefi et al., 2017). Increases in peak runoff and decreasing lag time increases flooding (Roodsari and Chandler, 2017; Zope et al., 2016), damaging public or private property. Urbanization also leads to higher sediment and nutrient loads delivered to downstream water bodies causing eutrophication and degrading water quality, threatening aquatic ecosystems (Daghighi, 2017; Liu et al., 2018; Luo et al., 2018; Stoner and Arrington, 2017). A variety of stormwater control measures (SCMs) also known as best management practices (BMPs) have been developed for mitigating urban impacts. Historically, management of urban runoff meant mitigating peaks using storage; this practice has given way to a more holistic focus on the restoration of the natural hydroperiod; known as low impact development (LID) or green stormwater infrastructure (GSI). SCMs that assist in these goals tend to focus on infiltration (Golden and Hoghooghi, 2017; Liu et al., 2018; Lucas and Sample, 2015).

Watershed models are used to: (1) simulate hydrology and water quality in runoff, streams, and water bodies; (2) evaluate the impacts of urban development; and (3) investigate effectiveness of watershed restoration strategies (Borah et al., 2019; Niazi et al., 2017). While numerous watershed models exist, limited information is available to guide in their selection. Two commonly used watershed models include the U.S. Environmental Protection Agency's (USEPA) Storm Water Management Model (SWMM) (USEPA, 2018) , and the Hydrologic

Simulation Program-Fortran (HSPF) (USEPA, 2014). SWMM is a dynamic/physically-based hydrologic and hydraulic model which is used to simulate runoff quantity and quality during discrete events and continuous periods (Huber and Dickinson, 1988; James et al., 2010; Rossman, 2010). Since, SWMM is able to simulate conveyance systems, it is mostly applied within urban watersheds. HSPF is a comprehensive process-based watershed model that simulates watershed hydrology and water quality (Bicknell et al., 2001; Linsley et al., 1975). Both SWMM and HSPF were developed by the USEPA. HSPF has been applied across large, regional watersheds, such as the Chesapeake Bay watershed, a 166,000 km^2 watershed (USEPA, 2010). The HSPF-based Chesapeake Bay watershed model discretizes subwatersheds based upon HUC-12 (hydrologic unit code) watershed delineations and geopolitical considerations, such as City, County, and State boundaries (Shenk et al., 2012). Due to the complexity inherent in urban storm drainage networks and their "flashy" runoff, SWMM models tend to be used at smaller scales to capture this response (Niazi et al., 2017).

Recent (<10 years) published research based upon use of SWMM or HSPF that used at least two statistical methods for evaluating model performance were compiled in Table 2.1. Based on the references provided in Table 2.1, SWMM has been applied to watershed ranging in size from 2 ha to 40,000 km^2, however, it has primarily been used within smaller urban watersheds (< 2 km^2). SWMM has specific functionality for simulation of SCMs and LID, incorporating a variety of physical processes such as storage routing and infiltration. On the other side, HSPF has also been applied across a wide range of larger watersheds (3 to 70,000 km^2). Although HSPF has been applied to urban watersheds, it has several limitations; HSPF does not directly simulate conveyance systems, nor does it directly simulate SCMs. HSPF models SCMs by shifting some of the watershed area's land use from urban to undeveloped and

changing the F-tables, as these govern stream dimensions in the HSPF model (Dudula and Randhir, 2016; Mohamoud et al., 2010; U.S.EPA, 2014). The lack of explicit SCM representation is a key weakness of HSPF (Mohamoud et al., 2010). HSPF is typically based upon readily available spatial data and must be calibrated to monitoring data. In contrast, SWMM depends upon physically based parameters that are collected or derived from spatial data gathered at smaller scales.

A comparative assessment of HSPF and SWMM in simulating hydrology of watersheds has been conducted only in a few studies; both were conducted in forested, not urban watersheds Lee et al. (2010) compared SWMM output with average streamflow from a large watershed during seven events. The authors indicated that both models performed adequately; however, HSPF simulated hourly streamflow better than SWMM. Tsai et al. (2017) applied SWMM and HSPF to a highly pervious, forested watershed. The authors indicated that HSPF matched observed streamflow better than SWMM. This may have been due to the highly permeable soil of the watershed which likely created a strong baseflow response. A key application of HSPF is the simulation of hydrology and water quality of the Chesapeake Bay watershed (USEPA, 2010). This is directly the result of HSPF's simplicity, which allows HSPF to execute simulations of this large watershed faster. This computational advantage is evident in execution of large watershed models for long times. SWMM's advantages are its ability to simulate "flashy" urban watersheds and assess SCM performance. As both models are widely used in urban areas, understanding the similarities and differences between them is critical, yet it has not been done. The objective of this study was to fill this research gap by comparing the capabilities of HSPF and SWMM as applied to a case study urban watershed. HSPF and SWMM were each assessed in terms of the (1) most sensitive hydrologic parameters in the watershed, (2) simulation of daily

and monthly streamflows in comparison with observed data, (3) simulation of peak flows, baseflows and their respective durations, and (4) predicted runoff coefficients during storm events with set return periods. These results were then used to compare the subcomponents of the long-term watershed hydrograph. Achieving a better understanding of the similarities and differences of SWMM and HSPF will help relate information from each model to the other, which will assist in meeting water quality goals at the regional scale.

2.2 Materials and methods

2.1.1 Site description

Stroubles Creek, located within Montgomery County, Virginia, lies within the Valley and Ridge physiographic province of Virginia. Stroubles Creek is a tributary to the New River, which is tributary to the Kanawha River, and part of the Mississippi River basin. An urbanized, 14.8-km^2 headwater portion of the Stroubles Creek watershed was selected for this study (Figure 2.1). This subwatershed includes much of downtown Blacksburg and the campus of Virginia Polytechnic Institute and State University (Virginia Tech). This watershed was selected because: 1) its headwaters are predominately (73.8%) urbanized, and 2) long-term monitoring data are available. The Virginia Tech Stream, Research, Education, and Management (StREAM) Lab (StREAM Lab, 2009) continuously measures groundwater levels, streamflows, and records precipitation and other climatological data within the Stroubles Creek watershed. Land cover is 73.8% urban (with a total imperviousness of 32%), 21% agricultural, 4% forested, and 1.2% water body (Multi-Resolution Land Use Consortium, 2011) (Figure 2.1). The Hydrologic Soil Group (HSG) of the headwaters and downstream is category C and B [as classified by the Natural Resource Conservation Service (NRCS, 2007, 1999a)], respectively. (Mostaghimi, S. et al., 2003).

Table 2.1. Summary of recent studies in simulation hydrology and water quality of watersheds by using SWMM and HSPF (sorted by watershed size).

Reference	Catchment area (km^2)	Indicator	[1] LID simulation	Simulation period	Streamflow Model performance		
					[2] R^2	[3] NSE	[4] PBIAS
SWMM							
Rai et al., (2017)	39269	Peak flows	–	1980 to 2012	–	0.66	-14%
Alamdari et al., (2017)	150	Peak flow, [5] TSS, [6] TN, [7] TP	–	2010 to 2013	0.78	0.73	12.1%
Moore et al., (2017)	1.5	Streamflow, peak flow, groundwater elevation	–	2013 to 2014	0.6	–	-38.7%
Guan et al., (2015)	0.12	Peak flows	Rain barrel, permeable pavement	2001 to 2006	0.84	0.9	–
Palla et al, (2015)	0.06	Runoff, peak flow, streamflow	Green roof, permeable pavement	7 events in 2005	–	0.84	-2%
Yazdi et al., (2019)	0.05	Runoff, TSS, TN, TP	–	2017 to 2018	0.71	0.69	19%
Rosa et al., (2015)	0.02	Runoff	Rain garden, permeable pavement, bioretention	2003 to 2005	0.8	0.68	–
HSPF							
Stern et al., (2016)	68000	Streamflow, sediment load	–	1958 to 2008	0.75	0.66	-15%
Huiliang et al., (2015)	6700	Streamflow, TP, TN	–	2004 to 2010	0.82	0.79	10.4%
Tong et al., (2012)	5840	Streamflow, TN, TP	–	1980 to 1989	0.82	0.72	-3.84%
Choi et al., (2017)	2330	Streamflow	–	1986 to 2005	–	0.70	5%
He and Hogue, (2012)	1680	Baseflow, peak flow, streamflow	–	1997 to 2006	0.85	0.69	10.5%
Dudula et al, (2016)	401	Streamflow	Bioretention, rain garden	1960 to 2008	0.73	0.71	–
Fonseca et al., (2014)	176	Temperature, fecal coliforms, TSS, pH	–	2003 to 2006	0.84	0.84	12.9%
Qiu et al., (2018)	3.27	Streamflow, TP, TN, sediment	–	2014 to 2015	0.90	0.80	–

[1] Low Impact Development
[2] The coefficient of determination
[3] Nash-Sutcliffe Efficiency
[4] Percent bias
[5] Total Suspended Solids
[6] Total Nitrogen
[7] Total Phosphorous

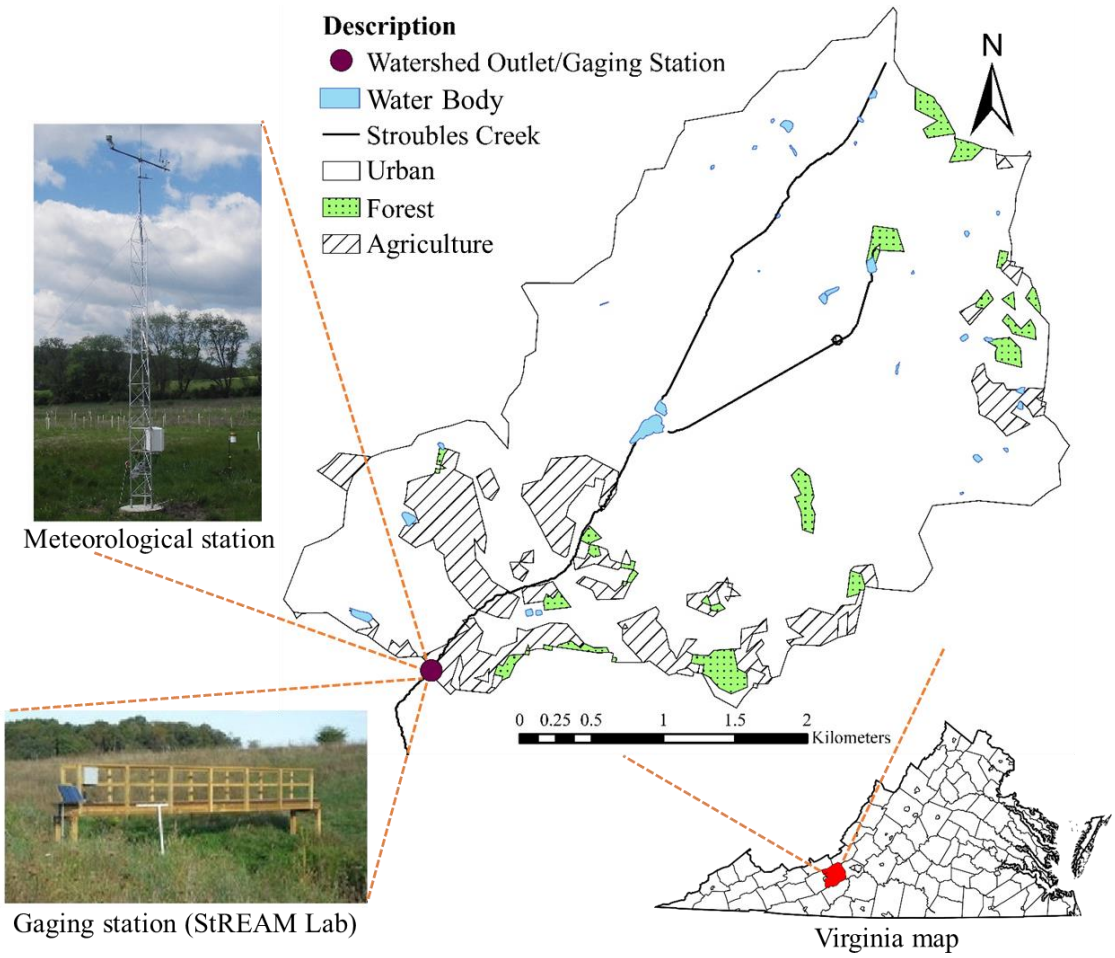

Figure 2.1. Stroubles Creek watershed land cover, with gaging and meteorological station locations.

The average elevation of the watershed is 670 m above sea level. Mean annual precipitation is 1030 mm (Liao et al., 2015).

2.1.2 Data collection

Storm sewer, street, parcel boundary, and surface elevation geographic information system (GIS) data were provided by the Town of Blacksburg (Town of Blacksburg, 2015) and Virginia Tech; separate datasets were merged. Soil information was obtained from the Soil Survey Geographic Database (SSURGO) of the Natural Resources Conservation Service, with scales ranging from 1:12,000 to 1:64,000 (NRCS, 1999b). The monitoring station measures stream stage every 15 minutes using a pressure transducer (CS451, Campbell Scientific Inc.,

Logan, UT, USA), with a water level resolution of 0.0035% FS (Full Scale / Full Span, the difference between the lowest and highest measured point) and a CR1000 datalogger (Campbell Scientific Inc., U.S). Stage was converted to discharge using a rating curve computed through the historical monitoring of stage-flow. Precipitation was recorded at 15-minute intervals at the StREAM Lab metrological station using a tipping bucket rain gages (TR-525USW, Texas Electronics, Inc., Dallas, TX, +/- 1%). The StREAM Lab weather station measured air temperature every 30 minutes at the Stroubles Creek monitoring station. StREAM Lab and the meteorological station are located at the watershed outlet. The depth to surficial groundwater was measured by two CS451 water level loggers (Campbell Scientific, U.S).

2.1.3 Model initialization

Land cover data was initially used to initialize the models in a process described by Ketabchy et al, (2018). The principal input parameters used in development of the HSPF and SWMM models were land use, soil properties, stream characteristics, and time series of precipitation and temperature. A total of 43 subwatersheds were delineated within the Stroubles Creek watershed. The watershed was delineated through ArcGIS 10.5 (Ketabchy et al., 2018), correcting the delineation for urban features (i.e. topography, slope, elevation, land use, etc.) where necessary. The differences and similarities of each process feature and main input/output variables for HSPF and SWMM are summarized in Table 2.2.

Table 2.2. Selected attributes of the HSPF and SWMM.

Feature	HSPF (Bicknell et al., 2001)	SWMM (Rossman, 2010)
Weather data	Precipitation, air temperature, solar radiation, cloud cover, wind, dew point, potential evapotranspiration	Precipitation, air temperature, wind speed, evaporation
Flow calibration parameters	20-25 parameters typically use for flow calibration	5-6 parameters typically use for flow calibration
Infiltration	Infiltration is calculated using Philip's equation	SWMM can use Horton or Green-Ampt or Curve number for calculating infiltration,
Water routing	Storage routing or kinematic wave method	Steady flow, Kinematic wave, or dynamic wave
Channel geometry	User-defined	User-defined
Shallow aquifer	Yes	Yes
Deep aquifer	Yes	Yes
LID control	No	Yes
Urban conveyance system	No	Yes

SWMM uses a simplified Darcy's law to simulate groundwater flows and interaction of surface water and groundwater of an aquifer through a number of parameters: bottom elevation of aquifer, groundwater-surface water interaction parameters (A_1, A_2, B_1, and B_2, which are listed in Table 2.3) (Rossman, 2010). These parameters control flow from the aquifer into the stream (and vice versa) and compute groundwater flow as a function of groundwater and surface water levels. Green-Ampt (GA) infiltration was applied for the infiltration module of SWMM, primarily because the watershed was semi-urbanized and the GA parameters such as hydraulic conductivity, suction head, and initial moisture values are available through the Soil Survey Geographic Database (SSURGO). The dynamic wave (DW) algorithm was selected for hydraulic routing within SWMM, because this method can simulate non-uniform and unsteady state flow

conditions, accurately. The longest flow paths of each subcatchment were used to calculate its hydraulic width (HW). Excess rainfall that exceeds depression storage is routed from each subcatchment through a nonlinear reservoir algorithm (Macro et al., 2019; Palla and Gnecco, 2015; Xing et al., 2016); each subcatchment is split into pervious and impervious portions, and runoff is directed to a user-defined outlet node or is routed across pervious areas. The Manning's roughness coefficient for pervious and impervious area is used to compute normal flow across a plane (the plane being the subcatchment); these eventually flow into either conveyance piping and/or streams, through which flow is calculated by use of the Manning's equation or through culvert formulas which depend upon upstream and downstream conditions.

HSPF includes three principle modules: PERLND (pervious land), IMPLND (impervious land segments), and RCHRES (routing through reaches). Processes in receiving streams can be simulated applying the RCHRES (reach and reservoir) module of HSPF. IMPLND module generates surface runoff, whereas the PERLND module analyzes all three major processes including surface runoff, interflow, and groundwater. All processes related to soil infiltration, soil moisture, groundwater, baseflow separation, etc., are analyzed in these modules, enabling HSPF to predict the hydrology and water quality of watersheds (Berndt et al., 2016; Bicknell et al., 2001; Mohamoud and Prieto, 2012; Xu et al., 2007). The PWATER and IWATER sections in HSPF control the water budget such as surface flow, interflow, baseflow, storage, and evaporation (ET). PWAT-PARM3 is one section of PWATER, which has two parameters of DEEPFR and AGWETP for simulating groundwater recharge. Philips equation (a physically-based method that uses an hourly time step), Chezy-Manning’s equation, and Kinematic Wave (KW) were applied within HSPF for simulating infiltration, streamflow, and hydraulic routing, respectively (Bicknell et al., 2001). Within HSPF, the parameters LZSN and UZSN (Table 2.3)

that control lower and upper zone storage are used to simulate water outflow from streams (Bicknell et al., 2001). The INFLT parameter is an index associated to Philips infiltration method to quantify soil infiltration capacity. There are three parameters controlling groundwater and baseflow in HSPF, named KVARY, AGWRC, DEEPER that are functions of baseflow recession variation and interactions between groundwater and surface water. BASETP is ET by riparian vegetation; when riparian vegetation is significant, its value starts with 0.03 (Singh et al., 2005). INTFW and IRC are interflow parameters, which are a function of soil, topography and land use (Bicknell et al., 2001).

The major components of the water balance within the Stroubles Creek watershed include: precipitation, total runoff (sum of overland flow, interflow and baseflow), total actual ET (sum of interception ET, aquifer upper zone ET, aquifer lower zone ET, baseflow ET, and active groundwater ET), and deep groundwater recharge. Each of the aforementioned water balance components have corresponding parameters in SWMM and HSPF (Table 2.3).

2.1.4 Baseflow separation

Direct runoff during storm events is the sum of overland flow and interflow, while baseflow consists of groundwater discharge from the saturated zone of an underlying aquifer directly to streams (Lott and Stewart, 2013; Miller et al., 2016; Rumsey et al., 2015). Baseflow affects aquatic habitats during dry periods and low-intensity storm events during periods of high groundwater levels (McCargo and Peterson, 2010). There are several methods to determine and separate baseflow from streamflow, which are grouped into three general categories: graphical, analytical, and mass balance methods (Lott and Stewart, 2016). Baseflow separation partitions a

Table 2.3. Selected parameters of HSPF and SWMM based on literature and field review, to assess the sensitivity analysis.

Parameter	Unit	Definition	Function of	Range
		HSPF		
LZSN	mm	Lower zone nominal soil moisture storage	Soils, Climate	2.54-381
INFILT	mm/hr.	Index to soil infiltration capacity	Soils, Land use	0.028-25
KVARY	1/mm	Variable groundwater recession flow	Baseflow recession	0-2540
AGWRC	1/day	Groundwater recession rate	Baseflow recession	0.001-0.999
DEEPFR	-	Fraction of inactive groundwater	Geology, Groundwater recharge	0-1
BASETP	-	Baseflow evapotranspiration	Riparian Vegetation	0-1
UZSN	mm	Upper zone Nominal Soil moisture storage	Surface soil conditions, land use	0.254-254
IRC	1/day	Interflow recession parameter	Soils, topography, land use	0.01-0.99
INTFW		Interflow inflow parameter	soils, topography, land use	1-10
		SWMM		
HW	m	Hydraulic Width	Longest flow path	±10% of each subwatershed
IMR	-	Impervious Manning roughness	Soil type, Land use	0.01–0.03
PMR	-	Pervious Manning roughness	Soil type, Land use	0.02–0.45
IDS	mm	Impervious depression storage	Pavement, Land use	0.3–2.3
PDS	mm	Pervious depression storage	Land cover	2.5–5.1
A_1	-	Groundwater flow coefficient	Discharge, Aquifer	0.0001–0.01
B_1	-	Groundwater flow exponent	Discharge, Aquifer	0.0001–1
A_2	-	Surface water flow coefficient	Aquifer	0.0001–0.01
B_2	-	Surface water flow exponent	Aquifer	0.0001–1
CND	mm/day	Conductivity	Soil type	±20% of initial values

hydrograph into baseflow and runoff. Analytical method is the most common baseflow separation methods (Lott and Stewart, 2016). Eckhardt, (2008) developed an equation with two parameters using numerical analysis provided in Eq. 1.

$$b_k = \frac{(1-BFI_{\max})ab_{k-1}+(1-a)BFI\times y_k}{1-aBFI_{max}} \quad (1)$$

where b is the baseflow, BFI_{max} is maximum baseflow index, a is the groundwater recession constant, k is the time step, and y is the total streamflow. Maximum baseflow index (BFI_{max}) determines based on the aquifer conditions. BFI_{max} can be 0.80, 0.50, and 0.25 for perennial streams with porous aquifers, ephemeral streams with porous aquifers, and perennial streams with hard rock aquifers, respectively. Since this method uses two parameter filters, it separates baseflow better than other numerical methods (Eckhardt, 2008; Neff et al., 2005). For our case study BFI_{max} was 0.80, because the stream was perennial with porous aquifers underneath.

2.1.5 Analysis of storm events

The behavior of each model during storms events with a set return period was assessed. Each calibrated model was used to simulate streamflow for the 1, 2, 5, 10, 25, 50, and 100-year 24-hr precipitation frequency (PF) estimates at the outlet of the Stroubles Creek watershed; the PF estimates were produced by National Oceanic and Atmospheric Administration (NOAA) ATLAS 14 with 90% confidence intervals (NOAA, 2016) using the partial duration time-series type. Natural Resources Conservation Service (NRCS) Type II storm distribution was used to develop time series of 24-hr precipitation events (NRCS, 2015). Groundwater discharge was assumed to be negligible during large storm events. The runoff volume simulated at the outlet of the watershed (by both models) during the 24-hr precipitation was normalized to runoff depth through dividing by the connected impervious area of the watershed. Further, runoff depth was divided by precipitation depth for calculating runoff coefficients, as, essentially all streamflow was runoff during the event.

2.1.6 Sensitivity analysis

Sensitivity analysis (SA) is process of the adjusting inputs of a model and calculating the rate of change in model results. SA techniques are grouped into local and global methods (Javaheri et al., 2018). Local SA methods evaluate the sensitivity of parameters around one local point. During simulation process, while the value of one input parameter was changed, the value of other parameters were held constant; hence, the sensitivity of streamflow as the main output of the models can be calculated by Eq. 2 (James and Burges, 1982).

$$S_c = (\frac{P}{Y})(\frac{Y_1 - Y_2}{P^{max} - P^{min}}) \quad (2)$$

where S_c is sensitivity coefficient; P is the value of input parameter; Y is the simulated output; P^{max} is the maximum range of the initial default value; P^{min} are the minimum range of the initial default value; and Y_1 and Y_2 are the corresponding output values. The most sensitive model parameters in watershed hydrology have higher values of S_c. In addition, Global sensitivity analysis (GSA) evaluates the sensitivity of parameters around the entire of parameter space (Dobler and Pappenberger, 2013; Javaheri et al., 2018). SA characterized key parameters that had a considerable effect on simulated results. The sensitive parameters have the potential to significantly influence SWMM and HSPF simulation results. In GSA, the calibrated value of each input was used as the baseline value, then the model was run for ±10% of the range of each parameter (Table 2.2). A total spread of 20% of parameter value was generated in this process. This approach is often applied to address the performance evaluation of best management practices (BMPs) and hydrologic models (Janke et al., 2013; Park et al., 2011).

2.1.7 Calibration and validation

HSPF and SWMM models simulate hydrologic and hydraulic of a watershed applying fixed and process-based parameters (Castanedo et al., 2006). A flow chart describing the process of developing the HSPF and SWMM models in this study is shown in Figure 2.2. Process-related parameters cannot normally be measured directly or cannot be calculated through GIS information; these include soil moisture storage, groundwater discharge into stream, ET, etc. (Bicknell et al., 2001; Castanedo et al., 2006). These parameters were adjusted manually during the calibration process between January 1, 2013 and December 30, 2013 for each model using hourly streamflow obtaining from StREAM Lab. There were 22 storm events during calibration period. Validation, which consists of running the models with the calibrated parameters without adjustment, was conducted for the period between January 1, 2009 and December 31, 2012, with 61 storm events.

Statistical analysis such as coefficient of determination (R^2) (Gebremariam et al., 2014; Nasr et al., 2007; Seong et al., 2015), Nash-Sutcliffe Efficiency (NSE) (Nash and Sutcliffe, 1970), and Percent bias (PBIAS) (Gupta et al., 1999) were performed to investigate the performance of models during calibration and validation periods. According to Duda et al., (2012) and Moriasi et al., (2015), multiple statistics should be used rather than a single criterion. A model performance rating system, which compared the simulated versus observed datasets qualitatively, was developed to assess model performance (Table 2.4) (Bennett et al., 2013; Ketabchy et al., 2019; Moriasi et al., 2015; Nayeb Yazdi et al., 2019a). If the statistical parameters showed good or satisfactory agreement (Table 2.4), the model calibration was considered complete; otherwise, the model calibration parameters were adjusted further. The

calibration process stops, when R^2 and NSE are greater than 0.6 and 0.5, respectively, and PBIAS is lower than 0.25% (Figure 2.3).

2.3 Results

2.3.1 Sensitivity analysis

The results of the local sensitivity analysis for selected input parameters are presented in Table 2.5. The most sensitive parameters in the HSPF model were groundwater parameters (DEEPFR, AGWRC), followed by INFILT, LZSN parameters, which are functions of soil and land use. The most sensitive parameters of the SWMM model was imperviousness ($S_c = 0.38$), impervious depression storage ($S_c = 0.11$).

Table 2.4. Performance assessment of watershed modeling[1].

Statistics	Very good	Good	Satisfactory	Unsatisfactory
R^2	$0.90 \leq R^2 < 1.00$	$0.75 \leq R^2 < 0.90$	$0.60 \leq R^2 < 0.75$	$R^2 \leq 0.60$
NSE	$0.75 \leq NSE < 1.00$	$0.65 \leq NSE < 0.75$	$0.50 \leq NSE < 0.65$	$NSE \leq 0.50$
BBIAS	BBIAS $< \pm 10$	$\pm 10 \leq BBIAS < \pm 15$	$\pm 15 \leq BBIAS < \pm 25$	BBIAS $\leq \pm 25$

[1] (Duda et al., 2012; Moriasi et al., 2007; Seong et al., 2015; Xu et al., 2007)

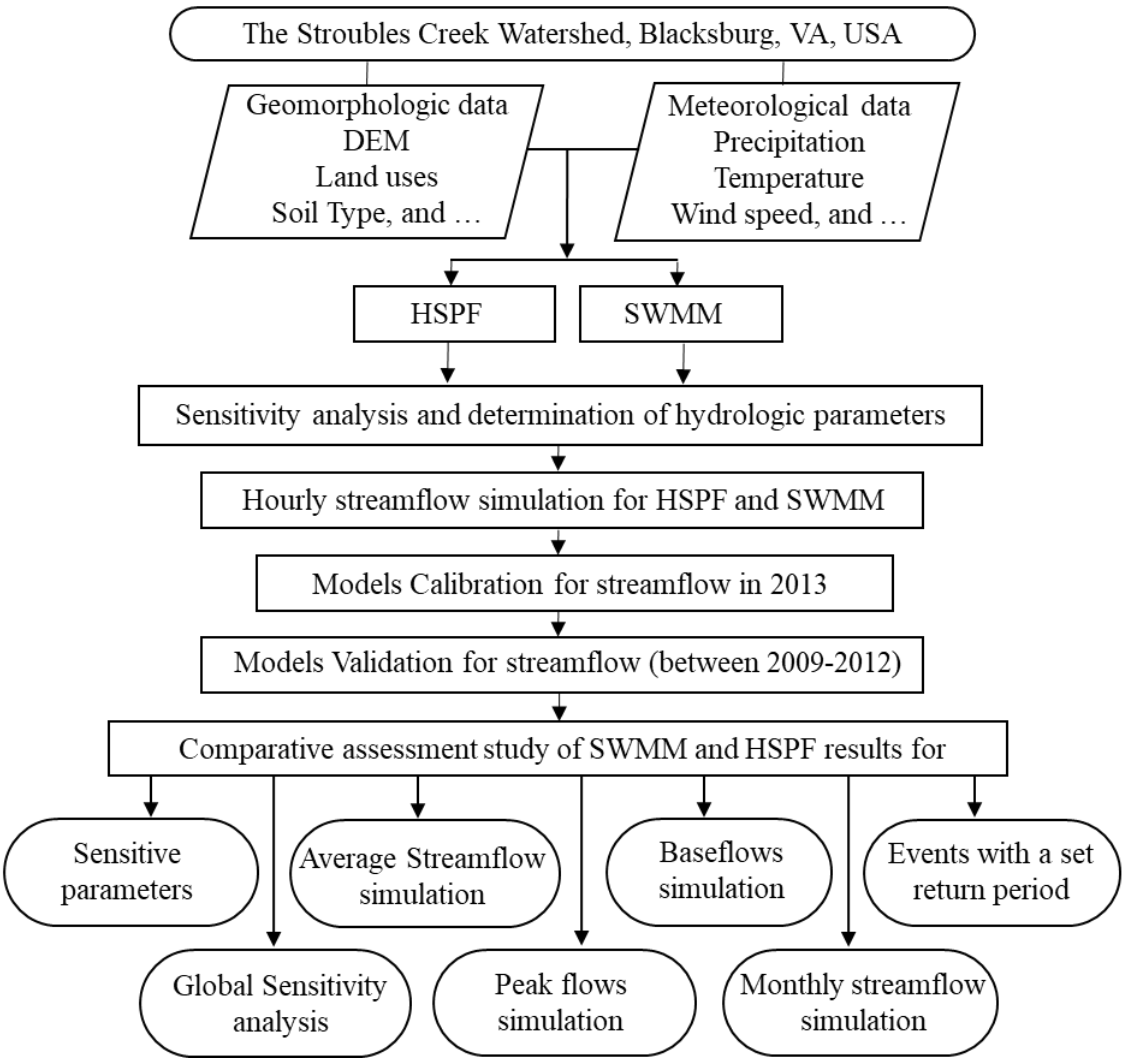

Figure 2.2. The flow chart of the application of HSPF-SWMM model.

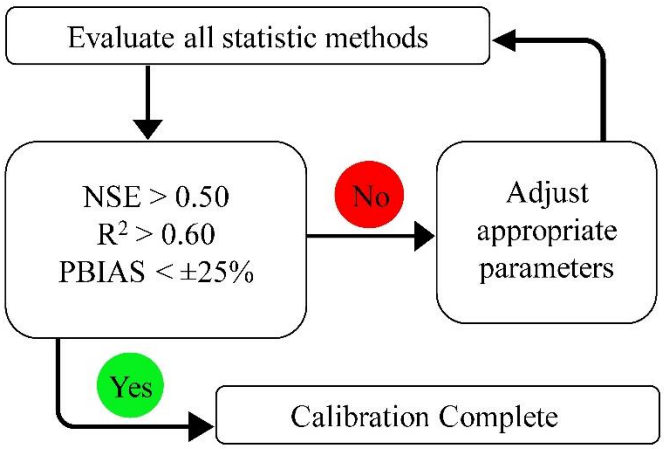

Figure 2.3. Diagram of model calibration steps.

Table 2.5. Ranking of the parameters according to the sensitivities of models output streamflow to them.

Level of sensitivity	Parameter	Sensitivity coefficient (Absolute value)
	HSPF	
High	DEEPFR	0.2100
	AGWRC	0.0860
	INFILT	0.0790
	LZSN	0.0710
	BASETP	0.0250
	UZSN	0.0091
	IRC	0.0028
	INTFW	0.0027
Low	KVARY	0.0005
	SWMM	
High	Imperviousness	0.3800
	Impervious depression storage	0.1100
	Hydraulic width	0.0300
	Pervious Manning's roughness	0.0080
Low	Conductivity	0.0070

These results are similar to previous studies (Ali and Bruen, 2016; Seong et al., 2015; Tsai et al., 2017; Xing et al., 2016). Compared to HSPF model, the groundwater parameters within SWMM including the groundwater flow coefficient, groundwater flow exponent, surface water flow exponent, and surface water flow coefficient did not substantially affect SWMM results.

2.3.2 Global sensitivity analysis results

The baseline values of model outputs i.e. average streamflow, average baseflow, and associated variation in modeled outputs are shown in Table 2.6. GSA was conducted on the most sensitive parameters in HSPF and SWMM, with the upper and lower bounds. During GSA, variability of average streamflow for SWMM was higher than that of HSPF, while variability of average baseflow for HSPF was significantly greater than that of SWMM. The most sensitive

Table 2.6. Global sensitivity analysis of HSPF and SWMM output simulation results.

Parameter	Average streamflow (m^3/s)	Average baseflow (m^3/s)
	HSPF	
Nominal	0.173	0.102
Variation of outputs	0.129 (-25%), 0.181 (+5%)	0.071 (-30%), 0.106 (+4%)
	SWMM	
Nominal	0.184	0.088
Variation of outputs	0.129 (-30%), 0.216 (+17)	0.79-10%), 0.093 (+5%)

parameters of the HSPF model were attributed to groundwater discharge, thus, altering those parameters had direct a significant effect on baseflow. This likely explains why HSPF-simulated baseflow had a larger variability during simulation than similar outputs from the corresponding SWMM model. The sensitive parameters of SWMM were primarily attributed to imperviousness and infiltration, which have a direct effect on runoff and/streamflow (Table 2.6).

2.3.3 Comparison of models without calibration

As a baseline for our study, the HSPF and SWMM models were initially run for the entire period of record, without calibration to assess the relative abilities of each model to match the observed data. Our supposition is that SWMM would perform better than HSPF without calibration for the aforementioned reasons. Parameter values for both models were left as estimated from external data sources or model defaults. NSE, R^2, and PBIAS for SWMM was 0.52, 0.58, and -22%, and for HSPF was 0.38, 0.47, and -0.42%, respectively. The results indicated that, without calibration, SWMM simulated streamflow far better than HSPF, earning an “acceptable” vs “poor” according to the metrics by Moriasi et al., (2015). This is due to the finer spatial scale of the inputs to SWMM, which are based more on the externally sourced data such as GIS and the physics of the hydrological processes which control the catchment response,

while HSPF is a process-based model that relies on many parameters which can only be determined through calibration. Thus, HSPF is not useful without calibration; whereas SWMM without calibration, while diminished somewhat, may still provide useful information. Thus, HSPF is better for watersheds with monitoring data but only limited physical information, the opposite is the case for SWMM.

2.3.4 Calibrated input parameters

The calibrated value ranges of input parameters for HSPF and SWMM models are presented in Table 2.7. The HSPF calibrated input parameters for soil and land use (LZSN, INFILT) were categorized for forest, agricultural, and urban land covers.

Table 2.7. Selected parameters of HSPF and SWMM for calibration.

Parameter	Unit	Calibrated value/ value range
	HSPF	
LZSN[1]	mm	381
LZSN[2]	mm	304
LZSN[3]	mm	254
INFILT[1]	mm/hr.	8.350
INFILT[2]	mm/hr.	7.050
INFILT[3]	mm/hr.	5.710
KVARY	1/mm	2.540
AGWRC	1/day	0.990
DEEPFR		0.300
BASETP		0.030
UZSN	mm	50.800
IRC	1/day	0.900
INTFW		5
	SWMM	
Hydraulic Width	m	72-1160
Impervious Manning roughness		0.008-0.014
Pervious Manning roughness		0.140-0.218
Imperviousness	%	7.000-68.670
Conductivity	mm/hr.	0.050-34.340

1. Forest land, 2. Agricultural land, 3. Urban land.

2.3.5 Comparison of models for average streamflow simulation

Statistical results for HSPF and SWMM model during calibration and validation periods are provided in Table 2.8. The statistical analysis results showed good agreement between the simulated and observed streamflow. The observed and simulated hydrographs of SWMM and HSPF for calibration and validation periods are shown in Figure 2.4. During the calibration and validation periods, SWMM showed slightly better agreement between simulated and observed streamflow than HSPF, based on the statistical values of NSE, R^2, and PBIAS. The positive values of PBIAS for models during validation period indicates the propensity of the models to underestimate streamflow. Since visual comparison of the models results using Figure 2.4b was hard to see, two months (i.e. December 2009, and May 2011) were separated for better visualization in a narrower data range (Figure 2.4c and d).

Scatter plots of observed and simulated streamflow in calibration and validation periods are shown in Figure 2.5. During storm events, SWMM simulated many of the stream peaks, well. The regression line slop for the HSPF calibration was less than 1.0 (Figure 2.5a), while that of

Table 2.8. Statistical results for HSPF and SWMM models during calibration and validation periods.

Parameters	Calibration	Validation	Model Performance Rating*
		HSPF	
NSE	0.66	0.51	Good / Satisfactory
R^2	0.70	0.64	Satisfactory / Satisfactory
PBIAS	-9.60%	23.40%	Good / Satisfactory
		SWMM	
NSE	0.69	0.59	Good / Satisfactory
R^2	0.76	0.74	Satisfactory / Satisfactory
PBIAS	-0.26%	18.20%	Good / Satisfactory

*First one represents performance of calibration period and second one indicates that of validation period.

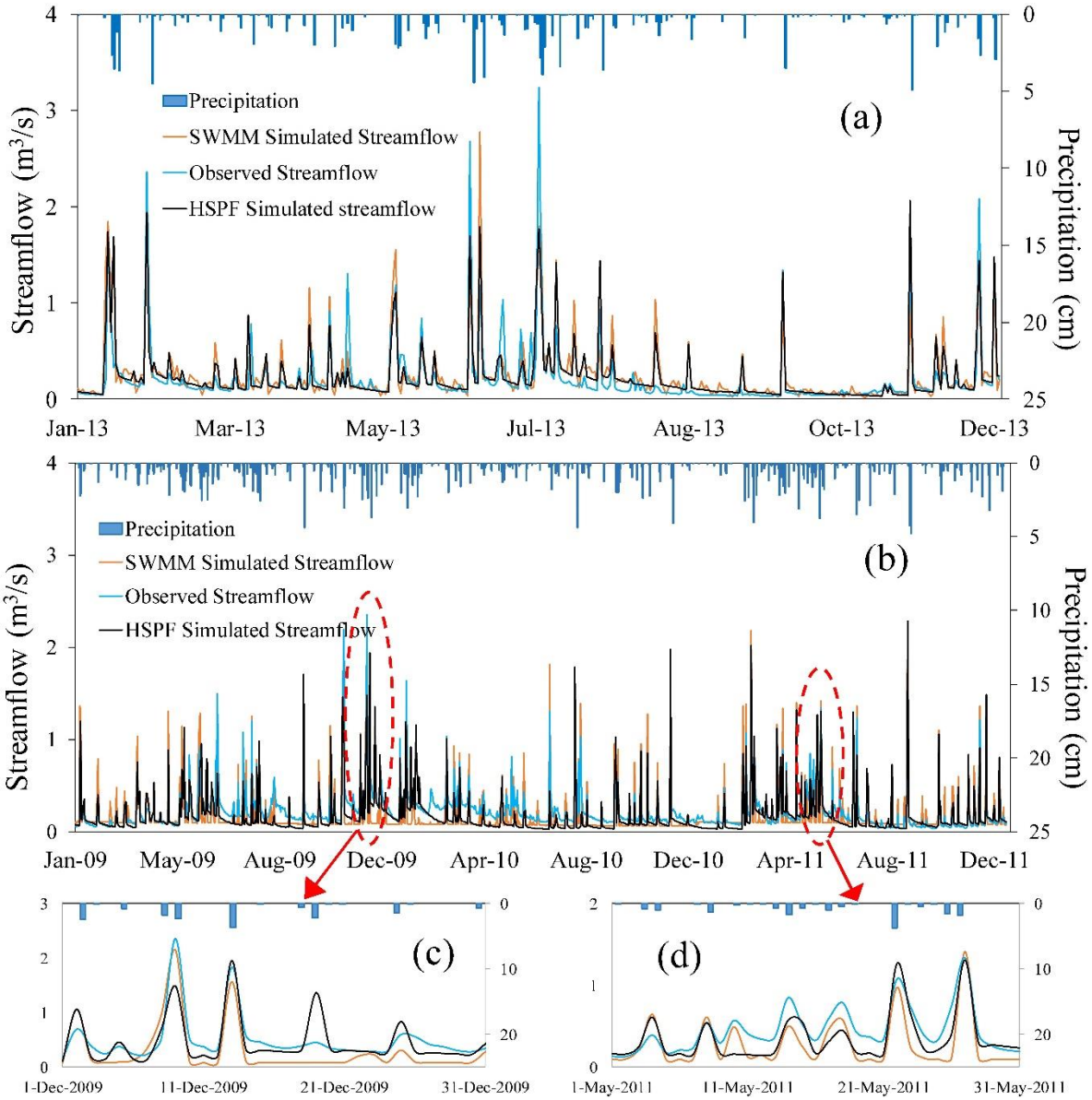

Figure 2.4. Comparison of hourly observed and simulated streamflow by HSPF and SWMM for calibration and validation periods (a) Calibration period for 2013 (b) Validation period for 2009-2011 (c) Data for December 2009 (d) Data for May 2011.

for SWMM calibration period was close to 1.0 (Figure 2.5b). The SWMM and HSPF models were not able to simulate peak flows for some of the storm events causing some errors in results (Figure 2.5a and Figure 2.5b). The slope of regression line for validation periods of SWMM and HSPF was approximately 0.7, indicating highly relative magnitude of the residuals to

standardized residuals (residuals equal to 0.0). SWMM generally overestimated high magnitude flood events (Figure 2.5d), while there was no certain pattern in simulating high magnitude flood events through HSPF (Figure 2.5c).

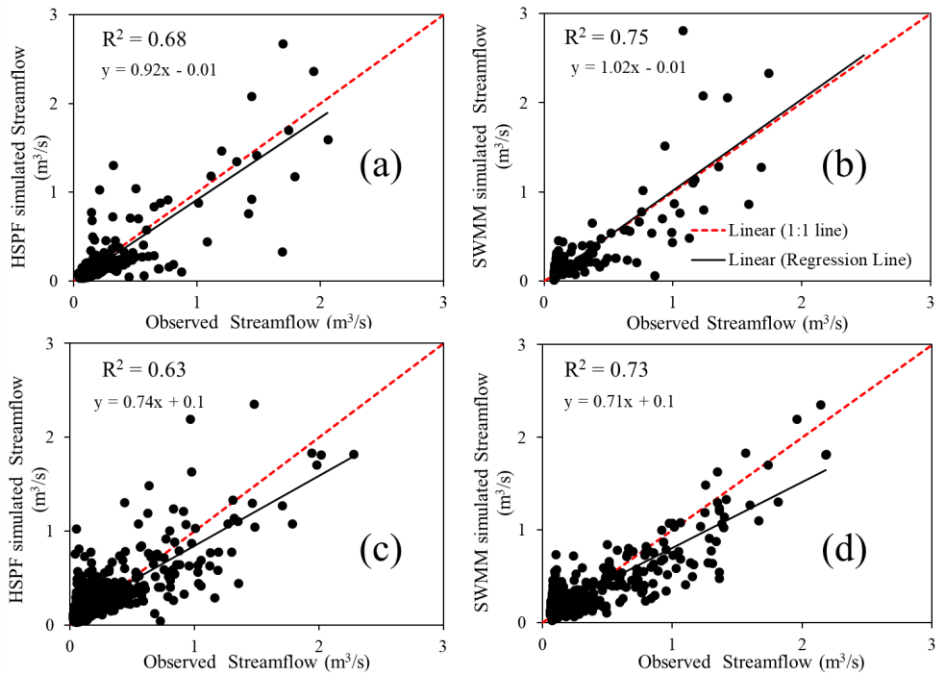

Figure 2.5. Scatter plots of observed and simulated streamflow along the 1:1 red line: (a) Calibration for HSPF; (b) Calibration for SWMM; (c) Validation for HSPF; (d) Validation for SWMM.

The residual time series of daily streamflow versus time and precipitation is provided in Figure 2.6. The HSPF streamflow simulation average error during wet periods (days with at least 0.25 cm precipitation) and dry periods were 0.002 and -0.067 m^3/s, respectively; while those of for SWMM streamflow simulation were 0.067 and -0.070 m^3/s, respectively. The aforementioned analysis indicates relatively better performance of both models in wet period than dry periods (in terms of averaged-error); HSPF appeared to be a better predictor of streamflow in wet periods rather than SWMM. During high magnitude storm events (days with

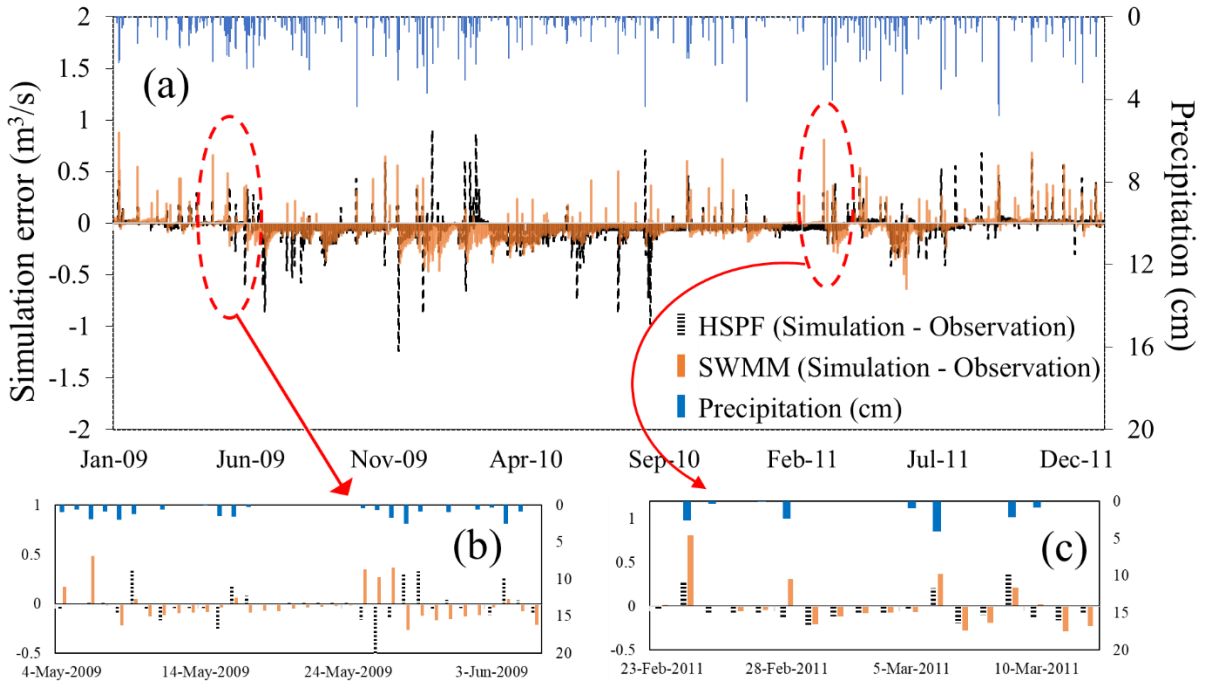

Figure 2.6. Comparison of residual error (simulated−observed) for daily streamflow simulation by HSPF and SWMM models (a) Between 2009 to 2012 (b) Between May-2009 to Jun-2009 (c) Between February-2011 to March-2011.

at least 2 cm precipitation), SWMM generally over-estimated the streamflow, while there was no specific pattern for HSPF simulation error.

Flow duration curves of simulated streamflow by HSPF and SWMM and observed streamflow are shown in Figure 2.7. Models simulated streamflow close to observed streamflow during high flows (between 0 – 10% flow exceedance Q_{10}). HSPF simulated streamflow between 10% and 90% of flow exceedance were slightly beneath observed streamflow, while SWMM over-predicted streamflow during low flow. Overall, based on a visual look, the HSPF simulation matched better in terms of flow exceedance pattern with observed streamflow compared to the SWMM simulation (Figure 2.7). The top 10% of streamflow in magnitude (according to Figure 2.7) were selected as peak flows to evaluate the capability of HSPF and SWMM in peak flow simulation (there was 81 days of high streamflow for observed dataset). The corresponding PBIAS values of SWMM and HSPF models for peak flow were -0.098 and 0.120, respectively,

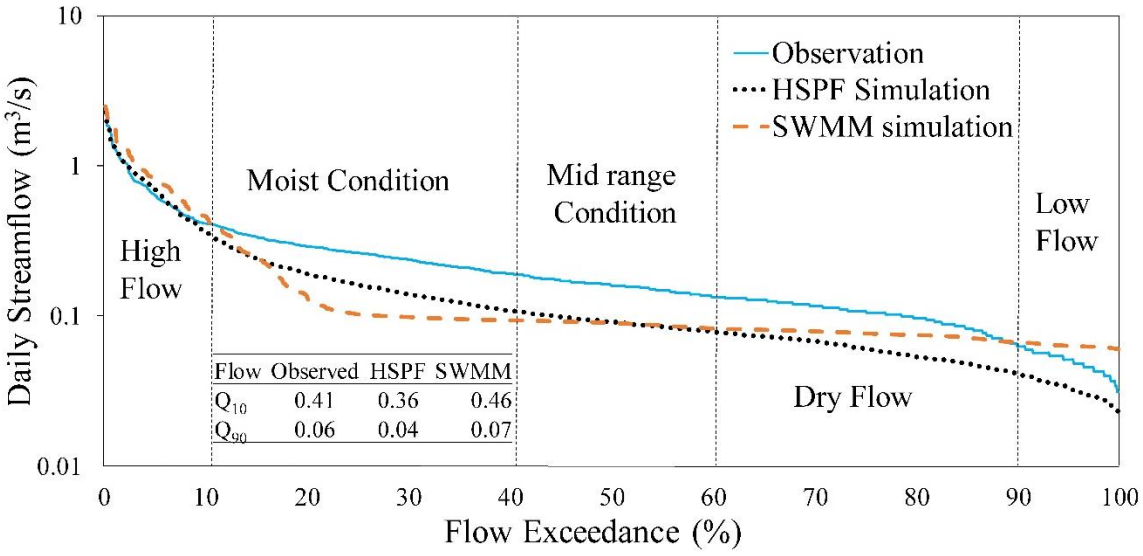

Figure 2.7. Comparison of flow duration curves of simulated streamflow by HSPF and SWMM and observed streamflow.

indicating that SWMM was better at reproducing observed peak flows. The average errors (simulated-observed) of peak flows (7.1% for SWMM and -8.1% for HSPF) confirmed the PBIAS statistical analysis results. The PBIAS values, average percent errors of models, and Figure 2.6 represent the overestimation and underestimation of peak flows by SWMM, and HSPF, respectively.

2.3.6 Comparison of models for monthly streamflow simulation

The average monthly streamflow (representing streamflow seasonally variation) indicated that HSPF and SWMM models achieve better agreement with observed streamflow during winter months (Jan and Feb), rather than summer months (May, Jun, Jul, and Aug) (Figure 2.8). The SWMM averaged-percent differences of all months resulted in -15%, while that of for HSPF was -22%, indicating SWMM is a better predictor of seasonally streamflow variation. The percentage difference between the SWMM and HSPF monthly simulated and observed streamflow ranged from 6% to 39%, and from 3% to 48%, respectively, which can be classified

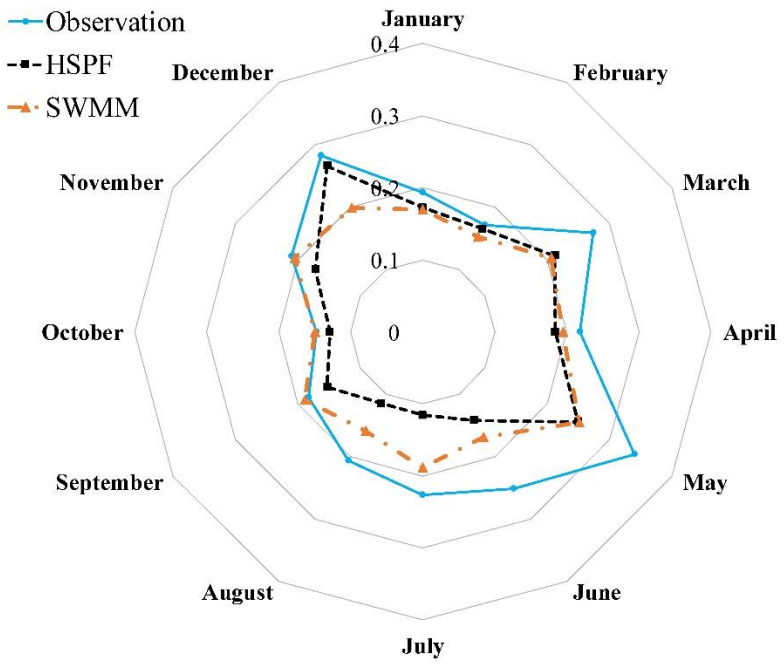

Figure 2.8. Radar plot of monthly average of observed and simulated streamflow.

as not good results for models when PBIAS is higher than 25% (Al-Abed and Al-Sharif, 2008). SWMM performed better than HSPF in summer months, while HSPF simulation matched relatively better with observed averaged-monthly streamflow in winter than SWMM. Generally, both models under-estimated the averaged-monthly streamflow between January 2009 and December 2013 (Figure 2.8). The simulation of average monthly streamflow can be beneficial for assessing impact of projected climate and land-use changes.

2.3.7 Comparison of models for baseflow simulation

The baseflow was plotted as (1) total baseflow and (2) baseflow for dry periods (DPs, or the periods in which precipitation and direct runoff are zero, and groundwater discharge is the only source of streamflow) (Figure 2.9). The observed DPs baseflows between 2009-2011 was 317 days, while that for SWMM and HSPF simulations were 693, and 199 days, respectively (Figure2. 9b); it indicates better performance of HSPF in coverage of the number of dry days

period. The PBIAS values of SWMM model for total baseflow and DPs baseflow were 0.4, and 0.61, respectively, while those of for HSPF model were 0.31 and, -0.53, respectively, indicating better performance of HSPF model in capturing observed total baseflow and DPs baseflow. Clearly, SWMM and HSPF models were not calibrated through observed baseflow; therefore, the aforementioned PBIAS calculations and the respective discussion were only based on baseflow calculation using the Eckhardt, (2008) method and the calibrated average streamflow. HSPF captured the observed baseflow pattern better than SWMM model (Figure 2.9a and b); in contrast, SWMM followed a relatively constant baseflow pattern throughout the DPs (Figure 2.9b). Our results are similar to previous study indicating that SWMM has a limitation concerning baseflow simulation during dry periods, particularly during winter months (Liu et al., 2013).

2.3.8 Comparison of model response to standard storm events

HSPF and SWMM models were compared during set return period events by running each using standard NRCS 24-hour storms. The Blacksburg, Virginia, 1-yr recurrence precipitation is 55 mm (2.2 in) (NOAA, 2016). During the monitoring period, an event (07-July, 2013) was identified and separated and are shown in Figure 2.10a. During this event, NSE, R^2, and PBIAS between observed and simulated data for SWMM were 0.51, 0.58, and %33, and for HSPF were 0.45, 0.52, and 20%, respectively. Since, the models were calibrated continuously, these results for that event can be can be considered to be acceptable (Moriasi et al., 2015). The simulated hydrograph for 1-yr recurrence interval are presented in Figure 2.10b. Results indicated that for extreme storm events SWMM simulated peak flows greater than HSPF, while HSPF simulated higher baseflow than SWMM. SWMM tended to produce more runoff than HSPF for simulated storms with recurrence interval equal or less than 10-yr (Figure 2.11).

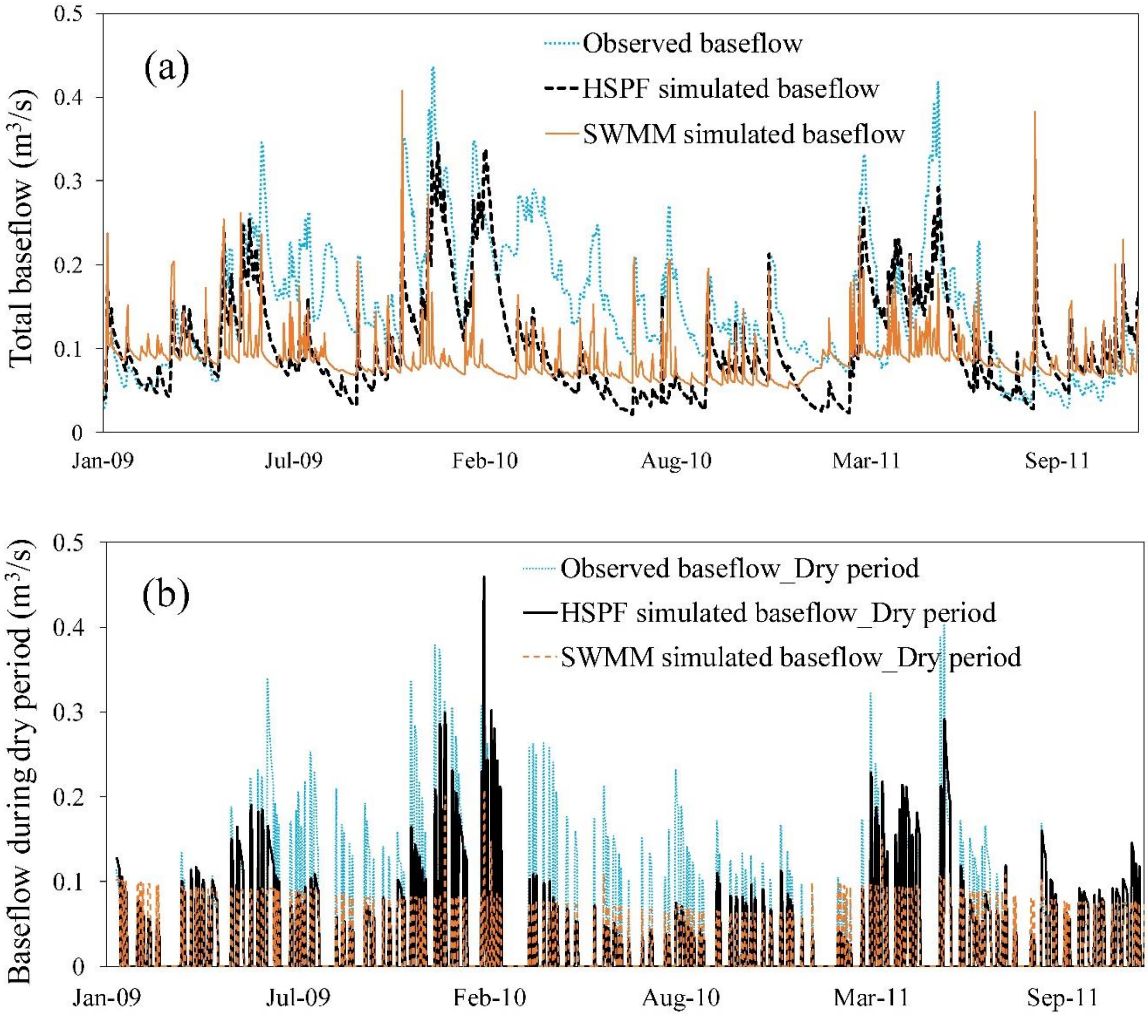

Figure 2.9. Comparison of observed, HSPF simulation, and SWMM simulation for total baseflow, and baseflow during dry periods (the periods without precipitation and direct runoff): (a) Total baseflow; (b) baseflow during dry periods.

Although the peak flows of SWMM and HSPF 24-hr. storm distribution for the 100-yr. recurrence interval were somewhat similar, a steeper receding limb was evident in the SWMM results compared to HSPF, this accounted for the difference in runoff volume.

2.4 Discussion

Statistical analysis indicated that both HSPF and SWMM models simulated streamflow adequately. However, the positive values of PBIAS for HSPF and SWMM indicated that both models had a propensity to underestimate streamflow. In addition, the performance of both

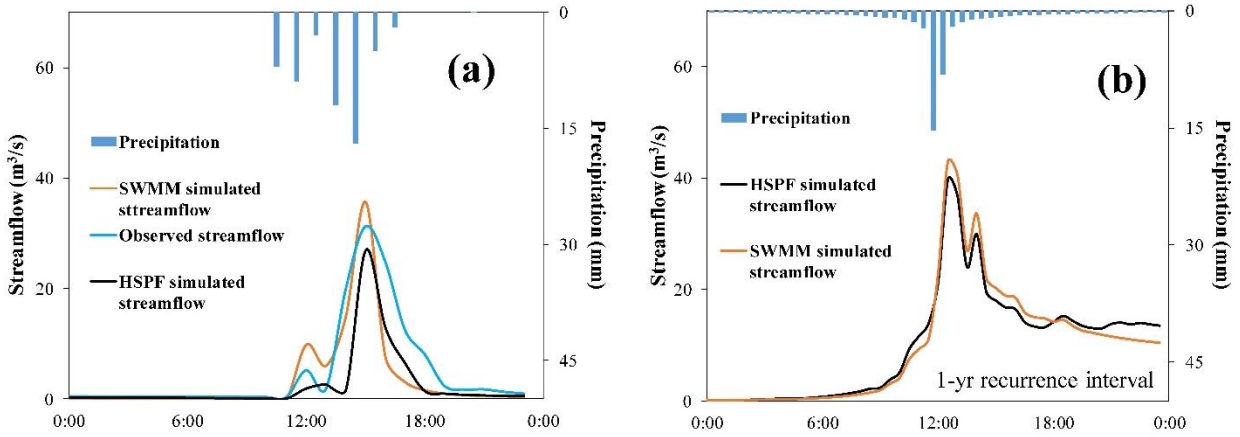

Figure 2.10. Comparison of HSPF and SWMM simulation during storm events (a) actual event in 07-July, 2013 (b) artificial 1-yr recurrence interval.

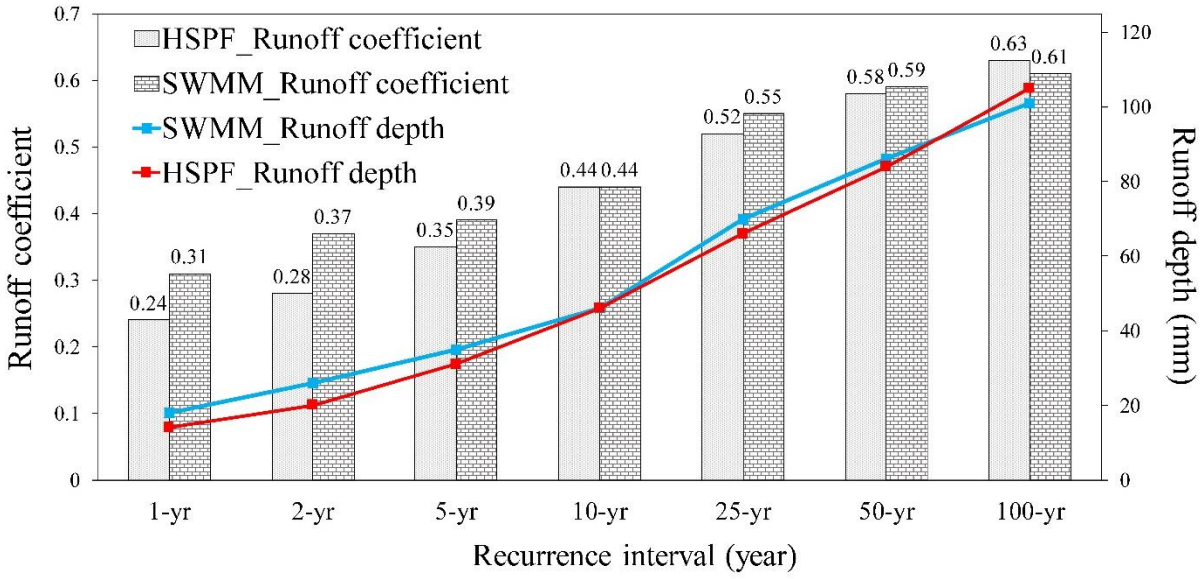

Figure 2.11. Predicted runoff depth, and runoff coefficients through SWMM and HSPF modeling tools for the case study watershed.

models for simulating streamflow during wet periods (days with at least 0.25 cm precipitation) was relatively better than dry periods. It may have been stemmed from the capability of the respective Philips and GA models, which were used for estimating infiltration rate in HSPF and SWMM, respectively. Because during storm events, these two models (i.e. Philips and GA) estimate infiltration rate relatively better than dry periods (Chahinian et al., 2005; Wilson, 2017).

During high magnitude storm events (days with at least 2 cm precipitation), SWMM generally over-estimated the streamflow, while there was no specific pattern for HSPF simulation error. HSPF appeared to be a relatively better predictor of streamflow in wet periods rather than SWMM. It may stem from the performance of GA and Philips models, which the Philips infiltration rate model represent wet periods relatively closer to reality than GA (Wilson, 2017). In terms of simulating streamflow seasonally, SWMM performed better than HSPF in summer months, while HSPF simulated streamflow better than SWMM in winter.

Generally, the Philip model estimated higher infiltration rates compared to GA (Turner, 2006; Wilson, 2017); this difference could be the main reason in the previously mentioned better performance of HSPF in capturing total baseflow and DPs baseflow in comparison to SWMM. Furthermore, HSFP and SWMM use KW and DW methods for runoff/stream routing, respectively. Previous studies indicated that DW method is more appropriate for obtaining the reference discharge and can capture high flows better than KW (Moramarco et al., 2008; Soentoro, 1991); this may be a main reason in better capturing peak flows using SWMM than HSPF. Overall, performance difference between HSPF and SWMM in simulating streamflow regime components may be prompted from different methods that the models employed for simulating infiltration rate and water routing. These methods explain why SWMM simulated streamflow better than HSPF within an urban watershed. In addition, in the absence of available monitoring data within a watershed, SWMM likely provides better results.

2.5 Conclusion

Models developed using HSPF and SWMM were used to simulate streamflow for a case study urban watershed, the Stroubles Creek watershed, in Blacksburg, Virginia. Sensitivity analysis was applied only on process-related parameters. Based on sensitivity analysis, the most

sensitive hydrologic parameters within HSPF were groundwater parameters i.e. DEEPFR and AGWRC, while for SWMM, it was the percentage of imperviousness. GSA indicated that variation for simulating baseflow-averaged for HSPF was greater than SWMM, while for simulating streamflow, the variability of SWMM outputs was greater than HSPF. SWMM performed better than HSPF sans calibration, due to the inclusion of more detailed watershed topology and SCMs. Analysis of the residual time series of daily streamflow (simulated-observed) indicated that both models performed better during wet rather than dry periods. The comparison results of models for dry periods indicated that HSPF could simulate the total baseflow and DPs baseflow better than SWMM, while the opposite was the case for peak flows. Analysis of extreme storm events was also conducted the runoff coefficient for SWMM was generally greater than HSPF for recurrence intervals of 1, 2, 5, and 10-yr, and the opposite for recurrence intervals larger than 10 years. The results of this study can assist urban watershed planners in translating their results from small scale urban watershed models where SCMs are implemented to larger, regional scale models where compliance is assessed. It can also guide in the selection of the most appropriate model for their urban watershed.

Acknowledgements

Funding for this work was provided in part by the Virginia Agricultural Experiment Station and the Hatch program of the National Institute of Food and Agriculture, U.S. Department of Agriculture. The authors appreciate the data provided by Town of Blacksburg, and StREAM Lab with W. Cully Hession and Laura Lehmann, as director and manager, respectively. The authors would like to acknowledge Karen Kline and Adil Godrej (Virginia Tech), and Robert Burgholzer (Virginia Department of Environmental Quality) for their helpful comments.

2.6 References for Chapter 2

Al-Abed, N., Al-Sharif, M., 2008. Hydrological modeling of Zarqa River Basin - Jordan using the hydrological simulation program - FORTRAN (HSPF) model. Water Resour. Manag. 22, 1203–1220. doi:10.1007/s11269-007-9221-9

Alamdari, N., Sample, D., Steinberg, P., Ross, A., Easton, Z., 2017. Assessing the effects of climate change on water quantity and quality in an urban watershed using a calibrated stormwater model. Water 9, 464. doi:10.3390/w9070464

Ali, I., Bruen, M., 2016. Methodology and Application of the Combined SWAT-HSPF Model. Environ. Process. 3, 645–661. doi:10.1007/s40710-016-0167-x

Bennett, N.D., Croke, B.F.W., Guariso, G., Guillaume, J.H.A., Hamilton, S.H., Jakeman, A.J., Marsili-Libelli, S., Newham, L.T.H., Norton, J.P., Perrin, C., Pierce, S.A., Robson, B., Seppelt, R., Voinov, A.A., Fath, B.D., Andreassian, V., 2013. Characterising performance of environmental models. Environ. Model. Softw. 40, 1–20. doi:10.1016/J.ENVSOFT.2012.09.011

Berndt, M.E., Rutelonis, W., Regan, C.P., 2016. A comparison of results from a hydrologic transport model (HSPF) with distributions of sulfate and mercury in a mine-impacted watershed in northeastern Minnesota. J. Environ. Manage. 181, 74–79. doi:10.1016/j.jenvman.2016.05.067

Bicknell, B.R., Imhoff, J.., Kittle Jr, J.., Jobes, T.., Donigian Jr, A.., Johanson, R., 2001. Hydrological simulation program–fortran: HSPF, version 12 user's manual. AQUA TERRA Consult. Mt. View, Calif.

Borah, D.K., Ahmadisharaf, E., Padmanabhan, G., Imen, S., Mohamoud, Y.M., 2019. Watershed Models for Development and Implementation of Total Maximum Daily Loads. J. Hydrol. Eng. 24, 03118001. doi:10.1061/(ASCE)HE.1943-5584.0001724

Castanedo, F., Patricio, M. a, Molina, J.M., 2006. Evolutionary computation technique applied to HSPF model calibration of a Spanish watershed BT - 7th International Conference on Intelligent Data Engineering and Automated Learning, IDEAL 2006, September 20, 2006 - September 23, 2006 4224 LNCS, 216–223.

Chahinian, N., Moussa, R., Andrieux, P., Voltz, M., 2005. Comparison of infiltration models to simulate flood events at the field scale. J. Hydrol. 306, 191–214. doi:10.1016/j.jhydrol.2004.09.009

Chen, J., Theller, L., Gitau, M.W., Engel, B.A., Harbor, J.M., 2017. Urbanization impacts on surface runoff of the contiguous United States. J. Environ. Manage. 187, 470–481. doi:10.1016/J.JENVMAN.2016.11.017

Choi, W., Pan, F., Wu, C., 2017. Impacts of climate change and urban growth on the streamflow of the Milwaukee River (Wisconsin, USA). Reg. Environ. Chang. 17, 889–899. doi:10.1007/s10113-016-1083-3

Daghighi, A., 2017. Harmful Algae Bloom Prediction Model for Western Lake Erie Using Stepwise Multiple Regression and Genetic Programming.

Dobler, C., Pappenberger, F., 2013. Global sensitivity analyses for a complex hydrological model applied in an alpine watershed. Hydrol. Process. 27, 3922–3940. doi:10.1002/hyp.9520

Duda, P.B., Hummel, P.R., Donigian, A.S.J., Imhoff, J.C., 2012. Basins/HSPF: model use, calibration, and validation. Trans. Asabe 55, 1523–1547. doi:10.13031/2013.42261

Dudula, J., Randhir, T.O., 2016. Modeling the influence of climate change on watershed systems: Adaptation through targeted practices. J. Hydrol. 541, 703–713. doi:10.1016/j.jhydrol.2016.07.020

Eckhardt, K., 2008. A comparison of baseflow indices, which were calculated with seven different baseflow separation methods. J. Hydrol. 352, 168–173. doi:10.1016/j.jhydrol.2008.01.005

Fonseca, A., Botelho, C., Boaventura, R.A.R., Vilar, V.J.P., 2014. Integrated hydrological and water quality model for river management: A case study on Lena River. Sci. Total Environ. 485–486, 474–489. doi:10.1016/j.scitotenv.2014.03.111

Gebremariam, S.Y., Martin, J.F., DeMarchi, C., Bosch, N.S., Confesor, R., Ludsin, S.A., 2014. A comprehensive approach to evaluating watershed models for predicting river flow regimes critical to downstream ecosystem services. Environ. Model. Softw. 61, 121–134. doi:10.1016/j.envsoft.2014.07.004

Golden, H.E., Hoghooghi, N., 2017. Green infrastructure and its catchment-scale effects: an emerging science. Wiley Interdiscip. Rev. Water 5, e1254. doi:10.1002/wat2.1254

Guan, M., Sillanpää, N., Koivusalo, H., 2015. Modelling and assessment of hydrological changes in a developing urban catchment. Hydrol. Process. 29, 2880–2894. doi:10.1002/hyp.10410

Gupta, H.V., Sorooshian, S., Yapo, P.O., 1999. Status of Automatic Calibration for Hydrologic Models: Comparison with Multilevel Expert Calibration. J. Hydrol. Eng. 4, 135–143. doi:10.1061/(ASCE)1084-0699(1999)4:2(135)

He, M., Hogue, T.S., 2012. Integrating hydrologic modeling and land use projections for evaluation of hydrologic response and regional water supply impacts in semi-arid environments. Environ. Earth Sci. 65, 1671–1685. doi:10.1007/s12665-011-1144-3

Hester, E.T., Bauman, K.S., 2013. Stream and retention pond thermal response to heated summer runoff from urban impervious surfaces. J. Am. Water Resour. Assoc. 49, 328–342. doi:10.1111/jawr.12019

Hofmeister, K.L., Cianfrani, C.M., Hession, W.C., 2015. Complexities in the stream temperature regime of a small mixed-use watershed, Blacksburg, VA. Ecol. Eng. 78, 101–111. doi:10.1016/J.ECOLENG.2014.05.019

Huber, W.C., Dickinson, R.E., 1988. Storm Water Management Model , Version 4 : User's Manual 720. doi:EPA/600/3-88/001a

Huiliang, W., Zening, W., Caihong, H., Xinzhong, D., 2015. Water and nonpoint source pollution estimation in the watershed with limited data availability based on hydrological simulation and regression model. Environ. Sci. Pollut. Res. 22, 14095–14103.

doi:10.1007/s11356-015-4450-6

James, L., Burges, S., 1982. Selection, calibration, and testing of hydrologic models, Hydrologic Modeling of Small Watersheds CT Haan, HP Johnson, DL Brakensiek, 437–472,. Joseph, Mich.

James, W., Rossman, L.A., James, W.R.., 2010. User's guide to SWMM5.

Janke, B.D., Herb, W.R., Mohseni, O., Stefan, H.G., 2013. Case study of simulation of heat export by rainfall runoff from a small urban watershed using MINUHET. J. Hydrol. Eng. 18, 995–1006.

Javaheri, A., Babbar-Sebens, M., Alexander, J., Bartholomew, J., Hallett, S., 2018. Global sensitivity analysis of water age and temperature for informing salmonid disease management. J. Hydrol. 561, 89–97. doi:10.1016/J.JHYDROL.2018.02.053

Ketabchy, M., 2018. Thermal Evaluation of an Urbanized Watershed using SWMM and MINUHET : a Case Study of the Stroubles Creek Watershed , Blacksburg , VA (in na) 1–117. doi:https://doi.org/10.13140/RG.2.2. 26726.47688

Ketabchy, M., Sample, D.J., Wynn-Thompson, T., Nayeb Yazdi, M., 2018. Thermal evaluation of urbanization using a hybrid approach. J. Environ. Manage. 226, 457–475. doi:10.1016/J.JENVMAN.2018.08.016

Ketabchy, M., Sample, D.J., Wynn-Thompson, T., Yazdi, M.N., 2019. Simulation of watershed-scale practices for mitigating stream thermal pollution due to urbanization. Sci. Total Environ. 671, 215–231. doi:10.1016/J.SCITOTENV.2019.03.248

Kyoung, J.L., Engel, B.A., Tang, Z., Choi, J., Kim, K.S., Muthukrishnan, S., Tripathy, D., 2005. Automated Web GIS based hydrograph analysis tool, WHAT. J. Am. Water Resour. Assoc. 41, 1407–1416. doi:10.1111/j.1752-1688.2005.tb03808.x

Lacher, I.L., Ahmadisharaf, E., Fergus, C., Akre, T., Mcshea, W.J., Benham, B.L., Kline, K.S., 2019. Scale-dependent impacts of urban and agricultural land use on nutrients, sediment, and runoff. Sci. Total Environ. 652, 611–622. doi:10.1016/J.SCITOTENV.2018.09.370

Lee, S.-B., Yoon, C.-G., Jung, K.W., Hwang, H.S., 2010. Comparative evaluation of runoff and water quality using HSPF and SWMM. Water Sci. Technol. 62, 1401. doi:10.2166/wst.2010.302

Li, H., Harvey, J.T., Holland, T.J., Kayhanian, M., 2013. Corrigendum: The use of reflective and permeable pavements as a potential practice for heat island mitigation and stormwater management. Environ. Res. Lett. 8, 049501. doi:10.1088/1748-9326/8/4/049501

Liao, H., Krometis, L.-A., Kline, K., Hession, W., 2015. Long-Term impacts of bacteria–sediment interactions in watershed-scale microbial fate and transport modeling. J. Environ. Qual. 44, 1483–1490. doi:10.2134/jeq2015.03.0169

Linsley, R.K., Kohler, M.A., Paulhus, J., 1975. HYDROLOGY FOR ENGINEERS.

Liu, A., Goonetilleke, A., Egodawatta, P., 2015. Role of Rainfall and Catchment Characteristicson Urban Stormwater Quality.

Liu, G., Schwartz, F.W., Kim, Y., 2013. Complex baseflow in urban streams: An example from central Ohio, USA. Environ. Earth Sci. 70, 3005–3014. doi:10.1007/s12665-013-2358-3

Liu, J., Shen, Z., Chen, L., 2018. Assessing how spatial variations of land use pattern affect water quality across a typical urbanized watershed in Beijing, China. Landsc. Urban Plan. 176, 51–63. doi:10.1016/j.landurbplan.2018.04.006

Locatelli, L., Mark, O., Mikkelsen, P.S., Arnbjerg-Nielsen, K., Deletic, A., Roldin, M., Binning, P.J., 2017. Hydrologic impact of urbanization with extensive stormwater infiltration. J. Hydrol. 544, 524–537. doi:10.1016/J.JHYDROL.2016.11.030

Lott, D.A., Stewart, M.T., 2016. Base flow separation: A comparison of analytical and mass balance methods. J. Hydrol. 535, 525–533. doi:10.1016/j.jhydrol.2016.01.063

Lott, D.A., Stewart, M.T., 2013. A Power Function Method for Estimating Base Flow. GroundWater 51, 442–451. doi:10.1111/j.1745-6584.2012.00980.x

Lucas, W.C., Sample, D.J., 2015. Reducing combined sewer overflows by using outlet controls for Green Stormwater Infrastructure: Case study in Richmond, Virginia. J. Hydrol. 520, 473–488. doi:10.1016/j.jhydrol.2014.10.029

Luo, K., Hu, X., He, Q., Wu, Z., Cheng, H., Hu, Z., Mazumder, A., 2018. Impacts of rapid urbanization on the water quality and macroinvertebrate communities of streams: A case study in Liangjiang New Area, China. Sci. Total Environ. 621, 1601–1614. doi:10.1016/J.SCITOTENV.2017.10.068

Macro, K., Matott, L.S., Rabideau, A., Ghodsi, S.H., Zhu, Z., 2019. OSTRICH-SWMM: A new multi-objective optimization tool for green infrastructure planning with SWMM. Environ. Model. Softw. 113, 42–47. doi:10.1016/J.ENVSOFT.2018.12.004

McCargo, J.W., Peterson, J.T., 2010. An evaluation of the influence of seasonal base flow and geomorphic stream characteristics on coastal plain stream fish assemblages. Trans. Am. Fish. Soc. 139, 29–48. doi:10.1577/T09-036.1

Miller, M.P., Buto, S.G., Susong, D.D., Rumsey, C.A., 2016. The importance of base flow in sustaining surface water flow in the Upper Colorado River Basin. Water Resour. Res. 52, 3547–3562. doi:10.1002/2015WR017963

Mohamoud, Y.M., Parmar, R., Wolfe, K., 2010. Modeling Best Management Practices (BMPs) with HSPF, in: Watershed Management 2010. American Society of Civil Engineers, Reston, VA, pp. 892–898. doi:10.1061/41143(394)81

Mohamoud, Y.M., Prieto, L.M., 2012. Effect of temporal and spatial rainfall resolution on hspf predictive performance and parameter estimation. J. Hydrol. Eng. 17, 377–388. doi:10.1061/(ASCE)HE.1943-5584.0000457

Moore, M.F., Vasconcelos, J.G., Zech, W.C., 2017. Modeling highway stormwater runoff and groundwater table variations with SWMM and GSSHA. J. Hydrol. Eng. 22, 04017025. doi:10.1061/(ASCE)HE.1943-5584.0001537

Moramarco, T., Pandolfo, C., Singh, V.P., 2008. Accuracy of kinematic wave approximation for flood routing. II. Unsteady analysis. J. Hydrol. Eng. 13, 1089–1096.

doi:10.1061/(ASCE)1084-0699(2008)13:11(1089)

Moriasi, D.N., Arnold, J.G., Van Liew, M.W., Binger, R.L., Harmel, R.D., Veith, T.L., 2007. Model evaluation guidelines for systematic quantification of accuracy in watershed simulations. Trans. ASABE 50, 885–900. doi:10.13031/2013.23153

Moriasi, D.N., Gitau, M.W., Pai, N., Daggupati, P., 2015. Hydrologic and Water Quality Models: Performance Measures and Evaluation Criteria. Trans. ASABE 58, 1763–1785. doi:10.13031/trans.58.10715

Mostaghimi, S., Benham, B., Brannan, K., Dillaha, T.A., Wagner, R., Wynn, J., G., Y., Zeckoski, R., 2003. Benthic TMDL for Stroubles Creek in Montgomery County, Virginia.

Multi-Resolution Land Use Consortium, 2011. Multi-Resolution Land Use Consortium National Land Cover Database (NLCD). doi:https://doi.org/http://www.mrlc.gov/nlcd11_data.php

Nash, J.E., Sutcliffe, J.V., 1970. River flow forecasting through conceptual models part I — A discussion of principles. J. Hydrol. 10, 282–290. doi:10.1016/0022-1694(70)90255-6

Nasr, A., Bruen, M., Jordan, P., Moles, R., Kiely, G., Byrne, P., 2007. A comparison of SWAT, HSPF and SHETRAN/GOPC for modelling phosphorus export from three catchments in Ireland. Water Res. 41, 1065–1073. doi:10.1016/j.watres.2006.11.026

Nayeb Yazdi, M., Arhami, M., Delavarrafiee, M., Ketabchy, M., 2019a. Developing air exchange rate models by evaluating vehicle in-cabin air pollutant exposures in a highway and tunnel setting: case study of Tehran, Iran. Environ. Sci. Pollut. Res. 1, 501–513. doi:10.1007/s11356-018-3611-9

Nayeb Yazdi, M., Sample, D.J., Scott, D., Owen, J.S., Ketabchy, M., Alamdari, N., 2019b. Water quality characterization of storm and irrigation runoff from a container nursery. Sci. Total Environ. 667, 166–178. doi:10.1016/j.scitotenv.2019.02.326

Neff, B.P., Day, S.M., Piggott, A.R., Fuller, L.M., 2005. Base flow in the Great Lakes basin. U.S. Geol. Surv. Sci. Investig. Rep. 32.

Niazi, M., Nietch, C., Maghrebi, M., 2017. Stormwater management model: Performance review and gap analysis, Journal of Sustainable Water in the Built Environment. doi:10.1061/JSWBAY.0000817.

NOAA, 2016. Precipitation Frequency Data Server [WWW Document]. Natl. Ocean. Atmos. Adm. URL https://hdsc.nws.noaa.gov/hdsc/pfds

NRCS, 2015. Storm Rainfall Depthand Distribution, Natural Resources Conservation Service.

NRCS, 2007. National Engineering Handbook Chapter 7 Hydrologic Soil Groups, United States Department of Agriculture. doi:https://directives.sc.egov.usda.gov/OpenNonWebContent.aspx?content=17757.wba

NRCS, 1999a. SSURGO. doi:https://websoilsurvey.sc.egov.usda.gov/App/HomePage.htm

NRCS, 1999b. Natural Resources Conservation Service. [WWW Document]. United States Dep. Agric. URL https://websoilsurvey.sc.egov.usda.gov/App/HomePage.htm

Palla, A., Gnecco, I., 2015. Hydrologic modeling of Low Impact Development systems at the urban catchment scale. doi:10.1016/j.jhydrol.2015.06.050

Park, D., Loftis, J.C., Roesner, L.A., 2011. Performance Modeling of Storm Water Best Management Practices with Uncertainty Analysis. J. Hydrol. Eng. 16, 332–344. doi:10.1061/(ASCE)HE.1943-5584.0000323

Qiu, J., Shen, Z., Wei, G., Wang, G., Xie, H., Lv, G., 2018. A systematic assessment of watershed-scale nonpoint source pollution during rainfall-runoff events in the Miyun Reservoir watershed. Environ. Sci. Pollut. Res. 25, 6514–6531. doi:10.1007/s11356-017-0946-6

Rai, P.K., Chahar, B.R., Dhanya, C.T., 2017. GIS-based SWMM model for simulating the catchment response to flood events. Hydrol. Res. 48, 384–394. doi:10.2166/nh.2016.260

Roodsari, B.K., Chandler, D.G., 2017. Distribution of surface imperviousness in small urban catchments predicts runoff peak flows and stream flashiness. Hydrol. Process. 31, 2990–3002. doi:10.1002/hyp.11230

Rosa, D.J., Clausen, J.C., Dietz, M.E., 2015. Calibration and Verification of SWMM for Low Impact Development. JAWRA J. Am. Water Resour. Assoc. 51, 746–757. doi:10.1111/jawr.12272

Rosburg, T.T., Nelson, P.A., Bledsoe, B.P., 2017. Effects of Urbanization on Flow Duration and Stream Flashiness: A Case Study of Puget Sound Streams, Western Washington, USA. JAWRA J. Am. Water Resour. Assoc. 53, 493–507. doi:10.1111/1752-1688.12511

Rossman, L.A., 2010. Storm water management model user's manual, version 5.0. Cincinnati: National Risk Management Research Laboratory, Office of Research and Development, US Environmental Protection Agency.

Rumsey, C.A., Miller, M.P., Susong, D.D., Tillman, F.D., Anning, D.W., 2015. Regional scale estimates of baseflow and factors influencing baseflow in the Upper Colorado River Basin. J. Hydrol. Reg. Stud. 4, 91–107. doi:10.1016/J.EJRH.2015.04.008

Seong, C., Herand, Y., Benham, B.L., 2015. Automatic calibration tool for hydrologic simulation program-FORTRAN using a shuffled complex evolution algorithm. Water (Switzerland) 7, 503–527. doi:10.3390/w7020503

Shenk, G.W., Wu, J., Linker, L.C., 2012. Enhanced HSPF Model Structure for Chesapeake Bay Watershed Simulation. J. Environ. Eng. 138, 949–957. doi:10.1061/(ASCE)EE.1943-7870.0000555

Singh, J., Knapp, H.V., Arnold, J.G., Demissie, M., 2005. Hydrological Modeling of The Iroquois River Watershed Using HSPF and SWAT. J. Am. Water Resour. Assoc. 41, 343–360. doi:10.1111/j.1752-1688.2005.tb03740.x

Soentoro, E., 1991. Comparison of flood routing methods. Doctoral dissertation, University of British Columbia. doi:http://resolver.ebscohost.com/openurl?url_ver=Z39.88-2004&rft_val_fmt=info:ofi/fmt:kev:mtx:journal&__char_set=utf8&rft_id=info:doi/10.14288/1.0050451&rfr_id=info:sid/libx%3Avirginiatech&rft.genre=article

Stern, M., Flint, L., Minear, J., Flint, A., Wright, S., 2016. Characterizing changes in streamflow and sediment supply in the sacramento River Basin, California, using Hydrological Simulation Program-FORTRAN (HSPF). Water (Switzerland) 8. doi:10.3390/w8100432

Stoner, E.W., Arrington, D.A., 2017. Nutrient inputs from an urbanized landscape may drive water quality degradation. Sustain. Water Qual. Ecol. 9–10, 136–150. doi:10.1016/J.SWAQE.2017.11.001

StREAM Lab, 2009. Stream Research, Education, and Management Lab (StREAM Lab), Virginia Tech. doi:https://www.bse.vt.edu/research/facilities/StREAM_Lab.html)

Tong, S.T.Y., Sun, Y., Ranatunga, T., He, J., Yang, Y.J., 2012. Predicting plausible impacts of sets of climate and land use change scenarios on water resources. Appl. Geogr. 32, 477–489. doi:10.1016/J.APGEOG.2011.06.014

Town of Blacksburg, 2015. Blacksburg GIS Database. doi:http://www.gis.lib.vt.edu/gis_data/Blacksburg/GISPage.html.

Tsai, L.-Y., Chen, C.-F., Fan, C.-H., Lin, J.-Y., 2017. Using the HSPF and SWMM Models in a High Pervious Watershed and Estimating Their Parameter Sensitivity. Water 9, 780. doi:10.3390/w9100780

Turner, E.R., 2006. Comparison of Infiltration Equations and T heir Field Validation With Rainfall Simulation 202.

U.S.EPA, 2014. HSPF BMP Web Toolkit: Ecosystems Research Division [WWW Document]. Environ. Prot. Agency. URL http://www.epa.gov/athens/research/modeling/HSPFWebTools/

USEPA, 2018. Storm Water Management Model (SWMM) [WWW Document]. URL https://www.epa.gov/water-research/storm-water-management-model-swmm (accessed 1.11.19).

USEPA, 2014. Hydrological Simulation Program - FORTRAN (HSPF).

USEPA, 2010. Chesapeake Bay Phase 5 Community Watershed Model [WWW Document]. U.S Environ. Prot. Agency.

Whitney, J.W., Glancy, P.A., Buckingham, S.E., Ehrenberg, A.C., 2015. Effects of rapid urbanization on streamflow, erosion, and sedimentation in a desert stream in the American Southwest. Anthropocene 10, 29–42. doi:10.1016/J.ANCENE.2015.09.002

Wilson, R.L., 2017. Comparing Infiltration Models to Estimate Infiltration Potential at Henry V Events. Portland State University. doi:http://pdxscholar.library.pdx.edu/cgi/viewcontent.cgi?article=1514&context=honorstheses

Xing, W., Li, P., Cao, S., Gan, L., Liu, F., Zuo, J., 2016. Layout effects and optimization of runoff storage and filtration facilities based on SWMM simulation in a demonstration area. Water Sci. Eng. 9, 115–124. doi:http://dx.doi.org/10.1016/j.wse.2016.06.007

Xu, Z., Godrej, A.N., Grizzard, T.J., 2007. The hydrological calibration and validation of a

complexly-linked watershed-reservoir model for the Occoquan watershed, Virginia. J. Hydrol. 345, 167–183. doi:10.1016/j.jhydrol.2007.07.015

Yousefi, S., Moradi, H.R., Keesstra, S., Pourghasemi, H.R., Navratil, O., Hooke, J., 2017. Effects of urbanization on river morphology of the Talar River, Mazandarn Province, Iran. Geocarto Int. 1–17. doi:10.1080/10106049.2017.1386722

Zope, P.E., Eldho, T.I., Jothiprakash, V., 2016. Impacts of land use–land cover change and urbanization on flooding: A case study of Oshiwara River Basin in Mumbai, India. CATENA 145, 142–154. doi:10.1016/J.CATENA.2016.06.009

Chapter 3. The effect of land use characteristics on urban stormwater quality and estimating watershed pollutant loads

Mohammad Nayeb Yazdi, David J. Sample, Durelle Scott

Submitted: Planned August 2020
To: *Environmental Pollution*
Status: Draft

Abstract

Urban development leads to higher runoff and nutrient loads transported during storm events to receiving waters. We quantified total nitrogen (TN), total phosphorus (TP) and total suspended solids (TSS) from 30 storm events within six urban land uses (i.e. commercial, industrial, transportation, open space, low density residential, and high density residential) in Virginia Beach during a 1-year period. We found median event mean concentrations (EMCs) within Virginia Beach for TSS, TP, and TN were 30 (19 – 34 $mg \cdot L^{-1}$), 0.31 (0.26 – 0.31 $mg \cdot L^{-1}$), and 0.94 (0.73 – 1.25 $mg \cdot L^{-1}$), respectively. Results indicated that the TSS EMCs from open space and industrial land uses were significantly greater than others, and there was a positive direct relationship between level of TN and imperviousness area, and level of TP and turf cover. We found that the amount and intensity of rainfall were correlated with TSS levels in runoff from all urban land uses. In addition, statistical results indicated that there was no significant difference between results of commercial and transportation land uses for TSS, TN and TP. Based upon our dataset and analysis, we developed a general equation relating pollutant load as a function of rainfall depth, and verified the equation with a 10-year simulation using the Storm Water Management Model (SWMM) simulation (2009–2019), to estimate pollutant loads for

TSS, TP, and TN from various land uses. Results indicated that average pollutant loads within urban coastal areas for TSS, TP, and TN were as 0.86, 0.03, and 0.01 $kg \cdot ha^{-1} \cdot cm^{-1}$, respectively.

3.1 Introduction

Most of the southeast U.S. lies within the Coastal Plain physiographic province, an area of approximately 1.2 million km^2 (Hupp, 2000). In the U.S., from 1970 to 2010, the population within Coastal Plain increased by almost 40% to 34.8 million, and is projected to increase by an additional 8% by 2020 (NOAA, 2017). To accommodate this growing population, coastal cities of the southeastern U.S. are expected to nearly double in urban landcover over the next 50 years (Terando et al., 2014). Urban development needed to accommodate this growing population alters watershed characteristics by transforming green areas into impervious surfaces for roads, roofs and parking lots, and transforming small creeks and streams into stormwater conveyance channels, resulting in increased urban runoff volume and peak flows, and decreasing the time to peak runoff (Chen et al., 2017; Locatelli et al., 2017; Rosburg et al., 2017). As runoff and subsurface travels across urban lands, sediments and nutrient are picked up and transported from landscapes to urban streams (Bettez and Groffman, 2012; Gold et al., 2017). The increased runoff and pollutant loads negatively impact streams, causing channel and bed erosion and loss of habitat (Russell et al., 2018). Understanding the factors that affect the fate and transport of pollutants from urban catchments is a critical first step in attempting to mitigate the effects of urbanization. Previous studies have shown that urban runoff is elevated in sediment and nutrients compared with runoff from forest areas. For example, event mean concentrations (EMCs) of total suspended solids (TSS) from urban watersheds ranges from 80 to 260, far greater than the range of EMC from forested lands, 8 to11 $mg \cdot L^{-1}$ (Badruzzaman et al., 2012; Li et al., 2015;

Métadier and Bertrand-Krajewski, 2012; Schiff et al., 2016; Sun et al., 2015; Toor et al., 2017; Yoon et al., 2010).

Coastal waters in the southeastern U.S. are particularly vulnerable to human impacts due to the proximity of urban areas and hydrologic connection of the Coastal Plain to receiving waters (Beckert et al., 2011; Phillips and Slattery, 2006). Further, water tables in coastal areas are high, decreasing soil infiltration in coastal area and increasing surface pollutant transport during storm events (Basha, 2011; Munõz-Carpena et al., 2018). The City of Virginia Beach is one of several large cities in the Coastal Plain that directly drains to the Bay (Johnson and Sample, 2017). These attributes, and its unique location at the outlet of the Bay, make the City of Virginia Beach an ideal location for detailed study of urban runoff quality that is representative of the Chesapeake Bay Coastal Plain.

Stormwater quality can be simulated by water quality models. The Storm Water Management Model (SWMM) (USEPA, 2018) and the Hydrologic Simulation Program-Fortran (HSPF) (USEPA, 2014) provide an approach to estimate runoff, TSS and nutrient loads from landscapes to adjacent streams. SWMM has been used for various sizes of watershed, from large (40,000 km^2) to small (2 ha) with different landscapes (e.g. urban, agricultural, and forest) (Beelen et al., 2015; Nayeb Yazdi et al., 2019; Yazdi et al., 2018). The required data for the SWMM model includes: rainfall, soil characteristics, land use, extent of imperviousness, and runoff EMCs or buildup/washoff characteristics. Despite the importance of rainfall and catchment characteristics on urban stormwater quality, there are few studies that have focused on the role of rainfall and land use on stormwater quality from coastal areas. While the Nationwide Urban Runoff Program (NURP) is still commonly used, conducted over three decades ago (Smullen et al., 1999; USEPA, 1983). Because of an increasing focus on urban stormwater

quality (e.g. Total Maximum Daily Load (TMDL), which restricts the levels of nutrient and sediment delivered to tributaries of the Chesapeake Bay), there is a need to better characterize runoff water quality delivered from Coastal Plain urban areas.

The objectives of this research are to: (1) estimate total nitrogen (TN), total phosphorous (TP), and TSS loading from six catchments with homogenous land use within a coastal urban area; (2) investigate the role of rainfall and land use characteristics on stormwater quality; (3) to develop an estimate of annual TSS, TP and TN loads delivered from Coastal Plain urban areas using a simple linear model, and 4) incorporating statistical variability using a Bootstrap method. To achieve these goals, monitoring stations were installed at the outlet of each study catchment to measure runoff flows and collect storm-weighted composite samples which were used to estimate nutrient and sediment EMCs by storm event for a 1-year period. While only providing a limited snapshot of the runoff response in a coastal watershed, the collected data is comparable to previous studies. The comparison was then used to assess general behavior and potential trends related to managing stormwater quality.

3.2 Methodology

3.2.1 Field measurements & sampling site

Land use in the urbanized portion of the City of Virginia Beach is composed of low density residential (41%), high density residential (21%), commercial (6%), industrial (4%), transportation (15%), and parks/open space (13%) land uses. For each of these six land uses, a catchment was identified that was predominately one of the six land uses (Figure 3.1). Maps of individual catchment areas with aerial photography are shown in Figure 3.2. Catchment characteristics are presented in Table 3.1. Our monitoring stations were equipped with: (1) an automatic sampler (model 6712; Teledyne ISCO, Lincoln, Nebraska) to collect flow-weighted,

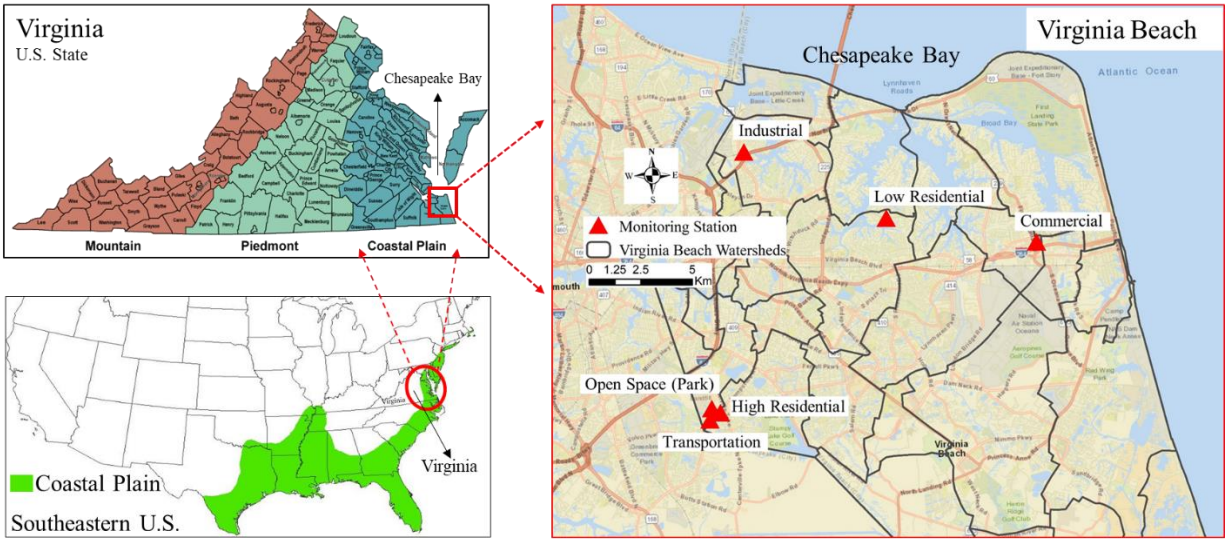

Figure 3.1. Location of six monitoring sites in Virginia Beach, Virginia.

Figure 3.2. Maps of each catchment with aerial photography of a) Commercial, b) Low density residential, c) Open space (park), d) High density residential, e) Transportation (road), f) Industrial.

composite stormwater samples; (2) a Palmer Bowlus flumes for measuring flow with a bubbler flow meter (model 730 Teledyne ISCO, Lincoln, Nebraska), or an area velocity sensor mounted in a pipe with no flume (model 750; Teledyne ISCO, Lincoln, Nebraska); (3) a rain gauge (model 674; Teledyne ISCO, Lincoln, Nebraska).

3.2.1 Sample collection methods

Monitoring was conducted between December 2018 and December 2019. Composite water samples were collected across 30 storm events. Total rainfall measured during the monitoring program was 1,140 mm; we note the historical average annual rainfall for Virginia Beach is 1,193 mm. The return period of rainfall events during the monitoring period varied from 1 to 5 years. Samples were transported from the field to the laboratory within 1 h of the end of each storm event, and then frozen at 0°C (USEPA, 1992). The analyte concentration within each single composite sample is defined as the event mean concentration (EMC). The composite samples collected approximately 75% of the storm runoff volume (Chapman and Horner, 2010). EMC is an effective way to characterize and report concentrations of stormwater constituents (Burant et al., 2018). The EMC multiplied by the flow volume of an event represents the total mass flux of a constituent from a given drainage area for the event.

Two sets of samples were collected. One set was analyzed for TN, TP, TSS, ortho-phosphorus (PO_4^{3-}), and total Kjeldahl nitrogen (TKN), nitrate (NO_3^-) and nitrite (NO_2^-), and ammonia (NH_4^+). TKN is the total concentration of organic nitrogen and NH_4^+, and TN is sum of TKN, NO_3^-, and NO_2^-. TP includes ortho-phosphate and organic phosphorus, i.e., the phosphorus in plant and animal fragments suspended in water. Another set of samples was analyzed for particle size distribution (PSD) by using laser diffraction analyzer (LA-950, Horiba, Kyoto,

Table 3.1. Study site characteristics.

Land use	Drainage area (ha)	Imperviousness (%)	General site characteristics
Low density residential (Single-family)	18	27	Detached housing units with large areas covered with grass.
High density residential (Multi-family)	2	40	Attached housing units, two or more units per structure. The surface is relatively flat with grass and trees.
Commercial	11	82	A complex with numbers of shops, restaurants. Most area is covered asphalt for parking lots.
Industrial	12	78	Light industrial area is directly in contact with adjacent urban areas and close to the airport. The road surface (asphalt) is not in the good condition.
Transportation (Roads)	3	75	Surface is covered by asphalt.
Open space (Park)	2	30	A park with a mixture of trees and vegetation, mainly turf, and a parking lot.

Japan). A collection of trip blanks, field blanks and equipment blanks were also collected (Burant et al., 2018).

A HACH nitrate kit (Model NI-14, Hach Company, Loveland, CO, detection limits 0.02 mg/L), nitrite kit (Model NI-14, detection limits 0.02 mg/L), ammonia kit (Model NI-14, detection limits 0.02 mg/L) and total phosphorus kit (model PO-24, detection limits 0.02 mg/L), were used for nitrogen and phosphorus analyses. The process for testing is described by Smith et al. (2004). For TSS, the weight of the pan and glass fiber filter were measured three times and the average taken for reporting purposes. The LA-950 directs multiple laser pulses into a water sample containing sediment particles; and uses multiple measurements of the resulting reflectance and adsorption of the sample to estimate the particle size distribution in the range of 0.01 - 3000 µm (Alberto et al., 2016; Goossens, 2008). For reference, particles size range

classifications are: clay (0.02-4 µm), silt (4-60 µm), very fine sand (60-125 µm), fine and medium sand (125-500 µm), and coarse sand (500-2000 µm) (Selbig and Bannerman, 2011; W. C. Krumbein, 1934). PSDs in the lower ranges indicate a propensity of the particles to bind with ions such as phosphorus (Gottselig et al., 2017; River and Richardson, 2018).

3.2.2 Role of precipitation on EMC

Suitable precipitation parameters were selected to evaluating the relationship between precipitation characteristics and stormwater quality. The selected precipitation parameters in this study were precipitation duration (PDu), precipitation depth (PDe), average precipitation intensity (API), maximum precipitation intensity (MPI), and antecedent dry periods (ADP). The average precipitation intensity was calculated by dividing the total precipitation depth by the precipitation duration. ADP was the number of dry days between storm events. We investigated these five rainfall parameters and EMCs for TN, TP, TSS, PO_4, and NO_3 for the 30 monitored events using Principal Component Analysis (PCA) within the SIMCA (version 14.0) statistical software.

3.2.2.1 Principal Component Analysis (PCA)

PCA is a technique that is applied to analyze relationships between objects and variables (Liu et al., 2013). PCA converts the variables to new set of principal components (PCs). The first PC (PC1) includes the variable that explains most of the variance in the dataset and the second PC (PC2) includes the variable that explains the second largest variance in the dataset and so on. The user is able to use the orthogonality of PCs for interpreting the variance with each PC independently. As the first few PCs contain most of the variance in this study, only these were included for analysis and interpretation. The PCA method reduces the number of variables that must be analyzed without losing information contained in the original dataset. By helping

process large datasets, PCA helps identify and understand relationships between variables efficiently (Espinasse et al., 1997; Kokot et al., 1998). In this study, these variables were included in PCA: PDu, PDe, API, MPI, ADP, and EMC values for TKN, TN, TP, TSS, PO_4, and NO_3, respectively. Accordingly, a data matrix (180 × 11) was generated which included 30 events for each land use (i.e. high density residential, low density residential, commercial, industrial, park, and transportation).

3.2.3 Statistical analysis

Statistical tests were performed to assess statistical differences between land uses. First, the Shapiro-Wilk Test was applied to assess normal distribution, the null hypothesis, H0 is that the distribution of each land use follows a normal distribution. If data follows a normal distribution, Welch's t-test with unequal variances and independent samples was used to assess the null hypothesis, H0: there was no difference between EMCs of the compared land uses, two at a time (Lucke and Nichols, 2015). If the distributions were not found to be normal, the Mann-Whitney test was used instead (Burant et al., 2018). The Mann-Whitney test was used for testing whether samples originated from the same distribution, thus the null hypothesis, H0 is that the distributions of the populations of the two land uses are the same. If the P value is less than the indicated significance level (0.05 and 0.10), the null hypothesis for the Mann-Whitney test can be rejected and the populations are distinct. In addition, ANOVA and the Kruskal–Wallis test (one-way ANOVA on ranks) were used for testing whether samples from two or more land uses have the same distribution (Hecke, 2012).

3.2.4 Develop pollutant loads equation for a watershed

An estimate of pollutant loading for each pollutant (i.e. TSS, TP, and TN) for a selected watershed in Virginia Beach (Figure 3.3) was calculated by multiplying runoff volume by EMC.

The City of Virginia Beach delineated and defined 32 Watersheds for administrative purposes, this one is called watershed 7. The area of the watershed is 10.31 km^2, and it currently includes 10% commercial (CO), 3% industrial (IN), 11% high density residential (HDR), 34% open space (OS), 24% low density residential (LDR), 17% transportation (TR), and 1% water (lake and pond) (Figure 3.3). Almost 35% of this watershed is impervious. The watershed drains directly to the Lynnhaven River, a tributary of the Chesapeake Bay. A monitoring station dedicated to assessing commercial land use was located in this watershed. Additionally, another monitoring station was installed in the watershed for measuring water levels (Figure 3.3). Total runoff volume in the watershed was estimated by Eq. (1) (De Leon and Lowe, 2009).

$$V = \frac{Pr}{100} \times \sum_{i=1}^{n} [A_i \times RC_i] \quad (1)$$

where, *Pr* is precipitation (cm), *n* is number of land uses located in the watershed, *A* is area of each land use (m^2), *RC* is the runoff coefficient for each land use. The runoff coefficient converts rainfall to runoff volume and is a function of imperviousness which was calculated by Eq. (2) (Schueler, 1987).

$$RC = 0.009 \times (percentage\ of\ impervious) + 0.05 \quad (2)$$

Thus, for storm events the loads for each constituent for the watershed was estimated by Eq. (3).

$$Pollutant\ Load\ (kg) = \frac{Pr}{100} \times \sum_{i=1}^{n} [A_i \times RC_i \times EMC_i] \quad (3)$$

where *EMC* is event mean concentration for each land use. EMC for each land use was obtained by the monitoring program.

3.2.1 Bootstrap for the pollutant load equation

We assumed that our samples were a representative sample of independent observations from a larger unknown population *X*. While there is no analytical method for deriving the distribution of the median for population *X*, the sample size is not large. A bootstrap method was

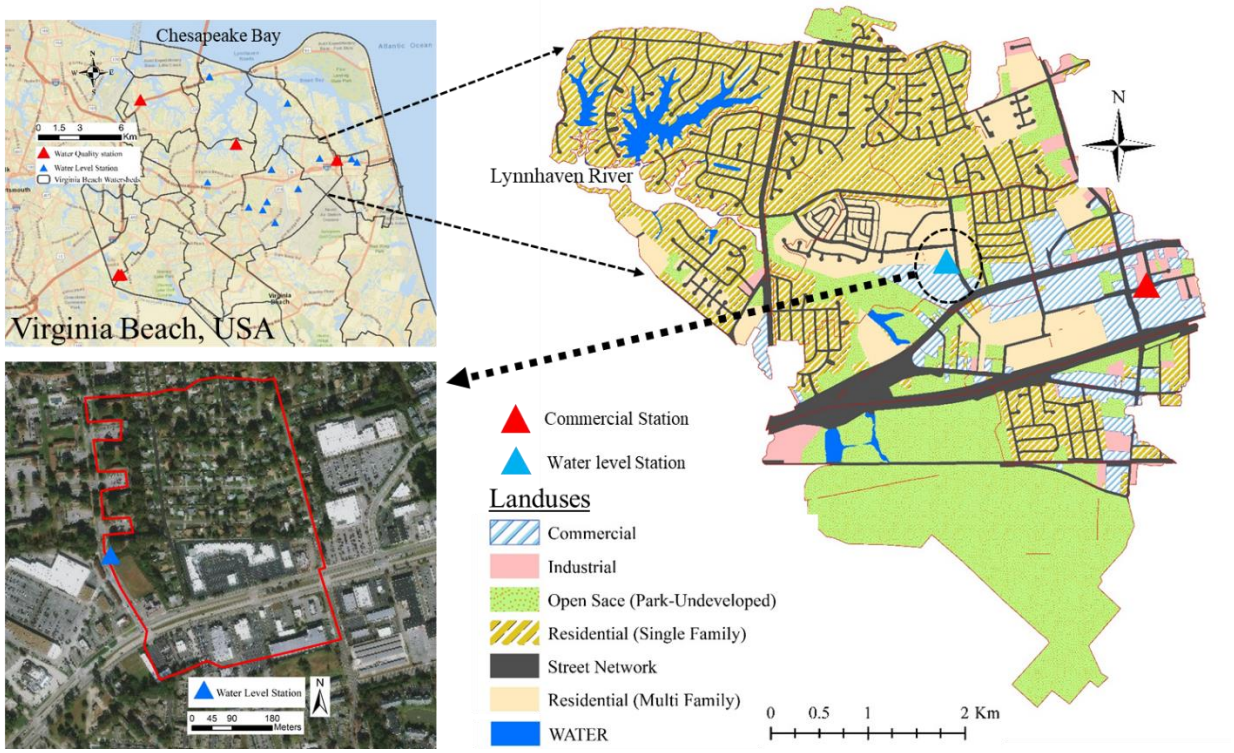

Figure 3.3. Map of the watershed in Virginia Beach.

used to derive the median EMC and 90% confidence intervals for each land use, assuming the distribution is unknown (Chernick, 2008; Wang and Sample, 2013). The percentile interval method generates the 50% and 95% confidence intervals (CIs) of the median EMC (Newman et al., 2000). Using Bootstrap, new data set with a similar median (M_c) were generated by sampled randomly the available *n* data set (i.e. EMCs) associated with *n* times replacement (Wang and Sample, 2013). The bootstrap method requires that the number of replications be increased until the estimate is stable (Chernick, 2008). We used RStudio (version 1.2) to apply these statistical methods. In this study, 100,000 resamples were taken to generate a conservative estimate of the sample median. Next, from the bootstrap replications, the median calculated and were ranked, and $Q_{2.5}$, Q_{25}, Q_{50}, Q_{75}, and $Q_{97.5}$ were related to the values of 2.5, 25, 50, 75, and 97.5 percentile, respectively. The intermediate data ($Q_{2.5} – Q_{97.5}$) were applied to define the best estimate of the

median EMC for TSS, TN and TP for each land use. Thus, Bootstrap generated five EMCs for each land use, subsequently we calculated five pollutant loads for each land use by Eq. 3.

3.2.2 SWMM model scenario development to verify the results

For this research, first, SWMM models were developed for each catchment (related to each land use) (Figure 3.2), and then a SWMM model was developed for the watershed in Virginia Beach (Figure 3.3), using landscape parameters such as soils, hydrography, land use, and digital elevation models provided by the City of Virginia Beach. Then, the model was assessed applying three statistical methods: the Nash-Sutcliffe Efficiency (NSE), coefficient of determination (r^2), and Percent bias (PBIAS). Moriasi et al., (2015) demonstrated multiple statistics should be applied instead of a single method. When r^2 and NSE were greater than 0.6, and PBIAS less than ±25%, the model calibration was considered complete (Ketabchy et al., 2018; Seong et al., 2015); otherwise, model calibration parameters were adjusted. After calibration SWMM manually, pollutant loads for the watershed were estimated by multiplying modelled 15-min runoff volume by EMCs of TSS, TP and TN and its results were compared with those from equation (Eq. 3).

3.3 Results

3.3.1 Continuous hydrograph for land uses

Flow was normalized by catchment area for each land use. Results of normalized flow, precipitation, and time of sampling for land use stations (CO, LDR, OS, HDR, TR, IN) are shown in Figure 3.4. Results indicate that normalized runoff for TR, CO, and IN are greater than that of LDR, HDR, and OS, because most area of TR, CO, and IN are impervious and covered by asphalt (Table 3.1). The runoff coefficients for TR, CO, IN, LDR, PA, and HDR were

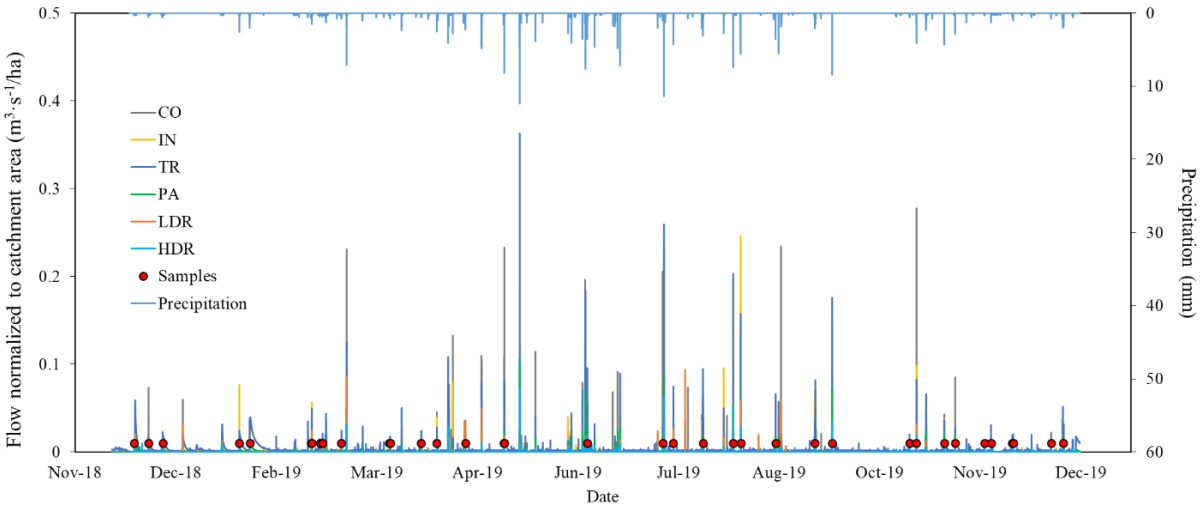

Figure 3.4. Flow normalized to catchment area of each land use with time of sampling.

calculated for the entire monitoring program, these were0.78, 0.71, 0.64, 0.27, 0.27, and 0.22, respectively. During the monitoring program, 30 storm events out of 53 storms were measured (Figure 3.4, red dots). Hydrograph for each catchment are shown in Appendix A.

3.3.2 EMC results for each land use

Median EMC results for each land use are shown in Table 3.2. The EMCs for TSS, TN, and TP through the monitoring period are provided in Figure 3.5a through Figure 3.5f, respectively. Box plots indicated that TSS EMC of park and industrial runoff is greater than other land uses. Park land use had the highest percentage of pervious area. High EMC of TSS for industrial land use may be caused by low quality of road surface (asphalt) and high truck traffic within the catchment. The TP for park and low density residential was greater than other land uses; much of these areas was covered by grass and trees. The elevated TP EMC may stem from excessive levels of fertilizer use. The lowest TP EMC were from the transportation and industrial land uses, which have the highest impervious coverage. Trends of the TN EMC for each land were opposite those of TP, the highest TN EMC were associated with transportation and industrial, and the lowest were associated with park and low density residential, respectively.

The elevated TN within transportation land use stems from high traffic density and higher atmospheric deposition in that area.

Table 3.2. Median EMCs ($mg \cdot L^{-1}$) for each land use.

Land use	NO_2+ NO_3	TKN	TN	PO_4	TP	TSS
Industrial	0.60	0.25	0.85	0.13	0.29	29.2
Commercial	0.29	0.65	0.93	0.12	0.30	27.2
Residential (low)	0.22	0.50	0.75	0.13	0.30	26.4
Residential (high)	0.38	0.50	1.07	0.10	0.27	15.3
Open space (Park)	0.25	0.67	0.92	0.30	0.40	46.7
Transportation	0.36	0.67	1.00	0.20	0.30	24.5

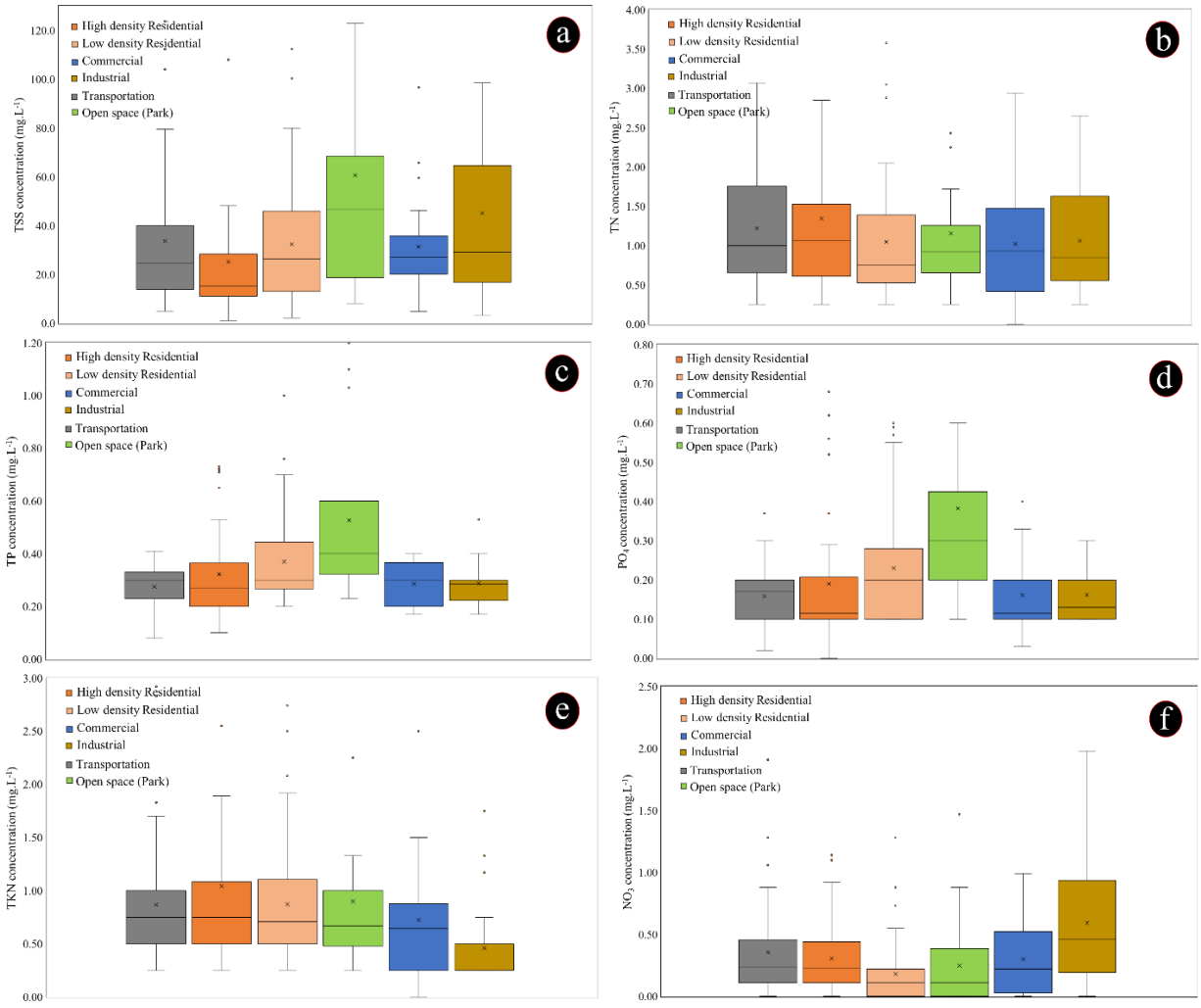

Figure 3.5. EMC variation of a) TSS, b) TN, c) TP, d) PO4, e) TKN, f) NO3.

3.3.3 Particle size distribution results

Suspended sediment particle size in this study were characterized by calculating D_{10}, D_{50}, and D_{90}. D_{90} describes the diameter of particles that 90% of the particles were smaller and 10% were larger, a similar definition governs D_{10}. D_{50} is the median particle size within the sample. Particle sizes were different for each land use (Figure 3.6). Particle sizes for transportation land use was greater than other land uses, so that the median D_{50} for transportation land use is almost 3 times higher than other land uses. Commercial and park land uses have the smallest particle size among these six land uses. Most stormwater particles delivered from these urban land uses were between 1 – 150 µm, which are fine particles. Miguntanna et al., (2013) showed that fine particles are the most common particle in urban runoff.

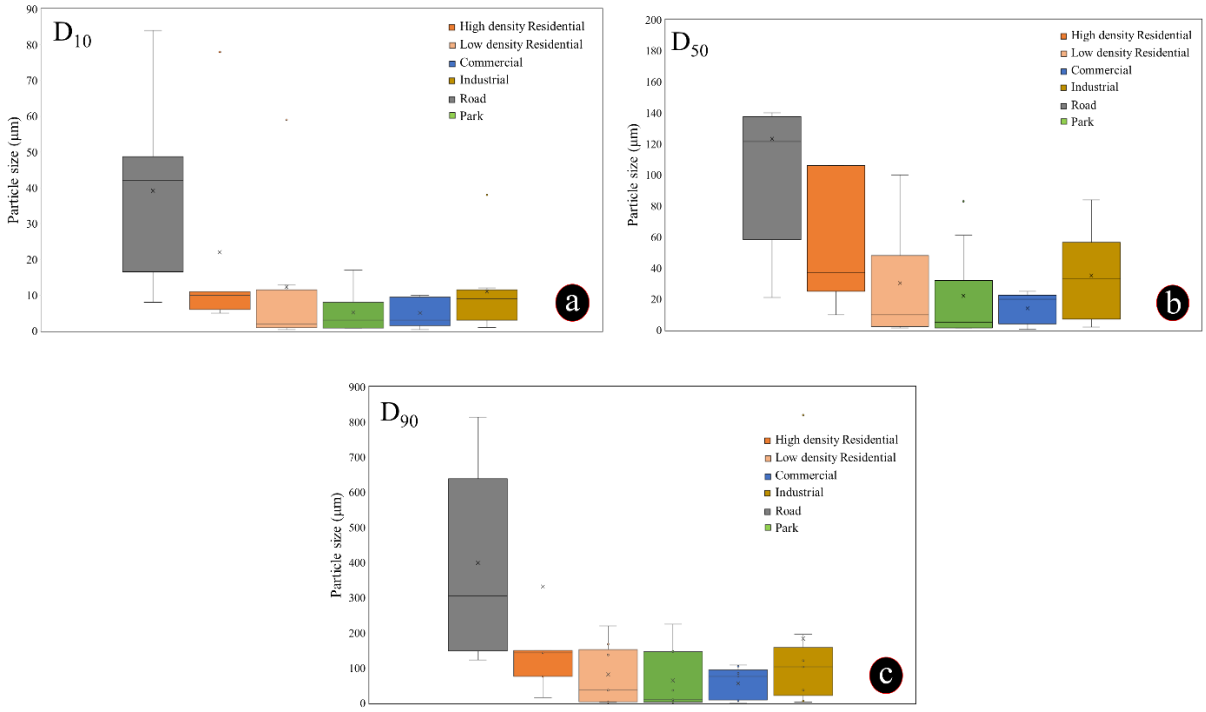

Figure 3.6. Particle sizes during monitoring program a) D_{10}, b) D_{50}, and c) D_{90}.

3.3.4 Statistical analysis results

Analysis of the results indicated that the data were not normally distributed, thus the Mann-Whitney U test was used for comparing between two land uses. Results indicated the p-value for the Mann-Whitney U test for TSS for some of these land uses was less than 0.05; thus, the null hypothesis for these results can be rejected (H0 is the distributions of populations for two land uses are equal) (Table 3.3). However, the p-value for three land uses including HDR, CO, and TR was greater than 0.05, suggesting there was not a significant difference between the EMC for TSS of these three land uses. In addition, the p-value of Kruskal–Wallis test for these three land uses (HDR, TR, CO) for TSS was 0.1265 (chi-squared = 4.1358) higher than 0.05 which means there was not a significant difference between the EMC for TSS of these three land uses (H0 is that the samples originated from populations with the same distribution). With respect to TN, the results showed that there was no significant different between EMC results of the land uses and the sample group comes from populations with similar distribution (Table 3.4). For TP, results indicated that there was a significant difference between HDR and TR, and HDR and CO, while there was no significant difference between CO and TR (Table 3.5). Overall, results indicated that there was no significant difference between commercial (CO) and transportation (TR) land uses for TSS, TP and TN, and the samples of these two land uses were from populations with the same distribution.

3.3.1 Role of precipitation characteristics on stormwater quality

The PCA analysis found that three PCs represent 64% of the total data variance (Figure 3.7). Two biplots where Figure 3.7a display the PC1 vs. PC2 biplot and Figure 3.7b shows the PC2 vs. PC3 biplot. The first three PCs explain 26.6, 20.2 and 17.5 % of the data variance,

Table 3.3. Statistical Results (p-values) for TSS between land uses.

Land uses	TR	HDR	LDR	IN	CO	OS
TR	--	8.7E-01	4.1E-02	6.5E-02	6.1E-01	4.3E-02
HDR	*Fr	--	4.0E-02	1.5E-02	8.6E-01	6.7E-02
LDR	*R	R	--	6.8E-02	6.0E-02	4.3E-02
IN	R	R	R	--	1.1E-02	3.5E-02
CO	Fr	Fr	R	R	--	6.1E-02
OS	R	R	R	R	R	--

*R: Reject, *Fr: Failing to Reject

Table 3.4. Statistical Results (p-values) for TN between land uses.

Land use	TR	HDR	LDR	IN	CO	OS
TR	--	7.2E-01	2.2E-01	5.1E-01	3.9E-01	9.0E-01
HDR	*Fr	--	2.4E-01	4.3E-01	3.6E-01	6.8E-01
LDR	Fr	Fr	--	5.2E-01	6.8E-01	3.6E-01
IN	Fr	Fr	Fr	--	8.2E-01	6.8E-01
CO	Fr	Fr	Fr	Fr	--	5.6E-01
OS	Fr	Fr	Fr	Fr	Fr	--

*Fr: Failing to Reject

Table 3.5. Statistical Results (p-values) for TP between land uses.

Land use	TR	HDR	LDR	IN	CO	OS
TR	--	7.0E-03	2.9E-02	6.7E-01	3.4E-01	8.7E-04
HDR	*R	--	1.5E-02	4.5E-02	1.5E-02	8.8E-05
LDR	R	R	--	2.2E-02	1.3E-02	7.6E-03
IN	*Fr	R	R	--	6.2E-01	6.6E-04
CO	Fr	R	R	Fr	--	4.1E-04
OS	R	R	R	R	R	--

*R: Reject, *Fr: Failing to Reject.

respectively. This shows that PC1, PC2 and PC3 axes contain an appropriate variance of the data. The three rainfall parameters, PDe, MPI, and API, show correlation with each other and with TSS (Figure 3.7a). The PDu vector has the same direction for TP and PO_4, indicating there is correlation between these parameters. As the angle between the TP, PO_4, and TSS vectors is small, most P is in particulate form (Figure 3.7b). Also, PDu, PDe, and MPI were correlated with TSS, TP, and PO_4, possibly because high intensity precipitation has high kinetic energy and cause more pollutants being entrenched and transported. ADP was not show strong correlated

with other rainfall characteristics and EMCs. These results are similar to previous studies indicating that rainfall intensity was correlated with TSS and TP EMCs (Liu et al., 2015, 2013; Mahbub et al., 2011).

3.3.2 Bootstrap results

Bootstrap results of EMCs for TSS, TN, and TP for each land use are presented in Table 3.6. Results show that 2.5 ($Q_{2.5}$) and 97.5 ($Q_{97.5}$) percentile have the lowest and highest EMC for each land use. The $Q_{97.5}$ for TSS and TN is 1.5 – 2.5 times greater than that of $Q_{2.5}$, while $Q_{97.5}$ for TP is 1.1 – 1.5 times higher than that of $Q_{2.5}$. These results indicate that variability between EMCs for TSS and TN are higher than those of TP.

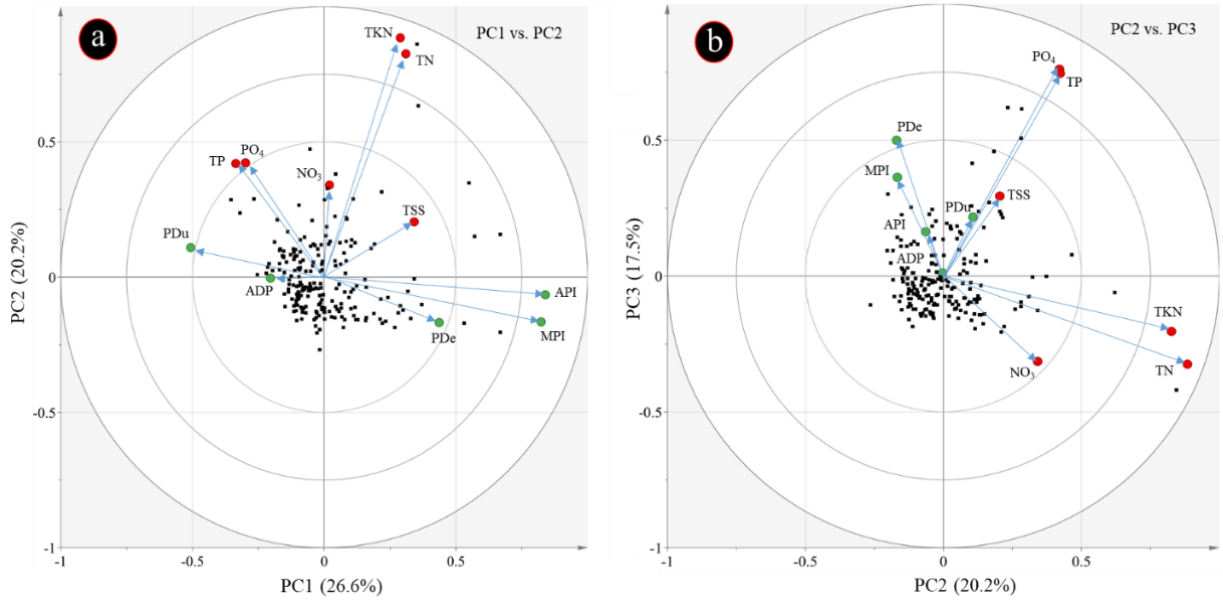

Figure 3.7. PCA biplots for rainfall characterization and nutrients.

Table 3.6. Bootstrap results of EMCs for TSS, TN, and TP for each land use ($mg \cdot L^{-1}$).

Land uses	2.5%	25%	50%	75%	97.5%
TSS					
Industrial	20.9	27.0	29.2	32.5	51.9
Commercial	20.9	22.3	27.2	31.1	34.5
Residential (low)	17.3	24.0	26.4	28.9	31.9
Residential (high)	13.1	14.8	15.3	17.1	21.5
Open space (Park)	32.6	42.7	46.7	51.9	61.2
Transportation	17.9	22.4	24.5	26.4	31.9
TN					
Industrial	0.75	0.81	0.85	0.94	1.10
Commercial	0.56	0.83	0.93	1.08	1.26
Residential (low)	0.64	0.75	0.75	0.84	1.03
Residential (high)	0.86	0.99	1.07	1.11	1.29
Open space (Park)	0.74	0.84	0.92	1.01	1.16
Transportation	0.83	0.86	1.00	1.04	1.38
TP					
Industrial	0.23	0.27	0.29	0.30	0.30
Commercial	0.20	0.29	0.30	0.30	0.30
Residential (low)	0.30	0.30	0.30	0.30	0.37
Residential (high)	0.23	0.27	0.27	0.30	0.30
Open space (Park)	0.37	0.40	0.41	0.47	0.50
Transportation	0.26	0.30	0.30	0.30	0.30

3.3.3 Hydrologic calibration results

The SWMM model was calibrated and validated for each catchment (related to each land use) at the catchment outlet. Goodness-of-fit was assessed by statistical analysis and by plotting the observed vs. simulated values of runoff for each station in Figure 3.8. Results indicate that NSE, r^2 were higher than 0.5 and 0.6, respectively, and PBIAS was lower than 25%, indicating there is a good agreement between the simulated and observed values for each station, and SWMM was able to simulate urban land uses reasonably well.

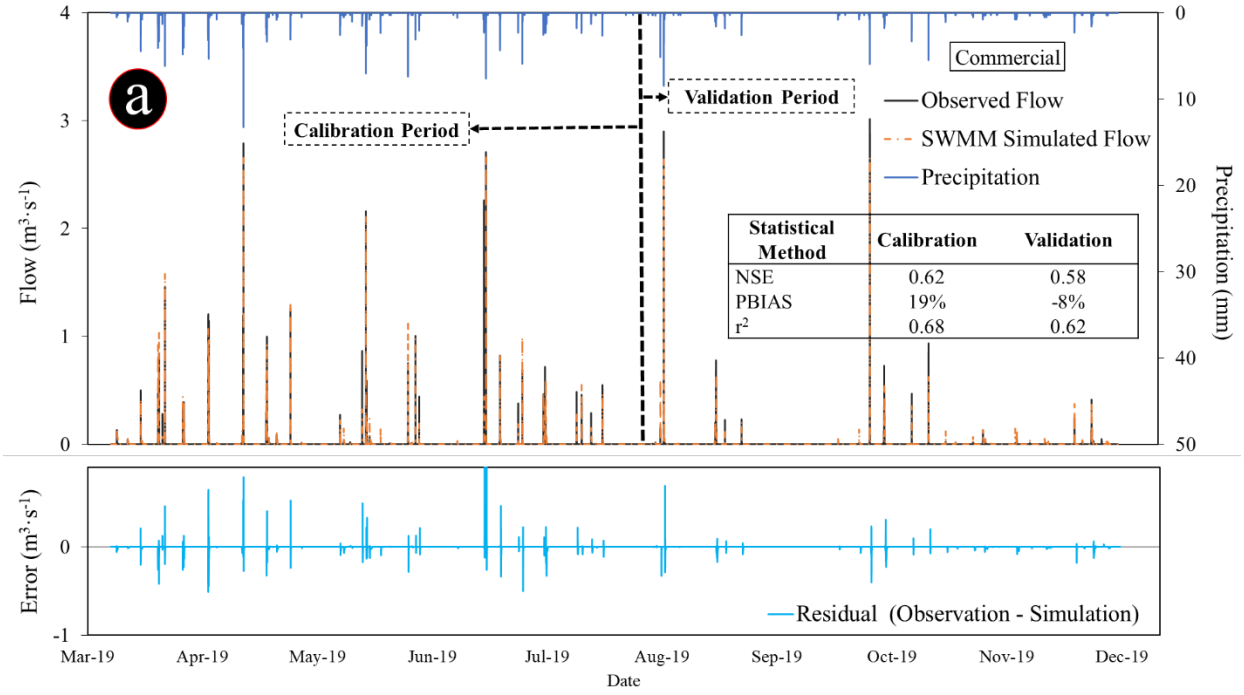
a
Commercial
Validation Period
Calibration Period
Observed Flow
SWMM Simulated Flow
Precipitation
Statistical Method | Calibration | Validation
NSE | 0.62 | 0.58
PBIAS | 19% | -8%
r2 | 0.68 | 0.62
Flow (m3·s-1)
Precipitation (mm)
Error (m3·s-1)
Residual (Observation - Simulation)
Mar-19
Apr-19
May-19
Jun-19
Jul-19
Aug-19
Sep-19
Oct-19
Nov-19
Dec-19
Date

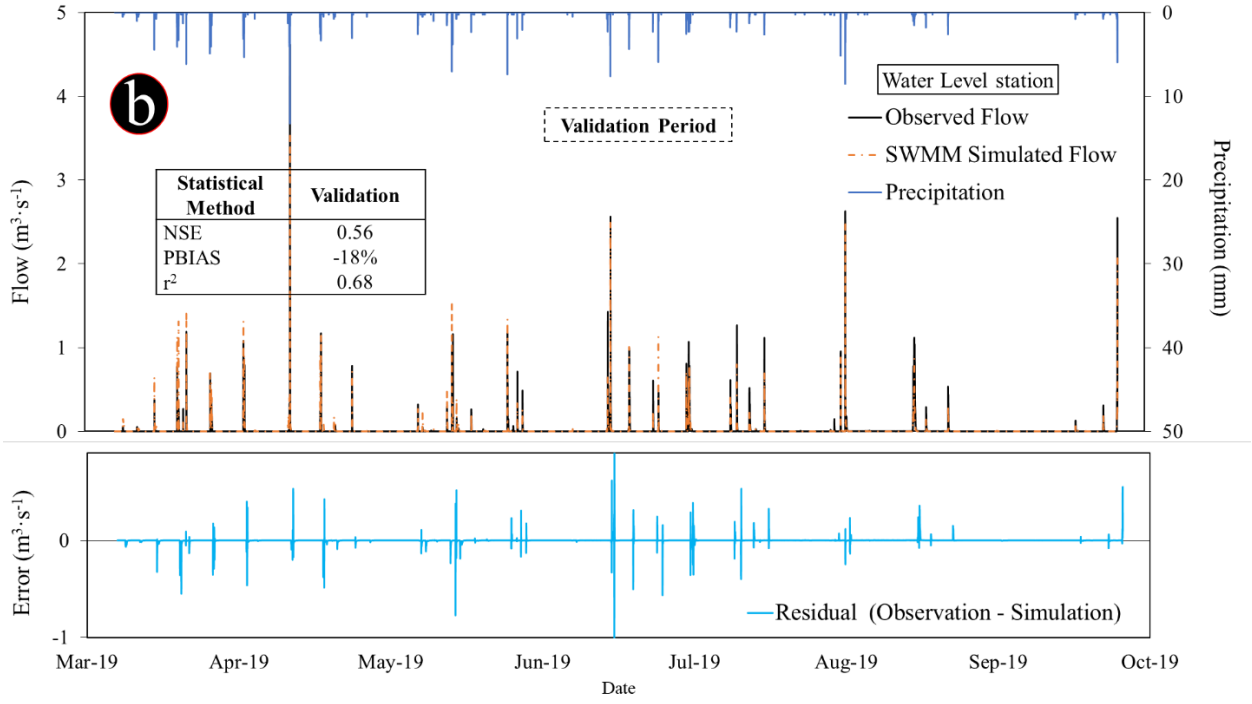
b
Water Level station
Validation Period
Observed Flow
SWMM Simulated Flow
Precipitation
Statistical Method | Validation
NSE | 0.56
PBIAS | -18%
r2 | 0.68
Flow (m3·s-1)
Precipitation (mm)
Error (m3·s-1)
Residual (Observation - Simulation)
Mar-19
Apr-19
May-19
Jun-19
Jul-19
Aug-19
Sep-19
Oct-19
Date

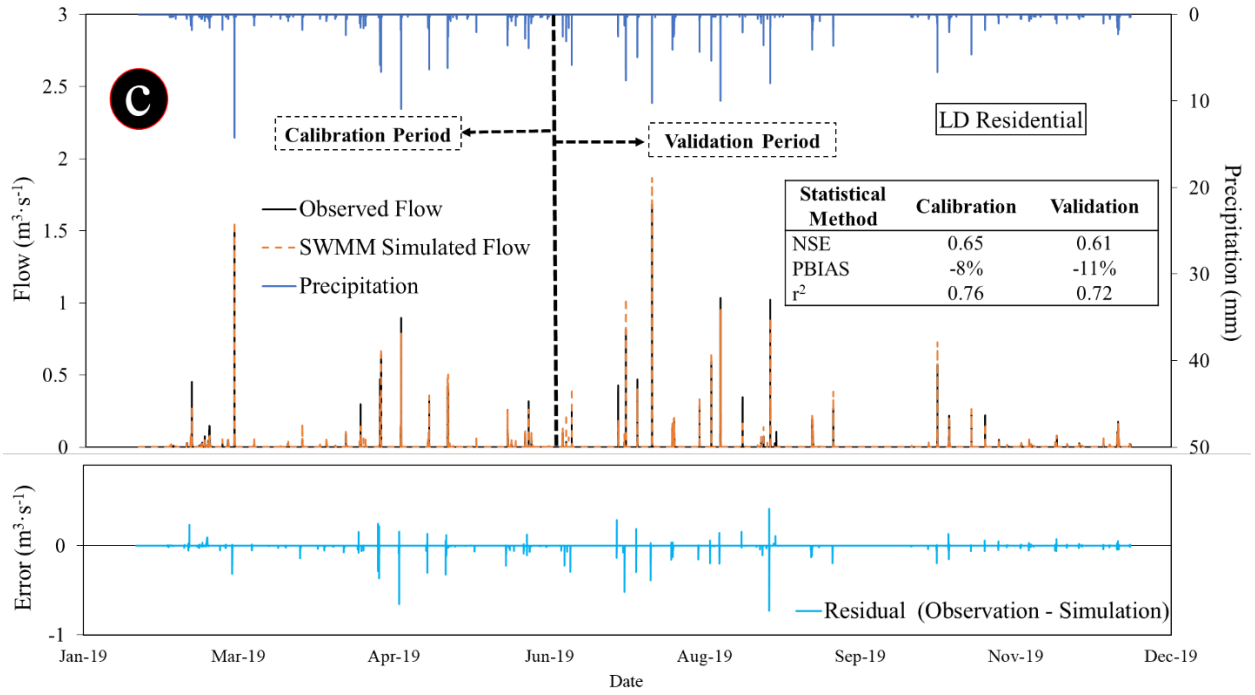
c
LD Residential
Calibration Period
Validation Period
Observed Flow
SWMM Simulated Flow
Precipitation
Statistical Method | Calibration | Validation
NSE | 0.65 | 0.61
PBIAS | -8% | -11%
r2 | 0.76 | 0.72
Flow (m3·s-1)
Precipitation (mm)
Error (m3·s-1)
Residual (Observation - Simulation)
Jan-19
Mar-19
Apr-19
Jun-19
Aug-19
Sep-19
Nov-19
Dec-19
Date

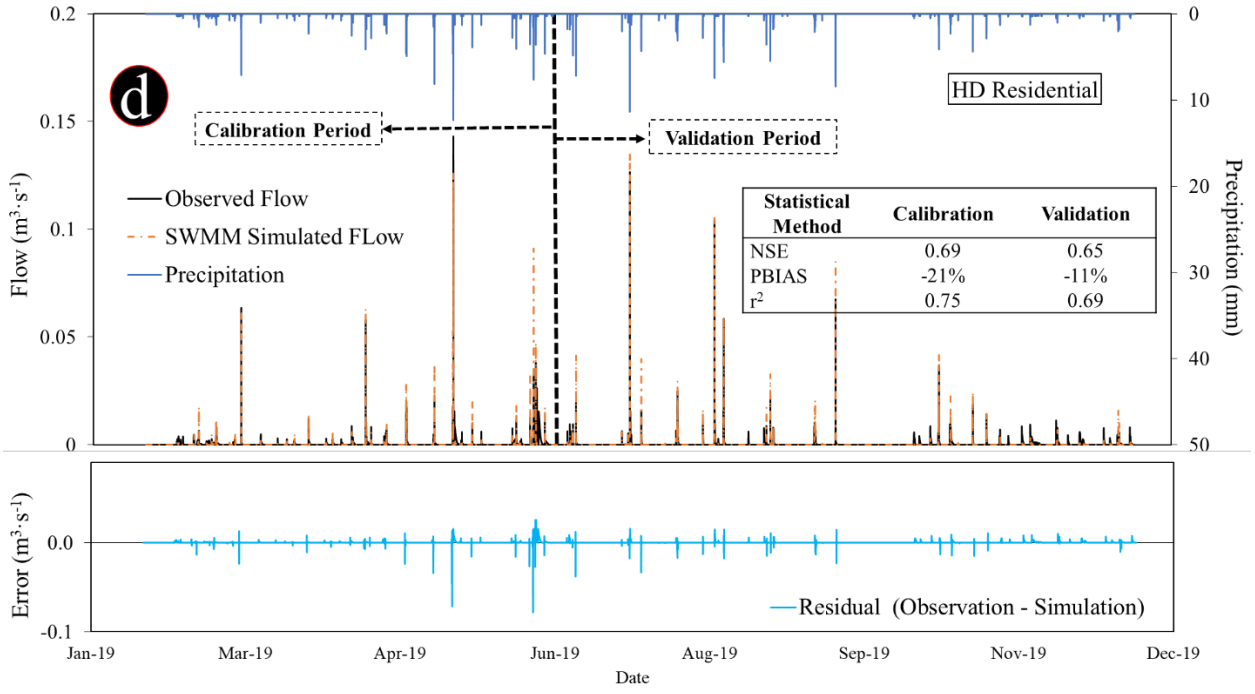
d
HD Residential
Calibration Period
Validation Period
Observed Flow
SWMM Simulated FLow
Precipitation
Statistical Method | Calibration | Validation
NSE | 0.69 | 0.65
PBIAS | -21% | -11%
r2 | 0.75 | 0.69
Flow (m3·s-1)
Precipitation (mm)
Error (m3·s-1)
Residual (Observation - Simulation)
Jan-19
Mar-19
Apr-19
Jun-19
Aug-19
Sep-19
Nov-19
Dec-19
Date

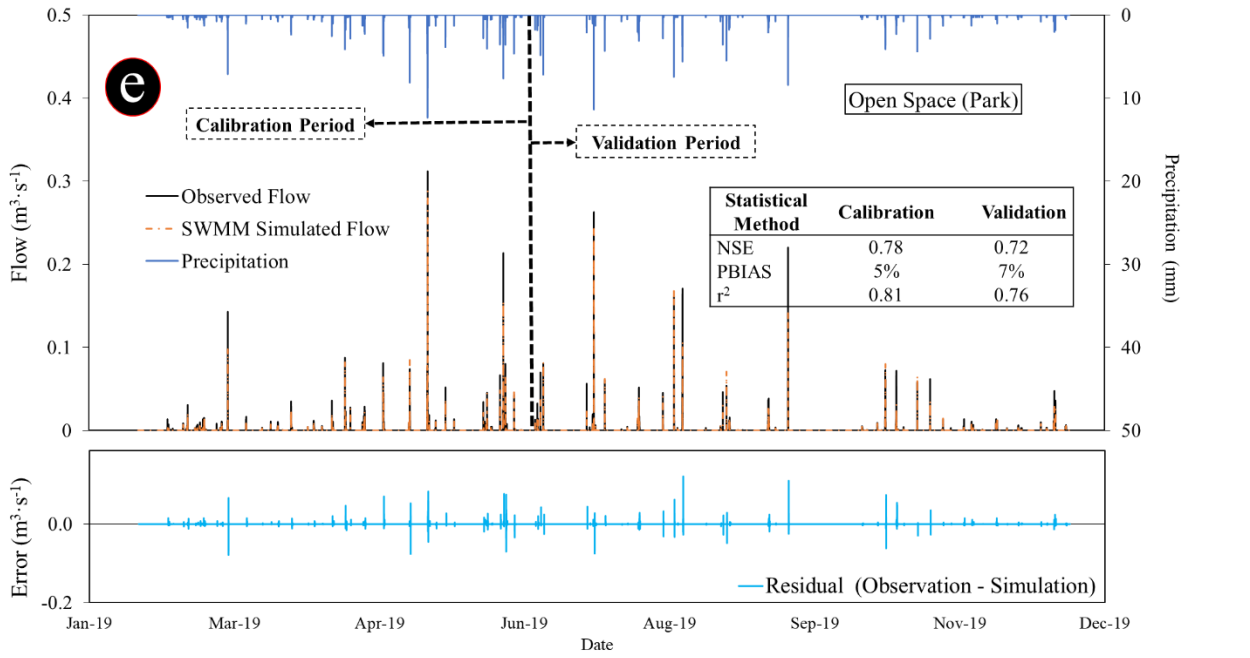
e
Open Space (Park)
Calibration Period
Validation Period
Observed Flow
SWMM Simulated Flow
Precipitation
Statistical Method | Calibration | Validation
NSE | 0.78 | 0.72
PBIAS | 5% | 7%
r² | 0.81 | 0.76
Flow (m³·s⁻¹)
Precipitation (mm)
Error (m³·s⁻¹)
Residual (Observation - Simulation)
Jan-19
Mar-19
Apr-19
Jun-19
Aug-19
Sep-19
Nov-19
Dec-19
Date

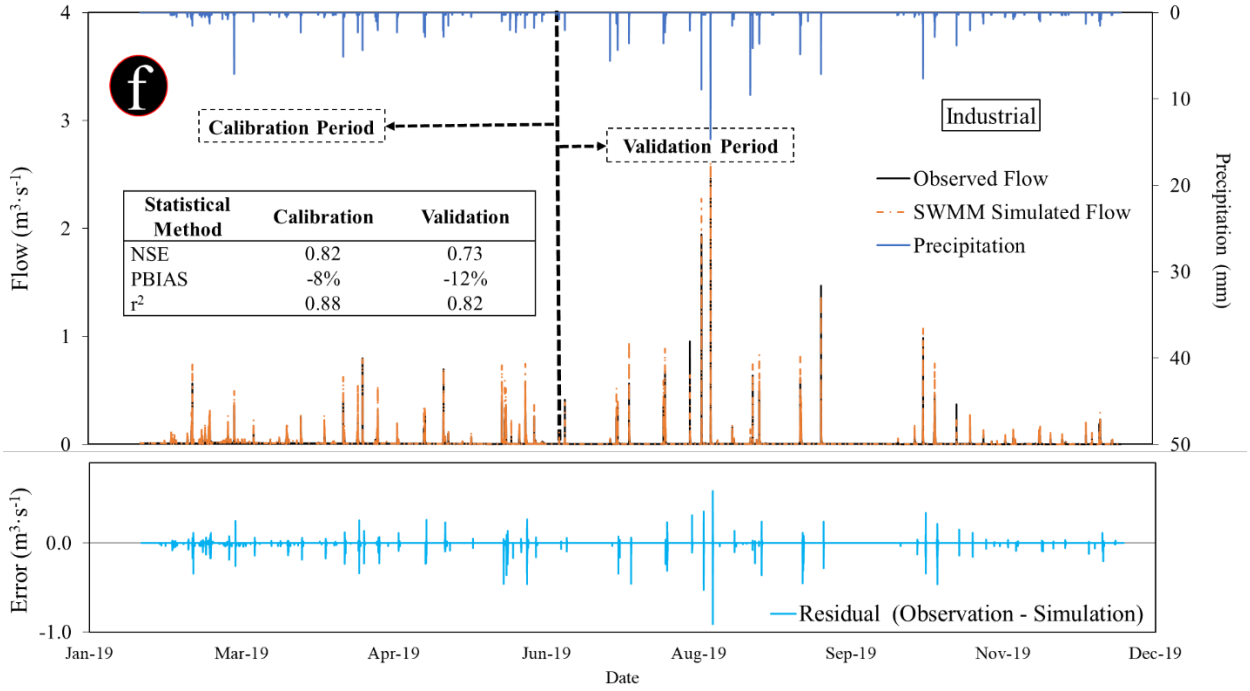
f
Industrial
Calibration Period
Validation Period
Observed Flow
SWMM Simulated Flow
Precipitation
Statistical Method | Calibration | Validation
NSE | 0.82 | 0.73
PBIAS | -8% | -12%
r² | 0.88 | 0.82
Flow (m³·s⁻¹)
Precipitation (mm)
Error (m³·s⁻¹)
Residual (Observation - Simulation)
Jan-19
Mar-19
Apr-19
Jun-19
Aug-19
Sep-19
Nov-19
Dec-19
Date

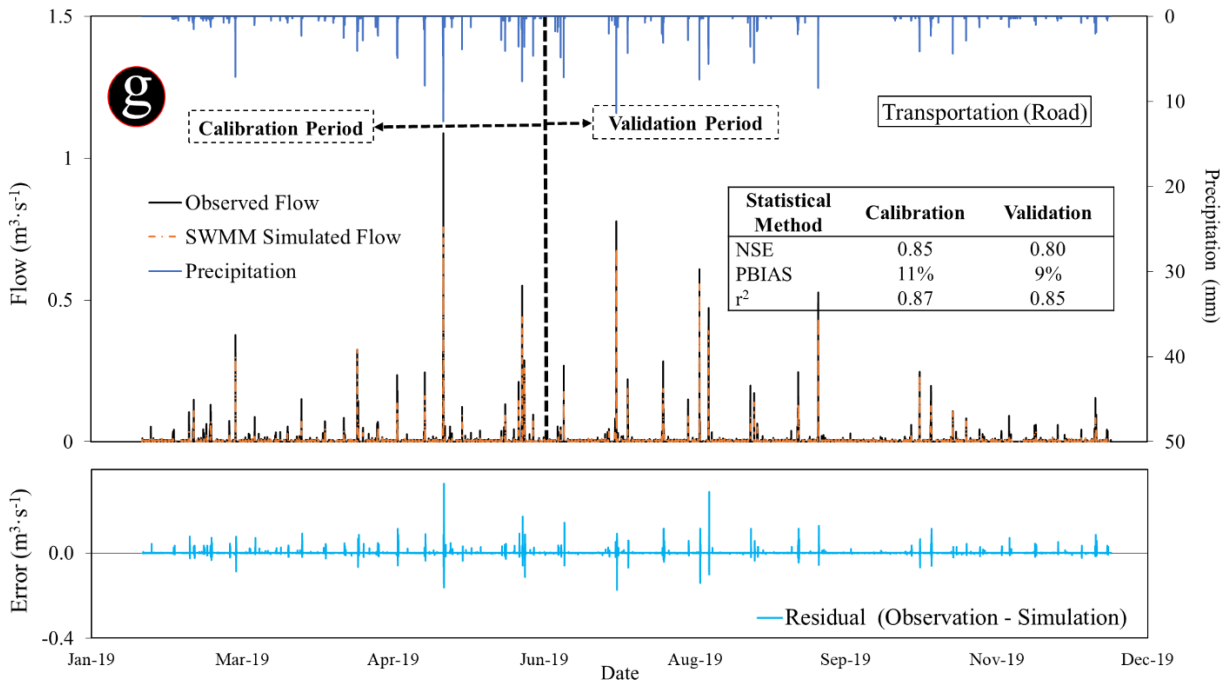

Figure 3.8. Comparison of observed and simulated runoff by storm events for each station a) Commercial (CO), b) Water level station, c) Low density residential, d) High density residential, e) Open space, f) Industrial, g) Transportation (road).

3.3.4 Water quality calibration results

We measured actual annual runoff volume at the outlet of each catchment, thus annual pollutant loads for each catchment was calculated by multiplying EMCs and annual runoff volume. The SWMM models were calibrated for water quality to estimate annual TSS, TP, and TN loads during the monitoring period for each catchment. Based upon percent error results, the SWMM estimated pollutant loads properly, as there was a good agreement between simulation and observation annual loads for TSS, TN, and TP (i.e., percent error was lower than ±25%) (Table 3.7).

Table 3.7. Results of sediment, TN and TP loads from observation and SWMM model.

Station	TSS load (kg/year)	TN load (kg/year)	TP load (kg/year)
CO Station			
Observation	4050	130	41.7
SWMM results	4300 (5.96%)	138 (6.85%)	45.3 (8.51%)
LDR Station			
Observation	1300	41.6	17.3
SWMM results	1430 (9.92%)	37.1 (-10.8%)	15.5 (-9.77%)
HDR Station			
Observation	74.0	3.95	1.03
SWMM results	80.0 (8.25%)	3.72 (-5.78%)	1.12 (8.78%)
OS Station			
Observation	370	7.28	3.16
SWMM results	340 (-7.8%)	6.87 (2.5%)	3.27 (3.3%)
IN Station			
Observation	8050	234	80.0
SWMM results	8200 (2.82%)	221 (-5.50%)	70.2 (-12.15%)
TR Station			
Observation	1210	63.7	18.55
SWMM results	1100 (-9.25%)	58.3 (-8.44%)	20.8 (12.25%)

3.3.5 Comparing SWMM results with regression equation results

The validated SWMM model was applied to simulate runoff volume and TSS, TN and TP concentrations from the watershed for 10 years (2008 to 2018). In addition, an equation (Eq.3) was developed to estimate pollutant loads for TSS, TP, and TN for the watershed. Correlation between results of the SWMM and the equation for these 10 years for TSS, TN, and TP was 0.87, 0.90, and 0.88, respectively (Figure 3.9). These results indicated that Eq. 3 can estimate pollutants loads for the watershed reasonably well.

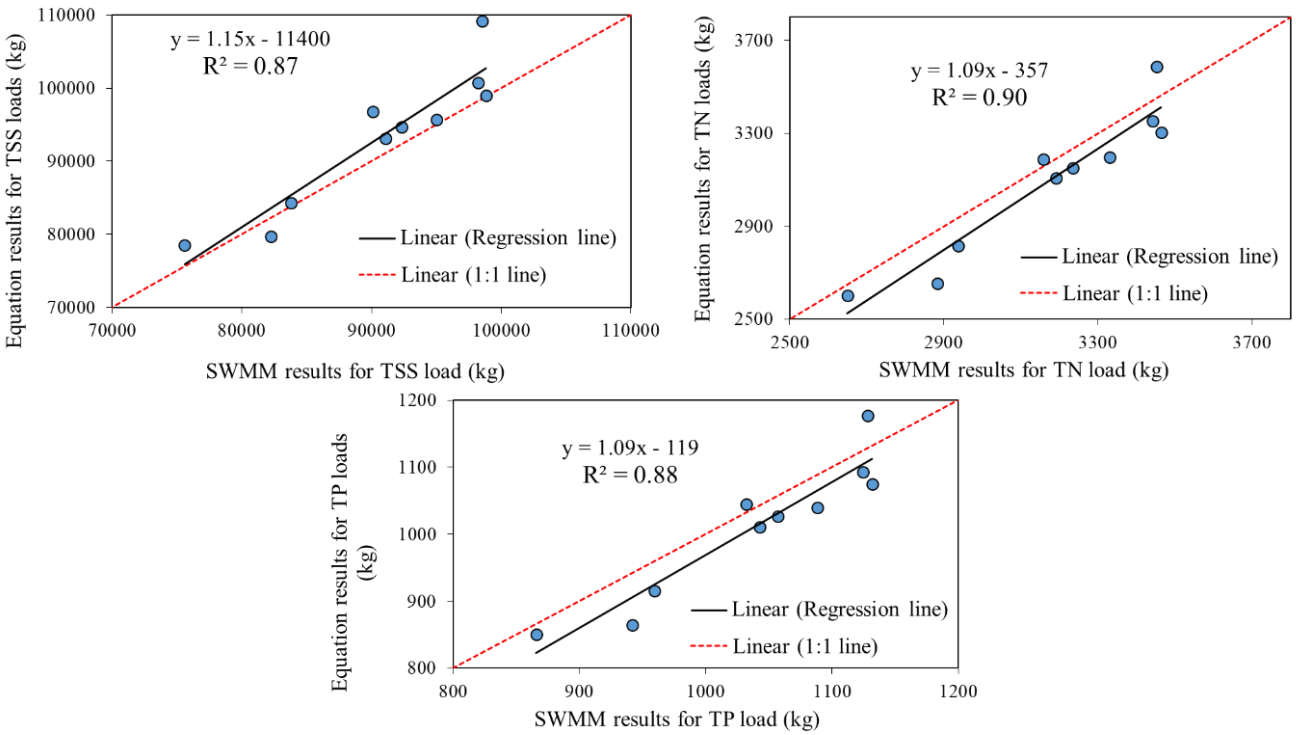

Figure 3.9. Scatter plots of SWMM and equation results for pollutant loads.

Using bootstrap, five EMC values corresponding to 2.5, 25, 50, 75, and 97.5 percentile were generated. Subsequently, five equations (line) with different confidence intervals (CI) were developed by Eq. 3 (Figure 3.10). The SWMM results for TSS is between 25% – 75% CI, for TN simulated results are mostly between 25% – 50% CI, and for TP are between 2.5 – 50 % CI (Figure 3.10). Results indicated that Eq. 3 could simulate pollutants loads for various annual rainfall, properly. However, the equation was not able to incorporate the effect of rainfall intensity. For example, the precipitation depth, in 2010, 2012, and 2014 was almost 141 cm, but because of the different rainfall intensity in these 3 years, the pollutant loads from the SWMM models for these 3 years are markedly different. In 2012, the intensity of storm events was higher than that of 2010 and 2014, thus the pollutant loads for 2012 year is greater than 2010 and 2014.

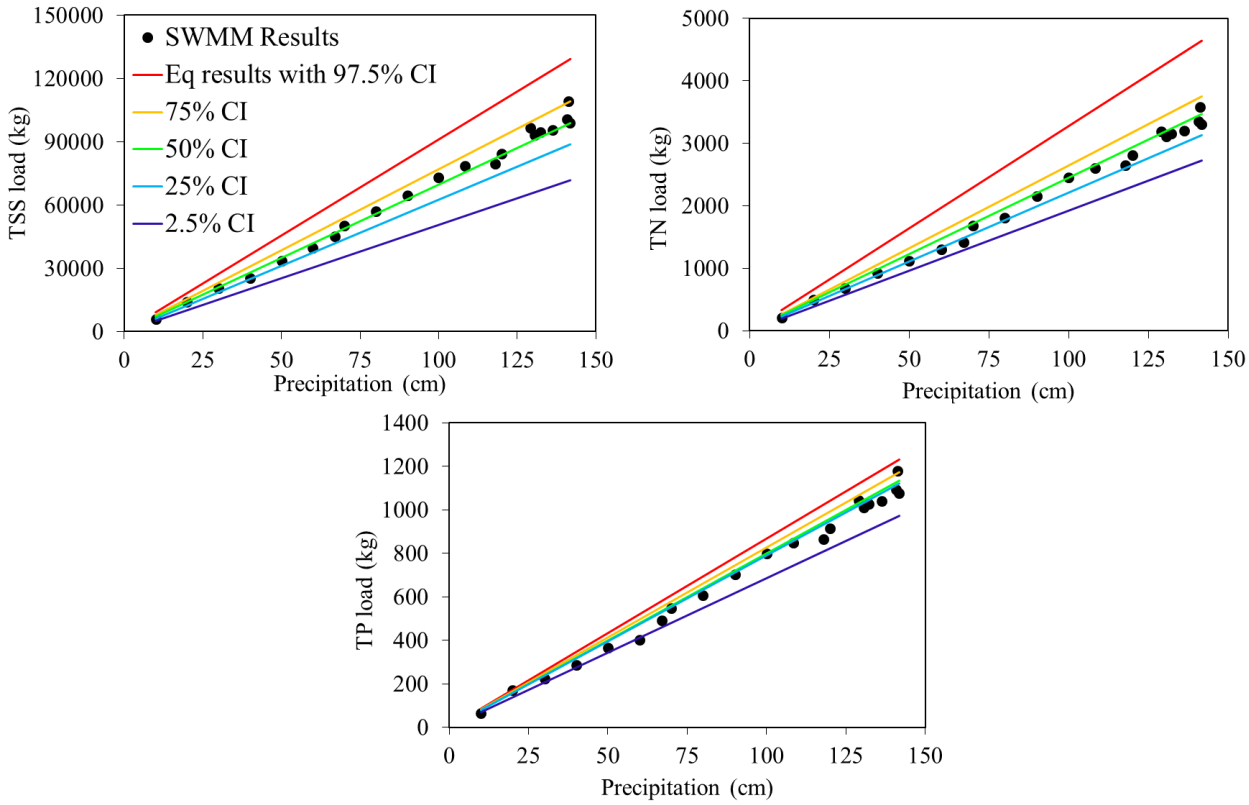

Figure 3.10. Pollutant loads results.

3.4 Discussion

The two most important studies that characterized stormwater discharged from urban areas with specific land use were the NURP (Smullen et al., 1999; USEPA, 1983) and the National Stormwater Quality Database (NSQD) v.3 (Pitt et al., 2008). NURP in comparison with NSQD used smaller and more homogenous with respect to land use) catchments, while the NSQD has larger catchments, and, as each entry is classified simply as having a majority of its area in that land use. Thus, the NURP's data could be more accurate that NSQD, but the database of NSQD within coastal area is much larger than that in the NURP. For instance, four land uses (i.e. residential, commercial, industrial, and open space) were monitored during NURP; however, within Coastal Plain area only EMCs in runoff discharged from residential and commercial land

uses are available (Table 3.8). Results of NSQD for TSS, TN and TP EMCs for various urban land uses in Virginia Coastal Plain are shown in Table 3.8.

The TSS and TN EMCs reported in those studies (Table 3.8) were greater than those found in our study. In contrast, we found that TP loads from our coastal urban watersheds were higher than that of NURP and NSQD. Thus, decision makers and storm water quality improvement strategies should consider these differences for each area. Previous studies reported that EMC for TSS, TP, and TN from urban catchments ranges from 80 to 260, 0.2 to 0.6, and 2.4 to 3.9 $mg \cdot L^{-1}$, respectively (Li et al., 2015; Métadier and Bertrand-Krajewski, 2012; Sun et al., 2015; Yang and Toor, 2017), also Hirschman et al., (2008) showed that the average concentration of TSS, TP and TN in urban storm runoff in Virginia Beach were 60.1, 0.32, and 2.21 $mg \cdot L^{-1}$, respectively, while our observations for Virginal Beach area were 30.1, 0.31, and 0.94 $mg \cdot L^{-1}$, respectively.

Our results are similar to previous study indicating that TKN forms on average were almost 78% of the total N during storm events (Lucke et al., 2018; Miguntanna et al., 2013). According to Goonetilleke et al., (2009), fine particles (1–150 μm range) are the most common size in urban stormwater, which is similar to our results, thus the strategies for improving the

Table 3.8. Coastal Plain EMC.

Land use	**TSS ($mg \cdot L^{-1}$)**	**TN ($mg \cdot L^{-1}$)**	**TP ($mg \cdot L^{-1}$)**
NURP			
Residential	21 – 56 *(34)	1.23 – 2.58 (1.8)	0.11 – 0.38 (0.28)
Commercial	9 – 22 (14)	0.68– 1.33 (0.94)	0.10 – 0.17 (0.14)
NSQD			
Residential	25 – 190 *(54)	1.01 – 3.04 (1.63)	0.16 – 0.70 (0.25)
Commercial	15 – 105 (31)	1.10– 5.12 (2.25)	0.17 – 0.76 (0.26)
Industrial	10 – 80 (29)	0.65 – 2.65 (1.3)	0.07 – 0.26 (0.13)
Open space	16 – 60 (32)	1.02 – 2.53 (1.53)	0.13 – 0.30 (0.17)

*(Median)

storm water quality should focus on this size range. There are three main measures for removing fine particles from stormwater including infiltration (e.g. permeable pavement), filtration (e.g. filter strips, grassed swales) and detention (e.g. wet and dry ponds) (Shammaa and Zhu, 2001; Winston and Hunt, 2017). However, particles larger than 100 μm settle easily, thus detention practices are the most important measure for capturing fine particle (Winston and Hunt, 2017). Atmospheric deposition, building materials and structure surfaces, road maintenance, industrial and construction activities, and vehicular transportation are main sources of fine particle in stormwater (Shammaa and Zhu, 2001) and Müller et al., (2020) reported that the vehicular transportation sources are the main sources of urban stormwater pollutants. Our PSD results show that particle sizes for transportation land use were larger than other land uses resulting from frequency of stopping and starting of vehicles (three traffic lights are located within the transportation catchment), traffic density and vehicle speed (De Silva et al., 2016; Revitt et al., 2014).

Our study found out there was no significant difference between results of commercial and transportation land uses, it means for conducting a stormwater quality program within urban areas, only one of these two land uses must be monitored, and there is no need to monitor 6 land uses. The regression equation estimates annual pollutant loads for TSS, TP, and TN as a function of annual rainfall depth. Although some measurements are required for verifying the model, we envision our model and this methodology for developing a general equation can be valid in many coastal urban areas of the country.

3.5 Conclusion

This study conducted to describe the water quality characteristics of stormwater constituents across a coastal urban area. The City of Virginia Beach is one of several large

coastal cities draining to the CB, directly. Thirty storm runoff samples were collected during a 1-year monitoring period from a six land uses (i.e. commercial, industrial, transportation, open space, low density residential, and high density residential) and were analyzed for TSS, TP, TN, TKN, NO_3, and PO_4. The SWMM was used to assess runoff, and pollutant loads, and then estimate annual loading for a typical watershed in the City of Virginia Beach.

Water quality results indicated that TSS EMCs from park and industrial runoff was greater than other land uses. The TP EMC from park and low density residential was greater than other land uses, most of these two land uses were covered by grass and trees. The highest TN EMCs were related to transportation and industrial land uses, and the lowest were related to park and low density residential land uses, respectively. Thus, there is a direct relationship between TN EMCs and percentage of imperviousness, and TP EMCs and portion of the catchment covered by turf.

PCA analyses indicated that the three rainfall parameters PDe, MPI, and API were correlated with each other and with TSS. There is strong correlation between TP and PO_4, which would mean that most P is primarily in phosphate form. There is also strong correlation between TN and TKN. PDu was correlated with TP and PO_4. Rainfall intensity and duration play a significant role in pollutant washoff, because high intensity and duration of rainfall lead to a greater kinetic energy release in the ensuing runoff (Whitney et al., 2015; Yousefi et al., 2017).

Based on calibration/validation results, SWMM was able to quantify the runoff quantity and quality from coastal urban areas reasonably well applying the EMC method. In addition, an equation was developed and verified by 10-year SWMM simulation (2009–2019), to estimate loads for TSS, TP, and TN by multiplying runoff volume by EMC. Results indicate that annual TSS, TN and TP load per km^2 within during storm events ranged from 9300 to 12100, 325 to

425, and 106 to 138 $kg \cdot yr^{-1} \cdot km^{-2}$. In addition, average pollutant loads within urban coastal areas for TSS, TP, and TN were calculated as 0.86, 0.03, and 0.01 $kg \cdot ha^{-1} \cdot cm^{-1}$, respectively.

3.6 References for Chapter 3

Alberto, A., St-Hilaire, A., Courtenay, S.C., van den Heuvel, M.R., 2016. Monitoring stream sediment loads in response to agriculture in Prince Edward Island, Canada. Environ. Monit. Assess. doi:10.1007/s10661-016-5411-3

Badruzzaman, M., Pinzon, J., Oppenheimer, J., Jacangelo, J.G., 2012. Sources of nutrients impacting surface waters in Florida: A review. J. Environ. Manage. 109, 80–92. doi:10.1016/j.jenvman.2012.04.040

Basha, H.A., 2011. Infiltration models for soil profiles bounded by a water table. Water Resour. Res. 47. doi:10.1029/2011WR010872

Beckert, K.A., Fisher, T.R., O'Neil, J.M., Jesien, R. V., 2011. Characterization and Comparison of Stream Nutrients, Land Use, and Loading Patterns in Maryland Coastal Bay Watersheds. Water, Air, Soil Pollut. 221, 255–273. doi:10.1007/s11270-011-0788-7

Beelen, R., Hoek, G., Raaschou-Nielsen, O., Stafoggia, M., Andersen, Z.J., Weinmayr, G., Hoffmann, B., Wolf, K., Samoli, E., Fischer, P.H., Nieuwenhuijsen, M.J., Xun, W.W., Katsouyanni, K., Dimakopoulou, K., Marcon, A., Vartiainen, E., Lanki, T., Yli-Tuomi, T., Oftedal, B., Schwarze, P.E., Nafstad, P., De Faire, U., Pedersen, N.L., Östenson, C.-G., Fratiglioni, L., Penell, J., Korek, M., Pershagen, G., Eriksen, K.T., Overvad, K., Sørensen, M., Eeftens, M., Peeters, P.H., Meliefste, K., Wang, M., Bueno-de-Mesquita, H.B., Sugiri, D., Krämer, U., Heinrich, J., de Hoogh, K., Key, T., Peters, A., Hampel, R., Concin, H., Nagel, G., Jaensch, A., Ineichen, A., Tsai, M.-Y., Schaffner, E., Probst-Hensch, N.M., Schindler, C., Ragettli, M.S., Vilier, A., Clavel-Chapelon, F., Declercq, C., Ricceri, F., Sacerdote, C., Galassi, C., Migliore, E., Ranzi, A., Cesaroni, G., Badaloni, C., Forastiere, F., Katsoulis, M., Trichopoulou, A., Keuken, M., Jedynska, A., Kooter, I.M., Kukkonen, J., Sokhi, R.S., Vineis, P., Brunekreef, B., 2015. Natural Cause Mortality and Long-Term Exposure to Particle Components: An Analysis of 19 European Cohorts within the Multi-Center ESCAPE Project. Environ. Health Perspect. 123, 525–33. doi:10.1289/ehp.1408095

Bettez, N.D., Groffman, P.M., 2012. Denitrification Potential in Stormwater Control Structures and Natural Riparian Zones in an Urban Landscape. Environ. Sci. Technol. 46, 10909–10917. doi:10.1021/es301409z

Burant, A., Selbig, W., Furlong, E.T., Higgins, C.P., 2018. Trace organic contaminants in urban runoff : Associations with urban. Environ. Pollut. 242, 2068–2077. doi:10.1016/j.envpol.2018.06.066

Chapman, C., Horner, R.R., 2010. Performance Assessment of a Street-Drainage Bioretention System. Water Environ. Res. 82, 109–119. doi:10.2175/106143009x426112

Chen, J., Theller, L., Gitau, M.W., Engel, B.A., Harbor, J.M., 2017. Urbanization impacts on surface runoff of the contiguous United States. J. Environ. Manage. 187, 470–481. doi:10.1016/J.JENVMAN.2016.11.017

Chernick, M.R., 2008. Bootstrap methods : a guide for practitioners and researchers. Wiley-Interscience.

De Leon, D., Lowe, J., 2009. Standard operating procedure for automatic sampling for stormwater monitoring 42.

De Silva, S., Ball, A.S., Huynh, T., Reichman, S.M., 2016. Metal accumulation in roadside soil in Melbourne, Australia: Effect of road age, traffic density and vehicular speed. Environ. Pollut. 208, 102–109. doi:10.1016/j.envpol.2015.09.032
Duda, P.B., Hummel, P.R., Donigian, A.S.J., Imhoff, J.C., 2012. Basins/HSPF: model use, calibration, and validation. Trans. Asabe 55, 1523–1547. doi:10.13031/2013.42261
Espinasse, B., Picolet, G., Chouraqui, E., 1997. Negotiation support systems: A multi-criteria and multi-agent approach. Eur. J. Oper. Res. 103, 389–409. doi:10.1016/S0377-2217(97)00127-6
Gold, A.C., Thompson, S.P., Piehler, M.F., 2017. Coastal stormwater wet pond sediment nitrogen dynamics. Sci. Total Environ. 609, 672–681. doi:10.1016/j.scitotenv.2017.07.213
Goonetilleke, A., Egodawatta, P., Kitchen, B., 2009. Evaluation of pollutant build-up and wash-off from selected land uses at the Port of Brisbane, Australia. Mar. Pollut. Bull. 58, 213–221. doi:10.1016/j.marpolbul.2008.09.025
Goossens, D., 2008. Techniques to measure grain-size distributions of loamy sediments: A comparative study of ten instruments for wet analysis. Sedimentology 55, 65–96. doi:10.1111/j.1365-3091.2007.00893.x
Gottselig, N., Nischwitz, V., Meyn, T., Amelung, W., Bol, R., Halle, C., Vereecken, H., Siemens, J., Klumpp, E., 2017. Phosphorus Binding to Nanoparticles and Colloids in Forest Stream Waters. Vadose Zo. J. 16, vzj2016.07.0064. doi:10.2136/vzj2016.07.0064
Hecke, T. Van, 2012. Power study of anova versus Kruskal-Wallis test. J. Stat. Manag. Syst. 15, 241–247. doi:10.1080/09720510.2012.10701623
Hirschman, D., Collins, K., Schueler, T., 2008. Technical memorandum: The tunoff reduction method, Center for Watershed Protection & Chesapeake Stormwater Network.
Hupp, C.R., 2000. Hydrology, geomorphology and vegetation of costal plain rivers in the south-eastern USA. Hydrol. Process. 14, 2991–3010. doi:10.1002/1099-1085(200011/12)14:16/17<2991::AID-HYP131>3.0.CO;2-H
Johnson, R.D., Sample, D.J., 2017. A semi-distributed model for locating stormwater best management practices in coastal environments. Environ. Model. Softw. 91, 70–86. doi:10.1016/j.envsoft.2017.01.015
Ketabchy, M., Sample, D.J., Wynn-Thompson, T., Nayeb Yazdi, M., 2018. Thermal Evaluation of Urbanization Using a Hybrid Approach. J. Environ. Manage. 226, 457–475. doi:10.1016/J.JENVMAN.2018.08.016
Kokot, S., Grigg, M., Panayiotou, H., Phuong, T.D., 1998. Data Interpretation by some Common Chemometrics Methods. Electroanalysis 10, 1081–1088. doi:10.1002/(SICI)1521-4109(199811)10:16<1081::AID-ELAN1081>3.0.CO;2-X
Li, D., Wan, J., Ma, Y., Wang, Y., Huang, M., Chen, Y., 2015. Stormwater runoff pollutant loading distributions and their correlation with rainfall and catchment characteristics in a rapidly industrialized city. PLoS One 10, 1–17. doi:10.1371/journal.pone.0118776
Liu, A., Egodawatta, P., Guan, Y., Goonetilleke, A., 2013. Influence of rainfall and catchment characteristics on urban stormwater quality. Sci. Total Environ. 444, 255–262. doi:10.1016/j.scitotenv.2012.11.053
Liu, A., Goonetilleke, A., Egodawatta, P., 2015. Role of Rainfall and Catchment Characteristicson Urban Stormwater Quality.
Locatelli, L., Mark, O., Mikkelsen, P.S., Arnbjerg-Nielsen, K., Deletic, A., Roldin, M., Binning, P.J., 2017. Hydrologic impact of urbanization with extensive stormwater infiltration. J. Hydrol. 544, 524–537. doi:10.1016/J.JHYDROL.2016.11.030

Lucke, T., Drapper, D., Hornbuckle, A., 2018. Urban stormwater characterisation and nitrogen composition from lot-scale catchments — New management implications. Sci. Total Environ. doi:10.1016/j.scitotenv.2017.11.105
Lucke, T., Nichols, P.W.B., 2015. The pollution removal and stormwater reduction performance of street-side bioretention basins after ten years in operation. Sci. Total Environ. 536, 784–792. doi:10.1016/j.scitotenv.2015.07.142
Mahbub, P., Goonetilleke, A., Ayoko, G.A., Egodawatta, P., 2011. Effects of climate change on the wash-off of volatile organic compounds from urban roads. Sci. Total Environ. 409, 3934–3942. doi:10.1016/j.scitotenv.2011.06.032
Métadier, M., Bertrand-Krajewski, J.L., 2012. The use of long-term on-line turbidity measurements for the calculation of urban stormwater pollutant concentrations, loads, pollutographs and intra-event fluxes. Water Res. 46, 6836–6856. doi:10.1016/j.watres.2011.12.030
Miguntanna, N.P., Liu, A., Egodawatta, P., Goonetilleke, A., 2013. Characterising nutrients wash-off for effective urban stormwater treatment design. J. Environ. Manage. 120, 61–67. doi:10.1016/j.jenvman.2013.02.027
Moriasi, D.N., Gitau, M.W., Pai, N., Daggupati, P., 2015. Hydrologic and Water Quality Models: Performance Measures and Evaluation Criteria. Trans. ASABE 58, 1763–1785. doi:10.13031/trans.58.10715
Müller, A., Österlund, H., Marsalek, J., Viklander, M., 2020. The pollution conveyed by urban runoff: A review of sources. Sci. Total Environ. doi:10.1016/j.scitotenv.2019.136125
Munõz-Carpena, R., Lauvernet, C., Carluer, N., 2018. Shallow water table effects on water, sediment, and pesticide transport in vegetative filter strips-Part 1: Nonuniform infiltration and soil water redistribution. Hydrol. Earth Syst. Sci. 22, 53–70. doi:10.5194/hess-22-53-2018
Nayeb Yazdi, M., Ketabchy, M., Sample, D.J., Scott, D., Liao, H., 2019. An evaluation of HSPF and SWMM for simulating streamflow regimes in an urban watershed. Environ. Model. Softw. 118, 211–225. doi:10.1016/J.ENVSOFT.2019.05.008
Newman, M.C., Ownby, D.R., Mézin, L.C.A., Powell, D.C., Christensen, T.R.L., Lerberg, S.B., Anderson, B.-A., 2000. Applying species-sensitivity distributions in ecological risk assessment: Assumptions of distribution type and sufficient numbers of species. Environ. Toxicol. Chem. 19, 508–515. doi:10.1002/etc.5620190233
NOAA, 2017. American population lives near the coast [WWW Document]. Natl. Ocean. Atmos. Adm. URL https://oceanservice.noaa.gov/facts/population.html
Phillips, J.D., Slattery, M.C., 2006. Sediment storage, sea level, and sediment delivery to the ocean by coastal plain rivers. Prog. Phys. Geogr. 30, 513–530. doi:10.1191/0309133306pp494ra
Pitt, R.E., Maestre, A., Hyche, H., Togawa, N., 2008. The updated stormwater quality database (NSQD), version 3. Proc. Water Environ. Fed. 16, 1007–1026.
Revitt, D.M., Lundy, L., Coulon, F., Fairley, M., 2014. The sources, impact and management of car park runoff pollution: A review. J. Environ. Manage. doi:10.1016/j.jenvman.2014.05.041
River, M., Richardson, C.J., 2018. Particle size distribution predicts particulate phosphorus removal. Ambio 47, 124–133. doi:10.1007/s13280-017-0981-z
Rosburg, T.T., Nelson, P.A., Bledsoe, B.P., 2017. Effects of Urbanization on Flow Duration and Stream Flashiness: A Case Study of Puget Sound Streams, Western Washington, USA.

JAWRA J. Am. Water Resour. Assoc. 53, 493–507. doi:10.1111/1752-1688.12511
Russell, K.L., Vietz, G.J., Fletcher, T.D., 2018. Urban catchment runoff increases bedload sediment yield and particle size in stream channels. Anthropocene 23, 53–66. doi:10.1016/j.ancene.2018.09.001
Schiff, K., Tiefenthaler, L., Bay, S., Greenstein, D., 2016. Effects of Rainfall Intensity and Duration on the First Flush from Parking Lots. Water 8, 320. doi:10.3390/w8080320
Schueler, T.R., 1987. Controlling urban runoff: A practical manual for planning and designing urban BMPs. Water Resour. Publ.
Selbig, W.R., Bannerman, R.T., 2011. Ratios of Total Suspended Solids to Suspended Sediment Concentrations by Particle Size. J. Environ. Eng. 137, 1075–1081. doi:10.1061/(asce)ee.1943-7870.0000414
Seong, C., Herand, Y., Benham, B.L., 2015. Automatic calibration tool for hydrologic simulation program-FORTRAN using a shuffled complex evolution algorithm. Water (Switzerland) 7, 503–527. doi:10.3390/w7020503
Shammaa, Y., Zhu, D.Z., 2001. Techniques for Controlling Total Suspended Solids in Stormwater Runoff. Can. Water Resour. J. 26, 359–375. doi:10.4296/cwrj2603359
Smith, D.P., Matthew E. McKenzie, Craig Bowe, Dean F. Martin, 2004. Uptake of phosphate and nitrate using laboratory cultures of Lemna minor L. Florida Sci. 67, 105–117.
Smullen, J.T., Shallcross, A.L., Cave, K.A., 1999. Updating the U.S. Nationwide Urban runoff quality data base. Water Sci. Technol. 39.
Sun, S., Barraud, S., Castebrunet, H., Aubin, J.B., Marmonier, P., 2015. Long-term stormwater quantity and quality analysis using continuous measurements in a French urban catchment. Water Res. 85, 432–442. doi:10.1016/j.watres.2015.08.054
Terando, A.J., Costanza, J., Belyea, C., Dunn, R.R., McKerrow, A., Collazo, J.A., 2014. The Southern Megalopolis: Using the Past to Predict the Future of Urban Sprawl in the Southeast U.S. PLoS One 9, e102261. doi:10.1371/journal.pone.0102261
Toor, G.S., Occhipinti, M.L., Yang, Y.Y., Majcherek, T., Haver, D., Oki, L., 2017. Managing urban runoff in residential neighborhoods: Nitrogen and phosphorus in lawn irrigation driven runoff. PLoS One 12, 1–17. doi:10.1371/journal.pone.0179151
USEPA, 2018. Storm Water Management Model (SWMM) [WWW Document]. URL https://www.epa.gov/water-research/storm-water-management-model-swmm (accessed 1.11.19).
USEPA, 2014. Hydrological Simulation Program - FORTRAN (HSPF).
USEPA, 1992. NPDES storm water sampling guidance document [WWW Document]. United States Environ. Prot. Agency.
USEPA, 1983. Results of the Nationwide National Urban Runoff Program: Volume 1 - Final Report [WWW Document]. United States Environ. Prot. Agency. URL https://www3.epa.gov/npdes/pubs/sw_nurp_exec_summary.pdf
W. C. Krumbein, W.C., 1934. Size Frequency Distributions of Sediments. SEPM J. Sediment. Res. Vol. 4, 65–77. doi:10.1306/D4268EB9-2B26-11D7-8648000102C1865D
Wang, C.Y., Sample, D.J., 2013. Assessing floating treatment wetlands nutrient removal performance through a first order kinetics model and statistical inference. Ecol. Eng. 61, 292–302. doi:10.1016/j.ecoleng.2013.09.019
Whitney, J.W., Glancy, P.A., Buckingham, S.E., Ehrenberg, A.C., 2015. Effects of rapid urbanization on streamflow, erosion, and sedimentation in a desert stream in the American Southwest. Anthropocene 10, 29–42. doi:10.1016/J.ANCENE.2015.09.002

Winston, R.J., Hunt, W.F., 2017. Characterizing Runoff from Roads: Particle Size Distributions, Nutrients, and Gross Solids. J. Environ. Eng. 143, 04016074–12. doi:10.1061/(ASCE)EE.1943-7870.0001148

Yang, Y.-Y., Toor, G.S., 2017. Sources and mechanisms of nitrate and orthophosphate transport in urban stormwater runoff from residential catchments. Water Res. 112, 176–184. doi:10.1016/j.watres.2017.01.039

Yazdi, M.N., Sample, D.J., Scott, D., Owen, J.S., 2018. Water Quality Characterization of Irrigation and Storm Runoff for a Nursery. Springer, Cham, pp. 788–793. doi:10.1007/978-3-319-99867-1_136

Yoon, S.W., Chung, S.W., Oh, D.G., Lee, J.W., 2010. Monitoring of non-point source pollutants load from a mixed forest land use. J. Environ. Sci. 22, 801–805. doi:10.1016/S1001-0742(09)60180-7

Yousefi, S., Moradi, H.R., Keesstra, S., Pourghasemi, H.R., Navratil, O., Hooke, J., 2017. Effects of urbanization on river morphology of the Talar River, Mazandarn Province, Iran. Geocarto Int. 1–17. doi:10.1080/10106049.2017.1386722

Chapter 4. Water Quality Characterization of Storm and Irrigation Runoff from a Container Nursery

Mohammad Nayeb Yazdi, David J. Sample, Durelle Scott, James S. Owen, Mehdi Ketabchy, and Nasrin Alamdari

Submitted: December 2018

To: *Science of The Total Environment*

Status: Published February 2019. DOI: 10.1016/j.scitotenv.2019.02.326

Abstract

Commercial nurseries grow specialty crops for resale using a variety of methods, including containerized production, utilizing soilless substrate, on a semipervious production surface. These "container" nurseries require daily water application and continuous availability of mineral nutrients. These factors can generate significant nutrients [total nitrogen (TN), and total phosphorus (TP)] and sediment [total suspended solids (TSS)] in runoff, potentially contributing to eutrophication of downstream water bodies. Runoff is collected in large ponds known as tailwater recovery basins for treatment and reuse or discharge to receiving streams. We characterized TSS, TN, and TP, electrical conductivity (EC), and pH in runoff from a 5.2 ha production portion of a 200-ha commercial container nursery during storm and irrigation events. Results showed a direct correlation between TN and TP, runoff and TSS, TN and EC, and between flow and pH. The Storm Water Management Model (SWMM) was used to characterize runoff quantity and quality of the site. We found during irrigation events that simulated event mean concentrations (EMCs) of TSS, TN, and TP were 30, 3.1 and 0.35 $mg \cdot L^{-1}$, respectively. During storm events, TSS, TN and TP EMCs were 880, 3.7, and 0.46 $mg \cdot L^{-1}$, respectively.

EMCs of TN and TP were similar to that of urban runoff; however, the TSS EMC from nursery runoff was 2-4 times greater. The average loading of TSS, TN and TP during storm events was approximately 900, 35 and 50 times higher than those of irrigation events, respectively. Based on a 10-year SWMM simulation (2008-2018) of runoff from the same nursery, annual TSS, TN and TP load per ha during storm events ranged from 9,230 to 13,300, 65.8 to 94.0 and 9.00 to 12.9 $kg \cdot ha^{-1} \cdot yr^{-1}$, respectively. SWMM was able to characterize runoff quality and quantity reasonably well. Thus, it is suitable for characterizing runoff loadings from container nurseries.

Keywords: container nursery; irrigation runoff; storm runoff, water quality, Storm Water Management Model (SWMM); eutrophication

4.1 Introduction

Agricultural runoff is the principal contributor to non-point source (NPS) pollution and subsequent impairments of streams, rivers, lakes, and estuaries (Carpenter et al., 1998; Chen et al., 2017; Liu et al., 2014). Agriculture is a major source of sediment, nitrogen (N) and phosphorus (P) loading to receiving waters due to excessive fertilizer, irrigation, and erosion from soil tillage (Hu and Huang, 2014; McDowell and Laurenson, 2014; Novotny, 2003; Zhang et al., 2015). Commercial nurseries yield marketable specialty crops of all sizes; 40% of which are produced in the ground, and 60% in containers (USDA-NASS, 2014). Nurseries are often located on affordable land on the fringe of urban areas for proximity to customers (Gant et al., 2011; Heimlich and Anderson, 2001). Container use in nurseries has become common due to their low cost and faster rates of growth in crop production (Majsztrik et al., 2011). “Container crops” are grown above ground, on a production surface known as a “pad” in containers using a soilless substrate with little water or nutrient retention capacity (Majsztrik et al., 2017).

Container nurseries produce a higher volume of runoff than field (in-ground) nurseries because of: (1) the porous nature and low water storage capacity of soilless substrates, (2) low container density per unit area, (3) mineral nutrients delivered using a multi-month controlled release fertilizer, sometimes supplemented through application of water soluble nutrients via overhead irrigation, and (4) the relative impermeability of the gravel and geotextile covered pads between gravel or bare soil roadways (Majsztrik et al., 2017). Nursery runoff carries sediment and fertilizer, namely N and P, making nurseries a potential contributor of NPS (Majsztrik et al., 2011; Mangiafico et al., 2009; White et al., 2011, 2010). The fate and transport of irrigation and storm runoff pollutants from a container nursery depends on precipitation, soil characteristics, slope, timing of storm or irrigation events, and antecedent dry period (Chen et al., 2016; Guo et al., 2014; Majsztrik et al., 2017; Yi et al., 2015).

Eutrophication in the Chesapeake Bay prompted the development of a total maximum daily load (TMDL), which limits discharges of nutrient and sediment loads from all sources, including agriculture watersheds (USEPA, 2010). Studies conducted on nurseries have shown that during the growing season, concentrations of total suspended solids (TSS), total N (TN), and total P (TP) in runoff are considerable, TP and TN have been reported to range from .41 - 8.27 $mg \cdot L^{-1}$ and 8.27 - 21.7 $mg \cdot L^{-1}$, respectively (Taylor et al., 2006; White et al., 2011). The recommended best management practice (BMP) for container nurseries in the Chesapeake Bay watershed is capturing 95% of the production area runoff from the first 1.27 to 2.54 cm of rainfall through installation of ponds, known as tailwater recover basins (TRBs) for the purpose of reducing sediment and nutrients loads (Bilderback et al., 2013; Mack et al., 2017; USEPA, 2010, 2005, VDEQ, 2012, 2010).

Our underlying assumption, based upon visual observation of runoff from a number of container nurseries, is that runoff from production areas is flashy, i.e., similar to runoff from urban areas, requiring sub hourly temporal resolution for accurate monitoring and subsequent modeling. The Storm Water Management Model (SWMM) (Rossman, 2010) is typically applied to urban watersheds with high imperviousness and a defined conveyance system of pipes and/or ditches (Guan et al., 2015; Moore et al., 2017; Palla and Gnecco, 2015) similar to that observed in container nurseries. SWMM has been applied across a wide range of watershed sizes, from large (Alamdari et al., 2017) to small (Lucas and Sample, 2015); and from urban to forested conditions (Tsai et al., 2017). Based upon the underlying assumption of a "flashy" hydrograph from nursery production areas, and the presence of runoff collection ditches, it was assumed that SWMM would be suitable for characterizing container nursery runoff. As part of the water balance of the nursery, irrigation needs to be accounted for and incorporated into the hydrologic model; fortunately, two previous studies developed methods which can be used this purpose (Sample and Heaney, 2006; Schoenfelder et al., 2006).

Despite being a potential source of NPS pollution, to date there have been only a few on-farm research studies that characterized water quality of nursery runoff (Fernandez et al., 2009; Hoskins et al., 2014b, 2014a; Mangiafico et al., 2008; Million et al., 2007; Million and Yeager, 2015; Newman et al., 2006; Owen et al., 2008; Ristvey et al., 2004). These studies assessed environmental impacts of varying irrigation, fertility, substrate, and plant spacing practices and lifecycle costs of operational changes. Development and application of computational models to characterize nurseries at larger scales could provide a more general understanding of fate and transport of runoff from nurseries, and help decision makers improve management of water quality before collection and reuse on their crop or discharge to the environment. This paper is

the first study that has modeled runoff quantity and quality at a nursery based upon collected data for calibration and validation.

The objectives of this study were (1) to characterize irrigation and storm runoff quantity and quality at a Mid-Atlantic nursery site; (2) to evaluate the ability of SWMM to simulate hydrology and water quality of runoff from the main production areas of that site; (3) to estimate average annual loading of TSS, TN, and TP from a container nursery production area for use in water quality planning. To achieve these goals, we conducted field monitoring during selected irrigation and storm events within a container nursery site in the Mid-Atlantic region; from this effort, we estimated event mean concentrations (EMCs) of TSS, TP and TN from five storm and seven irrigation events. A SWMM model was developed, calibrated and validated using the monitoring data collected during this study and then used to generate annual TSS, TN, and TP loads. The novelty of this research is the application of a hydrologic/water quality model to characterize runoff from a nursery site. Models such as SWMM can facilitate assessment of potential treatment options such as TRBs, and thus could become extremely valuable planning tools for the container nursery industry.

4.2 Methodology

4.2.1 Field measurements and sampling site

An anonymous container nursery in the Mid-Atlantic US was selected for this study (Figure 4.1). The nursery area is 200 ha, including forest (36 ha), ponds (12 ha), production areas or pads (38.5 ha), open areas, roads and buildings. The production areas drain to a downgradient TRB, which collects, stores, and treats runoff for later reuse; some treated runoff and baseflow is discharged. Approximately 20% of the nursery site is used for container production. Based upon field observation during storm events, we assumed that the pads were 100% impervious. While

desirable, performing a double ring infiltrometer test was not feasible for testing the pad due to access issues, the degree of soil compaction, and concerns of potential damage to the underlying geotextile membrane. A geodatabase of the site was developed using publicly accessible Geographic Information System (GIS) data, soils data from the Natural Resources Conservations Service (NRCS) Soil Survey Geographic database (SSURGO) (NRCS, 1999), 0.6-meter contour elevations and aerial photography which were used to delineate subwatersheds across the site. Based on watershed delineation, a downgradient monitoring site was selected (Figure 4.1).

The contributing drainage area upstream of the monitoring station was 5.2 ha, which consisted of 1.8 ha of roads and 3.4 ha of container pads, all of which drain to a central receiving

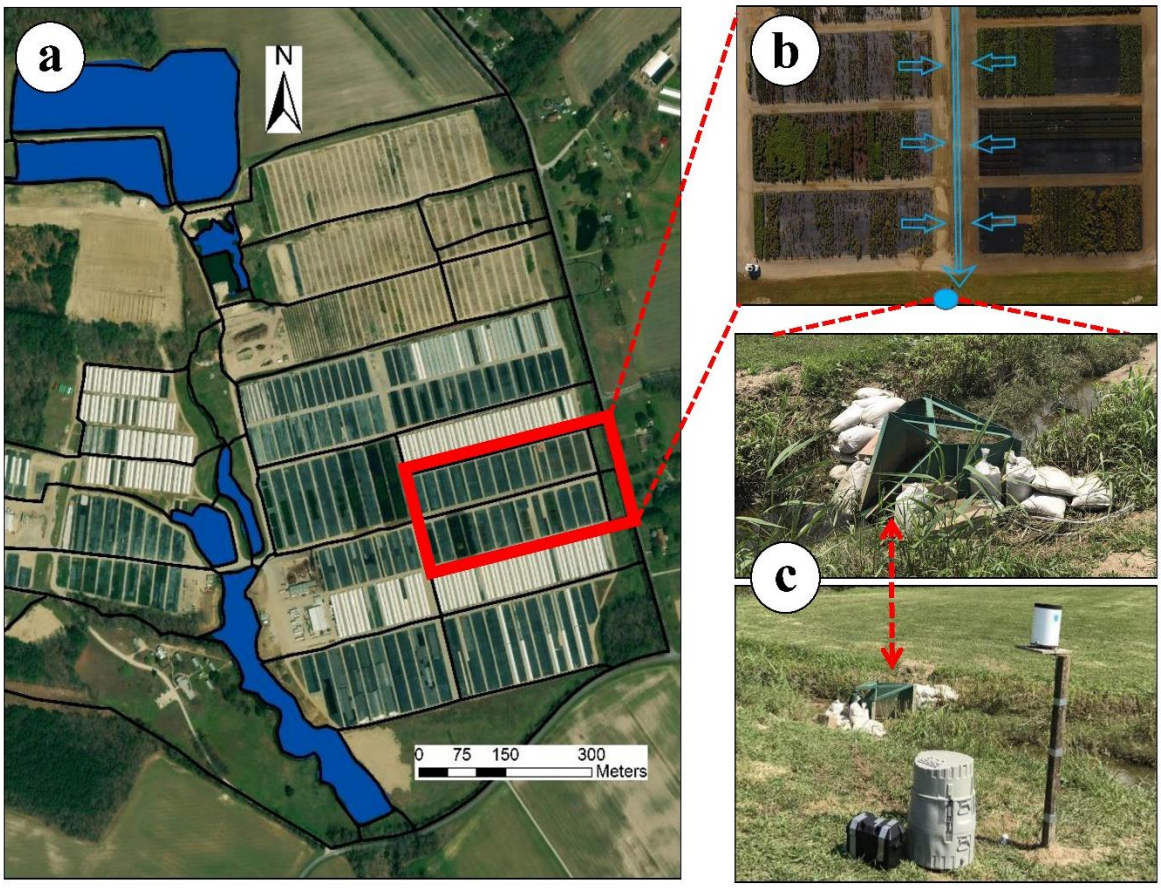

Figure 4.1. Location map of (a) monitoring site (b) pads and monitoring site outlet (c) H flume, automatic sampler, and rain gage.

ditch. The ditch drains runoff to the outlet of the monitoring site at which a 0.61 m H-flume with maximum flow capacity of 350 $L \cdot s^{-1}$ (Teledyne, 2011), an automatic sampler (model 6712; ISCO, Lincoln, Nebraska), a rain gauge (model 674; ISCO), and an bubbler flow meter (model 730; ISCO) were installed for measuring flows and collecting equal volume samples across irrigation and storm runoff hydrographs. An H-flume was selected due to its ability to accurately measure a large range of flows and prevent clogging. However, the access road and receiving ditch were regraded frequently, often with placement of new road base, leading to significant erosion and sediment deposition downstream, including in the H-flume, necessitating frequent maintenance after each storm event. Samples taken across the hydrograph were either composited or individually analyzed for five storm and seven irrigation events, to characterize runoff quality of the nursery. Samples were stored in 1 L polyethylene bottles (ISCO), which had been acid-washed by sulfuric acid and pre-rinsed three times with deionized water (USEPA, 1992). Irrigation and storm runoff samples were transported from the nursery to the laboratory within 1 hr. Samples were then analyzed for pH and electrical conductivity (EC) within 10 hrs. of collection, filtered for determination of TSS (USEPA, 1992), and were then frozen at < 0°C (USEPA, 1992) until analyzed for TN and TP applying automated flow injection analysis immediately following persulfate digestion (QuickChem® Method 10-107-04-4B and 10-115-01-4B; Lachat Instruments, Loveland, CO, USA).

4.2.2 Sample collection methods

Monitoring for irrigation and storm events was conducted in August, September, and October 2017, and May and July 2018; during two production or growing seasons. During this time span, runoff samples were collected during seven irrigation and five storm events. Monitoring was stopped during winter months when irrigation ceased, crops were not actively

growing, and container plants were consolidated, spaced, and grouped to reduce winter damage. The drainage area upstream of the monitoring site included 26 unique production areas within 52 irrigation zones that applied water at a rate of 4 $mm \cdot hr^{-1}$ on the site production areas and gravel-covered roads between them, each hosting different ornamental evergreen and deciduous shrubs in primarily 30 cm diameter, 11.3 L (3.7 – 18.9 L) spaced containers; space is typically left between each container to maximize growth. Plants were normally grouped based on size or water needs. Based upon field observation, approximately 70% of the pads were covered by plant containers during the study; however, actual land coverage and subsequent water interception efficiency of the target crop and container was <40% due to the effect of spacing. For purposes of our study, we assumed the differential due to differing vegetation species was small, and thus could be neglected in this initial research. Irrigation duration is typically determined for each watering zone based on plant need of the driest or most critical plant by the nursery operator. A bucket was placed on each pad to collect and measure quantity of water delivered via irrigation. Precipitation volume was checked by a randomly placed rain gauge that also provided the start and end time of irrigation cycle(s). Irrigation normally began at 0500 HR. Irrigation and/or rainfall, and runoff during each measured event was measured by the rain gage and H-flume located at the outlet of the monitoring site, respectively. Once irrigation started and runoff was evident, the auto-sampler collected samples of irrigation runoff at 5 min. intervals. However, during storm events, the auto-sampler collected samples of runoff by collecting equal volume samples across the hydrograph using the auto-samplers peristaltic pump; this facilitates collection of a runoff volume weighted sample. Each irrigation event was characterized with 12 samples, while the number of samples during storm events varied between 5 to 15 equal volume samples. Calculation of the incremental volume during storm event and obtaining an estimate

number of bottles (for collecting samples) requires an *a priori* estimate of total runoff volume from the production area. Total volume of runoff in the contributing drainage area can be estimated by Eq. (1) (De Leon and Lowe, 2009).

$$V = \frac{PF}{100} \times RC \times A \quad (1)$$

where V is the total volume of runoff (m^3); PF is the precipitation forecast (cm); A is the watershed area (m^2) and RC is the runoff coefficient. The runoff coefficient converts rainfall to runoff volume is a function of imperviousness for each drainage area calculated by Eq. (2) (Schueler, 1987).

$$RC = 0.009 \times (percentage\ of\ impervious) + 0.05 \quad (2)$$

Approximately 65% of monitoring site was covered by production areas and the remainder by gravel roadways. All production areas were considered to be impervious. The incremental volume was estimated by dividing total volume of runoff by the number of bottles in the sampler. The auto-sampler (model 6712, ISCO) used 24×1-liter polyethylene (PE) bottles for sample collection. Thus, the number of samples for each event was related to total runoff volume for that event.

4.2.3 Runoff coefficient and time of concentration

The runoff coefficient (*RC*) converts total irrigation and/or rainfall to runoff; and was calculated by dividing the total volume of irrigation and/or storm runoff by the total volume of irrigation or rainfall that occurred during the event in question (Merz et al., 2006; Yin et al., 2017). Time of concentration (t_c) is the time needed for irrigation and storm runoff to flow from the farthest point in a drainage area or watershed to its outlet. The longest flow path is the point with the longest travel time to the watershed outlet. The t_c of the sampling site, which has many controlling factors [rainfall volume and intensity, topography, geology, and land use (Li et al.,

2018)], was estimated using two primary methods developed by the NRCS, including: (a) the velocity method, and (b) the graphical method (Green and Nelson, 2002).

The segments used in the velocity method are assumed to have three types of flow; (1) sheet, (2) shallow concentrated, and (3) open channel (Merkel, 2001). Sheet flow and shallow concentrated flow occurred within the pads, and open channel flow occurred within the ditch. A simplified version of the Manning's kinematic solution can be used to compute t_c for sheet flow, developed by Welle and Woodward, (1986) Eq. (3):

$$T_{c,sf} = \frac{1.73\ (n.L)^{0.8}}{(P_2)^{0.5}.(S)^{0.4}} \quad (3)$$

where, $T_{c,\,sf}$ is t_c for sheet flow (min.); n is Manning's roughness coefficient for overland flow; L is the sheet flow length (m) (L for sheet flow should be less than 30 m); P_2 is 2-year, 24-hour rainfall (cm); and S is the slope of the land surface as a fraction. Thus, t_c for shallow concentrated flow within the pads was calculated by Eq. (4) (NRCS, 2010).

$$T_{c,cf} = \frac{L}{6.2 \times S^{0.5}} \quad (4)$$

where $T_{c,\,cf}$ is t_c for shallow concentrated flow (min.); L is the flow length, and S is the slope of the pads. Thus, t_c for open channel flow through the ditch was calculated by Eq. (5) (Michailidi et al., 2018).

$$T_{c,d} = \frac{n \times L}{R^{\frac{2}{3}} \times S^{\frac{1}{2}}} \quad (5)$$

where R is the hydraulic radius of the ditch; S is the slope of the ditch; and n is the roughness of the ditch bed. The t_c for the monitoring site is sum of the t_c for sheet flow ($T_{c,\,sf}$) and shallow concentrated flow ($T_{c,\,cf}$) for each pad, and the t_c for the ditch ($T_{c,\,d}$) (Figure 4.2).

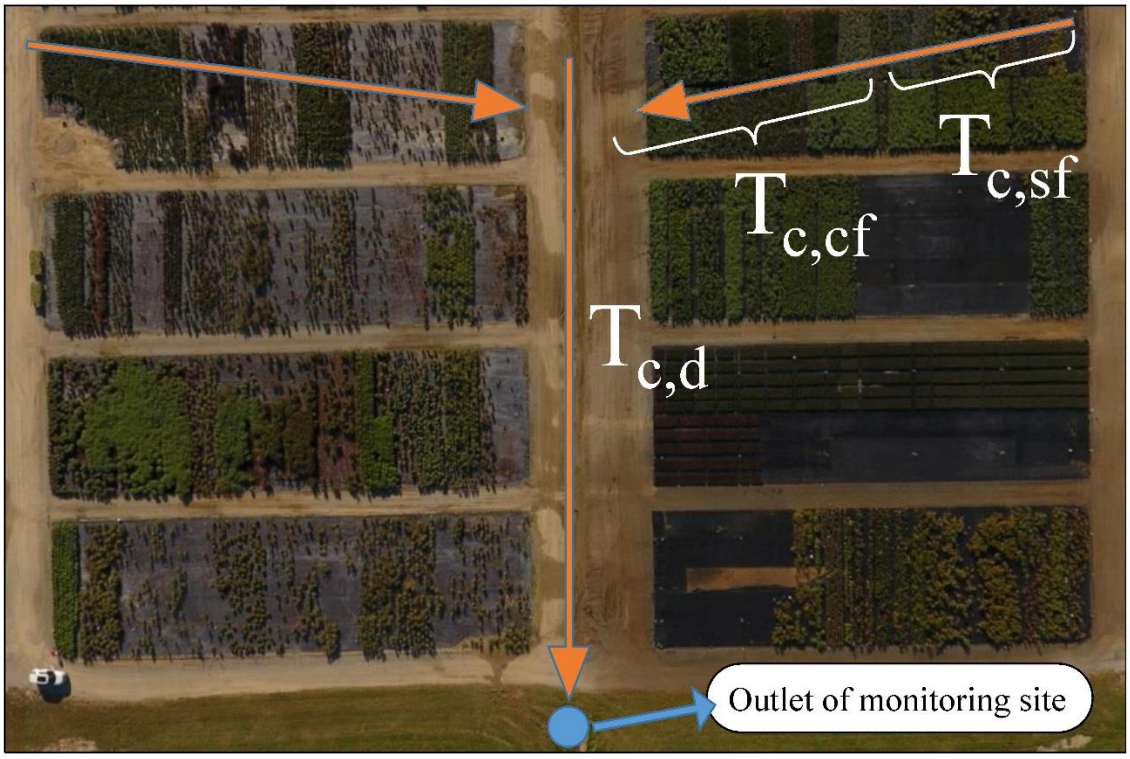

Figure 4.2. Sketch of the traveling time for sampling site.

Based on relation between lag time and t_c, the Soil Conservation Service (SCS) developed a graphical method for estimating t_c using Eq. (6) (Green and Nelson, 2002; Mishra and Singh, 2003).

$$t_c = 1.66\, t_{lag} \tag{6}$$

where t_{lag} is the time between the center of rainfall mass and the time to hydrograph peak; and t_c is the time for water to flow from the farther point within a watershed to the outlet.

4.2.4 Measuring event mean concentration

The concept of an EMC was used to characterize concentrations of NPS water pollution (Li et al., 2017; Wang et al., 2013; Yoon et al., 2010), and represents a flow weighted average concentration according to Eq. (7).

$$EMC = \frac{Total\ Constituent\ Mass}{Total\ volume\ of\ runoff} = \frac{\sum_{i=1}^{n} C_i Q_i \Delta t}{\sum_{i=1}^{n} Q_i \Delta t} = \frac{\sum_{i=1}^{n} C_i V_i}{\sum_{i=1}^{n} V_i} \tag{7}$$

where, Q_i is the runoff occurring during incremental samples ($L \cdot sec^{-1}$); C_i is the pollutant concentration during each incremental sample ($mg \cdot L^{-1}$); V_i is the volume of runoff during each incremental sample (L); t is the time (sec); and Δt is the discrete time interval of the incremental sample (sec). The EMCs for each event were then used to calculate the pollutant load flux for that event.

4.2.5 SWMM model scenario development

A SWMM Model was developed for the selected nursery sub-basin using landscape variables including property boundaries, soils characteristics, land use types, and digital elevation models obtained from the Isle of Wight County GIS Department. Other hydraulic variables (e.g. pipe inverts, diameters, ditch geometry, etc.) were directly measured. Precipitation inputs were developed from the rain gage (ISCO model 674), or a nearby weather station rain gage [WAKEFIELD, 448800, National Oceanic and Atmospheric Administration (NOAA)] for long term simulation. SWMM simulates the runoff quantity and quality for each subcatchment. Water quality is simulated within SWMM using buildup and washoff processes. Buildup is related to accumulation of pollutants on a surface during dry periods, and washoff is the process of sloughing simulated pollutants from a subcatchment surface during runoff events (Modugno et al., 2015). Direct measuring of buildup and washoff rates are difficult to obtain; normally these are assumed to be similar within the same land use. Often, runoff quality is reported only as an EMC. An EMC results from washoff of pollutants from the land surface; by definition, an EMC multiplied by runoff volume equals the mass of the pollutant washed during the event (Li et al., 2017; Wang et al., 2013). SWMM uses four methods for water quality calibration; however, the EMC and exponential buildup/washoff are the most widely used. In this study, the EMC and exponential buildup/washoff methods were applied to assess the best fit for estimating the

pollutant loads delivered from the nursery production area. The exponential buildup/washoff method requires multiple samples across a hydrograph of an irrigation or storm event to characterize how pollutants vary across the event. When calibrating based on EMC data, a composite sample for each event is sufficient; essentially the compositing process integrates concentration across the hydrograph; for more details on this procedure, see Sample et al., (2012). The exponential buildup/washoff method is given by Eq. 8 and 9

$$\mathrm{b} = B_{max} \,.\, (1 - e^{-K_B.t}) \tag{8}$$

where b is the buildup, B_{max} is the maximum buildup possible (kg), K_B is the buildup rate constant, and t is the buildup time interval (days):

$$\mathrm{W(t)} \;=\; M_b(0) \cdot (1 - e^{-K_W.q.t}) \tag{9}$$

where W is the cumulative mass of constituent washed off (kg·m^{-2}) at time t (hr), $M_b(0)$ is the initial mass of constituent on the surface (kg·m^{-2}) at time 0, K_W is washoff coefficient (cm^{-1}) and q is the runoff for the subcatchment (cm·hr^{-1}). The model was then evaluated using a group of statistical methods including: the Nash-Sutcliffe Efficiency (NSE), coefficient of determination (r^2), and Percent bias (PBIAS). Multiple statistics should be used rather than a single criterion (Ketabchy, 2018; Moriasi et al., 2015; Nayeb Yazdi et al., 2019). When the statistical parameters showed r^2 and NSE higher than 0.6 and 0.5, respectively, and PBIAS less than ±25%, the model calibration was considered complete and the calibration process stopped (Duda et al., 2012; Ketabchy et al., 2018; Seong et al., 2015); otherwise, model calibration parameters were adjusted. Annual pollutant loads were then estimated based on the calibrated SWMM model.

4.2.6 Integration of irrigation with rainfall data

A method was developed to estimate irrigation depths within each production area, and to integrate this data with precipitation for processing by SWMM. The method established a start and end time for each irrigation event and applied a pre-established irrigation volume daily to each production area. As a reflection of nursery operations, irrigation was suspended if a storm event over a given threshold occurred within a pre-established time period. An R program was developed to estimate irrigation and integrate it into a 10-year simulation (2008-2018) using precipitation data from a nearby weather station [WAKEFIELD, 448800, National Oceanic and Atmospheric Administration (NOAA)].

4.3 Results

4.3.1 Time of concentration and runoff coefficient during irrigation and storm events

Over the monitoring period, container crops were irrigated at 0500 HR for 30 to 60 min. with a solid-state impact irrigation system during the growing season. Seven irrigation and five storm events were selected. The characterization of each of these events is shown in Table 4.1.

Table 4.1. Runoff coefficient (RC) for monitoring site during irrigation and storm events.

Date	Period	Event length (min)	Depth (mm)	Intensity ($mm \cdot min^{-1}$)	Volume of irrigation/ rainfall ×100 (L)	Volume/ runoff ×100 (L)	Runoff Coefficient
Aug 7, 2017[S]	18:10-19:15	65	14.2	0.22	1,282	1,075	0.84
Sep 22, 2017[I]	5:45-6:45	60	3.46	0.06	1,170	715.0	0.61
Sep 29, 2017[I]	5:30-6:00	30	1.52	0.05	519.0	114.0	0.22
Sep 30, 2017[I]	5:15-6:15	60	2.21	0.04	753.0	294.0	0.39
Oct 01, 2017[I]	5:30-6:00	30	1.62	0.05	540.0	92.00	0.17
Oct 02, 2017[I]	5:30-6:00	30	1.76	0.06	595.0	179.0	0.30
Oct 05, 2017[I]	5:15-6:15	60	2.59	0.04	875.0	473.0	0.54
Oct 24, 2017[S]	1:25-5:10	390	18.3	0.05	1,648	1,434	0.87
May 16, 2018[S]	11:50-12:15	20	4.82	0.24	434.0	147.0	0.34
May 18, 2018[S]	12:50-13:00	10	13.0	1.3	1,172	897.0	0.76
June 03, 2018[S]	11:30-13:15	105	12.0	0.11	980.0	657.0	0.67
July 17, 2018[I]	5:15-6:15	60	2.08	0.04	621.0	176.0	0.28

[I] Irrigation event
[S] Storm event

Irrigation and storm events highlighted the variation in runoff coefficient, ranging from 0.17 to 0.61, and 0.35 to 0.87 for irrigation and storm events, respectively (Table 4.1). RC has a direct relationship with the volume of irrigation and/or rainfall, both increasing simultaneously.

The velocity method is a theoretical method that can be applied for both storm and irrigation events for estimating t_c, while the graphical method requires storm event data (lag time) to estimate t_c. Based on the velocity method, the t_c within the pads [sheet flow ($T_{c, sf}$) and shallow concentrated flow ($T_{c, cf}$)] was approximately 6 min., and the t_c for the farthest pad and outlet ($T_{c, d}$) through the ditch was approximately 21 min. Thus, total t_c ($T_{c, sf} + T_{c, cf} + T_{c, d}$) for the farthest pad (13th pad) was 27 min. Based on graphical method, lag times for two storm events (time between the center of mass precipitation and hydrograph for all storm event) was 18 min., so the total t_c for the monitoring site using the graphical method was 30 min. (Figure 4.3). Thus, the t_c for the monitoring site using two methods was estimated to be between 27 and 30 min.

4.3.2 Results of water quality characterization

During the monitoring program, we collected 130 samples (80 samples for irrigation and50 samples for storm events) over seven irrigation and five storm events. Sample analyses are

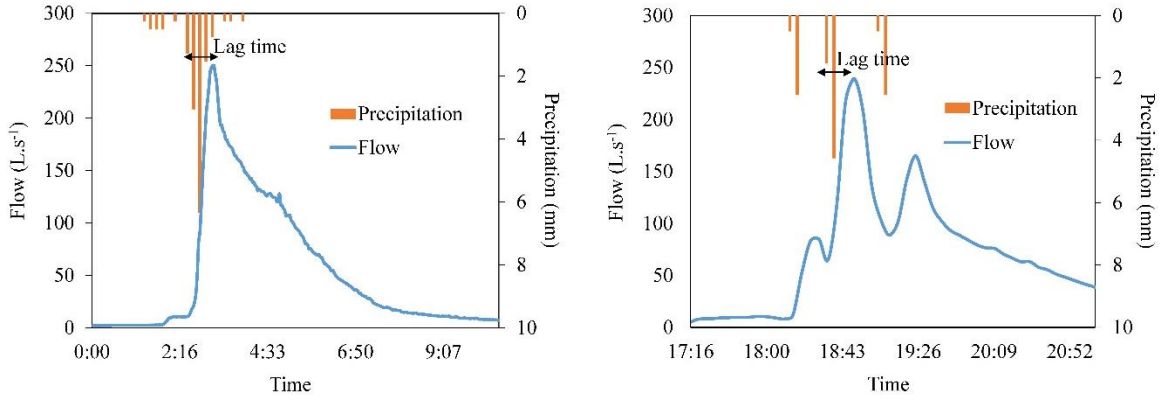

Figure 4.3. Hydrograph and precipitation of two storm events at the sampling site.

shown in Table 4.2. Results indicated that during storm events, due to higher intensity and duration of rainfall in comparison with irrigation, runoff volume and concentration of TSS were much higher than during irrigation events. On the other hand, TN and EC concentrations during storm events were less than irrigation events, most likely due to higher dilution. With respect to TP, concentrations were similar for irrigation and storm events, because in this study, most of the P likely originated from ortho-phosphate fertilizer (Shreckhise, 2018). Thus, intensity of rainfall would likely have less of an effect on concentration of TP unless it was sorbed to sediment. Since it had less the 26-30 min. of contact time, absorption to sediments was unlikely. In addition, pH varied between 7.7 – 8.7 during both events facilitating sorption or precipitation by calcium and magnesium, not metals such as iron or aluminum which are found in greater abundance in the dominant, poorly drained underlying Chickahominy silt loam (Ultisol).

Table 4.2. Results of measurements pooled across storm and irrigation events, respectively.

	Storm events	**Irrigation events**
Flow		
Mean ± SD ($L \cdot s^{-1}$)	160 ± 120	4.9 ± 4.1
Min – Max ($mg \cdot L^{-1}$)	1.6 – 432	1.0 – 16
TSS		
Mean ± SD ($mg \cdot L^{-1}$)	1,300 ± 1,300	32 ± 30
Min – Max ($mg \cdot L^{-1}$)	120 – 5,300	4.0 – 120
TN		
Mean ± SD ($mg \cdot L^{-1}$)	2.9 ± 1.4	3.4 ± 1.3
Min – Max ($mg \cdot L^{-1}$)	0.98 – 5.6	0.88 – 5.7
TP		
Mean ± SD ($mg \cdot L^{-1}$)	0.41 ± 0.15	0.41 ± 0.15
Min – Max ($mg \cdot L^{-1}$)	0.18 – 0.92	0.08 – 0.77
EC		
Mean ± SD ($uS \cdot cm^{-1}$)	270 ± 99	620 ± 42
Min – Max ($uS \cdot cm^{-1}$)	140 – 450	550 – 720
pH		
Mean ± SD	8.1 ± 0.25	8.0 ± 0.12
Min – Max	7.7 – 8.7	7.7 – 8.4

4.3.3 Correlation between all constituents

Correlation between flow, TSS, TN, TP, EC and pH are shown in Figure 4.4. For each constituent, the correlation coefficient, or *r* and p-value are presented in the upper panel of Figure 4.4; scatter plots are in the lower panels and the line in the scatter plots is a linear regression between two observed variables. Histograms with kernel density estimation are shown along the diagonal. According to Mukaka, (2012), the absolute value of *r* can be categorized as: 1) negligible correlation (below 0.30), 2) low correlation (between 0.30 and 0.50), 3) moderate correlation (between 0.50 and 0.70), and 4) high correlation (above 0.70). Based on the results, there is a direct relationship (moderate correlation) between TN and TP (*r*= 0.55), runoff and TSS (*r*= 0.57). Further, there is an inverse relationship between flow and EC (*r*= -0.82), TN and flow (*r*=-0.44) due to dilution, and TSS and EC (*r*= -0.55), and TN and TSS (*r*= -0.39). On the other hand, there was no observed relationship (negligible correlation) between TSS and TP (*r*= -0.15), substantiating our earlier assumption that phosphorus observed in runoff in this case study was mainly present in dissolved form as supported by the correlation between TP and TN. This result about dissolved forms of TP is similar to results reported by Shreckhise (2018).

4.3.4 EMCs and loads for pollutants

The EMCs and load fluxes of TSS, TP, and TN were calculated for irrigation and storm events (Table 4.3). TN and TP EMCs of nursery runoff ranged from 2.5 to 3.9 and 0.29 to 0.55 $mg \cdot L^{-1}$, respectively. The average TSS EMC for irrigation events from the nursery production area was 30 $mg \cdot L^{-1}$. The TSS EMC for storm events was 4 to 40 times greater than irrigation events. During our monitoring, there was a direct relationship between rainfall intensity and TSS

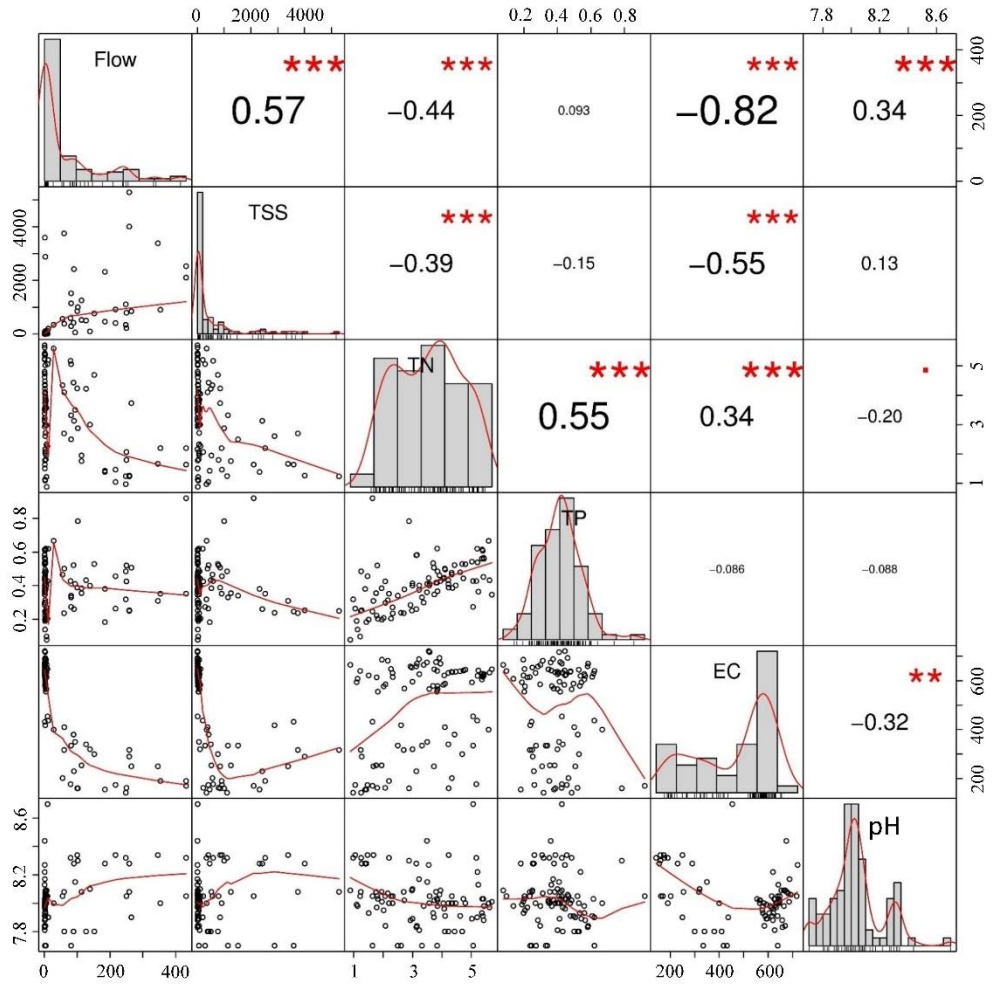

Figure 4.4. Results of correlation between all constituents. The line in the scatter plot represents simple linear regression between a pair of two variables.

EMC. For irrigation events, the highest TSS EMC was the Oct 05, 2017 irrigation runoff event with higher irrigation and peak flow, while the lowest value was in the Oct 02, 2017 irrigation event, with relatively low irrigation and peak flow. This indicates that the higher irrigation amounts can result in larger sediment transport. The average total load of TSS during irrigation and storm events was approximately 0.87 and 810 kg·day^{-1}, respectively. The average total load of TSS, TN and TP during storm events were approximately 900, 35 and 50 times higher than those of irrigation events, respectively.

Table 4.3. Estimated EMCs and pollutant load for irrigation and storm events.

Date	EMC ($mg \cdot L^{-1}$)			Load ($kg \cdot d^{-1}$)		
	TSS	TP	TN	TSS	TP	TN
Aug 7, 2017(S)	940	0.55	3.9	1600	0.52	1.9
Sep 22, 2017(I)	26	0.38	2.5	0.82	0.02	0.18
Sep 29, 2017(I)	26	0.35	3.0	0.68	0.006	0.05
Sep 30, 2017(I)	35	0.37	3.1	1.0	0.02	0.12
Oct 01, 2017(I)	27	0.36	3.8	0.25	0.004	0.03
Oct 02, 2017(I)	25	0.32	3.7	0.47	0.006	0.07
Oct 05, 2017(I)	42	0.29	2.5	1.9	0.014	0.12
Oct 24, 2017(S)	130	0.40	3.2	280	0.90	7.2
May 16, 2018(S)	1200	0.43	4.3	160	0.06	0.60
May 18, 2018(S)	1300	0.47	3.4	1200	0.45	3.2
June 03, 2018(S)	810	0.42	3.7	820	0.31	1.7
July 17, 2018(I)	30	0.37	3.2	0.98	0.008	0.09
Mean irrigation events	30	0.35	3.1	0.87	0.01	0.09
Mean storm events	880	0.46	3.7	810	0.45	2.9

(I) Irrigation event
(S) Storm event

4.3.5 Hydrologic calibration of irrigation and storm events

Goodness-of-fit was evaluated by plotting the observed vs. simulated runoff during irrigation and storm events in Figure 4.5 and 4.6, respectively. There were two time spans for irrigation, 30 and 60 min. Peak flows for irrigation events were between 2 to 7 $L \cdot s^{-1}$. SWMM was calibrated for these irrigation events based on runoff volume. r^2, NSE and PBIAS for irrigation events were 0.73, 0.68, and -8.90%, respectively, showing a good agreement between the simulated and observed values. With respect to storm events, SWMM was calibrated for the first 10 storm events during August of 2017, and validated for 16 storm events, between September 2017 and July 2018 (Figure 4.6). r^2, NSE and PBIAS for validation period were 0.71, 0.69, 19%, respectively indicating a good agreement between the simulated and observed runoff values for storm events (Figure 4.6 and 4.7). The results indicated that SWMM is able to characterize the hydrology of the production area adequately, and could be generalized.

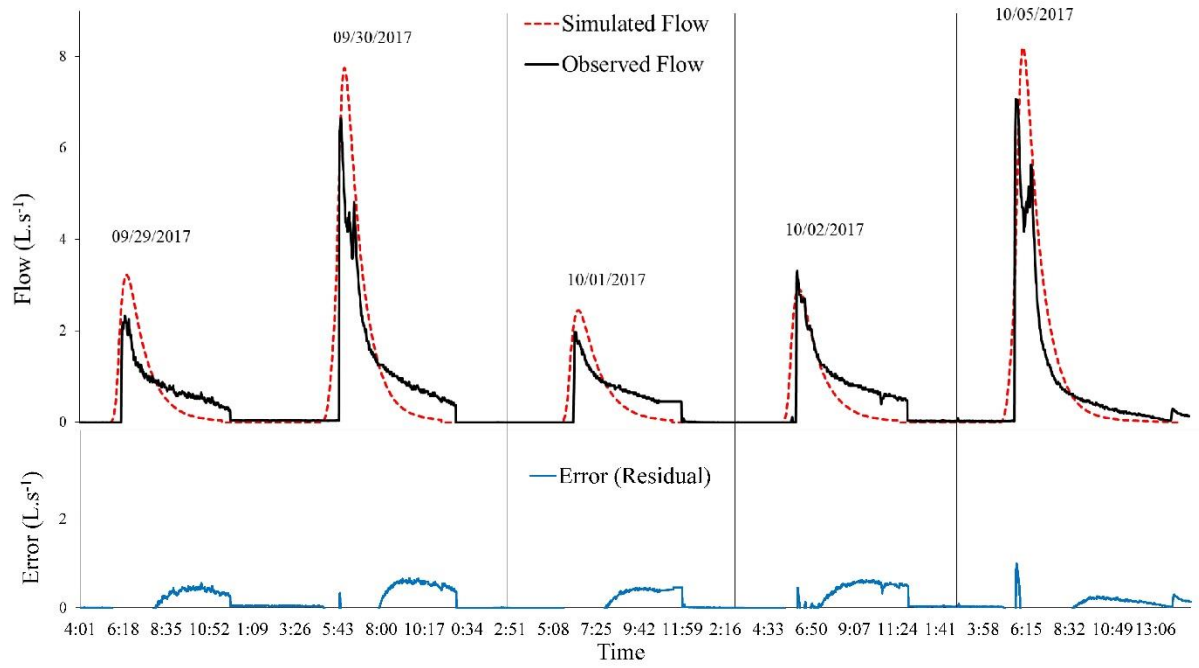

Figure 4.5. Comparison of observed and simulated runoff by SWMM for irrigation events, and error for each event.

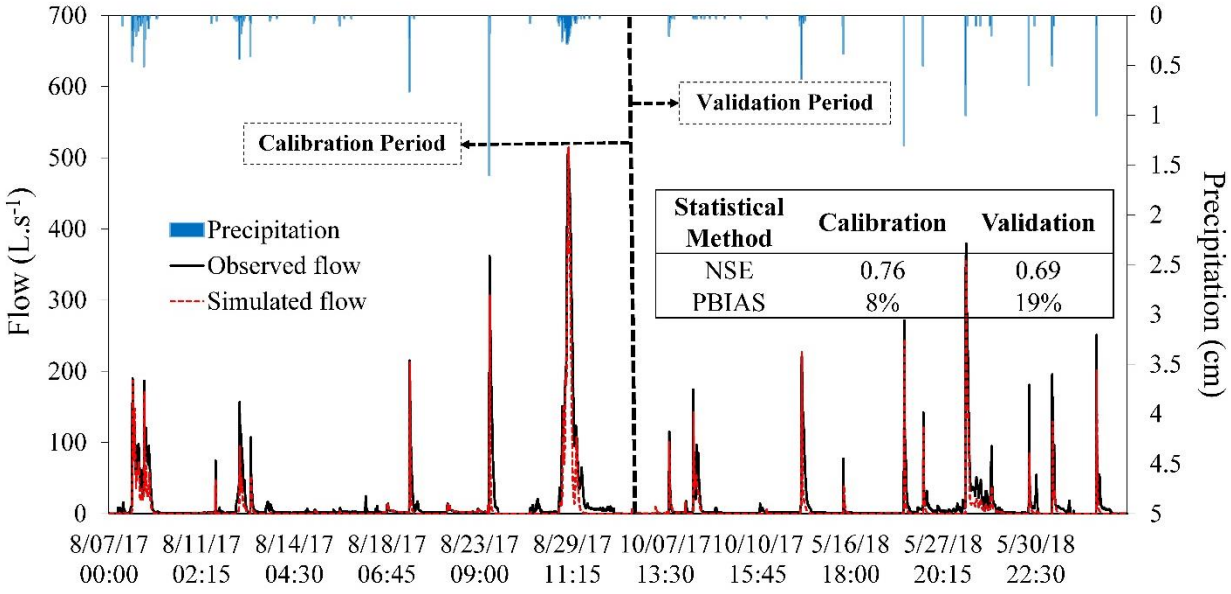

Figure 4.6. Comparison of observed and simulated runoff by SWMM for storm events.

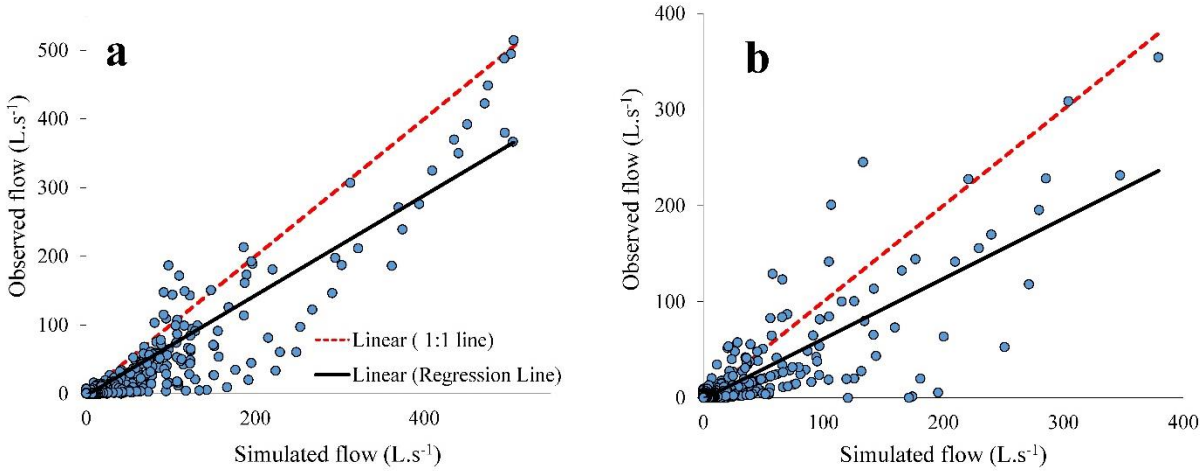

Figure 4.7. Scatter plots of observed and simulated flow along the 1:1 dashed line: (a) Calibration period, (b) Validation period.

4.3.6 Results of water quality calibration for the SWMM model

The EMC and exponential buildup/washoff method were qualified for two storm events, and used to estimate TSS, TP, and TN loads (Figure 4.8). The exponential buildup/washoff method (red line) followed the trend of TSS observation reasonably well; r^2 between simulation and observation for Oct 24, 2017 and Aug 7, 2017 were 0.91 and 0.62, respectively. However, using the buildup/washoff method for TN and TP resulted in an r^2 between simulated and observed TN and TP of less than 0.30, which is not acceptable, and the simulated plots could not mimic the trend of observation properly. In addition, pollutants loads were estimated using these two methods, these are shown in Table 4.4. Based upon percent error results, both methods could be considered to be valid for estimating pollutant loads, as there was a good agreement between simulation and observation loads (i.e., percent error was lower than ±25%). However, since the percent error for simulated TSS, TP and TP loads using the EMC method were less than those using the buildup/washoff method, the EMC method was used for calibrating TSS, TN and TP.

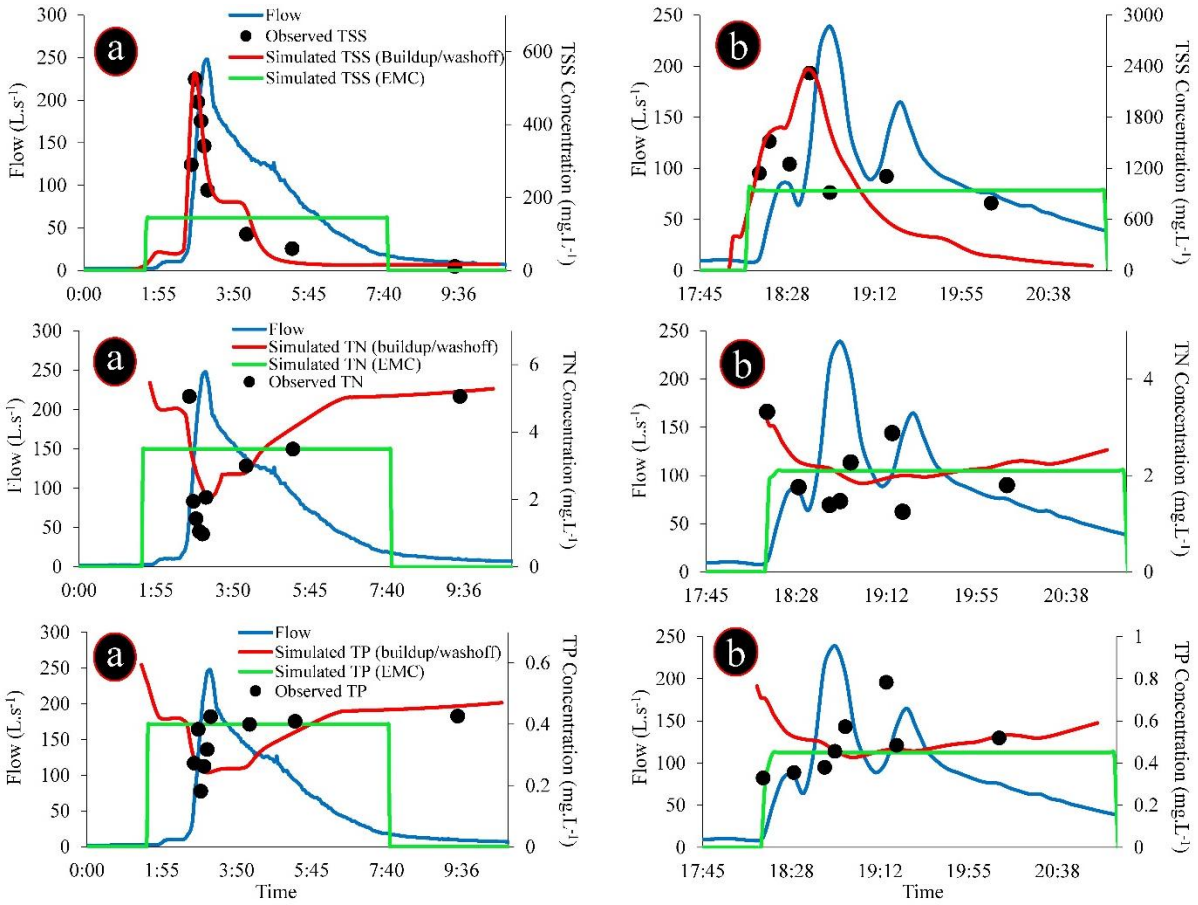

Figure 4.8. Water quality calibration through exponential buildup/washoff and EMC methods for the: (a) Oct 24, 2017 and (b) Aug 7, 2017 storm events.

Table 4.4. Results of pollutants loads from observation, buildup/washoff and EMC methods.

Method	TSS load (kg)	TN load (kg)	TP load (kg)
Oct 24, 2017			
Observation	285	7.21	0.910
Buildup/washoff	304 (-6.6 %)	6.99 (3.0 %)	0.710 (21.9 %)
EMC	278 (2.2 %)	7.18 (0.4 %)	0.740 (18.6 %)
Aug 7, 2017			
Observation	1,570	1.94	0.520
Buildup/washoff	1,430 (9.1 %)	2.17 (-11.8 %)	0.530 (-1.9 %)
EMC	1,500.0 (4.5 %)	2.06 (-6.1 %)	0.490 (5.7 %)

4.3.7 Pollutograph during irrigation and storm

Pollutographs of TSS, TN, TP, pH and EC for a selected storm and irrigation event are illustrated in Figure 4.9 and 4.10, respectively. There was a direct relationship between runoff

and TSS peaks, i.e., TSS peaks follow peak runoff, with a lag of approximately 15 min. (Figure 4.9a) (Hu and Huang, 2014; Huang et al., 2007). This lag results from the effect of first-flush (which is the initial runoff of the rainfall with high level of pollutants), so the TSS peak occurred prior to the arrival of the flow peak (Hu and Huang, 2014; Li et al., 2017; Obermann et al., 2009), while during irrigation, at the same time TSS and flow reached the peak; i.e., irrigation had no first-flush effect. After reaching its peak, the TSS concentration declined considerably (Figure 4.9a).

During irrigation, observed concentrations of TN and TP varied similarly. There was an inverse relationship between runoff and TN peaks (Figure 4.9b and 4.9c). The lowest concentration of TP and TN occurred 10 min. after peak runoff. During storm events, TP and TN exhibited behavior differently from irrigation runoff, likely because antecedence dry day (ADD) and rainfall intensity have a great role in concentration of TP (Yoon et al., 2010). There was no observed relationship between TN and precipitation, but generally, during peak flow, the concentration of TN is in the lowest value because of dilution (Figure 4.9b). During storm events, a similar pattern for TP and TN concentrations was observed, and the washoff process for dissolved mineral nutrients was different from that observed with TSS. During both irrigation and storm events, pH had an upward trend, and it varied from 7.5 – 8 (Figure 4.9d).

During irrigation runoff, EC exhibited two peaks; the first peak was related to the initial washoff of previous leachate that was present around the plant pots. Due to dilution, the level of EC then dropped suddenly to 550 $uS \cdot cm^{-1}$, returning to a second peak close to the initial peak

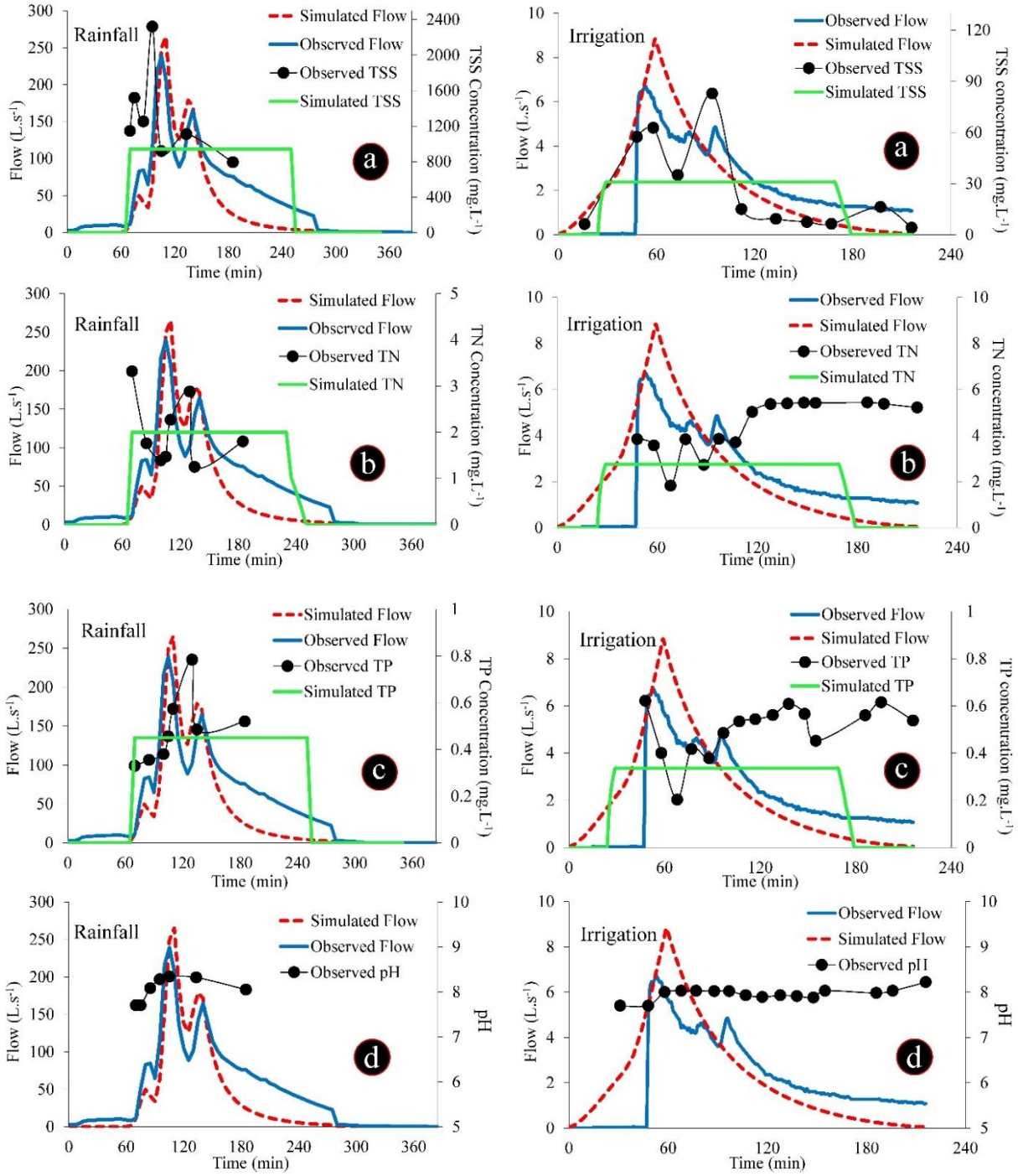

Figure 4.9. Pollutograph of a) TSS, b) TN, c) TP, and d) pH during a storm and an irrigation event.

near the end of the irrigation event, at about 650 uS·cm^{-1}, reflecting the arrival of mineral salts associated with controlled release fertilizers in the soilless substrate (Figure 4.10). Thus, two peaks in EC trend were related to the initial washoff of previous leachate, and leaching of

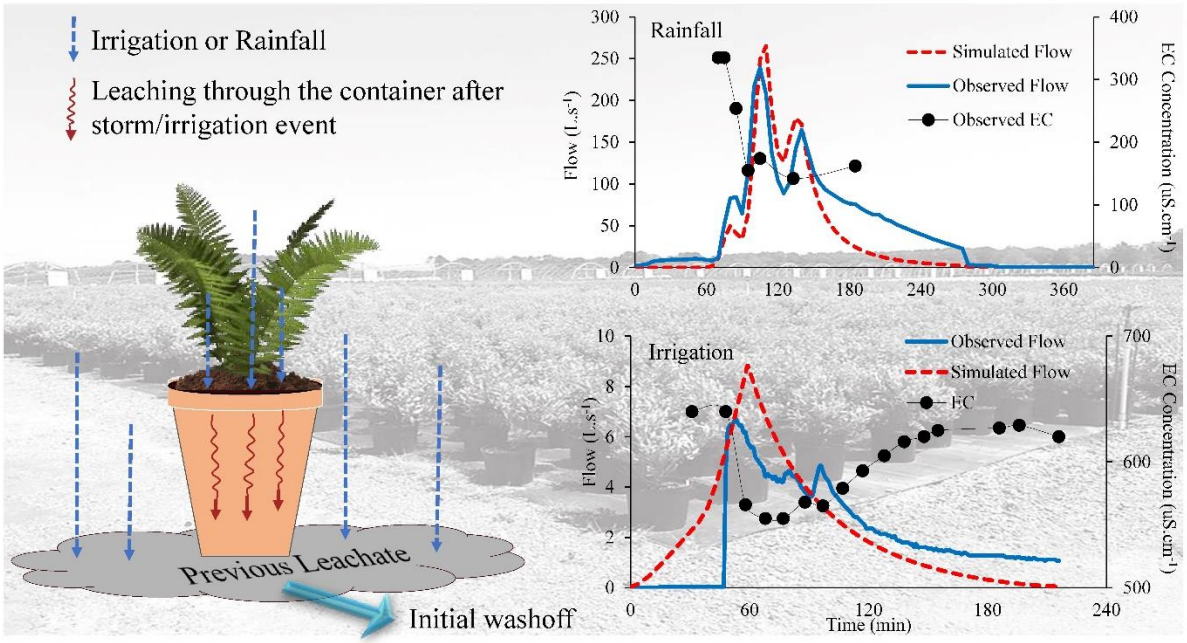

Figure 4.10. Sources of EC and pollutograph of that for a storm and an irrigation event.

containers with high salts. These results are similar to results reported by Hoskins et al., (2014a). The trend of EC concentration for the storm event was similar to the irrigation event, albeit the EC values during a storm event were lower due to dilution, so that minimum and maximum EC during storm events ranged from 150 to 350 uS·cm^{-1}, respectively.

4.3.8 Annual pollutant loads

The validated SWMM model was then used to simulate runoff flows and TSS, TN and TP concentrations from the nursery production area for 10 years (2008 to 2018). Annual pollutant loads were estimated by multiplying modeled 15-min. flows by concentrations of TSS, TP and TN; results of these calculations are presented in Table 4.5. During storm events, annual loads for TSS, TN and TP per ha ranged from 9,230 – 13,300, 65.8 – 94.0 and 9.00 – 12.9 kg·ha^{-1}·y^{-1}, respectively. The average daily loads of TSS, TN, and TP during irrigation events were 0.87, 0.09 and 0.01 kg·day^{-1}, respectively.

Table 4.5. Results of annual pollutants loads for storm events.

Year	Precipitation (cm)	Number of dry days	TSS load ($kg \cdot ha^{-1} \cdot yr^{-1}$)	TN Load ($kg \cdot ha^{-1} \cdot yr^{-1}$)	TP Load ($kg \cdot ha^{-1} \cdot yr^{-1}$)
2008	118	234	9,200	74.0	10.2
2009	142	211	11,600	88.6	12.2
2010	129	253	9,540	84.0	11.4
2011	141	232	11,700	89.8	12.4
2012	108	232	9,190	61.6	8.5
2013	141	231	11,800	87.9	12.1
2014	132	249	13,300	83.8	11.5
2015	136	228	13,300	83.4	11.5
2016	131	234	10,300	77.7	10.7
2017	120	244	10,900	72.5	10.0
Mean			11,100	80.3	11.1

4.4 Discussion

We characterized runoff quality for a nursery in the mid-Atlantic, US during irrigation and storm events. Based upon our monitoring results, TN and TP EMCs of nursery runoff during storm and irrigation events were similar and ranged from 2.5 to 3.9 and 0.29 to 0.55 $mg \cdot L^{-1}$, respectively. TN and TP EMCs of nursery runoff were similar to those of urban runoff which ranged from 2.5 to 4.5 and 0.2 to 0.6 $mg \cdot L^{-1}$, respectively (Badruzzaman et al., 2012; Graves et al., 2004; Harper and Baker, 2007; Li et al., 2015; Toor et al., 2017; Wei et al., 2013). Since the volume of storm runoff was higher than irrigation runoff, the average total load of TSS, TN and TP during storm events were approximately 900, 35 and 50 times higher than those of irrigation events, respectively. With regard to TSS, we observed a direct relationship between rainfall intensity and TSS EMC, which is similar to results reported by Yoon et al., (2010). Average TSS EMCs for irrigation events in nursery production areas was 30 $mg \cdot L^{-1}$ and TSS EMC of nursery for storm events was 4 to 40 times greater than irrigation events. The TSS EMC from storm runoff of nursery ranged from 130 to 1,300 $mg \cdot L^{-1}$ which is greater than that of urban runoff,

which typically ranges from 80 to 260 $mg \cdot L^{-1}$ (Line et al., 2002; Métadier and Bertrand-Krajewski, 2012; Sun et al., 2015). Concurrent unpublished research at Clemson University indicates an average nursery runoff TSS concentration > 400 $mg \cdot L^{-1}$, for irrigation events, this is ≈100 $mg \cdot L^{-1}$; decreases at particular nursery sites are likely due to flocculation or sedimentation with increasing hydraulic residence time through TRBs or other BMPs, if used (personal communication, John Majsztrik). There was a direct relationship between TN and TP (r= 0.55) and runoff and TSS (r = 0.57). Further, because of dilution, there was an inverse relationship between runoff and EC (r = -0.82), TN and flow (r =0.44).

This paper was the first study that characterized and modeled runoff quantity and quality from a container nursery production area, and the first to apply a model to such sites. The statistical results indicated that SWMM was able to characterize the hydrology and water quality of the container nursery adequately. The model provides the capability of assessing effects of changing fertilizer or irrigation practices, soils, and/or climate. The SWMM model developed for this study was generalized across time to simulate runoff flows and TSS, TN and TP concentrations for 10 years (2008 – 2018). Annual pollutant loads were estimated by multiplying modeled flows by modeled EMCs of TSS, TP and TN. Since SWMM can also simulate treatment performance of BMPs, future research related to this topic should focus upon specific metrics in water quality management at container nurseries to maintain TRBs or reduce runoff into the neighboring ecosystem contributing to surface water impairment. Coupled micro-scale hydrological and chemical models of the container or production surface could provide detailed insight into the impact of soilless substrate hydrological properties, metal speciation contributed by substrate versus native soils, crop growth and physiology, and surface covering types;

allowing for greater production system refinement to increase resource efficiency and minimize environmental impacts.

4.5 Conclusions

Several storm and irrigation runoff samples were collected from a large mid-Atlantic container nursery production area and were analyzed for pH, EC, TSS, TP, and TN. Samples from 5 storm events and 7 irrigation events were taken; and 130 samples were taken across the hydrograph to assess the temporal distribution of pollutants across the hydrograph. Samples were collected downstream from a 5.2 ha production area consisting of 1.82 ha of roads with a gravel base and 3.38 ha of production areas where containerized crop were produced, all of which drained to a central ditch within the middle of an 18 m roadway. A SWMM model was developed to characterize runoff during storm and irrigation events. The t_c for the monitoring site was between 26 to 30 min., which was estimated based on the velocity and graphical methods. The average runoff coefficient (RC) during irrigation and storm events was 0.35, and 0.70, respectively. Comparing results between runoff, TSS, TP, TN. EC and pH, indicated that there was a direct correlation between TN and TP, runoff and TSS, TN and EC, and flow and pH. Further, there was no relationship between TSS and TP, which indicated phosphorus was present mainly in dissolved form. During irrigation and storm events, TSS peaks followed peak runoff, after a nearly uniform lag. There was an observed inverse relationship between runoff peaks and concentrations of TN and TP.

During irrigation, EMCs of TSS, TN and TP were 30, 3.1 and 0.35 $mg \cdot L^{-1}$, respectively, and during storm events TSS, TN and TP EMCs were 880, 3.7, and 0.46 $mg \cdot L^{-1}$, respectively. During the storm events, annual loads for TSS, TN and TP per ha were between: 9,230 and 13,300, 65.8 and 94.0, 9.00 and 12.9 $kg \cdot ha^{-1} \cdot yr^{-1}$, respectively. Based on statistical results,

SWMM was able to characterize the runoff quantity and quality from nursery production areas reasonably well using the EMC method. Thus, this model, given sufficient data for calibration, could be applied to estimate runoff water quality loads from container nursery production areas, and assess treatment options.

Acknowledgements

Funding for this work was provided in part by the Virginia Agricultural Experiment Station, the Hatch Program and the Specialty Crop Research Initiative Project Clean WateR3 (2014-51181-22372), National Institute of Food and Agriculture, U.S. Department of Agriculture. Additional support was provided by the Virginia Nursery & Landscape Horticulture Research Foundation. The authors appreciate the field support provided by Zachary Landis and Michael Harrison, and the lab support provided by Jim Owen, Julie Brindley and Anna Birnbaum.

4.6 References for Chapter 4

Alamdari, N., Sample, D., Steinberg, P., Ross, A., Easton, Z., 2017. Assessing the effects of climate change on water quantity and quality in an urban watershed using a calibrated stormwater model. Water 9, 464. doi:10.3390/w9070464

Badruzzaman, M., Pinzon, J., Oppenheimer, J., Jacangelo, J.G., 2012. Sources of nutrients impacting surface waters in Florida: A review. J. Environ. Manage. 109, 80–92. doi:10.1016/j.jenvman.2012.04.040

Bilderback, T., Boyer, C., Chappell, M., Fain, G., Fare, D., Gilliam, C., Jackson, B., Lea-Cox, J., LeBude, A., Niemiera, A., Ruter, J., Tilt, K., Warren, S., White, S., Whitwell, T., Wright, R., Yeager, T., 2013. Best management practices: Guide for producing nursery crops. 3rd ed. South. Nurs. Assn., Acworth, GA.

Carpenter, S.R., Caraco, N.F., Correll, D.L., Howarth, R.W., Sharpley, A.N., Smith, V.H., 1998. Nonpoint pollution of surface waters with phosphorus and nitrogen. Ecol. Appl. 8, 559–568. doi:10.1890/1051-0761(1998)008[0559:NPOSWW]2.0.CO;2

Chen, L., Wang, G., Zhong, Y., Shen, Z., 2016. Evaluating the impacts of soil data on hydrological and nonpoint source pollution prediction. Sci. Total Environ. 563–564, 19–28. doi:10.1016/j.scitotenv.2016.04.107

Chen, Y., Wen, X., Wang, B., Nie, P., 2017. Agricultural pollution and regulation: How to subsidize agriculture? J. Clean. Prod. 164, 258–264. doi:10.1016/J.JCLEPRO.2017.06.216

De Leon, D., Lowe, J., 2009. Standard operating procedure for automatic sampling for stormwater monitoring 42.

Duda, P.B., Hummel, P.R., Donigian, A.S.J., Imhoff, J.C., 2012. Basins/HSPF: model use, calibration, and validation. Trans. Asabe 55, 1523–1547. doi:10.13031/2013.42261
Fernandez, R., Cregg, B., Andresen, J., 2009. Container-grown ornamental plant growth and water runoff nutrient content and volume under four irrigation treatments. HortScience 44, 1573–1580.
Gant, R.L., Robinson, G.M., Fazal, S., 2011. Land-use change in the 'edgelands': Policies and pressures in London's rural–urban fringe. Land use policy 28, 266–279. doi:10.1016/J.LANDUSEPOL.2010.06.007
Graves, G. a, Wan, Y.S., Fike, D.L., 2004. Water quality characteristics of storm water from major land uses in South Florida. J. Am. Water Resour. Assoc. 40, 1405–1419. doi:DOI 10.1111/j.1752-1688.2004.tb01595.x
Green, J., Nelson, J., 2002. Calculation of time of concentration for hydrologic design and analysis using geographic information system vector objects. J. Hydroinformatics 4, 75–81.
Guan, M., Sillanpää, N., Koivusalo, H., 2015. Modelling and assessment of hydrological changes in a developing urban catchment. Hydrol. Process. 29, 2880–2894. doi:10.1002/hyp.10410
Guo, W., Fu, Y., Ruan, B., Ge, H., Zhao, N., 2014. Agricultural non-point source pollution in the Yongding River Basin. Ecol. Indic. 36, 254–261. doi:10.1016/j.ecolind.2013.07.012
Harper, H.H., Baker, D.M., 2007. Evaluation of Current Stormwater Design Criteria within the State of Florida : Final Report. Florida Dep. Environ. Prot.
Heimlich, L.B.R., Anderson, W., 2001. Development at the urban fringe and beyond: impacts on agriculture and rural, Economic Research Service, Washington DC: US Department of Agriculture.
Hoskins, T., Owen, J., Fields, J., Altland, J., Easton, Z., Niemiera AX, 2014a. Solute Transport through a Pine Bark-based Substrate under Saturated and Unsaturated Conditions. J. Am. Soc. Hortic. Sci. 139, 634–641.
Hoskins, T., Owen, J., Niemiera, A., 2014b. Water Movement through a Pine-bark Substrate during Irrigation. HortScience 49, 1432–1436.
Hu, H., Huang, G., 2014. Monitoring of non-point source pollutions from an agriculture watershed in South China. Water (Switzerland) 6, 3828–3840. doi:10.3390/w6123828
Huang, J. liang, Du, P. fei, Ao, C. tan, Lei, M. heong, Zhao, D. quan, Ho, M. him, Wang, Z. shi, 2007. Characterization of surface runoff from a subtropics urban catchment. J. Environ. Sci. 19, 148–152. doi:10.1016/S1001-0742(07)60024-2
Ketabchy, M., 2018. Thermal evaluation an urbanized watershed using SWMM and MINUHET: a case study of Stroubles Creek Watershed, Blacksburg, VA. doi:10.13140/RG.2.2.26726.47688
Ketabchy, M., Sample, D.J., Wynn-Thompson, T., Nayeb Yazdi, M., 2018. Thermal Evaluation of Urbanization Using a Hybrid Approach. J. Environ. Manage. 226, 457–475. doi:10.1016/J.JENVMAN.2018.08.016
Li, D., Wan, J., Ma, Y., Wang, Y., Huang, M., Chen, Y., 2015. Stormwater runoff pollutant loading distributions and their correlation with rainfall and catchment characteristics in a rapidly industrialized city. PLoS One 10, 1–17. doi:10.1371/journal.pone.0118776
Li, S., Wang, X., Qiao, B., Li, J., Tu, J., 2017. First flush characteristics of rainfall runoff from a paddy field in the Taihu Lake watershed, China. Environ. Sci. Pollut. Res. 24, 8336–8351. doi:10.1007/s11356-017-8470-2
Li, X., Fang, X., Li, J., KC, M., Gong, Y., Chen, G., 2018. Estimating Time of Concentration for Overland Flow on Pervious Surfaces by Particle Tracking Method. Water 10, 379.

doi:10.3390/w10040379
Line, D.E., White, N.M., Osmond, D.L., Jennings, G.D., Mojonnier, C.B., 2002. Pollutant export from various land uses in the upper Neuse River Basin. Water Environ. Res. 74, 100–8.
Liu, R., Wang, J., Shi, J., Chen, Y., Sun, C., Zhang, P., Shen, Z., 2014. Runoff characteristics and nutrient loss mechanism from plain farmland under simulated rainfall conditions. Sci. Total Environ. 468–469, 1069–1077. doi:10.1016/J.SCITOTENV.2013.09.035
Lucas, W.C., Sample, D.J., 2015. Reducing combined sewer overflows by using outlet controls for Green Stormwater Infrastructure: Case study in Richmond, Virginia. J. Hydrol. 520, 473–488. doi:10.1016/j.jhydrol.2014.10.029
Mack, R., Owen, J.S., Niemiera, A.X., Latimer, J., 2017. Virginia Nursery and Greenhouse Grower Survey of Best Management Practices. Horttechnology 27, 386–392. doi:10.21273/HORTTECH03664-17
Majsztrik, J.C., Fernandez, R.T., Fisher, P.R., Hitchcock, D.R., Lea-Cox, J., Owen, J.S., Oki, L.R., White, S.A., 2017. Water Use and Treatment in Container-Grown Specialty Crop Production: A Review. Water. Air. Soil Pollut. 228. doi:10.1007/s11270-017-3272-1
Majsztrik, J.C., Ristvey, A.G., Lea-Cox, J.D., 2011. Water and Nutrient Management in the Production of Container-Grown Ornamentals. Hortic. Rev. (Am. Soc. Hortic. Sci). 38, 253. doi:10.1002/9780470872376.ch7
Mangiafico, S., Gan, J., Wu, L., Lu, J., Newman JP, Faber B, Merhaut, D., Evans, R., 2008. Detention and Recycling Basins for Managing Nutrient and Pesticide Runoff from Nurseries. HortScience 43, 393–398.
Mangiafico, S.S., Newman, J., Merhaut, D.J., Gan, J., Faber, B., Wu, L., 2009. Nutrients and pesticides in stormwater runoff and soil water in production nurseries and citrus and avocado groves in California. HortTechnology 19, 360–367.
McDowell, R.W., Laurenson, S., 2014. Water: Water Quality and Challenges from Agriculture. Encycl. Agric. Food Syst. 425–436. doi:10.1016/B978-0-444-52512-3.00085-1
Merkel, W., 2001. References on time of concentration with respect to sheet flow. Unpubl. Pap. Beltsville, MD.
Merz, R., Blöschl, G., Parajka, J., 2006. Spatio-temporal variability of event runoff coefficients. J. Hydrol. 331, 591–604. doi:10.1016/J.JHYDROL.2006.06.008
Métadier, M., Bertrand-Krajewski, J.L., 2012. The use of long-term on-line turbidity measurements for the calculation of urban stormwater pollutant concentrations, loads, pollutographs and intra-event fluxes. Water Res. 46, 6836–6856. doi:10.1016/j.watres.2011.12.030
Michailidi, E.M., Antoniadi, S., Koukouvinos, A., Bacchi, B., Efstratiadis, A., 2018. Timing the time of concentration: shedding light on a paradox. Hydrol. Sci. J. 63, 721–740. doi:10.1080/02626667.2018.1450985
Million, J., Yeager, T., 2015. Capture of Sprinkler Irrigation Water by Container-grown Ornamental Plants. HortScience 50, 442–446.
Million, J., Yeager, T., Albano, J., 2007. Consequences of excessive overhead irrigation on runoff during container production of sweet viburnum. J. Environ. Hortic. 25, 117–125.
Mishra, S.K., Singh, V.P., 2003. Soil Conservation Service Curve Number (SCS-CN) Methodology, Water Science and Technology Library. Springer Netherlands, Dordrecht. doi:10.1007/978-94-017-0147-1
Modugno, M., Gioia, A., Gorgoglione, A., Iacobellis, V., Forgia, G., Piccinni, A., Ranieri, E., 2015. Build-Up/Wash-Off Monitoring and Assessment for Sustainable Management of First

Flush in an Urban Area. Sustainability 7, 5050–5070. doi:10.3390/su7055050
Moore, M.F., Vasconcelos, J.G., Zech, W.C., 2017. Modeling highway stormwater runoff and groundwater table variations with SWMM and GSSHA. J. Hydrol. Eng. 22, 04017025. doi:10.1061/(ASCE)HE.1943-5584.0001537
Moriasi, D.N., Gitau, M.W., Pai, N., Daggupati, P., 2015. Hydrologic and Water Quality Models: Performance Measures and Evaluation Criteria. Trans. ASABE 58, 1763–1785. doi:10.13031/trans.58.10715
Mukaka, M.M., 2012. Statistics corner: A guide to appropriate use of correlation coefficient in medical research. Malawi Med. J. 24, 69–71.
Nayeb Yazdi, M., Arhami, M., Delavarrafiee, M., Ketabchy, M., 2019. Developing air exchange rate models by evaluating vehicle in-cabin air pollutant exposures in a highway and tunnel setting: case study of Tehran, Iran. Environ. Sci. Pollut. Res. 1, 501–513. doi:10.1007/s11356-018-3611-9
Newman, J., Albano, J., Merhaut, D., Blythe, E., 2006. Nutrient Release from Controlled-release Fertilizers in a Neutral-pH Substrate in an Outdoor Environment: I. Leachate Electrical Conductivity, pH, and Nitrogen, Phosphorus, and Potassium Concentrations. HortScience 41, 1674–1682.
Novotny, V., 2003. Water quality : diffuse pollution and watershed management. J. Wiley.
NRCS, 2010. Chapter 15: Time of Concentration. Nat. Resour. Conserv. Serv. 1–15.
NRCS, 1999. Natural Resources Conservation Service. [WWW Document]. United States Dep. Agric. URL https://websoilsurvey.sc.egov.usda.gov/App/HomePage.htm
Obermann, M., Rosenwinkel, K.-H., Tournoud, M.-G., 2009. Investigation of first flushes in a medium-sized mediterranean catchment. J. Hydrol. 373, 405–415. doi:10.1016/J.JHYDROL.2009.04.038
Owen, J., Warren, S., Bilderback, T., Albano, J., 2008. Phosphorus Rate, Leaching Fraction, and Substrate Influence on Influent Quantity, Effluent Nutrient Content, and Response of a Containerized Woody Ornamental Crop. HortScience 43, 906–912.
Palla, A., Gnecco, I., 2015. Hydrologic modeling of Low Impact Development systems at the urban catchment scale. J. Hydrol. 528, 361–368. doi:10.1016/J.JHYDROL.2015.06.050
Ristvey, A.G., Lea-Cox, J.D., Ross, D.S., 2004. nutrient uptake, partitioning and leaching losses from container-nursery production systems. Acta Hortic. 321–328. doi:10.17660/ActaHortic.2004.630.40
Rossman, L.A., 2010. Storm water management model user's manual, version 5.0. Cincinnati: National Risk Management Research Laboratory, Office of Research and Development, US Environmental Protection Agency.
Sample, D.J., Heaney, J.P., 2006. Integrated Management of Irrigation and Urban Storm-Water Infiltration. J. Water Resour. Plan. Manag. 132, 362–373. doi:10.1061/(ASCE)0733-9496(2006)132:5(362)
Sample, D.J.D.J., Grizzard, T.J.T.J., Sansalone, J., Davis, A.P.A.P., Roseen, R.M.R.M., Walker, J., 2012. Assessing performance of manufactured treatment devices for the removal of phosphorus from urban stormwater. J. Environ. Manage. 113, 279–291. doi:10.1016/j.jenvman.2012.08.039
Schoenfelder, C., Kenner, S., Hoyer, D., 2006. Hydraulic Model of the Belle Fourche Irrigation District Using EPA SWMM 5.0. World Environ. Water Resour. Congr. 2006 1–10. doi:doi:10.1061/40856(200)262
Schueler, T.R., 1987. Controlling urban runoff: A practical manual for planning and designing

urban BMPs. Water Resour. Publ.
Seong, C., Herand, Y., Benham, B.L., 2015. Automatic calibration tool for hydrologic simulation program-FORTRAN using a shuffled complex evolution algorithm. Water (Switzerland) 7, 503–527. doi:10.3390/w7020503
Shreckhise, J.H., 2018. Phosphorus Requirement and Chemical Fate in Containerized Nursery Crop Production. Virginia Tech.
Sun, S., Barraud, S., Castebrunet, H., Aubin, J.B., Marmonier, P., 2015. Long-term stormwater quantity and quality analysis using continuous measurements in a French urban catchment. Water Res. 85, 432–442. doi:10.1016/j.watres.2015.08.054
Taylor, M.D., White, S.A., Chandler, S.L., Klaine, S.J., Whitwell, T., 2006. Nutrient management of nursery runoff water using constructed wetland systems. Horttechnology 16, 610–614.
Teledyne, I.S.C.O., 2011. ISCO open channel flow measurement handbook.
Toor, G.S., Occhipinti, M.L., Yang, Y.Y., Majcherek, T., Haver, D., Oki, L., 2017. Managing urban runoff in residential neighborhoods: Nitrogen and phosphorus in lawn irrigation driven runoff. PLoS One 12, 1–17. doi:10.1371/journal.pone.0179151
Tsai, L.-Y., Chen, C.-F., Fan, C.-H., Lin, J.-Y., 2017. Using the HSPF and SWMM Models in a High Pervious Watershed and Estimating Their Parameter Sensitivity. Water 9, 780. doi:10.3390/w9100780
USDA-NASS, 2014. 2012 Census of Agriculture. United States Dep. Agric. Agric. Stat. Serv.
USEPA, 2010. Chesapeake Bay Total Maximum Daily Load for Nitrogen, Phosphorus and Sediment [WWW Document]. US Environ. Prot. Agency. URL https://www.epa.gov/chesapeake-bay-tmdl
USEPA, 2005. Protecting water quality from agricultural runoff [WWW Document]. US Environ. Prot. Agency.
USEPA, 1992. NPDES storm water sampling guidance document [WWW Document]. United States Environ. Prot. Agency.
VDEQ, 2012. Virginia Chesapeake Bay TMDL Watershed Implementation Plan - Phase II 81.
VDEQ, 2010. Virginia Chesapeake Bay TMDL Watershed Implementation Plan - Phase I 141.
Wang, S., He, Q., Ai, H., Wang, Z., Zhang, Q., 2013. Pollutant concentrations and pollution loads in stormwater runoff from different land uses in Chongqing. J. Environ. Sci. (China) 25, 502–510. doi:10.1016/S1001-0742(11)61032-2
Wei, Z., Simin, L., Fengbing, T., 2013. Characterization of urban runoff pollution between dissolved and particulate phases. ScientificWorldJournal. 2013, 964737. doi:10.1155/2013/964737
Welle, P.., Woodward, D.., 1986. Time of concentration [WWW Document]. Hydrol. Tech. Note No. N4. U.S. Dep. Agric. Soil Conserv. Serv. NENTC, Chester, PA.
White, S.A., Taylor, M.D., Albano, J.P., Whitwell, T., Klaine, S.J., 2011. Phosphorus retention in lab and field-scale subsurface-flow wetlands treating plant nursery runoff. Ecol. Eng. 37, 1968–1976. doi:10.1016/J.ECOLENG.2011.08.009
White, S.A., Taylor, M.D., Chandler, S.L., Whitwell, T., Klaine, S.J., 2010. Remediation of nitrogen and phosphorus from nursery runoff during the spring via free water surface constructed wetlands. Environ. Hortic. 28, 209.
Yi, Q., Li, H., Lee, J.W., Kim, Y., 2015. Development of EMC-based empirical model for estimating spatial distribution of pollutant loads and its application in rural areas of Korea. J. Environ. Sci. (China) 35, 1–11. doi:10.1016/j.jes.2015.01.024

Yin, H., Zhao, Z., Wang, R., Xu, Z., Li, H., 2017. Determination of urban runoff coefficient using time series inverse modeling. J. Hydrodyn. Ser. B 29, 898–901. doi:10.1016/S1001-6058(16)60803-X

Yoon, S.W., Chung, S.W., Oh, D.G., Lee, J.W., 2010. Monitoring of non-point source pollutants load from a mixed forest land use. J. Environ. Sci. 22, 801–805. doi:10.1016/S1001-0742(09)60180-7

Zhang, H., Richardson, P.A., Belayneh, B.E., Ristvey, A., Lea-Cox, J., Copes, W.E., Moorman, G.W., Hong, C., 2015. Characterization of water quality in stratified nursery recycling irrigation reservoirs. Agric. Water Manag. 160, 76–83. doi:10.1016/j.agwat.2015.06.027

Chapter 5. Assessing the ability of a Coastal Plain retention pond to treat nutrients and sediment

Mohammad Nayeb Yazdi, Durelle Scott, David J. Sample,

Submitted: Planned August 2020
To: *Environmental Pollution*
Status: Draft

Abstract

Urbanization alters watershed hydrology by increasing the area covered by impervious surfaces and channelizing or piping streams, resulting in increased runoff and decreased lag times. Increased runoff causes channel and streambed erosion, increasing transport of sediment and nutrients, degrading surface water quality. One method for mitigating these impacts is construction of retention ponds, a common stormwater control measure (SCM); which function by retaining large volumes of runoff for a period of time, releasing it slowly, which allows suspended sediments and associated pollutants to settle. Biological activity in retention ponds may also remove some pollutants through uptake and adsorption; however, retention ponds can also become a source of pollutants resuspended or mobilized from sediments. The goal of this study was to monitor the behavior of a coastal retention pond and to characterize its ability to treat nitrogen (N), phosphorous (P), and sediment as measured by total suspended sediment (TSS). Often, SCMs selected for similar studies are new and meet specific design guidelines for water quality. We selected a rather ordinary pond in the City of Virginia Beach for this study; the pond was chosen in part because it had no special water quality treatment features, such as a

forebay or a discharge structure with multiple outlets. We monitored water quality at the inlets and the outlet of the retention pond for one year and estimated its treatment efficiency for N, P, and sediment. We found that during cold weather, the pond reduced the level of TSS and P by an average of 62% and 10 %, respectively, while it exported N, increasing it in the pond outflows by an average of 8%. During warm weather, the treatment of the pond improved, achieving an average TSS reductions of 75% and an average N and P reduction of 47% and 10%, respectively. This may be due to biological activities like nitrification/denitrification that occur during warmer months. In addition, we used the Storm Water Management Model (SWMM) to characterize the behavior of the pond. We found SWMM was able to simulate TSS and Total P (TP) removal reasonably well, but its performance in simulating Total N (TN) removal was not satisfactory; this varied across the year. The results of this study indicate that, on an annual load basis, retention ponds may be providing significant treatment benefits that are being overlooked; and should be one of the tools available for mitigating negative effects of urbanization on hydrology and water quality.

5.1 Introduction

Most of the southeast U.S. lies within the Coastal Plain physiographic province, an area of approximately 1.2 million km^2 (Hupp, 2000). Urban landcover within this region is predicted to double in area over the next 50 years .(Terando et al., 2014). Urban development alters the hydrologic cycle by increasing areas covered by impervious surfaces and changing drainage patterns (Hester and Bauman, 2013; Li et al., 2013; Liu et al., 2015). These changes reduce infiltration and increase runoff peak and volume, and reduce lag time during storm events (Chen et al., 2017; Hamel et al., 2015; G. Liu et al., 2013; Locatelli et al., 2017; Rosburg et al., 2017; Taylor and Stefan, 2009; Wang et al., 2017). Furthermore, flooding risk increases, resulting in

higher peak stages and inundation (Roodsari and Chandler, 2017; Zope et al., 2016). Another result of increased runoff from urban development is increased channel and streambed erosion, and the increased transport of sediment and nutrient fluxes [Nitrogen (N), and Phosphorous (P)] to downstream waters including lakes, near coastal waters, and estuaries (DeLorenzo et al., 2012; Liu et al., 2018; Luo et al., 2018; Rosenzweig et al., 2011; Stephansen et al., 2014; Stoner and Arrington, 2017). This has led to eutrophication, hypoxia and other impairments to important estuaries and coastal waters such as the Chesapeake Bay (Diaz and Rosenberg, 2008).

To mitigate the impacts of urban runoff, a variety of stormwater control measures (SCMs) are employed during land development and urbanization. SCMs also known by the less specific term, best management practices or BMPs. Since the term "BMP" confuses structural and nonstructural approaches, instead, we use the term, SCMs, in this paper. SCMs can be small, decentralized practices that utilize infiltration and or evapotranspiration to reduce stormwater volume and improve water quality through a variety of unit processes, but predominately infiltration and evapotranspiration (Lucas and Sample, 2015; Palla and Gnecco, 2015). These are known as low impact development (LID) practices, or green infrastructure (GI). The central principle of LID design is to mimic or restore pre-development hydrology and water quality (Damodaram et al., 2010; Golden and Hoghooghi, 2017; Liu et al., 2014). SCMs may also include large, centralized facilities such as retention ponds or underground tanks that primarily remove pollutants through settling, but may also use biological uptake (USEPA, 2016). Retention ponds are often viewed as part of the conveyance system, or "gray" infrastructure. Due to the physiography of the Coastal Plain (low slope, high groundwater, poorly infiltrating soils), GI practices are somewhat restricted in their applicability and retention ponds are commonly used within the mid-Atlantic/southeast (Johnson and Sample, 2017; Steele et al., 2014).

Retention ponds have the ability to store runoff, and thus can control downstream hydrology. Retention ponds can also provide limited water quality treatment of runoff by trapping suspended sediments and associated pollutants and increasing pollutant residence time providing an opportunity for treatment (Damodaram et al., 2010; Hancock et al., 2010; Liu et al., 2014; Palla and Gnecco, 2015). Previous research has shown that hydrologic residence time (HRT) is the key variable that explains treatment efficiency of a retention pond (Chrétien et al., 2016; Ivanovsky et al., 2018; Schwartz et al., 2017). Within retention ponds, settling and denitrification are the most important treatment process for sediment and N, respectively (Bettez and Groffman, 2012; Collins et al., 2010; Ivanovsky et al., 2018), and for P removal the predominant processes are adsorption by sediments, precipitation, and uptake by plants (Stutter and Lumsdon, 2008; Vymazal, 2007; Xiao et al., 2016).

Generally, the water quality treatment that is provided by retention ponds, like most SCMs, varies considerably because of the physiographic provinces, the variability in urban runoff quality, design, and maintenance factors (McPhillips and Matsler, 2018; Sample et al., 2012). Although retention ponds can provide limited water quality treatment, some studies have indicated that retention ponds can be a source of pollutants at times and under some conditions, instead of removing them, this is particularly the case for N and P (Gold et al., 2017a; Rosenzweig et al., 2011). Since most monitoring studies of retention ponds have been performed for short periods of time, i.e., < 6 months, during the summer and early fall (Gold et al., 2018); seasonal variation in treatment has not been adequately qualified. Seasonal studies may provide insight on predicting how retention ponds may function on an annual basis and with climate change. Further, the connection between N and P cycling has not been fully characterized in retention ponds (Gold et al., 2018). This research addresses these gaps in knowledge by

conducting a monitoring program for one year on a coastal retention pond. In addition, hydrologic hydraulic/water quality models like the Stormwater Management Model (SWMM) was applied to evaluate the effect of the retention pond on long-term watershed loadings from stormwater.

The objectives of this study are: (1) to estimate the efficiency of a coastal retention pond for removing N, P, and sediment by event; (2) to evaluate the seasonal variability of treatment, particularly focusing on the potential of P to release from pond sediments during the summer; (3) to investigate the effect of rainfall characteristics on retention pond treatment; and (4) to refine water quality treatment process models within SWMM using knowledge gained from literature and the aforementioned field investigation, thus generalizing our results. The overarching objective is to improve the understanding of pond behavior and provide guidance on improving treatment with respect to sediment as measured by total suspended sediment (TSS), N, and P.

5.2 Methodology

5.2.1 Field measurements & sampling site

The City of Virginia Beach is part of the Hampton Roads region, a metropolitan area composed of nine cities and five counties in the Commonwealth of Virginia and two additional counties and one City in the State of North Carolina. All of Hampton Roads lies within the Coastal Plain physiographic region and much of it is tributary to the Chesapeake Bay (Johnson and Sample, 2017), which is the focus of an intensive restoration effort. These attributes make the City of Virginia Beach a good location for a case study of runoff water quality and treatment of retention ponds. Working with the City of Virginia Beach Public Works Department, a somewhat ordinary retention pond was selected; this pond is located within City View Park, (2073 Kempsville Road, 36°46'40.6"N 76°11'51.3"W), as shown in Figure 5.1. The pond has

three inlets and one outlet. Based on the location of monitoring station, inlets were labeled: (1) Parking lot, (2) Intersection, and (3) Street (Figure 5.1).

Total drainage area of the retention pond is 7.52 ha and the area of the pond is 0.22 ha, thus the ratio of the retention pond area to the catchment area is about 2.9%. The contributing drainage area is 51% impervious including parking lots, streets, driveways, and buildings. The retention pond has 3 inlets and each inlet has an associated drainage area. Maps of individual drainage areas with aerial photography are shown in Figure 5.1. Catchment characteristics are presented in Table 5.1.

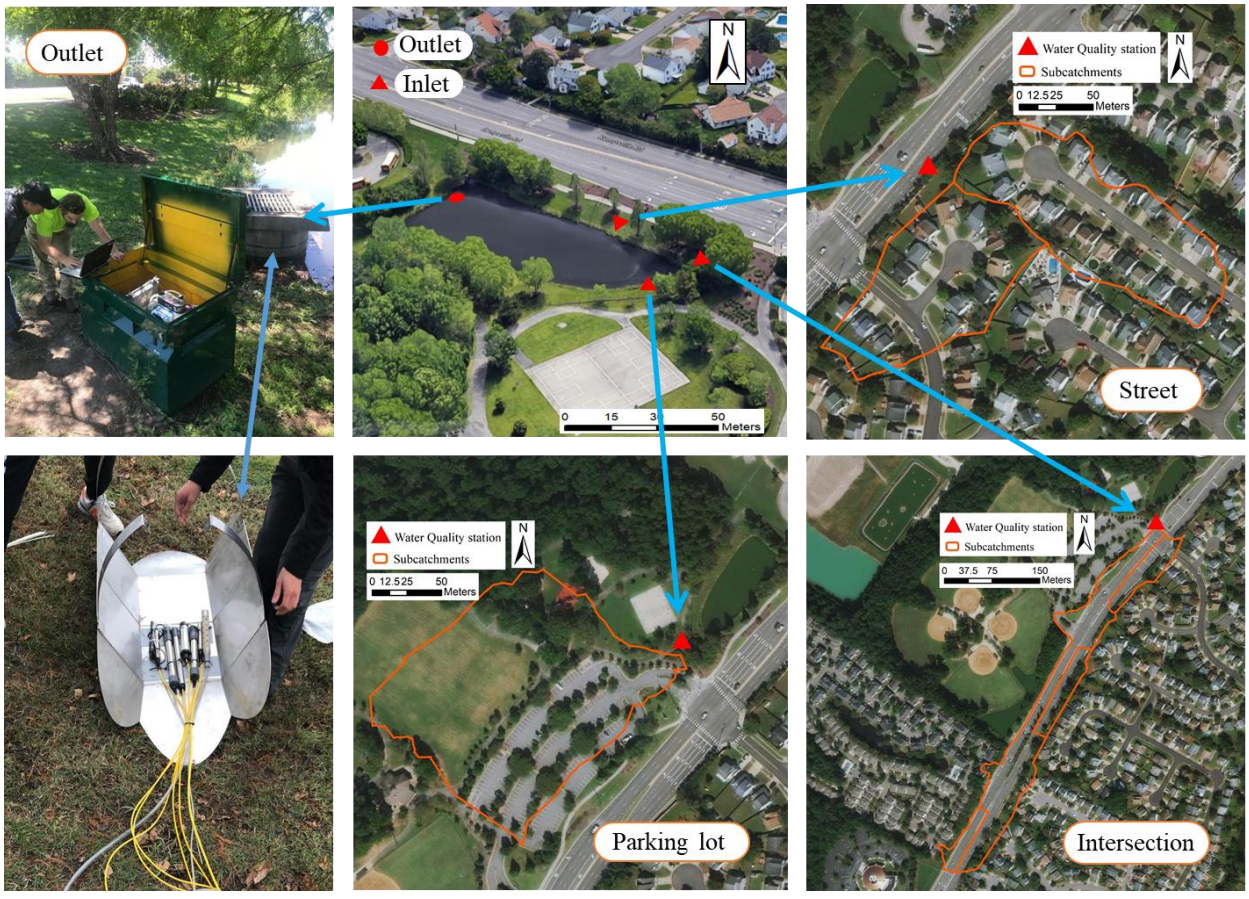

Figure 5.1. City View Park sampling location with maps of individual drainage areas with aerial photography.

Table 5.1. Study site characteristics.

Station	Drainage area (ha)	Imperviousness (%)
Street	2.04	40
Intersection	3.22	75
Parking lot	2.26	30

Bathymetric surveying was conducted on the retention pond using an acoustic Doppler current profiler (ADCP, Teledyne RD, Thousand Oaks, CA, US). Based on the bathymetric survey, the average and maximum depths of the pond were estimated as 1.57 m and 3.5 m, respectively (Figure 5.2). The elevation of the outlet is 2 meters. During dry periods, the water level is below 2 m, and the outlet is dry. Conversely, when the depth of water is higher than 2 m, water discharges through the outlet. Additionally, a stage-area curve for the pond was developed; the volume of the pond below the 2 m threshold was estimated to be approximately 3,700 m^3. There are various kinds of trees and vegetation around the pond and in its buffer zone including bald cypress, oak, loblolly pine tree (*Pinus taeda*), southern wax myrtle (*Morella cerifera*), a mix of grasses, sedges, rushes, red maple stump sprouts (*Acer rubrum*), and cattails (*Typha latifolia*) common to buffer areas.

Monitoring stations were installed at each inlet and at the outlet of the pond. Each station was equipped with: (1) an automatic sampler (model 6712; Teledyne-ISCO, Lincoln, Nebraska) to collect stormwater samples; (2) a rain gauge (model 674; ISCO, Lincoln, Nebraska); and (3) Area-Velocity meters (model 2150; ISCO, Lincoln, Nebraska) to measure inflows, which are installed at each inlet of the pond. At the outlet, a Palmer-Bowlus flume and a bubbler flow meter (model 730; ISCO, Lincoln, Nebraska) were installed to estimate outflow. A water quality data sonde (WQMS, Global Water Instrumentation, College Station, TX, USA) was installed at

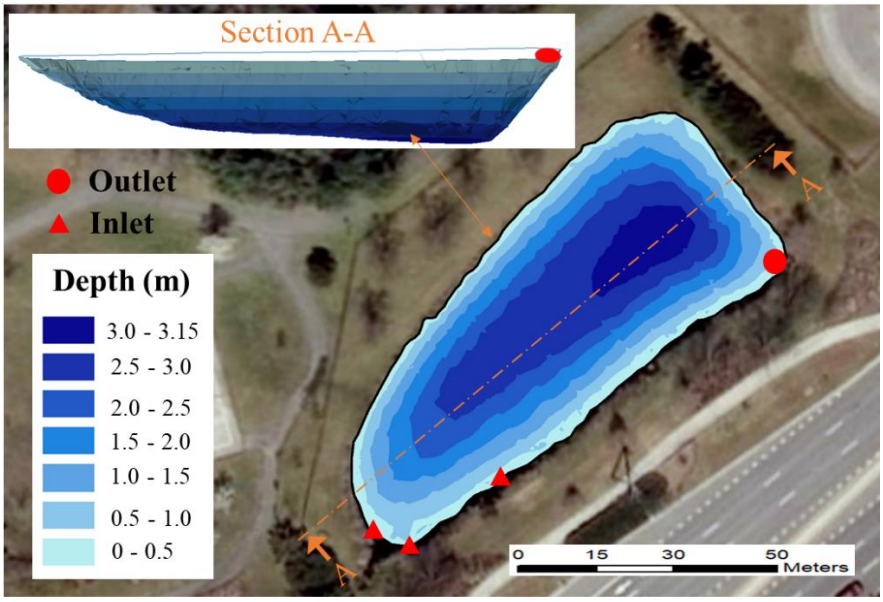

Figure 5.2. Bathymetry Survey of City view pond.

the outlet to continuously measure pond water level, pH, temperature, oxidation/reduction potential (ORP), conductivity, turbidity, and dissolved oxygen (DO) (Figure 5.1).

5.2.2 Sample collection methods

Water quality measurements and sampling were conducted at the inlets and outlet of the pond using similar procedures. Monitoring was initiated in December 2018 and continued over a 1-year period. All water samples were collected across the hydrograph for 30 storm events using the aforementioned auto-samplers, all were composite samples. The return period of observed storm events varied from 1 to 5 years. During each event, stormwater samples were collected and were transported from the field to the laboratory within 1 h of end of event, and then frozen at 0°C (USEPA, 1992).

A HACH total phosphorus kit (model PO-24, Hach Company, Loveland, CO, detection limits 0.02 mg/L), ammonia kit (Model NI-14, detection limits 0.02 mg/L), nitrate kit (Model

NI-14, detection limits 0.02 mg/L), and nitrite kit (Model NI-14, detection limits 0.02 mg/L) were applied for P and N analyses. The process for testing was described by Smith et al. (2004). For TSS, the weight of the pan and the glass fiber filter in the balance were measured three times.

Samples for Particle size distribution were collected unfiltered by vigorously shaking the composite sample, and subsampling into a 1 lit bottle. PSD was measured using a laser diffraction (LA-950, Horiba, Kyoto, Japan), which quantifies a particle size range of 0.01 - 3000 µm (Alberto et al., 2016; Goossens, 2008). Particles sort to 5 categories including clay (0.02-4 µm), silt (4-60 µm), very fine sand (60-125 µm), fine and medium sand (125-500 µm), and coarse (500-2000 µm) (Selbig and Bannerman, 2011; W. C. Krumbein, 1934). Summary statistics, including 10th percentile diameter (d_{10}), median particle diameter (d_{50}), and the 90th percentile diameter (d_{90}) were determined. Quality assurance/quality control (QA/QC), was provided in part by inclusion of blank samples, including: trip Blanks, sampling blanks and equipment blanks; these were run simultaneous with the monitoring program (Burant et al., 2018).

5.2.3 SWMM model development

Runoff quality is a function of land use and rainfall (Goonetilleke et al., 2005; A. Liu et al., 2013; Liu et al., 2015) which can be simulated by water quality models like SWMM (USEPA, 2018). The required data for the SWMM model includes rainfall, soil characteristics, land use, and extent of imperviousness. SWMM can determine pollutant-removal efficiency for a given SCMs like retention ponds. SWMM has a storage-Treatment component for simulating hydraulic storage and treatment. Required input for modeling a pond includes a storage-depth-area curve, which can be supplied by a bathymetric survey as was the case of our pond (Figure

5.2) and treatment equations for each pollutant. Pollutant removal was accounted for by applying first order decay equations to the storage node (i.e. pond) for TN, and TSS. Phosphorus in runoff has two forms including dissolve P (DP) and particulate P (PP), thus for P removal, DP and PP were considered separately, and the PP removal in the pond was characterized like TSS. In the mid-Atlantic region (EPA Rain Zone 2), analysis of data from the National Storm Water Quality Database indicates that DP is approximately 73% of TP (Pitt et al., 2008). Also, according to Vaze and Chiew (2004), DP is typically 20-30% of TP in urban runoff, i.e., 70-80% is associated with the sediment fraction. Thus, we assumed 50% of P was in particulate form. The removal rate a function of the irreducible concentration and a rate constant for each pollutant (Alamdari et al., 2017). The parameters in the storage node pollutant removal equations were calibrated to match the observed concentrations at the outlet of the pond for each storm event. Adjusted pollutant removal equation was estimated by Eq. 1 (Rossman and Huber, 2016; Smith, 2018).

$$C_{out} = a + (C_{in} - a) \times e^{\left(\frac{-b \times DT}{Depth}\right)} \quad (1)$$

where C_{out} = outflow concentration (concentration leaving the retention pond) (mg/L), C_{in} = inflow concentration to the pond (mg/L), DT = model time step (seconds), Depth = storage node water depth (m), a and b calibration parameters.

First, the SWMM model was calibrated for water quantity (hydrology) for each inlets and outlet and then the model was calibrated for water quality (pollutant-removal efficiency). Applying statistical methods such as the Nash-Sutcliffe Efficiency (NSE), coefficient of determination (r^2), and Percent bias (PBIAS), the SWMM model was assessed. The model calibration was complete, when r^2 and NSE became higher than 0.6 and 0.5, respectively, and PBIAS less than ±25 (Duda et al., 2012; Ketabchy et al., 2018; Seong et al., 2015); otherwise, model calibration parameters were adjusted. For water quality calibration, when the statistical

parameters showed r^2 and NSE higher than 0.4 and 0.35, respectively, and PBIAS less than ±30% (Moriasi et al., 2015) calibration was considered complete.

5.2.4 Pond treatment assessment

Removal pollutant efficiency for a pond is estimated by comparing inflow and outflow mass loads and change of concentration. Removal efficiency (RE) is an accepted method for calculating the pond efficiency. RE is a method for comparing average outlet EMCs with average inlet EMC (Eq. 2) (Lucke and Nichols, 2015; O'Driscoll et al., 2010).

$$RE = \left(1 - \frac{average\ of\ EMC_{outlet}}{average\ of\ EMC_{inlet}}\right) \times 100 \quad (2)$$

These parameters were calculated after each storm event over the monitoring program, and compared across the event intensity, duration, and season.

5.2.5 Assessing the role of precipitation on pond treatment using Principal Components Analysis

Suitable precipitation parameters were selected to assess the relationship between precipitation characteristics and retention pond treatment performance. The selected precipitation parameters in this study were precipitation duration (PDu), precipitation depth (PDe), average precipitation intensity (API), maximum precipitation intensity (MPI), and antecedent dry periods (ADP). ADP was the number of dry days between storm events. Average precipitation intensity was calculated by dividing the total precipitation depth by the precipitation duration. Precipitation characteristics using to represent event-to-event differences. These five parameters and pond treatment efficiency for TN, TP, TSS, PO_4, and TKN were estimated for the 30 monitored events, and then investigated using Principal Component Analysis (PCA). PCA is a technique that is applied for assessing relationships between objects and variables (Espinasse et

al., 1997; Kokot et al., 1998; A. Liu et al., 2013). In this study the PC variables are PDu, PDe, API, MPI, ADP, and RE values for TN, TP, TSS, PO_4, and TKN. Accordingly, a data matrix (30 × 10) including 30 events was generated.

5.2.6 Statistical analysis

Statistical tests were performed to evaluate statistical differences between inflow and outflow concentration from the retention pond. First, the Shapiro-Wilk Test was applied to assess whether the distribution of each inflow and outflow follow a normal distribution. The sampling program for collecting influent and effluent samples for retention ponds with long retention times may not enable to collect event-based pairing of monitoring data (Burant et al., 2018; Ivanovsky et al., 2018; Willard et al., 2017). Thus, if inflow and outflow follow a normal distribution, Welch's t-test was used to detect assess the null hypothesis, H0: there was no difference between inflow and outflow mean concentrations (Lucke and Nichols, 2015). While, if the distributions were not found to be normal, the Mann-Whitney test was used instead of Welch's t-test (Burant et al., 2018). The Mann-Whitney U test null hypothesis (H0) shows that the two groups originated from the same population. If the P value is less than the indicated significance level (0.05 and 0.10), the null hypothesis for the statistical tests can be rejected.

5.3 Results

5.3.1 Continuous hydrograph for the inlets and outlet

Results of flow and precipitation for three inlets (Parking lot, Intersection, and Street) and the outlet are shown in Figure 5.3. Results indicated that runoff flow during storm events for the Intersection and Parking lot stations was greater than the Street station. The effect of the attenuation of retention pond outflows compared with inflows to the pond is shown in Figure 5.3 (b) and (c), as a flattening in the outflow hydrograph. HRT was calculated for each event and it

was between 15 - 36 hours. The length of the HRT corresponded with storm magnitude. Monthly runoff volume delivered to the pond and discharged from the pond was presented in Table 5.2. Runoff reduction (RR) in the retention pond varied monthly between 1.76% and 7.00% (Figure 5.4). The maximum runoff reduction occurred in June, which is one of the warmest months in Virginia Beach, with high evapotranspiration, and the annual RR for the retention pond was

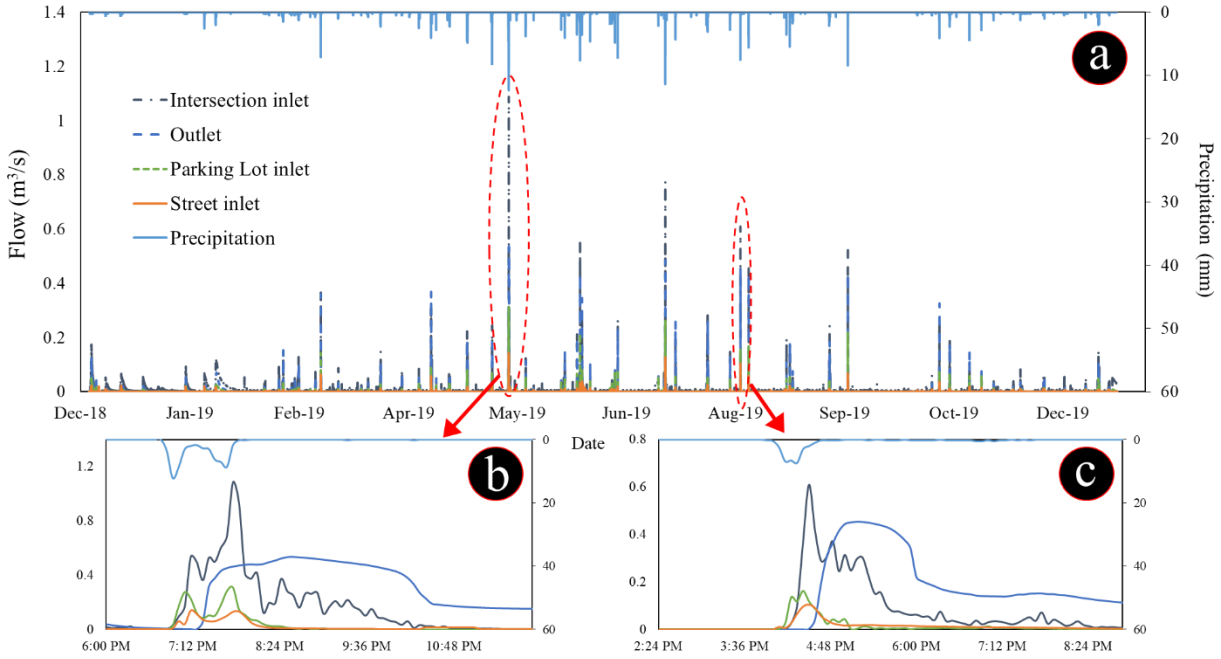

Figure 5.3. Hydrographs of each station a) between Dec-2018 to Dec-2019 b) May 19, 2019 c) Aug 4, 2019.

Table 5.2. Runoff reduction for the retention pond.

Month	Inflow (m^3)	Outflow (m^3)	Rainfall (mm)	Runoff Reduction (%)
Jan	7.39E+02	7.26E+02	79	1.76
Feb	8.42E+03	7.98E+03	111	5.15
Mar	6.72E+02	6.60E+02	76	1.76
Apr	4.03E+03	3.78E+03	116	6.11
May	7.24E+03	6.89E+03	126	4.90
Jun	2.12E+04	1.97E+04	142	7.00
Jul	4.40E+03	4.18E+03	125	4.95
Aug	2.50E+03	2.39E+03	116	4.51
Sep	2.00E+03	1.92E+03	92	4.31
Oct	1.42E+03	1.37E+03	95	3.61
Nov	8.88E+02	8.60E+02	62	3.16
Dec	7.69E+02	7.33E+02	50	4.63
Overall	5.43E+04	5.12E+04	1190	5.67

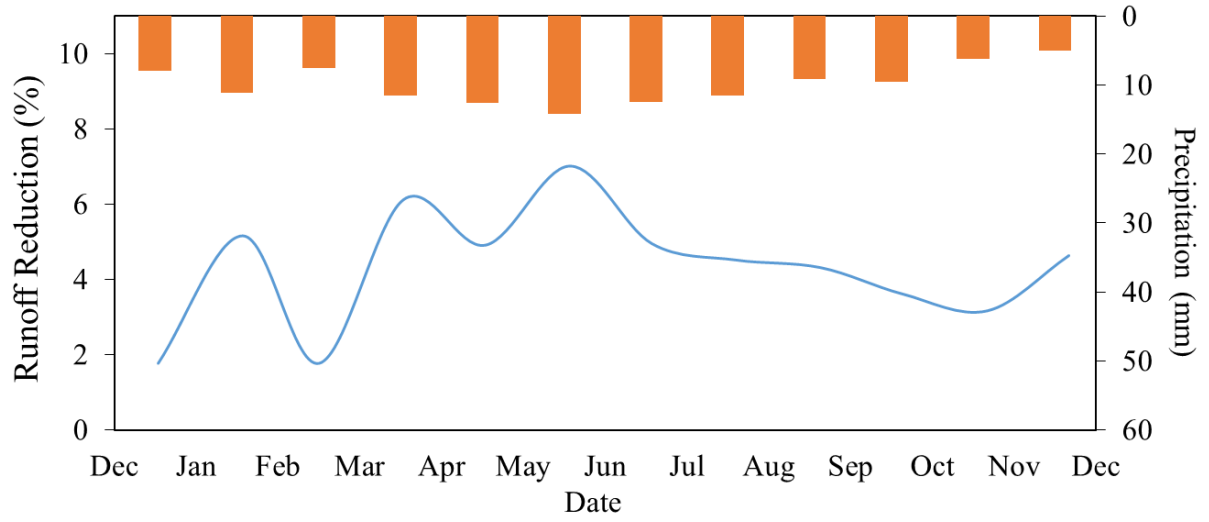

Figure 5.4. Monthly runoff reduction for the retention pond.

5.67%, while annual runoff volume reduction for wet ponds is considered 0% by Virginia Department of Conservation and Recreation (VA-DCR).

5.3.2 Results of water quality sonde

Results of temperature, pH, ORP, DO, and conductivity are shown in Figure 5.5. The highest and lowest temperatures were 28.5, and 11°C; these occurred during August and December,

respectively. The average and median of temperature were 21.5 and 24°C., respectively. After each storm, the temperature of the pond increased slightly. Impervious surfaces such as pavement have a low albedo, and thus absorb thermal energy, increasing the temperature of storm runoff (Ketabchy et al., 2018). pH varied between 7.48 and 6.82 and the highest and lowest pH occurred during September and May, respectively. Results indicated that there is direct relationship between temperature and pH, so as temperature increased during the summer, pH likewise increased; the opposite was the case during cold weather. Oxidation-reduction potential is measured in millivolts (mV). There is a relationship between ORP and DO, and when oxygen is low (low DO), ORP could be negative. ORP varied between 24.1 and -442.8 mV. Most of the time, particularly during warm seasons, ORP in the retention pond was negative (average -231 mV), which is a suitable environment for denitrification and P release from sediments (Spagni et al., 2001). DO varied between 98 and 1%, that shows sometimes the pond faced with anoxic condition. Most of time (particularly during dry periods), DO was low (average 39.3), however after storm events, because of turnover and new inflows, DO increased significantly. Turbidity varied between 32.2 and 1021.7 NTU (Nephelometric Turbidity Units). The average of turbidity was 472.2 NTU (median was 388.3 NTU), while after storm events it declined to as low as 100 NTU after the event.

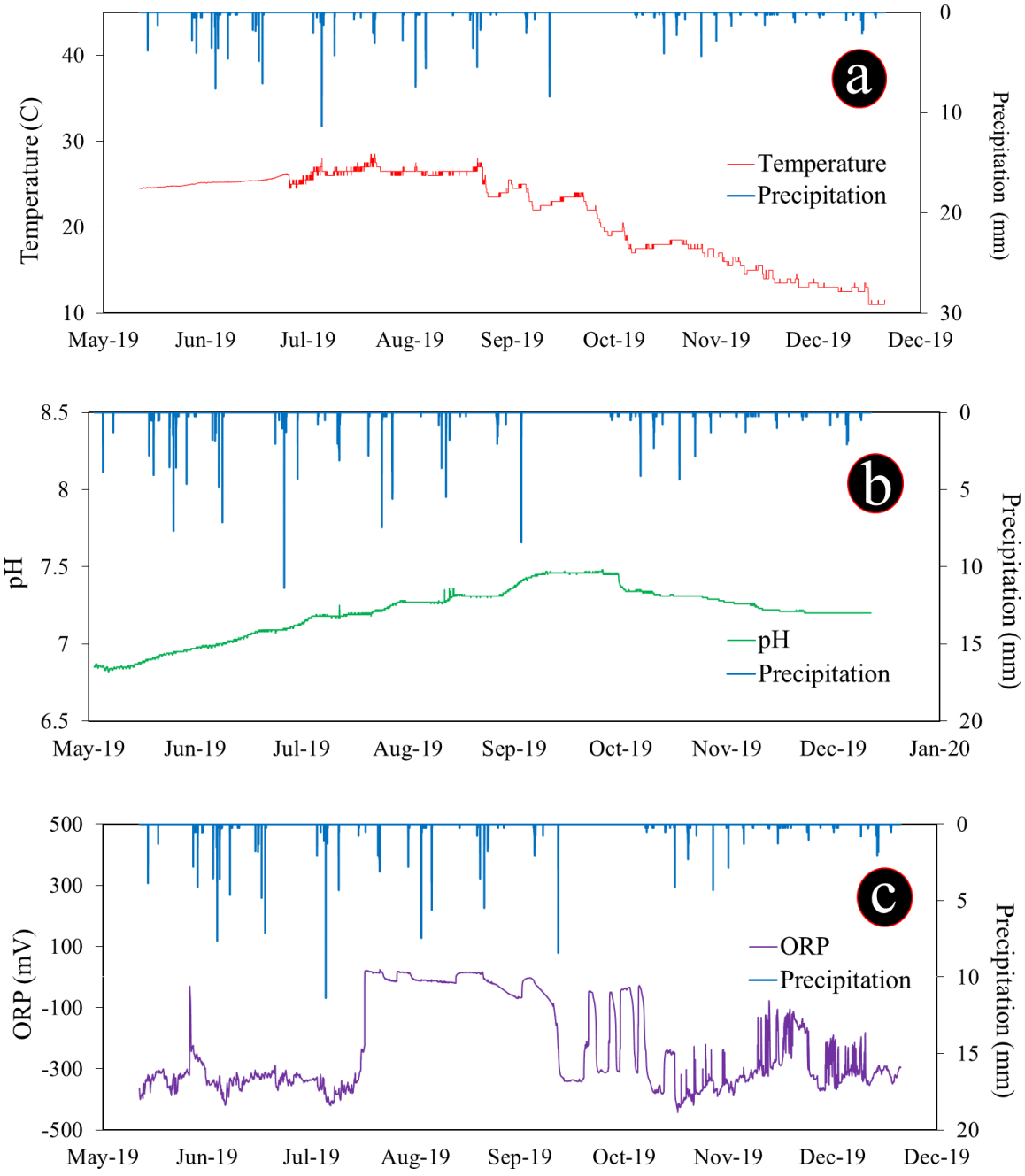
a
Temperature (C)
Precipitation (mm)
Temperature
Precipitation
40
30
20
10
0
10
20
30
May-19
Jun-19
Jul-19
Aug-19
Sep-19
Oct-19
Nov-19
Dec-19
Dec-19
b
pH
Precipitation (mm)
pH
Precipitation
8.5
8
7.5
7
6.5
0
5
10
15
20
May-19
Jun-19
Jul-19
Aug-19
Sep-19
Oct-19
Nov-19
Dec-19
Jan-20
c
ORP (mV)
Precipitation (mm)
ORP
Precipitation
500
300
100
-100
-300
-500
0
5
10
15
20
May-19
Jun-19
Jul-19
Aug-19
Sep-19
Oct-19
Nov-19
Dec-19
Dec-19

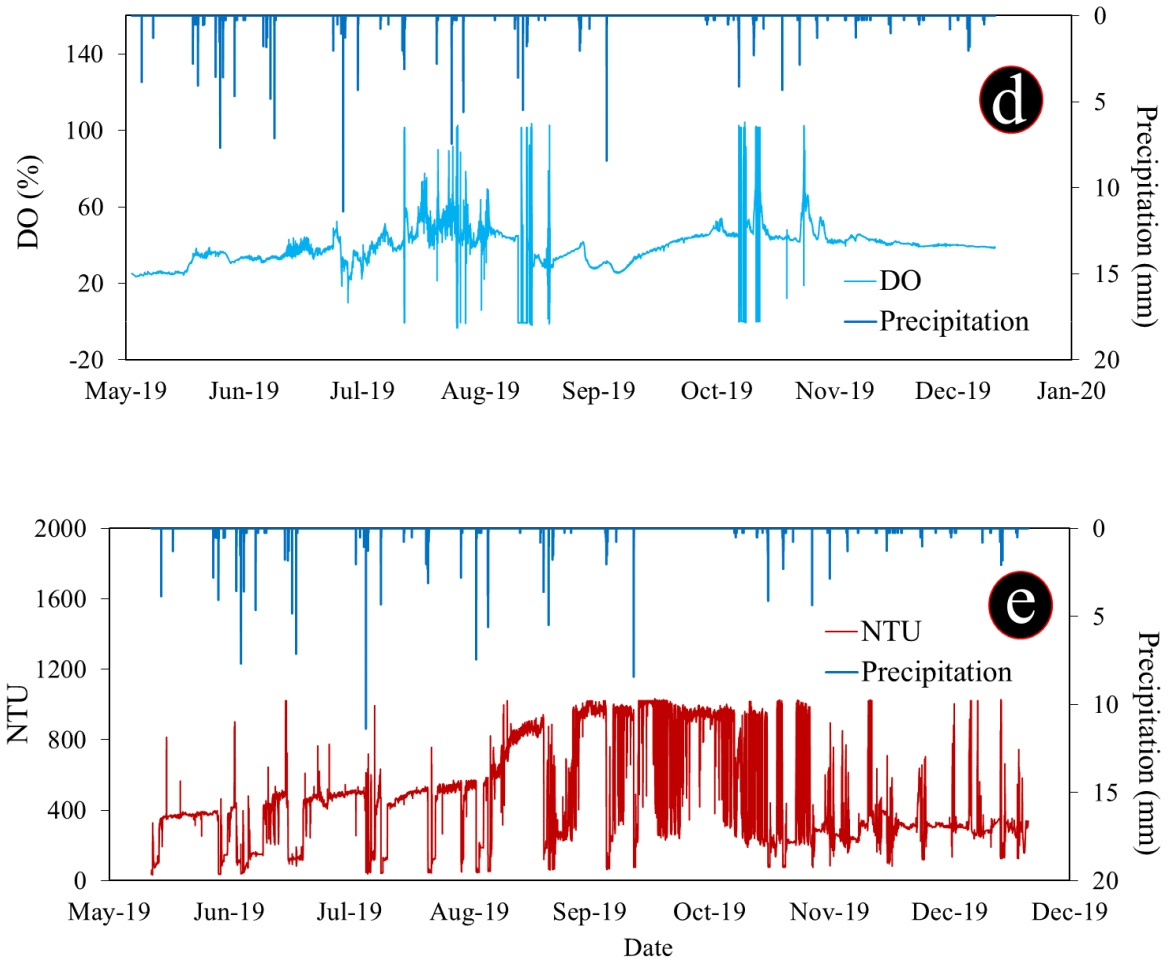

Figure 5.5. Water quality for a) temperature, b) pH, c) ORP, d) DO and, e) turbidity.

5.3.3 Temperature within the pond

Results of water temperature sensors inside the pond at 1 and 2.5 m depth are shown in Figure 5.6. Results indicate that there is a thermal stratification during warm weather (June – September). The temperature differential between these two layers is almost 5 degrees, and the maximum differential of 7 degree occurred in July. Song et al. (2013) and Wilhelm (2007) showed that between late spring and early fall, retention ponds and shallow water bodies face with thermal stratification. During September, the temperature differential between these two layers declined and in October they were the same temperature (a well-mixed condition). There

was no thermal stratification observed during cold weather. After each storm, temperature inside the pond increased as much as 2 degrees C.

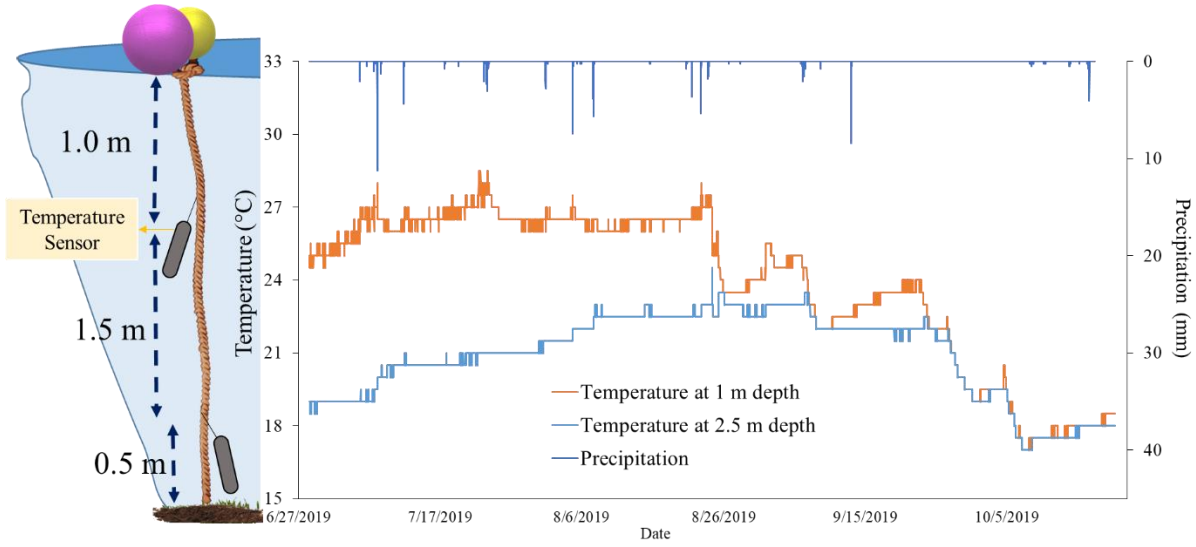

Figure 5.6. Temperature inside the retention pond.

stratification between late spring and early fall. During September, the temperature differential between these two layers declined and in October they were the same temperature (a well-mixed condition). There was no thermal stratification observed during cold weather. After each storm, temperature inside the pond increased as much as 2 degrees C.

5.3.4 Results of water quality sampling

Stormwater samples were analyzed for 30 events throughout one year. Composite samples were collected from runoff the Parking-lot, Intersection, Street, and the Outlet Station(s), respectively. Since the drainage areas and characteristics of each inlet and resulting flows and pollutant concentrations are unique, a method for combining them was developed. Total runoff volume for each inlet was estimated by using the results of hydrograph. Total mass loads of inlets were calculated and then divided by total volume of runoff delivered to the pond, and a single EMC for inflow was calculated. The inflow annual average EMC was 0.37 $mg \cdot L^{-1}$

(Coefficient of Variation, or CV=60%) for NH_3, 0.41 mg·L^{-1} (CV=60%) for NH_4, 0.01 mg·L^{-1} (CV=40%) for NO_2, 0.37 mg·L^{-1} (CV=80%) for NO_3, 0.54 mg·L^{-1} (CV=73%) for TKN, 0.63 mg·L^{-1} (CV=66%) for TN, 0.21 mg·L^{-1} (CV=17%) for PO_4, 0.33 mg·L^{-1} (CV=24%) for TP, and 34.5 mg·L^{-1} (CV=77%) for TSS. During the monitoring period, inflow TSS varied between 10 and 113 mg·L^{-1}, respectively. TSS, TP and TN concentrations for inflow through the monitoring period are shown in Fig 5.7a. The outflow had an annual average EMC of 0.25 mg·L^{-1} (CV=54%) for NH_3, 0.27 mg·L^{-1} (CV=53%) for NH_4, 0.006 mg·L^{-1} (CV=90%) for NO_2, 0.25 mg·L^{-1} (CV=95%) for NO_3, 0.36 mg·L^{-1} (CV=65%) for TKN, 0.42 mg·L^{-1} (CV=67%) for TN, 0.15 mg·L^{-1} (CV=34%) for PO_4, 0.28 mg·L^{-1} (CV=20%) for TP, and 7.5 mg·L^{-1} (CV=49%) for TSS. Variability in TSS, TP and TN concentration for outflow are presented in Fig 5.7b. Results showed that the outflow concentrations of TN and TP has less variability than those of inflow. In

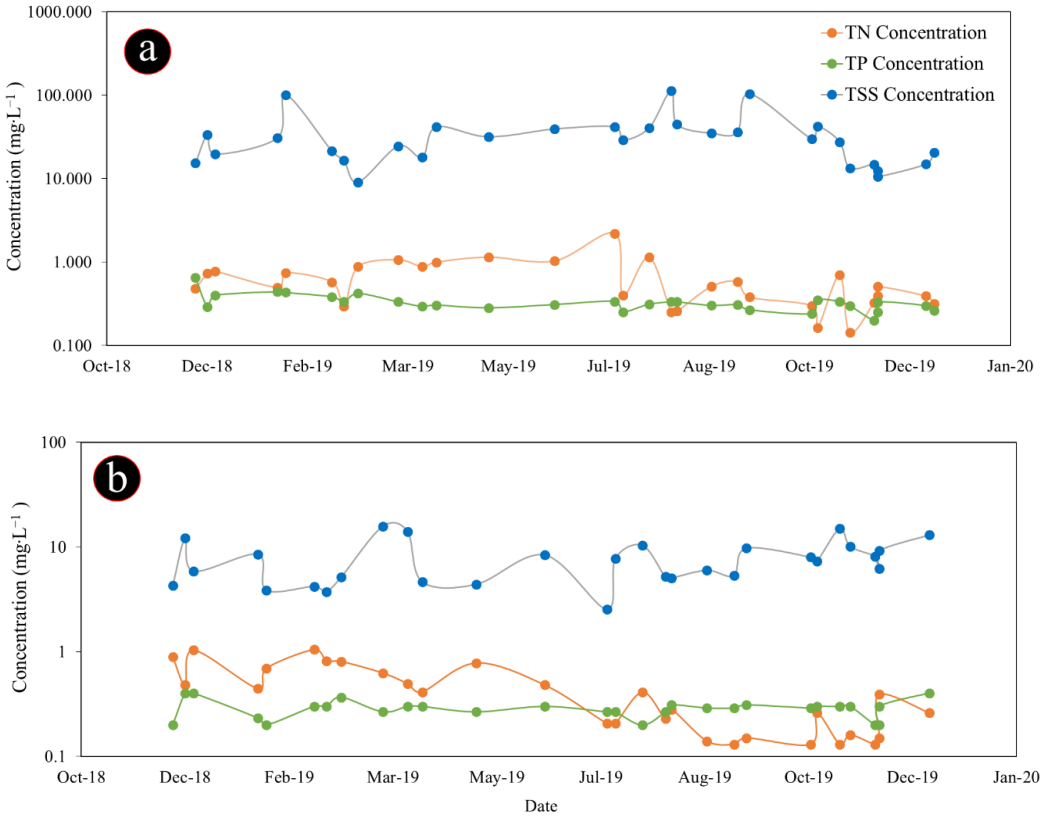

Figure 5.7. Concentrations of TN, TP, and TSS within monitoring period for a) inflow and b) outflow.

addition, the inflow concentrations of TSS varied between 10 – 100 $mg \cdot L^{-1}$, while for outflow varied between 4 – 15 $mg \cdot L^{-1}$.

5.3.5 Pond performance with statistical results

Results of water quality and RE were divided into warm and cold weather groups and are presented in Table 5.3. Negative or positive of removal efficiency (RE) means, the pond can be either a source or sink for those pollutants, respectively. We found, during cold weather, the pond reduced the level of TSS and P by 62% and 8.8%, respectively, while it exported N and the level of N increased in the outflow of the pond by 6%. During warm weather, due to biological activities like nitrification/denitrification, the performance of the pond changed, it reduced TSS, TN and P by 74%, 47%, and 8%, respectively (Table 5.3). Performance of the retention pond during warm weather was similar to results of a literature search for published studies, reported by Koch et al. (2014) which showed RE of N for wet ponds were about 40%.

5.3.6 Statistical analysis results

Results of Shapiro test indicated that, except for TSS, the data were not normally distributed, thus Welch's t-test was used for assessing TSS and Mann-Whitney U test for everything else (Table 5.4). Also, data were assessed in 3 groups including overall concentrations, concentrations in cold weather and concentrations in warm weather.

Table 5.3. Results of removal efficiency for the retention pond, %.

Attribute	NO_2+ NO_3	TKN	TN	PO_4	TP	TSS
Warm weather	56.3	44.3	47.0	27.6	8.1	74.2
Cold weather	33.9	-16.2	-6.1	10.0	8.8	62.2
Overall	44.4	12.1	18.7	18.2	8.4	67.8

Table 5.4. Statistical Results (P-values).

	Statistical methods	TSS	TN	TKN	TP	PO_4
Overall	t-test	5.7E-06 R	-	-	-	-
	Whitney	-	2.3E-02 R	2.5E-02 R	1.1E-02 R	7.9E-03 R
Warm Weather	t-test	5.0E-04 R	-	-	-	-
	Whitney	-	4.7E-03 R	4.4E-03 R	1.7E-02 R	7.0E-04 R
Cold Weather	t-test	3.5E-03 R	-	-	-	-
	Whitney	-	6.1E-01 Fr	8.1E-01 Fr	1.5E-01 Fr	5.4E-02 Fr

*R: Reject, *Fr: Failing to Reject

Results indicated P-value for Welch's t-test for all three groups was less than 0.05, so the null hypothesis (H0: there was no difference between inflow and outflow mean concentrations) for the test can be rejected. Thus, the sample means for TSS of inflow and outflow were significantly different. On the other hand, P-values for TN, TKN, TP, and PO4 overall were less than 0.05, meaning that the null hypothesis (H0: inflow and outflow concentrations come from the same population) for the Mann-Whitney U test is rejected. Analysis of results during warm weather were similar to the overall, however, during cold weather, all P-values were greater than 0.05, in which case the null hypothesis cannot be rejected, and the groups of data for inflow and outflow likely come from the same population. This means that during cold weather, the retention pond has no significant treatment effect for P and N, while during warm weather, the effect of pond treatment for P and N is significant.

5.3.7 Principal Component Analysis

PC1, PC2 and PC3 axes in the analysis shows a suitable variance of the data. There are two biplots where displays the PC1 vs. PC2 and the PC2 vs. PC3, respectively (Figure 5.8). The first three PCs contain 27.4, 25.2 and 13.3% of the data variance, respectively, which adds to a

total data variance of approximately 61.5 %. This demonstrates that PC1, PC2 and PC3 axes contain an appropriate variance of the data. The three rainfall parameters PDe, MPI, and API exhibit strong correlation with each other and with RE of TSS, TP, and PO_4. There is strong correlation between RE of TP, PO_4, and TSS, which is understandable in most P is primarily in particulate form, while the opposite is true of nitrogen. There is strong correlation between TN and TKN as the angle between the vectors is very small, indicating most TN is in organic form. The lengths of PDe and API vectors are longer than the vector for ADP and PDu. This demonstrates that PDe and API could have more effect on the pond treatment efficiency than PDu and ADP. There is not a strong correlation between ADP with other precipitation characteristics and ERs and thus could be an independent parameter.

5.3.8 Particle size distribution results

Particle size in this study are presented in 3 size fractions, i.e. D_{10}, D_{50}, and D_{90}. Particle

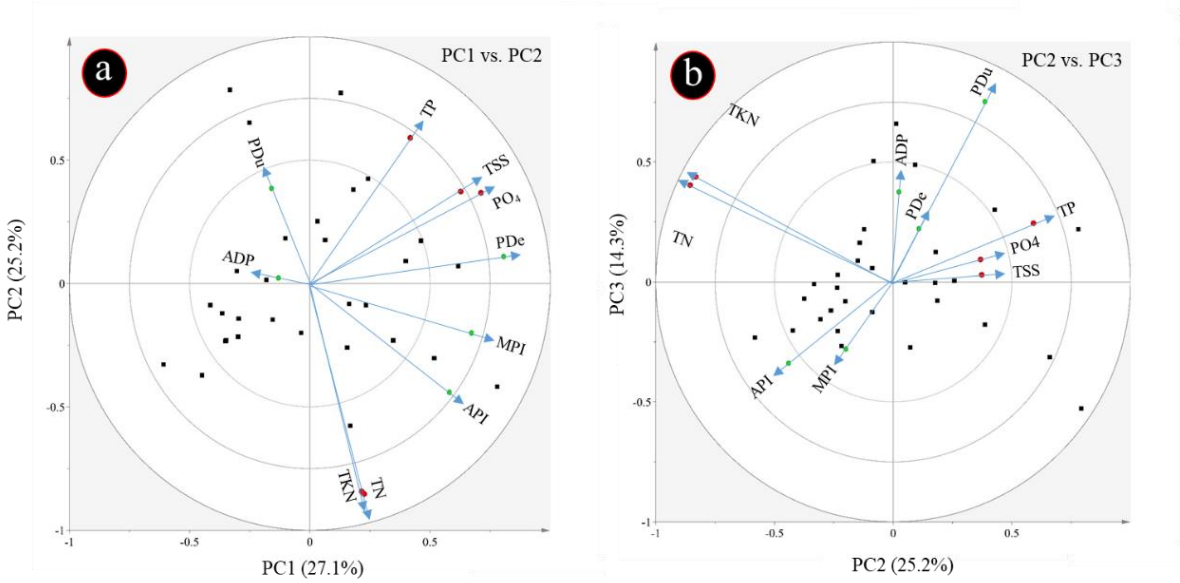

Figure 5.8. PCA biplots for rainfall parameters and REs.

size varied between inflows and outflow (Figure 5.9). D_{50} for inflows varied between 0.2 and 320 µm, while for outflow varied between 0.15 and 0.84 µm, and only for two events was 120 and 240 µm. PSD indicated that D_{10}, D_{50}, and D_{90} in outflow of the pond decreased by 40%, 46%, and 42%, respectively, in comparison to inflows.

5.3.1 Modeling results

A SWMM model was developed and calibrated for the retention pond. Since the pond has 3 inlets and one outlet, four hydrographs are shown in Figure 5.10. Analysis of the goodness-of-fit metrics r^2, NSE and PBIAS showed SWMM simulated water quantity (i.e. inflows and

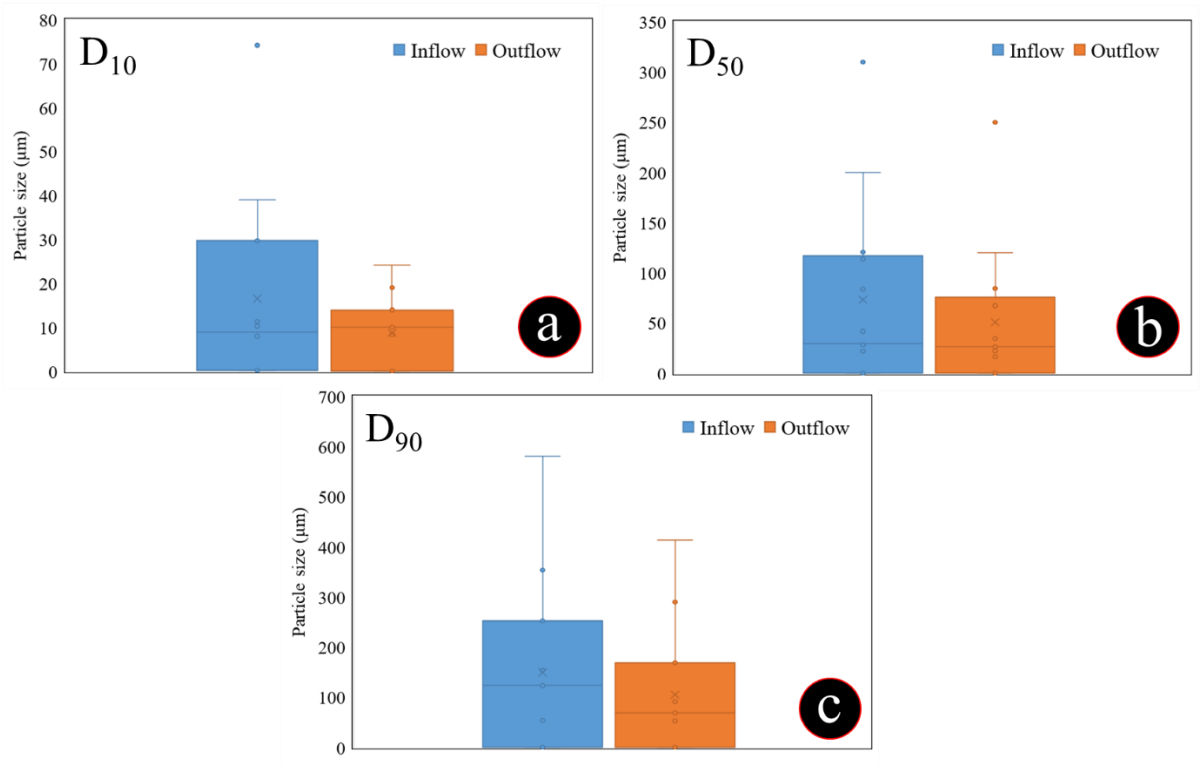

Figure 5.9. Particle sizes during monitoring program a) D_{10}, b) D_{50}, and c) D_{90}

outflow) of the retention pond well (Table 5.5). Regarding water quality, treatment equations for TN, TSS and TP was considered for the retention pond (Eq 3, 3, 4, 5 and 7). Treatment equations for TP has two parts, which Eq. 5 and Eq. 6 are related to DP and PP, respectively, and TP removal is sum of DP and PP removal (Eq. 7). PP associated with the sediment fraction, so there is similar behavior between PP and TSS (Eq. 6). The SWMM model for water quality was calibrated based upon the EMCs of the outflows. Results of r^2 indicated that the SWMM simulated TSS removal well, and for TP, the model performance was satisfactory (Figure 5.11). Since the variability of TN concentrations during warm weather was high, SWMM was unable to adequately simulate TN during warm weather (Figure 5.11c) using the aforementioned equation (1), but during cold weather the performance of SWMM for simulating TN was satisfactory (Figure 5.11d).

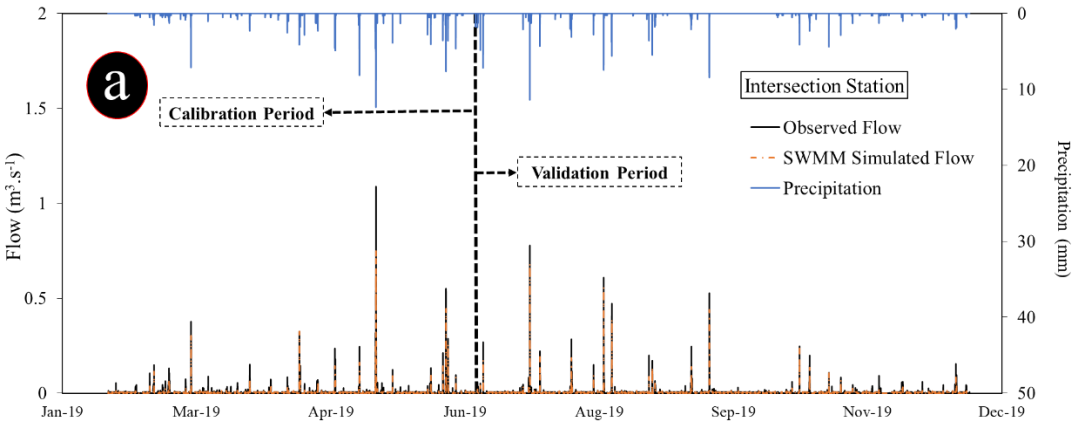

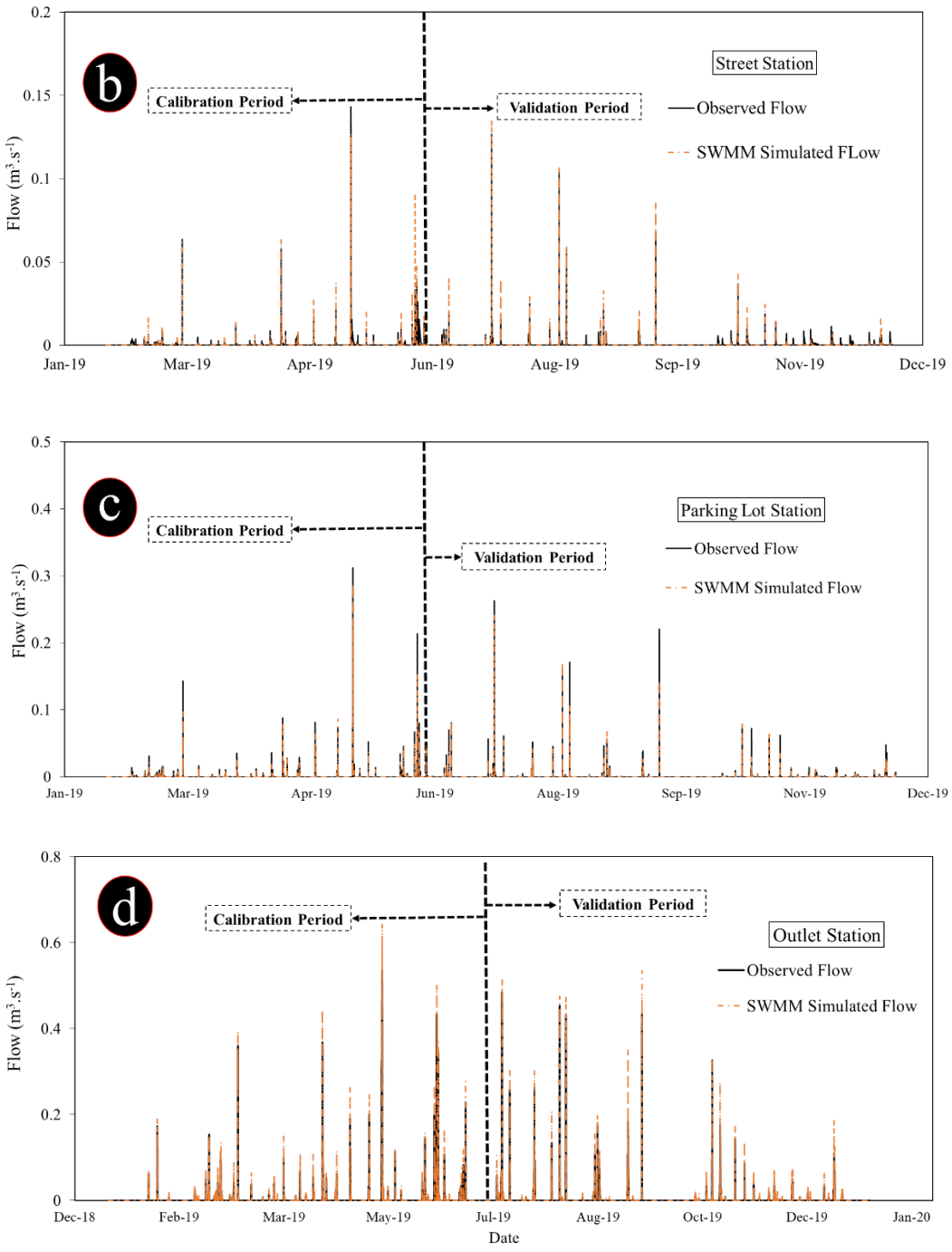

Figure 5.10. Comparison of observed and simulated runoff for each station a) Intersection, b) Street, c) Parking Lot, d) Outlet station.

Table 5.5. Calibration and validation results of statistical analysis for hydrology.

Statistical Method	Calibration	Validation
Intersection Station		
NSE	0.85	0.80
PBIAS	11%	9%
r^2	0.87	0.85
Parking lot Station		
NSE	0.78	0.72
PBIAS	5%	7%
r^2	0.81	0.76
Street Station		
NSE	0.69	0.65
PBIAS	-16%	-21%
r^2	0.75	0.69
Outlet Station		
NSE	0.71	0.63
PBIAS	12%	16%
r^2	0.78	0.72

$$TSS_{out} = 4.5 + (TSS_{in} - 4.5) \times e^{\left(\frac{-0.003 \times DT}{Depth}\right)} \quad (3)$$

$$TN_{out} = 0.2 + (TN_{in} - 0.2) \times e^{\left(\frac{-0.001 \times DT}{Depth}\right)} \quad (4)$$

$$DP_{out} = 0.05 + (0.5 \times TP_{in} - 0.05) \times e^{\left(\frac{-0.0004 \times DT}{Depth}\right)} \quad (5)$$

$$R = R\_TSS\ for\ PP \quad (6)$$

$$TP = SRP + PP \quad (7)$$

where DT = model time step (seconds), Depth = pond water depth, R = fractional removal.

5.4 Discussion

5.4.1 Removal process for TSS, TP and TN within the retention pond

Statistical analysis showed that, overall, the pond has positive effect on water quality treatment, however the pond treatment during cold and warm weather was completely different. During

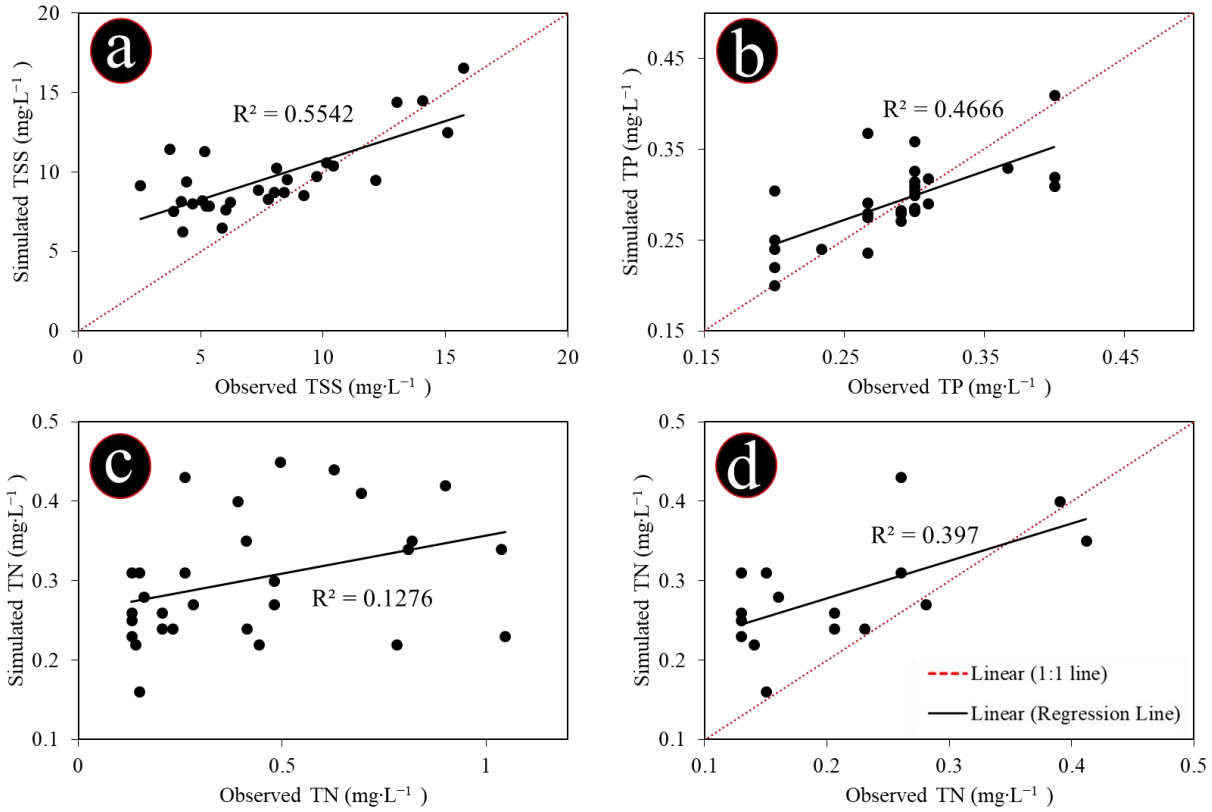

Figure 5.11. Scatter plots of simulated and observed results for each pollutant.

warm weather, biological activities could play a role in the observed better treatment of P and N, while during cold weather, there was no significant difference between concentrations of inflow and outflow for P and N. Thus, water quality results of TSS, TP and TN are shown for warm and cold weather (Figure 5.12).

5.4.1 TSS removal

Retention ponds are impediment for TSS removal by decreasing velocity of inflows, resulting in suspended solids to settle (NCDENR, 2009). Excess amounts of TSS, can has negative impact on aquatic life by decreasing sunlight entering water column and subsequently lowering water temperature (Bilotta and Brazier, 2008), and decreasing DO levels by increasing organic material into the water column (Waterman et al., 2011). TSS treatment within retention ponds occurs

mainly due to settling (Ivanovsky et al., 2018). In the present study, The TSS concentration of inflow in our study varied between 10 to 100 mg·L^{-1}, while the TSS concentration for outflow varied between 1 to 15 mg·L^{-1}, thus the retention pond was able to decrease the TSS concentrations very well, irrespective of season.

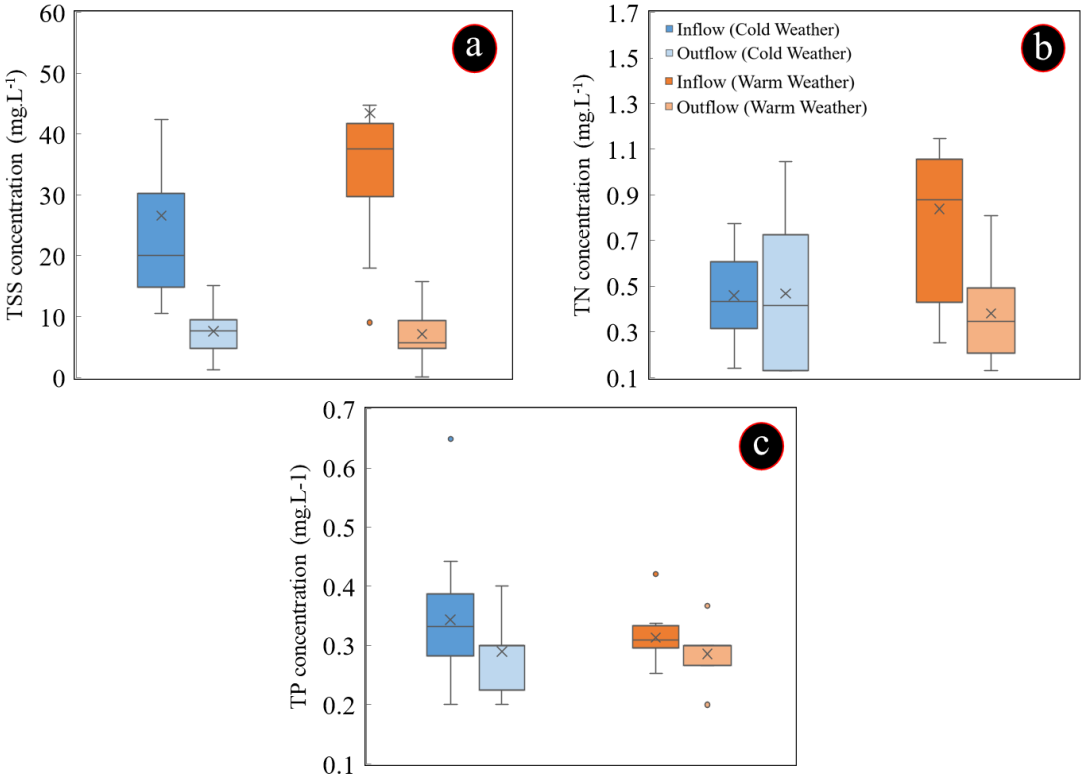

Figure 5.12. Removal process for a) TSS, b) TN and, c) TP.

5.4.2 TN removal

Within retention ponds, nitrogen exists inorganic and organic forms. Several factors can have effect on N removal in retention ponds including water column N:P ratios, the presence of pond vegetation, pH, temperature, the length and depth of the pond, flow path, sediment carbon quality, and HRT (Collins et al., 2010; Gold et al., 2018; Koch et al., 2014). In retention ponds, nitrogen is mainly removed through nitrification/denitrification, assimilation, and sedimentation (Bettez and Groffman, 2012; Collins et al., 2010; Troitsky et al., 2019).

Assimilation is uptake N into organic form by macrophytes and phytoplankton. Sedimentation of N mostly happens when organic materials die and accumulate in the bed of the retention pond (Troitsky et al., 2019). Clearly, HRT is the most important factor in sedimentation rates of N (Gu et al., 2017), since retention ponds have relatively high HRTs, Saunders and Kalff, (2001) reported, sedimentation process is the second largest N removal within retention ponds.

Nitrification is the biological oxidation of NH_4^+ and NH_3 to NO_3^- followed by denitrification, which nitrate (NO_3^-) is converted to nitrite (NO_2^-) in an anoxic condition and finally to molecular nitrogen (N_2) (Gold et al., 2017b). Thus, to make the reaction of NH_4^+ to N_2 occur, the pond should have aerobic and anaerobic sections to support the growth of nitrifying and denitrifying bacteria, respectively. Denitrification is conducted in sediment and bottom of the pond, and is the largest N removal process in most retention ponds (Kadlec and Wallace, 2008). In general, shallow retention ponds (lower than 3 m) are more effective than deeper pond in N removal (Koch et al., 2014), particularly when the temperature and pH of the retention ponds are greater than 20 °C and 7, respectively (De Assunção and Von Sperling, 2013). Also, HRTs increases the level of denitrification because more time allows the bacteria to reduce N levels further (Perryman et al., 2011).

During warm weather, nitrification and denitrification were occurring within our retention pond, so that the retention pond treatment changed, decreasing the level of N at the outlet. pH increased and ORP was negative, indicating suitable conditions for nitrification and denitrification (Troitsky et al., 2019). During warm weather, algal and microbial stocks in the retention pond causing N assimilation. During cold weather, due to an decrease in algal and microbial stocks, N release occurred (Bell et al., 2019). That may be the reason behind the

performance of our retention pond, which was a source of N (exported N), and the level of N increased at the outlet during cold weather.

In addition, dissimilatory nitrate reduction to ammonium (DNRA) is a process similar to denitrification, occurs in anaerobic conditions and transfers NO_3^- to soluble NH_4^+ directly (Gold et al., 2018). Low concentrations of NO_3^- and DO, high levels of iron, and organic rich sediments are favored conditions for DNRA (Kessler et al., 2018). The required conditions for DNRA are similar to denitrification conditions. Koch et al., (2014) showed that there is an increase in NH_4^+ concentrations that occurs within deeper ponds based upon short-term loading, which may be caused by DNRA. However, in our case study, the NH_4^+ concentrations didn't increase at the outlet, and the removal rate was similar to TN, thus it can be assumed DNRA was not occurring within the retention pond or at least it is not a prevalent process within it, in comparison to denitrification. Overall N treatment of our retention pond was 19%, similar to the Scenario Builder for the Chesapeake Bay Watershed Model (Chesapeake Bay Program, 2013), and research about SCMs conducted by Simpson et all, (2009).

5.4.3 TP removal

Phosphorus is removed or captured by sorption and plant uptake (Stutter and Lumsdon, 2008; Vymazal, 2007; Xiao et al., 2016). Particulate P was the dominant form in the water column (Sønderup et al., 2016; Song et al., 2017), thus the most effective way of P removal is through sedimentation. The P concentration for inflow during cold weather was higher than warm weather, but the treatment efficiency of the retention pond during both time periods were similar (within 10%). It demonstrates that the treatment of the pond for P during cold weather was better than warm weather. It can be assumed, during cold weather, P was adsorbed in sediment. During warm weather, the decomposition of sediment organic matter, higher

temperatures, and summer stratification resulted in a decline in DO and hypoxic conditions in the bottom of the retention pond (Song et al., 2015). Hypoxic conditions likely caused the release sorbed P from sediment, this phenomenon has been observed and reported by Duan et al. (2016); and Song et al. (2017). These processes may explain negative P removal efficiencies that sometimes occurs in retention ponds. Although the treatment of our retention pond changed slightly during warm weather, it was still a sink for P with the exception of two events where the RE was negative (-12.2 % and -24.9%), which is similar to results reported by Topçu et al. (2014).

5.4.4 Particle sizes effect

PSD may be an important factor in predicting retention pond treatment. Without knowledge of the specific PSD in retention pond inflows, predicting the percentage of particles captured in pond is difficult (Berretta and Sansalone, 2011). Particle sizes of water sediment entering the retention pond varied widely for storm events. Particle size (D_{50}) ranged from 0.15 to 320 μm. For reference, clays are 4 μm or less, silts are between 4 μm and 60 μm, very fine sands are between 60 μm and 120 μm, and fine and medium sand are between 100 μm and 250 μm, and coarse sands are between 500 μm and 2000 μm (Selbig and Bannerman, 2011; W. C. Krumbein, 1934). Particle size plays a key role in pollutant treatment, because 85% of TP and TN are attached to particle sizes smaller than 300 μm. Additionally, particulate TP and TN in storm runoff adhere to sediment sizes between 11 and 150 mm (Vaze and Chiew, 2004). Thus, the results suggest that to effectively remove TP and TN, the retention pond should have a long HRT sufficient to allow particles to settle. For example, D_{50} for outflow in the retention pond was smaller than 80 μm, except for two storm events, within which it was 120 and 240 μm. During those two storm events the

concentration of TP for outflow was higher than inflows (RE was negative), and the retention was a source of P instead of being sink.

5.5 Conclusion

A monitoring program was conducted for one year on a coastal retention pond within Virginia Beach, USA. The performance of the retention pond was evaluated for reducing runoff and concentrations for 30 storms events between December 2018 and December 2019. Storm water samples for the inlets and the outlet of the pond were analyzed for NO_2, NO_3, TKN, TN, PO_4, TP, TSS, and PSD. A SWMM model was developed and calibrated to simulate the retention pond treatment for stormwater quantity and quality. HRT was calculated for each event and it ranged from 15 - 36 hours. Results indicated that the runoff reduction for the retention pond varied monthly between 1.76 to 7.00 %. Between late spring and early fall, the retention pond experienced long periods of thermal stratification. With regard to water quality, the inflow annual average EMC was 0.63 $mg \cdot L^{-1}$ for TN, 0.33 $mg \cdot L^{-1}$ for TP, and 34.5 $mg \cdot L^{-1}$ for TSS, while the outflow had an annual average EMC of 0.42, 0.28 and 7.5 $mg \cdot L^{-1}$ for TN, TP and TSS, respectively. During cold weather, the retention pond had no significant treatment effect for P and N, while during warm weather, the effect of pond treatment for P and N was significant. Results indicated that during cold weather, the pond reduced the level of TSS and TP by 62% and 8.8%, respectively, while the pond exported N and the level of TN increased in the outflow of the pond by 6%. During warm weather, due to biological activities like nitrification and denitrification, the performance of the pond improved, and the pond reduced TSS, TN and TP by 74%, 47%, and 8%, respectively. In addition, results indicated that rainfall characteristics play an important role in the removal efficiency of the retention pond so that the three rainfall parameters including precipitation depth, maximum precipitation intensity, and antecedent dry period had

strong correlation with RE of TSS and TP. Analysis of goodness-of-fit parameters indicates that SWMM simulated water quantity (i.e. inflows and outflow) of the retention pond well. SWMM was able to model TSS removal reasonably well, and for TP the performance of SWMM was satisfactory, however SWMM was unable to simulate TN during warm weather, and only could simulate TN during cold weather. While this retention pond was not designed for water quality treatment, the results of this study indicate that the retention pond provides significant improvement in the water quality of urban runoff and can be implemented to mitigate adverse impact of urbanization on hydrology and water quality. However, the ability of retention ponds to reduce N has been much variable during cold and warm weather due to biological activities. The N cycling processes inside the retention ponds should be characterized and efficient management strategies should be implemented to improve retention ponds treatment.

5.6 Reference for Chapter 5

Alamdari, N., Sample, D., Steinberg, P., Ross, A., Easton, Z., 2017. Assessing the effects of climate change on water quantity and quality in an urban watershed using a calibrated stormwater model. Water 9, 464. doi:10.3390/w9070464

Alberto, A., St-Hilaire, A., Courtenay, S.C., van den Heuvel, M.R., 2016. Monitoring stream sediment loads in response to agriculture in Prince Edward Island, Canada. Environ. Monit. Assess. doi:10.1007/s10661-016-5411-3

Bell, C.D., Tague, C.L., McMillan, S.K., 2019. Modeling runoff and nitrogen loads from a watershed at different levels of impervious surface coverage and connectivity to stormwater control measures. Water Resour. Res. 1–18. doi:10.1029/2018wr023006

Berretta, C., Sansalone, J., 2011. Hydrologic transport and partitioning of phosphorus fractions. J. Hydrol. 403, 25–36. doi:10.1016/j.jhydrol.2011.03.035

Bettez, N.D., Groffman, P.M., 2012. Denitrification Potential in Stormwater Control Structures and Natural Riparian Zones in an Urban Landscape. Environ. Sci. Technol. 46, 10909–10917. doi:10.1021/es301409z

Bilotta, G.S., Brazier, R.E., 2008. Understanding the influence of suspended solids on water quality and aquatic biota. Water Res. 42, 2849–2861. doi:10.1016/J.WATRES.2008.03.018

Burant, A., Selbig, W., Furlong, E.T., Higgins, C.P., 2018. Trace organic contaminants in urban runoff : Associations with urban. Environ. Pollut. 242, 2068–2077. doi:10.1016/j.envpol.2018.06.066

Chen, J., Theller, L., Gitau, M.W., Engel, B.A., Harbor, J.M., 2017. Urbanization impacts on surface runoff of the contiguous United States. J. Environ. Manage. 187, 470–481. doi:10.1016/J.JENVMAN.2016.11.017

Chesapeake Bay Program, 2013. Estimates of County-Level Nitrogen and Phosphorus Data for Use in Modeling Pollutant Reduction: Documentation for Scenario Builder Version 2.4.

Chrétien, F., Gagnon, P., Thériault, G., Guillou, M., 2016. Performance Analysis of a Wet-Retention Pond in a Small Agricultural Catchment. J. Environ. Eng. 142, 04016005. doi:10.1061/(ASCE)EE.1943-7870.0001081

Collins, K.A., Lawrence, T.J., Stander, E.K., Jontos, R.J., Kaushal, S.S., Newcomer, T.A., Grimm, N.B., Cole Ekberg, M.L., 2010. Opportunities and challenges for managing nitrogen in urban stormwater: A review and synthesis. Ecol. Eng. 36, 1507–1519. doi:10.1016/j.ecoleng.2010.03.015

Damodaram, C., Giacomoni, M.H., Prakash Khedun, C., Holmes, H., Ryan, A., Saour, W., Zechman, E.M., 2010. Simulation of Combined Best Management Practices and Low Impact Development for Sustainable Stormwater Management1. JAWRA J. Am. Water Resour. Assoc. 46, 907–918. doi:10.1111/j.1752-1688.2010.00462.x

De Assunção, F.A.L., Von Sperling, M., 2013. Influence of temperature and pH on nitrogen removal in a series of maturation ponds treating anaerobic effluent. Water Sci. Technol. 67, 2241–2248. doi:10.2166/wst.2013.111

DeLorenzo, M.E., Thompson, B., Cooper, E., Moore, J., Fulton, M.H., 2012. A long-term monitoring study of chlorophyll, microbial contaminants, and pesticides in a coastal residential stormwater pond and its adjacent tidal creek. Environ. Monit. Assess. 184, 343–359. doi:10.1007/s10661-011-1972-3

Diaz, R.J., Rosenberg, R., 2008. Spreading Consequences Dead Zones and Consequences for Marine Ecosystems. Science (80-.). 321, 926–929.

Duan, S., Newcomer-Johnson, T., Mayer, P., Kaushal, S., 2016. Phosphorus retention in stormwater control structures across streamflow in urban and suburban watersheds. Water (Switzerland) 8. doi:10.3390/w8090390

Duda, P.B., Hummel, P.R., Donigian, A.S.J., Imhoff, J.C., 2012. Basins/HSPF: model use, calibration, and validation. Trans. Asabe 55, 1523–1547. doi:10.13031/2013.42261

Espinasse, B., Picolet, G., Chouraqui, E., 1997. Negotiation support systems: A multi-criteria and multi-agent approach. Eur. J. Oper. Res. 103, 389–409. doi:10.1016/S0377-2217(97)00127-6

Gold, A.C., Thompson, S.P., Piehler, M.F., 2018. Nitrogen cycling processes within stormwater control measures: A review and call for research. Water Res. 149, 578–587. doi:10.1016/j.watres.2018.10.036

Gold, A.C., Thompson, S.P., Piehler, M.F., 2017a. Water quality before and after watershed-scale implementation of stormwater wet ponds in the coastal plain. Ecol. Eng. 105, 240–251. doi:10.1016/j.ecoleng.2017.05.003

Gold, A.C., Thompson, S.P., Piehler, M.F., 2017b. Coastal stormwater wet pond sediment nitrogen dynamics. Sci. Total Environ. 609, 672–681. doi:10.1016/j.scitotenv.2017.07.213

Golden, H.E., Hoghooghi, N., 2017. Green infrastructure and its catchment-scale effects: an emerging science. Wiley Interdiscip. Rev. Water 5, e1254. doi:10.1002/wat2.1254

Goonetilleke, A., Thomas, E., Ginn, S., Gilbert, D., 2005. Understanding the role of land use in urban stormwater quality management. J. Environ. Manage. 74, 31–42. doi:10.1016/j.jenvman.2004.08.006

Goossens, D., 2008. Techniques to measure grain-size distributions of loamy sediments: A comparative study of ten instruments for wet analysis. Sedimentology 55, 65–96. doi:10.1111/j.1365-3091.2007.00893.x

Gu, L., Dai, B., Zhu, D.Z., Hua, Z., Liu, X., van Duin, B., Mahmood, K., 2017. Sediment modelling and design optimization for stormwater ponds. Can. Water Resour. J. / Rev. Can. des ressources hydriques 42, 70–87. doi:10.1080/07011784.2016.1210542

Hamel, P., Daly, E., Fletcher, T.D., 2015. Which baseflow metrics should be used in assessing flow regimes of urban streams? Hydrol. Process. 29, 4367–4378. doi:10.1002/hyp.10475

Hancock, G.S., Holley, J.W., Chambers, R.M., 2010. A Field-Based Evaluation of Wet Retention Ponds: How Effective Are Ponds at Water Quantity Control?1. JAWRA J. Am. Water Resour. Assoc. 46, 1145–1158. doi:10.1111/j.1752-1688.2010.00481.x

Hester, E.T., Bauman, K.S., 2013. Stream and retention pond thermal response to heated summer runoff from urban impervious surfaces. J. Am. Water Resour. Assoc. 49, 328–342. doi:10.1111/jawr.12019

Hupp, C.R., 2000. Hydrology, geomorphology and vegetation of costal plain rivers in the south-eastern USA. Hydrol. Process. 14, 2991–3010. doi:10.1002/1099-1085(200011/12)14:16/17<2991::AID-HYP131>3.0.CO;2-H

Ivanovsky, A., Belles, A., Criquet, J., Dumoulin, D., Noble, P., Alary, C., Billon, G., 2018. Assessment of the treatment efficiency of an urban stormwater pond and its impact on the natural downstream watercourse. J. Environ. Manage. 226, 120–130. doi:10.1016/j.jenvman.2018.08.015

Johnson, R.D., Sample, D.J., 2017. A semi-distributed model for locating stormwater best management practices in coastal environments. Environ. Model. Softw. 91, 70–86. doi:10.1016/j.envsoft.2017.01.015

Kadlec, R., Wallace, S., 2008. Treatment wetlands.

Kessler, A.J., Roberts, K.L., Bissett, A., Cook, P.L.M., 2018. Biogeochemical Controls on the Relative Importance of Denitrification and Dissimilatory Nitrate Reduction to Ammonium in Estuaries. Global Biogeochem. Cycles 32, 1045–1057. doi:10.1029/2018GB005908

Ketabchy, M., Sample, D.J., Wynn-Thompson, T., Nayeb Yazdi, M., 2018. Thermal Evaluation of Urbanization Using a Hybrid Approach. J. Environ. Manage. 226, 457–475. doi:10.1016/J.JENVMAN.2018.08.016

Koch, B.J., Febria, C.M., Gevrey, M., Wainger, L.A., Palmer, M.A., 2014. Nitrogen Removal by Stormwater Management Structures: A Data Synthesis. JAWRA J. Am. Water Resour. Assoc. 50, 1594–1607. doi:10.1111/jawr.12223

Kokot, S., Grigg, M., Panayiotou, H., Phuong, T.D., 1998. Data Interpretation by some Common Chemometrics Methods. Electroanalysis 10, 1081–1088. doi:10.1002/(SICI)1521-4109(199811)10:16<1081::AID-ELAN1081>3.0.CO;2-X

Li, H., Harvey, J.T., Holland, T.J., Kayhanian, M., 2013. Corrigendum: The use of reflective and permeable pavements as a potential practice for heat island mitigation and stormwater management. Environ. Res. Lett. 8, 049501. doi:10.1088/1748-9326/8/4/049501

Liu, A., Egodawatta, P., Guan, Y., Goonetilleke, A., 2013. Influence of rainfall and catchment characteristics on urban stormwater quality. Sci. Total Environ. 444, 255–262. doi:10.1016/j.scitotenv.2012.11.053

Liu, A., Goonetilleke, A., Egodawatta, P., 2015. Role of Rainfall and Catchment Characteristicson Urban Stormwater Quality.

Liu, G., Schwartz, F.W., Kim, Y., 2013. Complex baseflow in urban streams: An example from central Ohio, USA. Environ. Earth Sci. 70, 3005–3014. doi:10.1007/s12665-013-2358-3

Liu, J., Shen, Z., Chen, L., 2018. Assessing how spatial variations of land use pattern affect water quality across a typical urbanized watershed in Beijing, China. Landsc. Urban Plan. 176, 51–63. doi:10.1016/j.landurbplan.2018.04.006

Liu, W., Chen, W., Peng, C., 2014. Assessing the effectiveness of green infrastructures on urban flooding reduction: A community scale study. Ecol. Modell. 291, 6–14. doi:10.1016/J.ECOLMODEL.2014.07.012

Locatelli, L., Mark, O., Mikkelsen, P.S., Arnbjerg-Nielsen, K., Deletic, A., Roldin, M., Binning, P.J., 2017. Hydrologic impact of urbanization with extensive stormwater infiltration. J. Hydrol. 544, 524–537. doi:10.1016/J.JHYDROL.2016.11.030

Lucas, W.C., Sample, D.J., 2015. Reducing combined sewer overflows by using outlet controls for Green Stormwater Infrastructure: Case study in Richmond, Virginia. J. Hydrol. 520, 473–488. doi:10.1016/J.JHYDROL.2014.10.029

Lucke, T., Nichols, P.W.B., 2015. The pollution removal and stormwater reduction performance of street-side bioretention basins after ten years in operation. Sci. Total Environ. 536, 784–792. doi:10.1016/j.scitotenv.2015.07.142

Luo, K., Hu, X., He, Q., Wu, Z., Cheng, H., Hu, Z., Mazumder, A., 2018. Impacts of rapid urbanization on the water quality and macroinvertebrate communities of streams: A case study in Liangjiang New Area, China. Sci. Total Environ. 621, 1601–1614. doi:10.1016/J.SCITOTENV.2017.10.068

McPhillips, L.E., Matsler, A.M., 2018. Temporal Evolution of Green Stormwater Infrastructure Strategies in Three US Cities. Front. Built Environ. 4, 26. doi:10.3389/fbuil.2018.00026

Moriasi, D.N., Gitau, M.W., Pai, N., Daggupati, P., 2015. Hydrologic and Water Quality Models: Performance Measures and Evaluation Criteria. Trans. ASABE 58, 1763–1785.

doi:10.13031/trans.58.10715

NCDENR, 2009. Stormwater BMP Manual [WWW Document]. Chapter 10. Wet Deten. Basin. North Carolina Dep. Environ. Nat. Resour. URL https://ncdenr.s3.amazonaws.com/s3fs-public/Water Quality/ Surface Water Protection/SPU/SPU - BMP Manual Documents/BMPMan-Ch10- WetPonds-20090616-DWQ-SPU.pdf

O'Driscoll, M., Clinton, S., Jefferson, A., Manda, A., McMillan, S., 2010. Urbanization Effects on Watershed Hydrology and In-Stream Processes in the Southern United States. Water 2, 605–648. doi:10.3390/w2030605

Palla, A., Gnecco, I., 2015. Hydrologic modeling of Low Impact Development systems at the urban catchment scale. J. Hydrol. 528, 361–368. doi:10.1016/J.JHYDROL.2015.06.050

Perryman, S.E., Rees, G.N., Walsh, C.J., Grace, M.R., 2011. Urban Stormwater Runoff Drives Denitrifying Community Composition Through Changes in Sediment Texture and Carbon Content. Microb. Ecol. 61, 932–940. doi:10.1007/s00248-011-9833-8

Pitt, R.E., Maestre, A., Hyche, H., Togawa, N., 2008. The updated stormwater quality database (NSQD), version 3. Proc. Water Environ. Fed. 16, 1007–1026.

Roodsari, B.K., Chandler, D.G., 2017. Distribution of surface imperviousness in small urban catchments predicts runoff peak flows and stream flashiness. Hydrol. Process. 31, 2990–3002. doi:10.1002/hyp.11230

Rosburg, T.T., Nelson, P.A., Bledsoe, B.P., 2017. Effects of Urbanization on Flow Duration and Stream Flashiness: A Case Study of Puget Sound Streams, Western Washington, USA. JAWRA J. Am. Water Resour. Assoc. 53, 493–507. doi:10.1111/1752-1688.12511

Rosenzweig, B.R., Smith, J.A., Baeck, M.L., Jaffé, P.R., 2011. Monitoring Nitrogen Loading and Retention in an Urban Stormwater Detention Pond. J. Environ. Qual. 40, 598. doi:10.2134/jeq2010.0300

Rossman, L.A., Huber, W.C., 2016. Storm water management model reference manual volume III–water quality. Cincinnati, OH, USA USEPA.

Sample, D.J.D.J., Grizzard, T.J.T.J., Sansalone, J., Davis, A.P.A.P., Roseen, R.M.R.M., Walker, J., 2012. Assessing performance of manufactured treatment devices for the removal of phosphorus from urban stormwater. J. Environ. Manage. 113, 279–291. doi:10.1016/j.jenvman.2012.08.039

Saunders, D.L., Kalff, J., 2001. Nitrogen retention in wetlands, lakes and rivers. Hydrobiologia 443, 205–212. doi:10.1023/A:1017506914063

Schwartz, D., Sample, D.J., Grizzard, T.J., 2017. Evaluating the performance of a retrofitted stormwater wet pond for treatment of urban runoff. Environ. Monit. Assess. 189. doi:10.1007/s10661-017-5930-6

Selbig, W.R., Bannerman, R.T., 2011. Ratios of Total Suspended Solids to Suspended Sediment Concentrations by Particle Size. J. Environ. Eng. 137, 1075–1081. doi:10.1061/(asce)ee.1943-7870.0000414

Seong, C., Herand, Y., Benham, B.L., 2015. Automatic calibration tool for hydrologic simulation program-FORTRAN using a shuffled complex evolution algorithm. Water (Switzerland) 7, 503–527. doi:10.3390/w7020503

Simpson, T., Weammert, S., 2009. Developing best management practice definitions and effectiveness estimates for nitrogen, phosphorus and sediment in the Chesapeake bay watershed, University of Maryland Mid-Atlantic Water Program.

Smith, C.D.M., 2018. Watershed 5 water quality model report, Virginia Beach.

Smith, D.P., Matthew E. McKenzie, Craig Bowe, Dean F. Martin, 2004. Uptake of phosphate and nitrate using laboratory cultures of Lemna minor L. Florida Sci. 67, 105–117.

Sønderup, M.J., Egemose, S., Hansen, A.S., Grudinina, A., Madsen, M.H., Flindt, M.R., 2016. Factors affecting retention of nutrients and organic matter in stormwater ponds. Ecohydrology 9, 796–806. doi:10.1002/eco.1683

Song, K., Winters, C., Xenopoulos, M.A., Marsalek, J., Frost, P.C., 2017. Phosphorus cycling in urban aquatic ecosystems: connecting biological processes and water chemistry to sediment P fractions in urban stormwater management ponds. Biogeochemistry 132, 203–212. doi:10.1007/s10533-017-0293-1

Song, K., Xenopoulos, M.A., Buttle, J.M., Marsalek, J., Wagner, N.D., Pick, F.R., Frost, P.C., 2013. Thermal stratification patterns in urban ponds and their relationships with vertical nutrient gradients. J. Environ. Manage. 127, 317–323. doi:10.1016/J.JENVMAN.2013.05.052

Song, K., Xenopoulos, M.A., Marsalek, J., Frost, P.C., 2015. The fingerprints of urban nutrients: dynamics of phosphorus speciation in water flowing through developed landscapes. Biogeochemistry 125, 1–10. doi:10.1007/s10533-015-0114-3

Spagni, A., Buday, J., Ratini, P., Bortone, G., 2001. Experimental considerations on monitoring ORP, pH, conductivity and dissolved oxygen in nitrogen and phosphorus biological removal processes. Water Sci. Technol. 43, 197–204. doi:10.2166/wst.2001.0683

Steele, M.K., Heffernan, J.B., Bettez, N., Cavender-Bares, J., Groffman, P.M., Grove, J.M., Hall, S., Hobbie, S.E., Larson, K., Morse, J.L., Neill, C., Nelson, K.C., O'Neil-Dunne, J., Ogden, L., Pataki, D.E., Polsky, C., Chowdhury, R.R., 2014. Convergent Surface Water Distributions in U.S. Cities. Ecosystems 17, 685–697. doi:10.1007/s10021-014-9751-y

Stephansen, D.A., Nielsen, A.H., Hvitved-Jacobsen, T., Arias, C.A., Brix, H., Vollertsen, J., 2014. Distribution of metals in fauna, flora and sediments of wet detention ponds and natural shallow lakes. Ecol. Eng. 66, 43–51. doi:10.1016/j.ecoleng.2013.05.007

Stoner, E.W., Arrington, D.A., 2017. Nutrient inputs from an urbanized landscape may drive water quality degradation. Sustain. Water Qual. Ecol. 9–10, 136–150. doi:10.1016/J.SWAQE.2017.11.001

Stutter, M.I., Lumsdon, D.G., 2008. Interactions of land use and dynamic river conditions on sorption equilibria between benthic sediments and river soluble reactive phosphorus concentrations. Water Res. 42, 4249–4260. doi:10.1016/j.watres.2008.06.017

Taylor, C.A., Stefan, H.G., 2009. Shallow groundwater temperature response to climate change and urbanization. J. Hydrol. 375, 601–612. doi:10.1016/j.jhydrol.2009.07.009

Terando, A.J., Costanza, J., Belyea, C., Dunn, R.R., McKerrow, A., Collazo, J.A., 2014. The Southern Megalopolis: Using the Past to Predict the Future of Urban Sprawl in the Southeast U.S. PLoS One 9, e102261. doi:10.1371/journal.pone.0102261

Topçu, A., Pulatsü, S., 2014. Phosphorus Fractions and Cycling in the Sediment of a Shallow Eutrophic Pond. J. Agric. Sci. 20, 63–70.

Troitsky, B., Zhu, D.Z., Loewen, M., van Duin, B., Mahmood, K., 2019. Nutrient processes and modeling in urban stormwater ponds and constructed wetlands. Can. Water Resour. J. / Rev. Can. des ressources hydriques 44, 230–247. doi:10.1080/07011784.2019.1594390

USEPA, 2018. Storm Water Management Model (SWMM) [WWW Document]. URL https://www.epa.gov/water-research/storm-water-management-model-swmm (accessed 1.11.19).

USEPA, 2016. Operating and Maintaining Underground Storage Tank Systems: Practical Help and Checklists.

USEPA, 1992. NPDES storm water sampling guidance document [WWW Document]. United States Environ. Prot. Agency.

Vaze, J., Chiew, F.H.S., 2004. Nutrient loads associated with different sediment sizes in urban stormwater and surface pollutants. J. Environ. Eng. 130, 391–396. doi:10.1061/(ASCE)0733-9372(2004)130:4(391)

Vymazal, J., 2007. Removal of nutrients in various types of constructed wetlands. Sci. Total Environ. 380, 48–65. doi:10.1016/j.scitotenv.2006.09.014

W. C. Krumbein, W.C., 1934. Size Frequency Distributions of Sediments. SEPM J. Sediment. Res. Vol. 4, 65–77. doi:10.1306/D4268EB9-2B26-11D7-8648000102C1865D

Wang, P., Pozdniakov, S.P., Vasilevskiy, P.Y., 2017. Estimating groundwater-ephemeral stream exchange in hyper-arid environments: Field experiments and numerical simulations. J. Hydrol. 555, 68–79. doi:10.1016/J.JHYDROL.2017.10.004

Waterman, D.M., Waratuke, A.R., Motta, D., Cataño-Lopera, Y.A., Zhang, H., García, M.H., 2011. In Situ Characterization of Resuspended-Sediment Oxygen Demand in Bubbly Creek, Chicago, Illinois. J. Environ. Eng. 137, 717–730. doi:10.1061/(ASCE)EE.1943-7870.0000382

Wilhelm, S., Adrian, R., 2007. Impact of summer warming on the thermal characteristics of a polymictic lake and consequences for oxygen, nutrients and phytoplankton. Freshw. Biol. 0, 071004210218001-??? doi:10.1111/j.1365-2427.2007.01887.x

Willard, L.L., Wynn-Thompson, T., Krometis, L.A.H., Neher, T.P., Badgley, B.D., 2017. Does it pay to be mature? Evaluation of bioretention cell performance seven years postconstruction. J. Environ. Eng. 143, 04017041. doi:10.1061/(ASCE)EE.1943-7870.0001232

Xiao, Y., Cheng, H.-K., Yu, W.-W., Li, Z.-W., 2016. Effects of water flow on the uptake of

phosphorus by sediments: An experime- ntal investigation 28, 329–332. doi:10.1016/S1001-6058(16)60636-4

Zope, P.E., Eldho, T.I., Jothiprakash, V., 2016. Impacts of land use–land cover change and urbanization on flooding: A case study of Oshiwara River Basin in Mumbai, India. CATENA 145, 142–154. doi:10.1016/J.CATENA.2016.06.009

Chapter 6. Conclusions and Future Research

6.1 Key findings

This research evaluated the behavior of urban and agricultural watershed within urbanized Coastal Plain watersheds through monitoring and modeling that can be utilized for estimating pollutant loads delivered to receiving water.

First, in Chapter 2, we focused on watershed models. While numerous hydrologic models exist, there is limited information about how to select the most appropriate model for a given watershed, and how to evaluate its effectiveness at streamflow simulation. Hydrologic models such as SWMM and HSPF are widely used to assess the effects of urbanization on receiving waters. We developed SWMM and HSPF model for an urbanized watershed and compared the ability of these two models at simulating streamflow, peak flow, and baseflow. The most sensitive hydrologic parameters for HSPF were related to groundwater; for SWMM, it was imperviousness. Both models simulated streamflow adequately; however, HSPF simulated baseflow better than SWMM, while, SWMM simulated peak flow better than HSPF (Nayeb Yazdi et al., 2019a).

In chapter 3, we focused on the effect of urban land uses on stormwater quality. We estimated N, P, and sediment loading from these six catchments (i.e. commercial, low density residential, high density residential, industrial, transportation, and open space) with homogenous land use within coastal urban area and investigated the effect of rainfall characteristics on stormwater quality. A model was developed to estimate annual TSS, TP, TN loads delivered from urban areas using a simple linear model and incorporating statistical variability by use of a Bootstrap method. We calculated EMCs within Virginia Beach for TSS, TP, and TN were 30 (19 – 34 $mg \cdot L^{-1}$), 0.31 (0.26 – 0.31 $mg \cdot L^{-1}$), and 0.94 (0.73 – 1.25 $mg \cdot L^{-1}$), respectively, and average

pollutant loads within urban coastal areas for TSS, TP, and TN were as 0.86, 0.03, and 0.01 $kg \cdot ha^{-1} \cdot cm^{-1}$, respectively.

In Chapter 4, we conducted a monitoring and modeling program on a nursery as an urban agriculture. We quantified TSS, TN, and TP in runoff from a 5.2 ha production portion of a 200 ha commercial container nursery during storm and irrigation events. A SWMM model was developed to simulate hydrology and water quality at the main production areas of that site. In addition, an estimate of average annual loading of TSS, TN and TP from a nursery production area was developed. As in the first study, we modeled runoff quantity and quality at a container nursery. Results showed the average loading of TSS, TN and TP during storm events was approximately 900, 35 and 50 times higher than those of irrigation events, respectively. SWMM was able to quantify runoff quality and quantity, well. Thus, SWMM is suitable for characterizing runoff loadings from container nurseries (Nayeb Yazdi et al., 2019b; Yazdi et al., 2018)

A variety of SCMs have been developed for mitigating urban and agricultural impacts. Due to the physiography of the Coastal Plain (low slope, high groundwater, poorly infiltrating soils), retention ponds are commonly used within the mid-Atlantic/southeast (Johnson and Sample, 2017; Steele et al., 2014). Thus, in Chapter 5, we assessed the ability of a Coastal Plain retention pond to treat nutrients and sediment. We selected a rather ordinary pond in the City of Virginia Beach for this study, and a monitoring program was conducted at the inlets and the outlet of the retention pond for one year. A SWMM model was developed and calibrated to simulate the retention pond treatment for stormwater quantity and quality. Results indicated that during cold weather, the pond reduced the level of TSS and TP by 62% and 8.8%, respectively, while the pond exported N and the level of TN increased in the outflow of the pond by 6%.

During warm weather, due to biological activities like nitrification and denitrification, the performance of the pond improved, and the pond reduced TSS, TN and TP by 74%, 47%, and 8%, respectively. SWMM was able to model TSS removal reasonably well, and for TP the performance of SWMM was satisfactory, however SWMM was unable to simulate TN during warm weather, and only could simulate TN during cold weather. While this retention pond was not designed for water quality treatment, the results of this study indicate that the retention pond provides significant improvement in the water quality of urban runoff and can be implemented to mitigate negative effects of urbanization on hydrology and water quality. Understanding the function of the retention pond in detail and characterizing it with a numerical model may provide a means of improving treatment across an entire watershed and thus improve the health of downstream ecosystems.

Collectively, these studies take an important step towards understanding behavior of urban and agricultural watershed within Coastal Plain area. Nonetheless, future work is needed to improve our overall understanding of runoff quality delivered from Coastal Plain area to receiving waters.

6.2 Suggestions for future research

The presented research provides scientific findings that can be useful for better understanding urban and agricultural runoff quality within coastal Plain area. However, suggestions are provided to aid future studies in effectively modeling and monitoring:

1) There are two common methods for water quality calibrating SWMM including event mean concentration (EMC), and buildup and washoff. In this research, EMC was applied as a water quality method in SWMM model. EMC method works properly, when the focus is on annual loads. However, buildup and washoff method is more accurate than EMC in simulating

runoff quality, because precipitation characteristics such as intensity, duration, and antecedent dry periods have effect on buildup and washoff method. Thus, Future research should seek to develop a water quality model based on buildup and washoff.

2) There are three sources of uncertainty in: model parameters and structure, input data (i.e. precipitation, soil infiltration, etc.), and observation (i.e. flow, pollutant concentrations) used to calibrate models (Asgari-Motlagh et al., 2019; Butts et al., 2004; Yen et al., 2014). Future research should seek to characterize uncertainly in processes and variables relating to the hydrologic and water quality of urban and agricultural runoff. In addition, treatment performance of SCMs is also uncertain that can have effects on variability in incoming loads, hydrology, and site characteristics (Fassman, 2012; Park and Roesner, 2013, 2012; Shahed Behrouz et al., 2020). Thus, future monitoring research should identify uncertainly in retention pond performance, as well.

3) Performance of the retention pond varied during cold and warm weather, it means temperature and rainfall characteristic can play a great role in the retention pond treatment. Thus, future research should seek to evaluate effect of climate change (CC) on the performance of the retention pond. Historical assessments of the U.S. climate between 1950 and 2009 indicated that temperature for almost all U.S. cities increased because of CC (Mishra and Lettenmaier, 2011). In addition, Because of CC, rainfall characteristics has changed so that the extreme rainfall intensity has increased at the global scale (Westra et al., 2014). Thus, CC can have serious effect of retention ponds treatment.

6.3 References for Chapter 6

Asgari-Motlagh, X., Ketabchy, M., Daghighi, A., 2019. Probabilistic Quantitative Precipitation Forecasting Using Machine Learning Methods and Probable Maximum Precipitation. Int. Acad. J. Sci. Eng. 6, 1–14. doi:10.9756/IAJSE/V6I1/1910001

Butts, M.B., Payne, J.T., Kristensen, M., Madsen, H., 2004. An evaluation of the impact of model structure on hydrological modelling uncertainty for streamflow simulation. J. Hydrol. 298, 242–266. doi:10.1016/j.jhydrol.2004.03.042

Fassman, E., 2012. Stormwater BMP treatment performance variability for sediment and heavy metals. Sep. Purif. Technol. 84, 95–103. doi:10.1016/j.seppur.2011.06.033

Johnson, R.D., Sample, D.J., 2017. A semi-distributed model for locating stormwater best management practices in coastal environments. Environ. Model. Softw. 91, 70–86. doi:10.1016/j.envsoft.2017.01.015

Mishra, V., Lettenmaier, D.P., 2011. Climatic trends in major U.S. urban areas, 1950-2009. Geophys. Res. Lett. 38, L16401. doi:10.1029/2011GL048255

Nayeb Yazdi, M., Ketabchy, M., Sample, D.J., Scott, D., Liao, H., 2019a. An evaluation of HSPF and SWMM for simulating streamflow regimes in an urban watershed. Environ. Model. Softw. 118, 211–225. doi:10.1016/J.ENVSOFT.2019.05.008

Nayeb Yazdi, M., Sample, D.J., Scott, D., Owen, J.S., Ketabchy, M., Alamdari, N., 2019b. Water quality characterization of storm and irrigation runoff from a container nursery. Sci. Total Environ. 667, 166–178. doi:10.1016/j.scitotenv.2019.02.326

Park, D., Roesner, L.A., 2013. Effects of Surface Area and Inflow on the Performance of Stormwater Best Management Practices with Uncertainty Analysis. Water Environ. Res. 85, 782–792. doi:10.2175/106143013x13736496908825

Park, D., Roesner, L.A., 2012. Evaluation of pollutant loads from stormwater BMPs to receiving water using load frequency curves with uncertainty analysis. Water Res. 46, 6881–6890. doi:10.1016/j.watres.2012.04.023

Shahed Behrouz, M., Zhu, Z., Matott, L.S., Rabideau, A.J., 2020. A new tool for automatic calibration of the Storm Water Management Model (SWMM). J. Hydrol. 581, 124436. doi:10.1016/j.jhydrol.2019.124436

Steele, M.K., Heffernan, J.B., Bettez, N., Cavender-Bares, J., Groffman, P.M., Grove, J.M., Hall, S., Hobbie, S.E., Larson, K., Morse, J.L., Neill, C., Nelson, K.C., O'Neil-Dunne, J., Ogden, L., Pataki, D.E., Polsky, C., Chowdhury, R.R., 2014. Convergent Surface Water Distributions in U.S. Cities. Ecosystems 17, 685–697. doi:10.1007/s10021-014-9751-y

Westra, S., Fowler, H.J., Evans, J.P., Alexander, L. V., Berg, P., Johnson, F., Kendon, E.J., Lenderink, G., Roberts, N.M., 2014. Future changes to the intensity and frequency of short-duration extreme rainfall. Rev. Geophys. doi:10.1002/2014RG000464

Yazdi, M.N., Sample, D.J., Scott, D., Owen, J.S., 2018. Water Quality Characterization of Irrigation and Storm Runoff for a Nursery. Springer, Cham, pp. 788–793. doi:10.1007/978-3-319-99867-1_136

Yen, H., Wang, X., Fontane, D.G., Harmel, R.D., Arabi, M., 2014. A framework for propagation of uncertainty contributed by parameterization, input data, model structure, and calibration/validation data in watershed modeling. Environ. Model. Softw. 54, 211–221. doi:10.1016/j.envsoft.2014.01.004

APPENDIX A. Hydrographs of each station

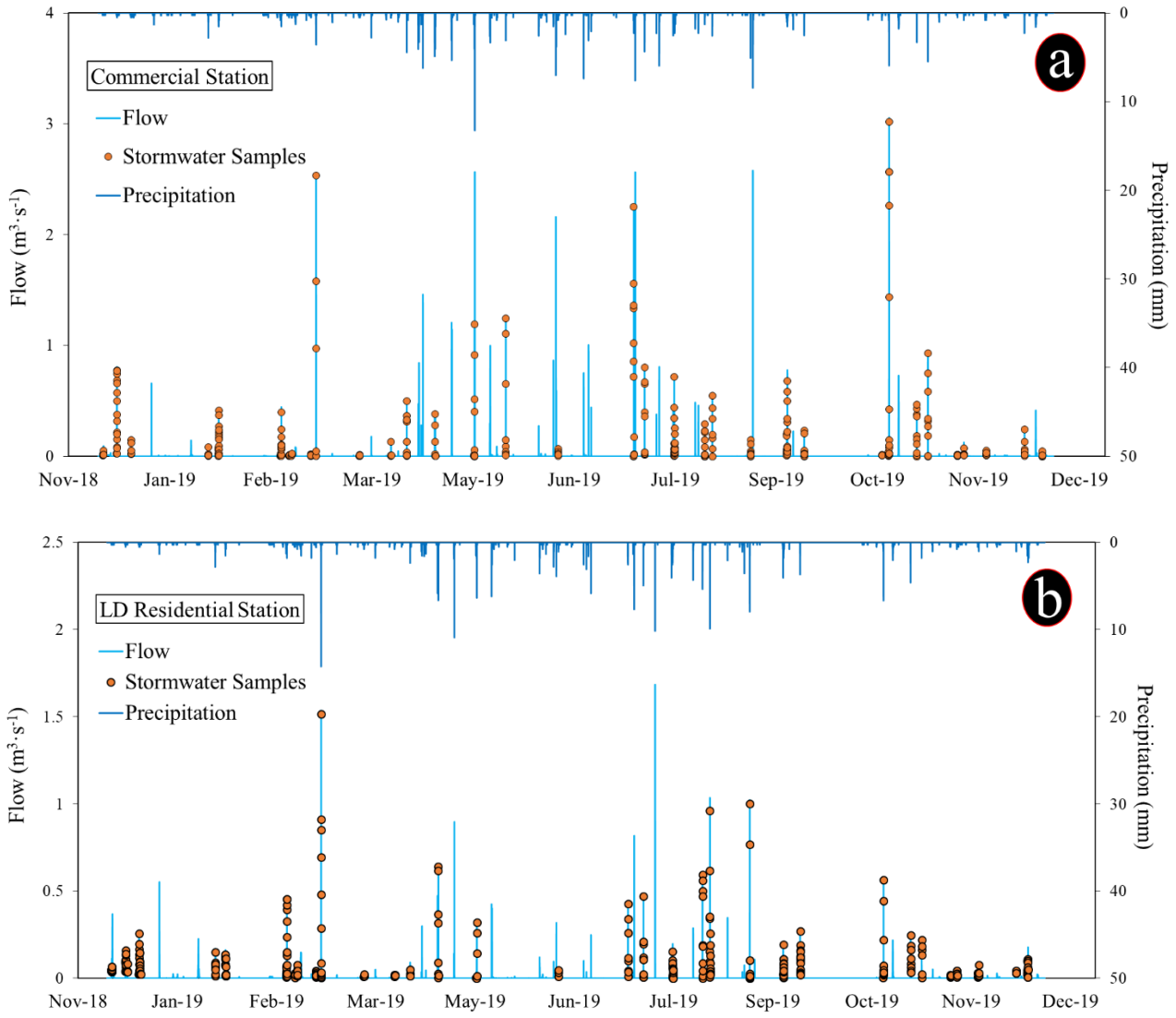

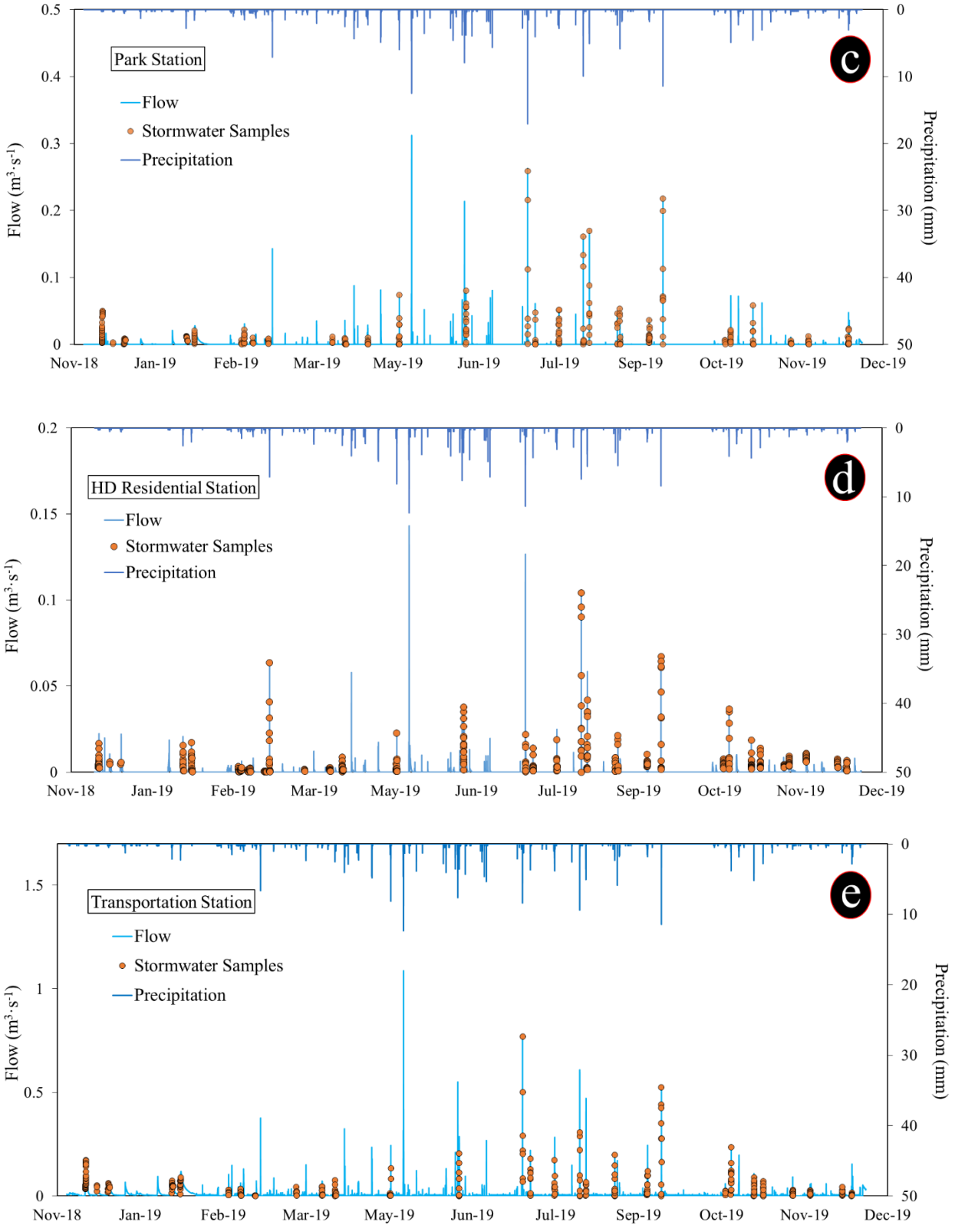
Park Station
Flow
Stormwater Samples
Precipitation
c
Flow (m³·s⁻¹)
Precipitation (mm)
0.5
0.4
0.3
0.2
0.1
0
0
10
20
30
40
50
Nov-18
Jan-19
Feb-19
Mar-19
May-19
Jun-19
Jul-19
Sep-19
Oct-19
Nov-19
Dec-19
HD Residential Station
Flow
Stormwater Samples
Precipitation
d
Flow (m³·s⁻¹)
Precipitation (mm)
0.2
0.15
0.1
0.05
0
0
10
20
30
40
50
Nov-18
Jan-19
Feb-19
Mar-19
May-19
Jun-19
Jul-19
Sep-19
Oct-19
Nov-19
Dec-19
Transportation Station
Flow
Stormwater Samples
Precipitation
e
Flow (m³·s⁻¹)
Precipitation (mm)
1.5
1
0.5
0
0
10
20
30
40
50
Nov-18
Jan-19
Feb-19
Mar-19
May-19
Jun-19
Jul-19
Sep-19
Oct-19
Nov-19
Dec-19

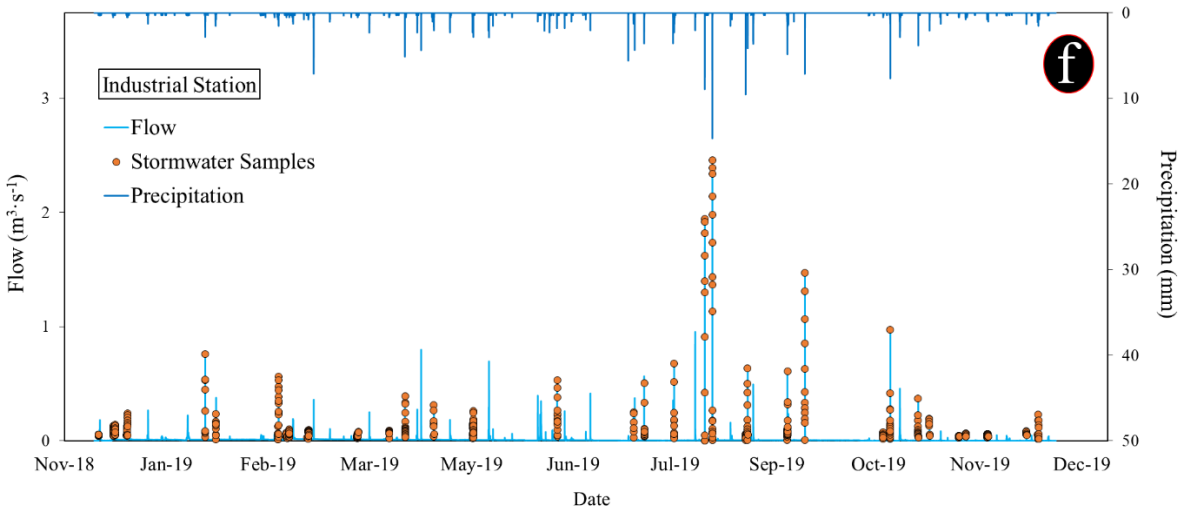

Figure A.1. Hydrographs of each station a) Commercial, b) Low density residential, c) Open space (park), d) High density residential, e) Transportation (road), f) Industrial.